# "*In vitro* methods to study the cytotoxicity, cell transformation capacity and genotoxicity of nanoparticles—application to cobalt ferrite and silver nanoparticles".

**Francesca Broggi**

Thesis submitted for a Ph.D. degree in Life Sciences

Prof. Vicki Stone
*Supervisor*

Heriot-Watt University
Edinburgh
EH14 4AS
UK

Jessica Ponti, PhD
François Rossi, PhD
*Co-Supervisors*

European Commission
Joint Research Centre
Ispra (VA)
Italy

**December, 2011**

## Abstract

The objective of this thesis was to investigate the *in vitro* cytotoxic, genotoxic and transforming effects induced by nanoparticles (NPs) of industrial interest on a range of cell cultures.

The cytotoxicity of two sizes of $CoFe_2O_4$ NPs, paramagnetic particles of interest in different biomedical applications, was investigated using the Neutral Red uptake (NR) and Colony Forming Efficiency (CFE) assays using six mammalian cell lines at concentrations between 10 and 120 µM. More specifically, cytotoxicity was evaluated after 72-hour treatment of five cell lines (A549, CaCo2, HaCaT, HepG2, MDCK) with 10, 20, 40, 60, 80, 100 and 120 µM concentrations of NPs using NR, and 10, 20, 30, 40, 50, 60, 80, 100 and 120 µM concentrations of NPs using CFE. In parallel with these tests, cytotoxicity was also evaluated in mouse Balb3T3 fibroblasts using (i) NR after 72-hour treatment with 10, 20, 40, 60, 80, 100 and 120 µM concentrations of NPs, and (ii) CFE after both 72-hour treatment with 1, 5, 10, 20, 30, 40, 50, 60, 80, 100 and 120 µM concentrations of NPs, and 24-hour treatment with 1, 10, 60 and 120 µM concentrations of NPs. The cytotoxic effect exhibited a dose-effect relationship for Balb3T3 cells as assessed using the CFE assay. The testing of a more extensive concentration range of NPs in Balb3T3 cells (i.e., 1 and 5 µM in addition to the concentrations tested in the other five cell lines) over a 72-hour exposure time using CFE, together with the additional test using a 24-hour exposure time allowed appropriate concentration ranges to be determined for use in subsequent experiments using the Cell Transformation (CTA) and Cytokinesis-Block Micronucleus (CBMN) assays.

The cell transformation capacity and genotoxicity of $CoFe_2O_4$ NPs were investigated using the Balb3T3 model, and assessed using the CTA (specifically at concentrations of 1, 5, 20 and 60 µM for 72 hours of treatment) and CBMN (specifically at concentrations of 1, 10 and 60 µM for 24 hours of treatment). The $CoFe_2O_4$ NPs induced neither effect at the doses and time points investigated.

Four sizes of Ag NPs, chosen for their antimicrobial properties, were assessed for cytotoxicity (using CFE at concentrations of 0.1, 0.5, 1, 5 and 10 µM for 24 hours of treatment and of 0.01, 0.1, 0.5, 1, 2.5, 5 and 10 µM for 72 hours of treatment), cell transformation capacity (using CTA at concentrations of 0.5, 2.5 and 5 µM for 72 hours

of treatment) and genotoxicity to Balb3T3 mouse fibroblasts (using CBMN at concentrations of 1, 5 and 10 μM for 24 hours of treatment). The Ag NPs had a significant cytotoxic effect, but no cell transformation or genotoxic effects at the doses and time points investigated.

Physicochemical characterization of the chosen NPs was performed; size distribution and surface charge were measured by Dynamic Light Scattering (DLS), imaging by Scanning Electron Microscopy (SEM), the purity and ion leakage by Inductively Coupled Plasma Mass Spectrometry (ICP-MS), and the sedimentation by UV-Visible spectrometry.

*To my family*

## Acknowledgements

Thanks to:

Professor Vicki Stone for her support during the PhD thesis preparation and for her precious contribution;

Dr. Jessica Ponti for her precious help during these three years of nanotoxicology research; she has encouraged me to improve my work and knowledge and has supported me throughout the difficult times;

Dr. François Rossi and Hermann Stamm for giving me the opportunity to carry out the laboratory work at the Joint Research Center;

All my colleagues who shared this special work experience with me, particularly Valentina, Rosella, Chiara, Sabrina, Patrick, Laura, Silvia and Elisa;

The NP synthesis and characterization group for its fundamental collaboration in exploring the world of NPs and in particular to Dr. Guido Giudetti (Nanobiosciences Unit, JRC) for DLS sample analysis and his contribution to all DLS clarifications, as well as Ag NPs sample preparation for SEM imaging; Dr. Fabio Franchini (Nanobiosciences Unit, JRC) for ICP-MS sample analysis and explanation of the ICP-MS technique; Dr. Douglas Gilliland (Nanobiosciences Unit, JRC) for elucidation of the NPs' chemistry; Dr. Hubert Rauscher (Nanobiosciences Unit, JRC) for his contribution with the UV-Vis sample analysis; Dr. Thierry Darmanin (Nanobiosciences Unit, JRC) for Ag NPs' synthesis and preparation of Ag NP dispersants; Dr. Cesar Pascual Garcia (Nanobiosciences Unit, JRC) for Ag NPs' imaging;

Alla mia famiglia, che mi ha affiancato ed incoraggiato in ogni momento di questa avventura;

Paula and Gabriella, secretaries at the Nanobiosciences Unit, for their assistance in helping me to solve all administrative matters; Mrs Dorothy Haston for her precious help and support for the administrative procedures at Heriot-Watt University.

ACADEMIC REGISTRY
# Research Thesis Submission

| | | | |
|---|---|---|---|
| Name*:* | Francesca Broggi | | |
| School/PGI: | School of Life Sciences | | |
| Version: *(i.e. First, Resubmission, Final)* | First | Degree Sought (Award **and** Subject area) | PhD Life Science |

**Declaration**

In accordance with the appropriate regulations I hereby submit my thesis and I declare that:

1) the thesis embodies the results of my own work and has been composed by myself
2) where appropriate, I have made acknowledgement of the work of others and have made reference to work carried out in collaboration with other persons
3) the thesis is the correct version of the thesis for submission and is the same version as any electronic versions submitted*.
4) my thesis for the award referred to, deposited in the Heriot-Watt University Library, should be made available for loan or photocopying and be available via the Institutional Repository, subject to such conditions as the Librarian may require
5) I understand that as a student of the University I am required to abide by the Regulations of the University and to conform to its discipline.

* *Please note that it is the responsibility of the candidate to ensure that the correct version of the thesis is submitted.*

| | | | |
|---|---|---|---|
| Signature of Candidate*:* | Francesca Broggi | Date: | |

**Submission**

| | |
|---|---|
| Submitted By *(name in capitals):* | |
| Signature of Individual Submitting: | |
| Date Submitted: | |

**For Completion in the Student Service Centre (SSC)**

| | | | |
|---|---|---|---|
| Received in the SSC by *(name in capitals):* | | | |
| *Method of Submission*<br>*(Handed in to SSC; posted through internal/external mail):* | | | |
| *E-thesis Submitted (**mandatory for final theses)*** | | | |
| Signature: | | Date: | |
| | | | |

## Table of contents

## List of Tables

($Co^{2+}$) was calculated as the difference between the cobalt detected at 24 or 72 hours and at time 0 in filtered fractions. The percentage release was calculated using the corresponding average of the total fractions.

**B.5** Cobalt concentrations (µM) detected by ICP-MS in P703 $CoFe_2O_4$ samples prepared in MEM basal medium in total and filtered fractions, both at time 0 and after 24 and 72 hours of incubation under standard culture conditions (37°C, 5% $CO_2$, 90% humidity). Expected concentrations in total fractions were calculated using 98 mM as concentration of the stock suspension for P703. The release of cobalt ($Co^{2+}$) was calculated as the difference between the cobalt detected at 24 or 72 hours and at time 0 in filtered fractions. The percentage release was calculated using the corresponding average of the total fractions.

**B.6** Cobalt concentrations (µM) detected by ICP-MS in P601 $CoFe_2O_4$ samples prepared in Balb3T3 complete culture medium in total and filtered fractions, both at time 0 and after 24 and 72 hours of incubation under standard culture conditions (37°C, 5% $CO_2$, 90% humidity). Expected concentrations in total fractions were calculated using 119 mM as concentration of the stock suspension for P601. The release of cobalt ($Co^{2+}$) was calculated as the difference between the cobalt detected at 24 or 72 hours and at time 0 in the filtered fractions. The percentage release was calculated using the corresponding average of the total fractions.

**B.7** Cobalt concentrations (µM) detected by ICP-MS in P703 $CoFe_2O_4$ samples prepared in Balb3T3 complete culture medium in total and filtered fractions, both at time 0 and after 24 and 72 hours of incubation under standard culture conditions (37°C, 5% $CO_2$, 90% humidity). Expected concentrations in total fractions were calculated using 98 mM as concentration of the stock suspension for P703. The release of cobalt ($Co^{2+}$) was calculated as the difference between the cobalt detected at 24 or 72 hours and at time 0 in filtered fractions. The percentage release was calculated using the corresponding average of the total fractions.

**B.8** Metal impurities detected by ICP-MS analysis in P601 and P703 $CoFe_2O_4$ stock suspensions. The metal amounts detected are reported as a percentage of the stock suspension (119 mM and 98 mM stock concentrations for P601 and P703, respectively), the corresponding concentration as micromolarity and the maximum concentration present in the maximum dose of $CoFe_2O_4$ tested. At these levels, any of the impurities can potentially induce toxic effects after 72 hours of treatment on Balb3T3 cells, which appear to be the most sensitive culture of the cell lines used to test the $CoFe_2O_4$ NPs (Ponti, unpublished data).

**B.9** Z-potential measurements of all Ag NPs evaluated in this study. The Ag NPs dilutions in ultrapure water were investigated to determine their surface charge. Values are expressed as mV ± standard deviation (SD). All Ag NPs had a negative surface charge, but only Ag 44 nm, Ag 84 nm and Ag 100 nm showed values lower than -30 mV, which indicated that they

were stable in an aqueous environment.

**B.10** The mean NP diameter (Mean NPs Ø) (nm) of all Ag NPs investigated in this study. The DLS measurements were done for Ag NP dilutions in ultrapure water, Phosphate Buffer Saline (PBS), MEM basal medium and Balb3T3 complete culture medium (100 µM for all Ag NPs investigated) at time 0 and after 24 and 72 hours of incubation under standard culture conditions (37°C, 90% humidity, 5% $CO_2$). The standard deviation (SD) was used to assess variability in the measurements.

**B.11** Mean NP diameter (Mean NPs Ø) (nm) of 100 µM Ag NP samples prepared in ultrapure water and determined by Nanoparticle Tracking Analysis. Standard deviation (SD) is shown.

**B.12** The different units of measure by which Ag NP concentration can be expressed. The number of NPs per mL (No. NPs/mL) was calculated using formula B.1, the hydrodynamic diameters measured in ultrapure water by DLS (46 nm, 44 nm, 84 nm and 100 nm for NM-300, Ag 44 nm, Ag 84 nm and Ag 100 nm, respectively) and the densities determined by weighing three samples of 500 µL of stock suspension for each Ag NP (1.113, 0.9885, 0.9779 and 0.9773 $g/cm^3$ for NM-300, Ag 44 nm, Ag 84 nm and Ag 100 nm, respectively).

## List of Figures

**1.7** The possible fates of cultured, cytokinesis-blocked cells following exposure to cytotoxic/genotoxic agents. Using CBMN assay, biomarkers, such as the frequency of chromosome breakage (MN), chromosome loss (MN), and chromosome rearrangement, for example, dicentric chromosomes (NPB), gene amplification (NBUDs), necrosis and apoptosis can be measured. In addition, cytostatic effects can be estimated from the ratio of mono-, bi- and multinucleated cells (Fenech, 2007).

**1.8A, B, C, D, E, F, G, H and I** Optical microscope images (40X) from positive control slides prepared in the CBMN assay using Balb3T3 mouse fibroblasts. In particular, an example of a mononucleated cell (A), a binucleated cell (B), a polynucleated cell (C), a binucleated cell with one or more micronuclei (D and E respectively), a binucleated cell with nuclear bud (F), a binucleated cell with nucleoplasmic bridge (G), a binucleated cell with double nucleoplasmic bridge and a micronucleus (H) and a binucleated cell with nucleoplasmic bridge and nuclear buds (I) (EC, JRC-Ispra, IHCP, NBS).
To calculate the NDI, mononucleated, binucleated (with or without micronuclei) and polynucleated cells are scored. In this study, the genotoxic potential of $CoFe_2O_4$ and Ag NPs, demonstrated by the induction of micronuclei formation, was evaluated on Balb3T3 mouse fibroblasts.

**1.9** Mechanisms of primary and secondary genotoxicity induced by particles and fibres; ROS may play a major role in primary genotoxicity, whilst the excessive and persistent formation of ROS from inflammatory cells may be responsible for secondary genotoxicity (Schins, 2002).

**2.1** A549 cells in culture (100X magnification at the optical microscope) (NBS, IHCP, JRC)

**2.2** Balb3T3 cells in culture (100X magnification at the optical microscope) (NanoBioSciences Unit, IHCP, JRC).

**2.3** CaCo2 cells in culture (100X magnification at the optical microscope) (NanoBioSciences Unit, IHCP, JRC).

**2.4** HaCaT cells in culture (100X magnification at the optical microscope) (NanoBioSciences Unit, IHCP, JRC).

**2.5** HepG2 cells in culture (100X magnification at the optical microscope) (NBS, IHCP, JRC).

**2.6** MDCK cells in culture (100X magnification at the optical microscope) (NBS, IHCP, JRC).

**2.7A, B, C, D, E and F** Images of colonies from negative controls at the end of a CFE assay: (A) A549 colonies (45X magnification), (B) Balb3T3 colonies (15X magnification), (C) CaCo2 colonies (45X magnification), (D) HaCaT colonies (45X magnification), (E) HepG2 colonies (15X magnification) and (F) MDCK colonies (15X magnification) (EC, JRC-Ispra, IHCP,

NBS).

**2.8A, B, C, D, E and F** Normal and morphologically transformed Balb3T3 mouse fibroblasts as seen at the stereo microscopic level after the CTA: (A) negative control cells (45X of magnification) and some examples of type III foci from positive control dishes (B, C, D, E and F) (15X magnification). In the negative control dishes, cells grow in a monolayer as they retain their morphology and contact-inhibition. When cells are transformed into tumorigenic cells, they lose contact-inhibition and begin to grow spindle shaped with no ordered orientation and as a multilayer (EC, JRC-Ispra, IHCP, NBS). Only type III foci are scored because these alone can induce tumour formation in nude mice with an 85% frequency (Saffiotti et al., 1984; IARC/INCI/EPA, 1985).

**2.9** A typical binucleated, micronucleated Balb3T3 cell after 24-hour exposure to mytomicin C (0.5 µM) as a positive control. The black arrows highlight micronuclei in the cytosol (400X of magnification, EC, JRC-Ispra, NBS). In this study, the genotoxic potential of $CoFe_2O_4$ and Ag NPs in Balb3T3 mouse fibroblasts was indicated by the induction of micronuclei formation.

**3.1** Six cell lines exposed to dialyzed diethylene glycol (DEG) for 72 hours. Cytotoxicity was evaluated using Neutral Red uptake. Results are expressed as Cell Viability (% of control) and are a mean of three independent experiments, ± standard error of the mean (SEM). The red ring highlights the concentration of dialyzed DEG that was chosen as control for the solvent (Control DEG 0.1% v/v) in the experiments with cobalt ferrites.

**3.2** Six cell lines exposed to dialyzed diethylene glycol (DEG) for 72 hours. Cytotoxicity was evaluated by Colony Forming Efficiency (CFE). Results are expressed as CFE (% of control) and are the mean of three independent experiments, ± standard error of the mean (SEM). The red ring highlights the concentration of dialyzed DEG that was chosen as control for the solvent (control DEG 0.1 % v/v) in the experiments with cobalt ferrites.

**3.3** Six cell lines exposed to $CoFe_2O_4$ NPs P601 for 72 hours. Cytotoxicity was evaluated using the Neutral Red assay. Results are expressed as Cell Viability (% of the dialyzed DEG 0.1% v/v) and are the mean of three independent experiments, ± standard error of the mean (SEM).

**3.4** Six cell lines exposed to $CoFe_2O_4$ NPs P601 for 72 hours. Cytotoxicity was evaluated using CFE. Results are expressed as Colony Forming Efficiency (CFE% of the solvent control, i.e., CFE% of dialyzed DEG 0.1% v/v) and are the mean of three independent experiments, ± standard error of the mean (SEM).

**3.4A** Three cell lines exposed to $CoFe_2O_4$ NPs P601 for 72 hours. The statistical significance was evaluated by one-way ANOVA (*$p<0.05$ and **$p<0.01$) with respect to dialyzed DEG 0.1% v/v control. Significant differences

were found in A549, Balb3T3 and CaCo2 cells when compared to dialyzed DEG 0.1% v/v control. Results are the mean of three independent experiments, ± standard error of the mean (SEM).

**3.4B** Three cell lines exposed to $CoFe_2O_4$ NPs P601 for 72 hours. The statistical significance was evaluated by one-way ANOVA (*$p<0.05$ and **$p<0.01$) with respect to dialyzed DEG 0.1% v/v control. Significant differences were found in MDCK cells compared to dialyzed DEG 0.1% v/v control. Results are the mean of three independent experiments, ± standard error of the mean (SEM).

**3.5** Six cell lines exposed to $CoFe_2O_4$ NPs P703 for 72 hours. Cytotoxicity was evaluated using NR. Results are expressed as Cell Viability (% of dialyzed DEG 0.1% v/v control) and are the mean of three independent experiments, ± standard error of the mean (SEM). For ease of comparing the cytotoxicity results of P601 NPs to those of the P703 NPs, the concentrations of P703 NPs reported in the cytotoxicity graphs were the expected ones.

**3.6** Six cell lines exposed to $CoFe_2O_4$ NPs P703 for 72 hours. Cytotoxicity was evaluated using CFE. Results are expressed as Colony Forming Efficiency (% of the dialyzed DEG 0.1% v/v control) and are the mean of three independent experiments, ± standard error of the mean (SEM).

**3.6A** Three cell lines exposed to $CoFe_2O_4$ NPs P703 for 72 hours. The statistical significance was evaluated by one-way ANOVA (*$p<0.05$ and **$p<0.01$) with respect to dialyzed DEG 0.1% v/v control. Significant differences compared to dialyzed DEG 0.1% v/v control were found in A549 and Balb3T3 cells. Results are the mean of three independent experiments, ± standard error of the mean (SEM).

**3.6B** Three cell lines exposed to $CoFe_2O_4$ NPs P703 for 72 hours. The statistical significance was evaluated by one-way ANOVA (*$p<0.05$ and **$p<0.01$) with respect to dialyzed DEG 0.1% v/v control. Significant differences were found in HepG2 cells ($p<0.05$) compared to the dialyzed DEG 0.1% v/v control. Results are the mean of three independent experiments, ± standard error of the mean (SEM).

**3.7A and 3.7B** The comparison of cytotoxicity in Balb3T3 cells induced by P601 (A, light blue histograms) and P703 (B, dark blue histograms), NPs and $Co^{2+}$ (A and B, yellow histograms) after 72 hours of exposure, evaluated using the CFE assay. Results are the mean of three independent experiments, ± standard error of the mean (SEM = standard deviation/√number of experiments or replicates). The CFE values for $Co^{2+}$ treatments of 72 hours were extrapolated from a previous study (Ponti et al., 2009). Concentrations indicated in the graphs are related to the expected µM concentrations of NPs in total fraction samples, considering 119 and 98 mM as concentration of the stock suspensions of P601 and P703; see Tables B.6 and B.7 for the respective $Co^{2+}$ concentrations detected in Balb3T3 complete culture medium after 72 hours of incubation for both

P601 and P703 NPs.
The P601 NPs showed the highest cytotoxicity with respect to $Co^{2+}$ at all doses considered; in contrast, P703 NPs showed less cytotoxicity than $Co^{2+}$. Data were statistically analyzed using t-test (http://www.graphpad.com/quickcalcs/ttest1.cfm). There was no significant difference when P601 or P703 data were compared to those of $Co^{2+}$.

**3.8A and 3.8B** CFE results after exposing Balb3T3 cells to P601 (A) and P703 (B) NPs for 72 hours. In order to define the concentrations at which the transformation capacity of these NPs could be assessed as accurately as possible, the cytotoxicity on Balb3T3 fibroblasts (in contrast to the other cell lines) was investigated testing additional concentrations including 1 and 5 µM. Statistically significant differences are not shown here (please see Figures 3.4A and 3.6A).

**3.9A** The cytotoxicity induced by P601 and P703 NPs after 72 hours of exposure, evaluated by concurrent CFE and CTA assays. Results are the mean of three independent experiments, ± standard error of the mean (SEM = standard deviation/√number of experiments or replicates). Statistical significance was evaluated using one-way ANOVA (*$p<0.05$, ***$p<0.001$).

**3.9B** The cell transformation capacity induced by P601 and P703 NPs in Balb3T3 cells after 72 hours of exposure, evaluated using CTA. Results are a mean of three independent experiments, ± standard error of the mean (SEM = standard deviation/√number of experiments or replicates). Statistical significance was evaluated by Fisher's exact test for CTA data (***$p<0.001$).

**3.10** The cytotoxicity induced by P601 and P703 NPs in Balb3T3 cells after 24 hours of exposure, evaluated by CFE. Results are the mean of three independent experiments, ± standard error of the mean (SEM = standard deviation/√number of experiments or replicates). Results of the statistical analysis are not shown here (please see Figure 3.11A).

**3.11A and 3.11B** The cytotoxicity (A) and genotoxicity (B) induced by P601 and P703 NPs after 24 hours of exposure on Balb3T3 cells evaluated by CFE and CBMN assays. Results are the mean of three independent experiments, ± standard error of the mean (SEM = standard deviation/√number of experiments or replicates). The statistical significance of CFE and CBMN data was evaluated using one-way ANOVA and Fisher's exact test, respectively (***$p<0.001$).

**3.12A and 3.12B** The comparison between cytotoxicity induced by P601 (A, light blue histograms), P703 (B, dark blue histograms) NPs and $Co^{2+}$ (A and B, yellow histograms) in Balb3T3 cells after 24 hours of exposure, evaluated using the CFE assay. Results are the mean of three independent experiments, ± standard error of the mean (SEM = standard deviation/√number of experiments or replicates). The CFE values for $Co^{2+}$

treatments of 24 hours were extrapolated from a previous study (Ponti et al., 2009). The concentrations shown relate to the expected µM concentrations of NPs in total fraction samples, considering 119 and 98 mM as the concentration of the stock suspensions of P601 and P703, respectively; please see Tables B.6 & B.7 for the respective $Co^{2+}$ concentrations detected in Balb3T3 complete culture medium after 24 hours of incubation for both P601 and P703 NPs.
Statistical analysis was done using the t-test (http://www.graphpad.com/quickcalcs/ttest1.cfm) and significant differences were found when comparing P601 or P703 data to those of $Co^{2+}$ (*$p<0.05$; **$p<0.01$).

**3.13** The cytotoxicity of NM-300 NPs on Balb3T3 cells after 72 hours of exposure, assessed using CFE; the NP concentration is expressed as µM. Results are the mean of three independent experiments, ± standard error of the mean (SEM = standard deviation/√number of experiments or replicates). Statistical significance was evaluated using one-way ANOVA (*$p<0.05$; **$p<0.01$).

**3.14** The cytotoxicity of Ag 44 NPs on Balb3T3 cells after 72 hours of exposure, assessed using CFE; the NP concentration is expressed as µM. Results are the mean of three independent experiments, ± standard error of the mean (SEM = standard deviation/√number of experiments or replicates). Statistical significance was evaluated using one-way ANOVA (**$p<0.01$).

**3.15** The cytotoxicity of Ag 84 NPs on Balb3T3 cells after 72 hours of exposure, assessed using CFE; the NP concentration is expressed as µM. Results are the mean of three independent experiments, ± standard error of the mean (SEM = standard deviation/√number of experiments or replicates). Statistical significance was evaluated using one-way ANOVA (**$p<0.01$).

**3.16** The cytotoxicity of Ag 100 NPs on Balb3T3 cells after 72 hours of exposure, assessed using CFE; the NP concentration is expressed as µM. Results are the mean of three independent experiments, ± standard error of the mean (SEM = standard deviation/√number of experiments or replicates). Statistical significance was evaluated using one-way ANOVA (**$p<0.01$).

**3.17A and 3.17B** The cytotoxicity of Ag NPs on Balb3T3 cells after 72 hours of incubation, assessed using CFE and expressed as a function of the NP concentration in either µM (A) or the number of NPs/mL (No. NPs/mL) (B). Results are the mean of three independent experiments, ± standard error of the mean (SEM = standard deviation/√number of experiments or replicates).

**3.18A and 3.18B** The cytotoxicity and cell transformation induced by Ag NPs in Balb3T3 cells after 72 hours of exposure as evaluated with concurrent CFE and CTA assays. Due to the absence of type III foci, the transformation frequency (x $10^{-4}$) was zero for Ag 100 nm at 2.5 and 5 µM, and zero for

| | |
|---|---|
| | Ag 44 nm at 5 µM. The results are the mean of three independent experiments, ± standard error of the mean (SEM = standard deviation/√number of experiments or replicates). Statistical significance was evaluated using one-way ANOVA and Fisher's exact test for CFE and CTA results, respectively (***p<0.001). |
| **3.19** | The cytotoxicity of Ag NPs on Balb3T3 cells after 24 hours of exposure, assessed using CFE. Results of the statistical analyses are shown in Figure 3.20A. Results are the mean of three independent experiments, ± standard error of the mean (SEM = standard deviation/√number of experiments or replicates). |
| **3.20A and 3.20B** | The cytotoxicity of Ag NPs in Balb3T3 cells after 24 hours of exposure, assessed using CFE (A), and genotoxicity of Ag NPs in Balb3T3 cells after 24 hours of exposure (B), assessed using the CBMN assay. Results are the mean of three independent experiments, ± standard error of the mean (SEM = standard deviation/√number of experiments or replicates). Statistical significance was evaluated by one-way ANOVA (*p<0.05; ***p<0.001) and Fisher's exact test for CFE and CBMN assay data, respectively. |
| **B.1A and B.1B** | DLS correlograms of basal media HAM and MEM, used to dilute $CoFe_2O_4$ P601 and P703 NPs for DLS sample analysis. The correlation coefficient is expressed as a function of time (µs). The Y intercepts at time 0 were lower than 0.1 and no correlogram had a sigmoid shape. These observations indicated that no nano-sized objects were detected in these samples using DLS and thus suggested they were particle-free. |
| **B.2A and B.2B** | DLS correlograms of basal media DMEM and NPs dispersant DEG, used to dilute $CoFe_2O_4$ P601 and P703 NPs for DLS sample analysis. The correlation coefficient is expressed as a function of time (µs). The Y intercepts at time 0 were lower than 0.1 and no correlogram had a sigmoid shape. These observations indicated that no nano-sized objects were detected in these samples using DLS and thus suggested they were particle-free. |
| **B.3** | DLS correlograms of ultrapure water, used to dilute $CoFe_2O_4$ P601 and P703 NPs for DLS sample analysis. The correlation coefficient is expressed in function of time (µs). The Y intercept at time 0 was lower than 0.1 and the correlogram did not show a sigmoid shape. These observations indicated that no nano-sized objects were detected in these samples using DLS and thus suggested they were particle-free. |
| **B.4A and B.4B** | DLS correlograms of A549 and Balb3T3 complete culture media. The curves showed a sigmoid shape and Y intercepts at time 0 had values close to 1. Correlograms of this type are usually associated with samples that contain nano-sized objects. |
| **B.5A and** | DLS correlograms of CaCo2 and HaCaT complete culture media. The |

**B.5B** curves showed a sigmoid shape and Y intercepts at time 0 had values close to 1. Correlograms of this type are usually associated with samples that contain nano-sized objects.

**B.6A and B.6B** DLS correlograms of HepG2 and MDCK complete culture media. The curves showed a sigmoid shape and Y intercepts at time 0 had values close to 1. Correlograms of this type are usually associated with samples that contain nano-sized objects.

**B.7** DLS size distribution average of six measurements by intensity (upper graph) and volume (lower graph) of complete culture medium employed for A549 cells. In both graphs, the percentage values (% Intensity and % Volume) are shown as a function of the nanometer size.

**B.8** DLS size distribution average of six measurements by intensity (upper graph) and volume (lower graph) of complete culture medium employed for Balb3T3 cells. In both graphs, the percentage values (% Intensity and % Volume) are shown as a function of the nanometer size.

**B.9** DLS size distribution average of six measurements by intensity (upper graph) and volume (lower graph) of complete culture medium employed for CaCo2 cells. In both graphs, the percentage values (% Intensity and % Volume) are shown as a function of the nanometer size.

**B.10** DLS size distribution average of six measurements by intensity (upper graph) and volume (lower graph) of complete culture medium employed for HaCaT cells. In both graphs, the percentage values (% Intensity and % Volume) are shown as a function of the nanometer size.

**B.11** DLS size distribution average of six measurements by intensity (upper graph) and volume (lower graph) of complete culture medium employed for HepG2 cells. In both graphs, the percentage values (% Intensity and % Volume) are shown as a function of the nanometer size.

**B.12** DLS size distribution average of six measurements by intensity (upper graph) and volume (lower graph) of complete culture medium employed for MDCK cells. In both graphs, the percentage values (% Intensity and % Volume) are shown as a function of the nanometer size.

**B.13A and B.13B** DLS measurements of P601 and P703 NPs dilutions in dialyzed DEG (2% v/v), ultrapure water, basal media and complete culture media (100 µM expected test concentration) after 72 hours of incubation in standard culture conditions (37°C, 5% $CO_2$, 90% humidity). The standard deviation (SD) is shown. Both $CoFe_2O_4$ NPs increase in size in the basal media environment (>1.5 µm); neither of the P601 and P703 preparations in dialyzed DEG and in ultrapure water increased in size. The PdI values for 2% v/v of P601 in dialyzed DEG and ultrapure water were 0.16 ± 0.02 and 0.23 ± 0.06, respectively. The PdI values for all other P601 preparations were ≥0.3. The PdI values for P703 preparations showed behaviour similar to that of P601 and corresponded to 0.180 ± 0.05 in both dialyzed DEG and ultrapure water.

**B.14A and B.14B** DLS measurements of $CoFe_2O_4$ P601 and P703 NP (100 µM) dilutions in basal medium MEM and Balb3T3 complete culture medium after 0, 24 and 72 hours of incubation, under standard culture conditions (37°C, 5% $CO_2$, 90% humidity). The standard deviation (SD) is shown. Both P601 and P703 NPs tended to form aggregates/agglomerates that were larger in medium without serum than those in the completed medium at all incubation time points studied. The PdI values for P601 were consistently >0.3; the PdI ranged between 0.361 ± 0.03 and 0.399 ± 0.04, and 0.468 ± 0.01 and 0.587 ± 0.04 for samples in MEM and Balb3T3 complete medium, respectively. In contrast, the PdI values for P703 ranged between 0.289 ± 0.03 and 0.390 ± 0.10, and 0.378 ± 0.05 and 0.500 ± 0.02 for MEM and Balb3T3 complete medium, respectively.

**B.15A and B.15B** Some of the 144 cycles of the UV-Vis measurements in a $CoFe_2O_4$ P601 sample (60 µM) in complete culture medium without Phenol Red at fixed height (upper cuvette region) made every 30 minutes over 72 hours (A), and normalized absorption of the same sample at 500 nm (upper cuvette region) (B).

**B.16A and B.16B** Normalized absorption of a sample of $CoFe_2O_4$ P601 (A) and P703 (B) at a concentration of 60 µM in complete culture medium at fixed height (bottom cuvette region) in complete culture medium without Phenol Red at 500 nm.

**B.17A, B.17B, B.17C and B.17D** Figures B.17A, B.17B, B.17C and B.17D: Mean NP diameter (nm) of all Ag NPs investigated in this study. DLS measurements were done for Ag NP dilution in ultrapure water, Phosphate Buffer Saline (PBS), MEM basal medium and Balb3T3 complete culture medium (100 µM for all Ag NPs investigated) at time 0 and after 24 and 72 hours of incubation (for preparations in Balb3T3 complete culture medium) under standard culture conditions (37°C, 90% humidity, 5% CO2). The standard deviation (SD) was used to assess variability in the measurements.

**B.18A, B.18B, B.18C and B.18D** Scanning Electron Microscope images of 100 µM samples of Ag NM-300 (A), Ag 44 nm (B), Ag 84 nm (C) and Ag 100 nm (D) prepared in ultrapure water. No aggregates/agglomerates of relevance were found in these preparations.

## Glossary

| | |
|---|---|
| **AFM** | Atomic Force Microscopy |
| **Ag** | Silver |
| **A549** | Human Lung Carcinoma cells |
| **APTS** | 3-aminopropyltriethoxysilane |
| **Balb3T3** | Immortalized Mouse fibroblasts |
| **Bhas 42** | Balb3T3 cells v-Ha-ras-transfected |
| **BHK21** | Baby hamster kidney cells |
| **BN** | Binucleated cells |
| **BSI** | British Standards Institution |
| **CaCo2** | Human Caucasian Colon adenocarcinoma cells |
| **CBMN** | Cytokinesis-block Micronucleus assay |
| **CFE** | Colony Forming Efficiency |
| **C3H/10T½** | Mouse fibroblasts aneuploid established cell line |
| **CNTs** | Carbon nanotubes |
| **Co** | Cobalt |
| **$CoFe_2O_4$** | Cobalt ferrite |
| **CPPs** | Cell penetrating peptides |
| **CTA** | Cell Transformation Assay |
| **DEG** | Diethylene glycol |
| **DLS** | Dynamic Light Scattering |
| **DMEM** | Dulbecco's Modified Eagle Medium |
| **DMEM/F12** | Dulbecco's modified Eagle's medium/F12 |
| **DMSO** | Dimethyl sulphoxide |
| **EC** | European Commission |
| **ECVAM** | European Centre for the Validation of Alternative Methods |
| **Fe** | Iron |
| **HaCaT** | Immortalized Human keratinocyte cells |
| **HAM** | HAM F-12 with GlutaMAX-I |
| **HepG2** | Human hepatoma cells |
| **IARC** | Agenzia Internazionale per la Ricerca sul Cancro |
| **ICP-MS** | Inductively-Coupled Mass Spectrometry |

| | |
|---|---|
| **IHCP** | Institute for Health and Consumer Protection |
| **JB6** | Pre-neoplastic mouse epidermal cells |
| **JRC** | Joint Research Centre |
| **MCA** | 3-methylcholanthrene |
| **MDCK** | Madin Darby Canine Kidney cells |
| **MEM** | Minimum Essential Medium with Earle's salts and L-glutamine |
| **MMC** | Mitomycin C |
| **MN** | Mononucleated cells |
| **MR** | Magnetic Resonance |
| **MTS** | 3-(4,5-dimethylthiazol-2-yl)-5-(3-carboxymethoxyphenyl)-2-(4-sulfophenyl)-2H-tetrazolium |
| **MTT** | 3-(4,5-Dimethylthiazol-2-yl)-2,5-diphenyltetrazolium bromide |
| **NBS** | NanoBiosciences Unit |
| **NBUDs** | Nuclear buds |
| **NDI** | Nuclear Division Index |
| **Ni** | Nickel |
| **NMs** | Nanomaterials |
| **NOs** | Nano-objects |
| **NPBs** | Nucleoplasmic bridges |
| **NPs** | Nanoparticles |
| **NR** | Neutral Red |
| **OECD** | Organization for Economic Co-operation and Development |
| **PBS** | Phosphate Buffer Saline (1X) solution |
| **PdI** | Polydispersity Index |
| **PN** | Polynucleated cells |
| **REACH** | Registration Evaluation and Authorization of Chemicals |
| **RES** | Reticulo-endothelial system |
| **ROS** | Reactive oxygen species |
| **SCENIHR** | Scientific Committee on Emerging and Newly Identified Health Risks |
| **SD** | Standard deviation |
| **SEM** | Standard error of the mean |
| **SHE** | Syrian Hamster Embryo cells |
| **swCNTs** | Single wall carbon nanotubes |

| | |
|---|---|
| **TEM** | Transmission Electron Microscopy |
| **UV-Vis** | UltraViolet-Visible spectroscopy |
| **VMT** | Validation Management Team |
| **w/o** | Without |
| **WST** | Water soluble salts |
| **XPS** | X-ray Photoelectron Spectroscopy |
| **XRD** | Powder X-Ray Diffractometry |
| **XTT** | 2,3-bis-(2-methoxy-4-nitro-5-sulfophenyl)-2H-tetrazolium-5-carboxanilide |
| **Z-potential** | Zeta potential |

## Publications by the candidate

Ceriotti L., Ponti J., Broggi F., Kob A., Drechsler S., Thedinga E., Colpo P., Sabbioni E., Ehret R., Rossi F., 2007, "Real-time assessment of cytotoxicity by impedance measurement on a 96-well plate", Sensors and Actuators B, 123, 769-778;

Sirghi L., Ponti J., Broggi F., Rossi F., 2008, "Probing elasticity and adhesion of live cells by atomic force microscopy indentation", European BioPhysics Journal, 37, 6, 935-945;

Ponti J., Sabbioni E., Munaro B., Broggi F., Marmorato P., Franchini F., Colognato R., Rossi F., 2009, "Genotoxicity and morphological transformation induced by cobalt nanoparticles and cobalt chloride: an *in vitro* study in Balb/3T3 mouse fibroblasts", Mutagenesis, 1-7;

Ponti J., Colognato R., Rauscher H., Gioria S., Broggi F., Franchini F., Pascual C., Giudetti G., Rossi F., 2010, "Colony Forming Efficiency and microscopy analysis of multi-wall carbon nanotubes cell interaction", Toxicology Letters, 197, 29-37;

Comes Franchini M., Ponti J., Lemor R., Fournelle M., Broggi F., Locatelli E., 2010, "Polymeric entrapped thiol-coated gold nanorods: cytotoxicity and suitability as molecular optoacustic contrast agent", Journal of Materials Chemistry, 20, 10908-10914;

Rauscher H., Broggi F., Mariani V., Ponti J., Rossi F., 2010, "Sedimentation of nanoparticles in *in vitro* assays", European Cells and Materials, Vol. 20, Suppl. 3, 210;

Mariani V., Ponti J., Giudetti G., Broggi F., Marmorato P., Gioria S., Franchini F., Rauscher H. and Rossi F., 2011, "Online monitoring of cell metabolism to assess the toxicity of nanoparticles: the case of cobalt ferrite", Nanotoxicology;

Uboldi C., Giudetti G., Broggi F., Gilliland D., Ponti J., Rossi F., 2011, "Amorphous silica nanoparticles do not induce cytotoxicity, cell transformation nor genotoxicity in Balb/3T3 mouse fibroblasts", accepted for publication as Special Issue of Mutation Research - Genetic Toxicology and Environmental Mutagenesis on nanogenotoxicology;

Ponti J., Broggi F., Mariani V., De Marzi L., Colognato R., Marmorato P., Gioria S., Gilliland D., Pascual Garcia C., Meschini S., Stringaro A., Molinari A., Rauscher H., Rossi F., 2012, "Morphological transformation induced by multiwall carbon nanotubes on Balb/3T3 cell model as an *in vitro* end point of carcinogenic potential", Nanotoxicology;

Locatelli E., Broggi F., Ponti J., Marmorato P., Franchini F., Lena S. and Comes Franchini M., 2012, "Lipophilic Silver Nanoparticles and Their Polymeric Entrapment into Targeted-PEG-based micelles for the treatment of Glioblastoma", Communication on Advanced Healthcare Materials;

## Objectives

The main objective of this Ph.D. research project was to study and understand the *in vitro* toxicological effects induced by specific nanoparticles (NPs) of industrial and biomedical interest.

Nanoparticles of both cobalt ferrites ($CoFe_2O_4$ NPs) and silver (Ag NPs) were selected for an *in vitro* study using the Balb3T3 cell model. The model employs mouse fibroblasts; their A-31-1-1 clone enables a single cell type to be screened for different endpoints, such as cytotoxicity, cell transformation capacity and genotoxicity.

Indeed, the A-31-1-1 clone is suitable for the Colony Forming Efficiency (CFE) assay, the Cell Transformation Assay (CTA) and the Cytokinesis-Block Micronucleus assay (CBMN), which detect cytotoxicity as inhibition of colony growth, the cell transformation capacity as induction of type III foci formation, and DNA damage as induction of micronuclei, respectively. The CFE and CTA are pre-validated assays, whilst the CBMN has been the object of retrospective validation by the Validation Management Team (VMT) of the European Centre for the Validation of Alternative Methods (ECVAM). These assays appear to be suitable for NP *in vitro* testing, since their endpoints can be achieved without using any dye that can potentially interact with NPs, thereby invalidating the results. These methods have all been recommended by the Registration Evaluation and Authorization of Chemicals (REACH) legislation and the Organization for Economic Cooperation and Development (OECD, Working Party on Manufactured Nanomaterials, WPMN) as promising assays for studying the toxicological profile of nanomaterials.

The different sizes or synthesis of NPs and different testing methods and cell lines were also compared, where possible, to elucidate test limitations and the influence of NP physicochemical characteristics (e.g., size or synthesis) and cell type on experimental outcomes. Thus, two and four sizes of $CoFe_2O_4$ NPs and Ag NPs, respectively, were studied here. The cytotoxicity induced by $CoFe_2O_4$ NPs on other mammalian cell lines that model different exposure routes was also investigated using Neutral Red uptake (NR) and CFE tests in parallel. The six specific cell lines tested were the: (i) A549 human lung carcinoma cells, (ii) Balb3T3 mouse fibroblasts, (iii) CaCo2 human Caucasian colon

adenocarcinoma cells, (iv) HaCaT human keratinocytes, (v) HepG2 human hepatoma cells, and (vi) MDCK Madin Darby Canine Kidney cells.

In addition, extensive physicochemical characterization of the NPs was performed to clarify and complete the toxicological results.

In summary, the Ph.D. study focused on the following three main objectives:

(i) Assessment of cytotoxicity induced by two sizes of $CoFe_2O_4$ NPs on six different mammalian cell lines using CFE and NR

(ii) Assessment of cytotoxicity, cell transformation capacity and genotoxicity induced by two sizes of $CoFe_2O_4$ NPs on the Balb3T3 model using the CFE, CTA and CBMN assays

(iii) Assessment of cytotoxicity, cell transformation capacity and genotoxicity induced by four Ag NPs on the Balb3T3 model using the CFE, CTA and CBMN assays.

# Chapter 1: Introduction

## 1.1 Location and goal of the research

The experimental work described in this PhD thesis was carried out in the NanoBiosciences Unit (NBS) at the Institute for Health and Consumer Protection (IHCP) of the European Commission's (EC) Joint Research Centre (JRC) located in Ispra (Varese, Italy). The work was conducted during the period 2008-2011.

The NBS is involved in nanotechnology research, focusing both on the production of nanomaterials (NMs) (nanoparticles and nanosurfaces) and the evaluation of their potential *in vitro* toxicity using *in vitro* cell models as alternatives to animal models (Russell et al., 1959).

For this thesis, a series of established standard *in vitro* tests that have been proposed by the Registration Evaluation and Authorization of Chemicals (REACH) legislation or recognized in the Organization for Economic Co-operation and Development (OECD) guidelines for the study of the toxicological profiles of chemicals were used to investigate the cytotoxicity of NPs. In addition, the Neutral Red uptake (NR) and Colony Forming Efficiency (CFE) assays were chosen to assess the cytotoxicity induced by NMs, whilst their cell transformation capacity and genotoxic potential were investigated using the Cell Transformation Assay (CTA) and Cytokinesis-Block Micronucleus test (CBMN), respectively.

The primary reason for studying the potential toxicity of NMs is that their use is becoming increasingly widespread and consequently there is a growing risk of unintentional exposure to humans and the environment (Aitken et al., 2006; Dunphy Guzmán et al., 2006). The special, often unique, properties of certain nanoscale materials make them highly attractive in many different areas of application, including consumer products (e.g., computers chips, cosmetics, sunscreens, food packaging, and for drug delivery or targeted treatment of tumours in medicine (http://www.nanotechproject.org/inventories/consumer/, last accessed in February 2011). Occupational exposure to NMs can occur during the production processes by inhalation, ingestion or skin contact, whilst the increasing volume of consumer products containing

NMs means that there is greater exposure potential directly related to the general public (Aitken et al., 2006).

Although the potential benefits arising from the use of nanoproducts and nanodevices are well documented, much less information is available on their potential toxic effects on human and environmental health (Aitken et al., 2006). Whilst the volume of relevant scientific data is increasing gradually, it is still insufficient to perform adequate risk assessments. In addition, despite evidence that some NMs may be toxic, legislation regulating the safe production and use of such NMs is still incomplete (Oberdörster et al., 2005).

In order to address concerns about the potentially harmful effects of NMs on public and environmental health whilst promoting the secure development of nanotechnology, the EC has established actions that support the scientific research related to the risk assessment of NMs. These actions are documented in the 7$^{th}$ Framework Programme (2007-2013) and include several nanotoxicology research projects that have been undertaken (http://cordis.europa.eu/projects/index.cfm?fuseaction=app.search&TXT=nanomaterials&FRM=1&STP=10&SIC=SICNNT&PGA=FP7-NMP&CCY=&PCY=&SRC=&LNG=en&REF=, last accessed in February 2012). These aim to provide technical input for the advancement of legislation for the safe and responsible development of nanotechnology (http://cordis.europa.eu/nanotechnology/actionplan.htm, last accessed in October 2010).

## 1.2 Nanotechnology and NMs

The term "nanotechnology" was coined in 1974 in Japan by Norio Taniguchi, a researcher at the University of Tokyo (Singh et al., 2008). Nanotechnology involves the design, production and characterization of materials with at least one dimension in the nanoscale ($10^{-9}$m) (**Figure 1.1**).

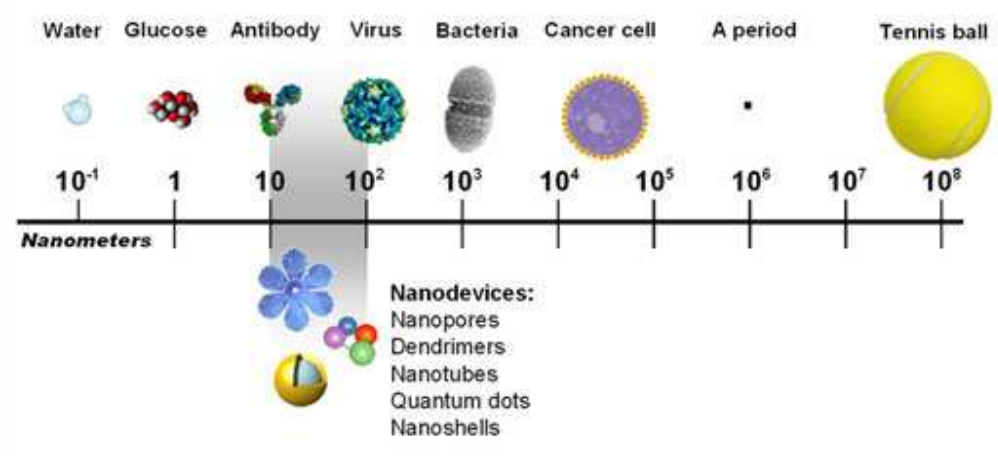


**Figure 1.1: Nanotechnology products are 100–10000-fold smaller than a human cell (image taken from the National Cancer Institute website, http://nano.cancer.gov/learn/understanding/, last accessed in September 2011).**

Although there have been various definitions of a NM, the term "nano" is now generally accepted to refer to dimensions ≤100 nm. In a recent review on environmental risk assessment studies for NMs (Stone et al., 2009), the specific definitions for nanomaterial (NM), nanoobject (NO) and nanoparticles (NPs) according to the British Standards Institution (BSI) and the Scientific Committee on Emerging and Newly Identified Health Risks (SCENIHR) were discussed. More specifically, a general NM has just one dimension of ≤100 nm (e.g., carbon nanotubes and nano-structured surfaces), whilst NOs and NPs have two and three dimensions of ≤100 nm, respectively (Stone et al., 2009).

It is now well known that matter reaching such small sizes can change its physicochemical properties and behave completely differently than the corresponding bulk material (Lu et al., 2009; Wijnhoven et al., 2009). This change in physicochemical properties can be explained primarily by the increase in the relative surface area (surface area per mass unit) and associated quantum effects (Buzea et al., 2007). Indeed, any increase in relative surface area corresponds to an increase in chemical reactivity, resistance to mechanical stress and electrical properties, making some NMs useful catalysts (Stone et al., 2010). Moreover, the quantum effects become so relevant at the nanometre level that they can influence and change the optical, magnetic and electrical properties of matter (Aitken et al., 2006).

The size-dependant properties of some compounds have been exploited unwittingly for years, for example, the use of gold and silver NPs as pigments in glass and ceramic staining since the $10^{th}$ century B.C. (Min'ko et al., 2008).

Nanomaterials can be classified into different groups according to their dimensions, phase composition or manufacturing processes. They can be classified into two main groups based on their origin, i.e., incidental NMs and engineered NMs (Oberdörster et al., 2005) (**Figure 1.2**). In fact, NMs present in the environment can have different origins (Borm et al., 2006). Typically, incidental NMs (e.g., diesel exhaust particles) are the result of unintended anthropogenic sources (e.g., combustion derived) or are produced by natural processes (e.g., volcanic activity, forest fires, sea spray and erosion processes) (Oberdörster et al., 2005) (see Figure 1.2).

The human race has been exposed to incidental NMs throughout its evolutionary history. The discovery of fire meant that a million more NMs could be inhaled when starting a fire to cook food (The Royal Society and The Royal Academy of Engineering, 2004). Unsurprisingly, therefore, the human race is now surrounded by NMs; a typical room has been estimated to contain 1–2 x $10^4$ NPs per $cm^3$, whilst 5 x $10^4$ NPs per $cm^3$ and $10^5$ NPs per $cm^3$ can be found in woodland areas and urban streets, respectively (http://copublications.greenfacts.org/en/nanotechnologies/l-3/7-exposure-nanoparticles.htm#2p0, last accessed in February 2012).

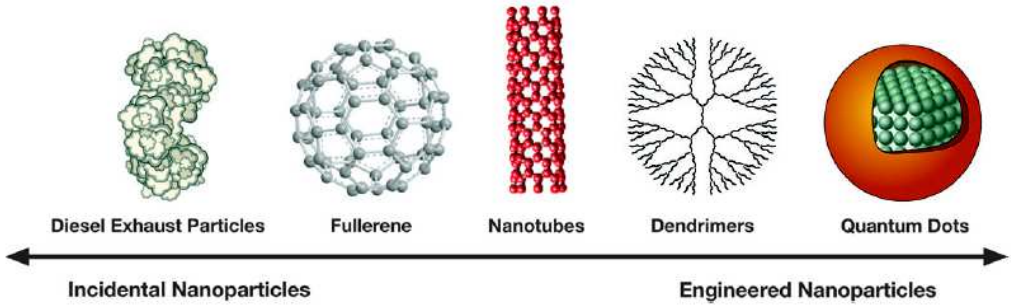


**Figure 1.2: Examples of incidental and engineered NPs. Diesel exhaust particles are defined as particles either from unintended anthropogenic sources or of natural origin. Some particles, such as fullerenes and carbon nanotubes, are considered to be both engineered materials and incidental components of pollution, while dendrimers and quantum dots are considered to be manufactured NMs (Image from Stern & McNeil, 2008).**

Many examples of nanostructures can also be found in Nature, both in plants and animals. The Lotus leaf, for example, is naturally water-repellent due to cone-shaped nano-crystals of hydrophobic wax that are distributed on its upper surface; these structures are so small that drops of water cannot spread and flow away, leading to a phenomenon known as the "Lotus effect" (**Figure 1.3**). Another well-known example of a nanostructure in Nature is the nanofilaments found on the feet of Gecko lizards (**Figure 1.4**); these act like Velcro and allow this reptile to climb smooth surfaces (Buzea et al., 2007).

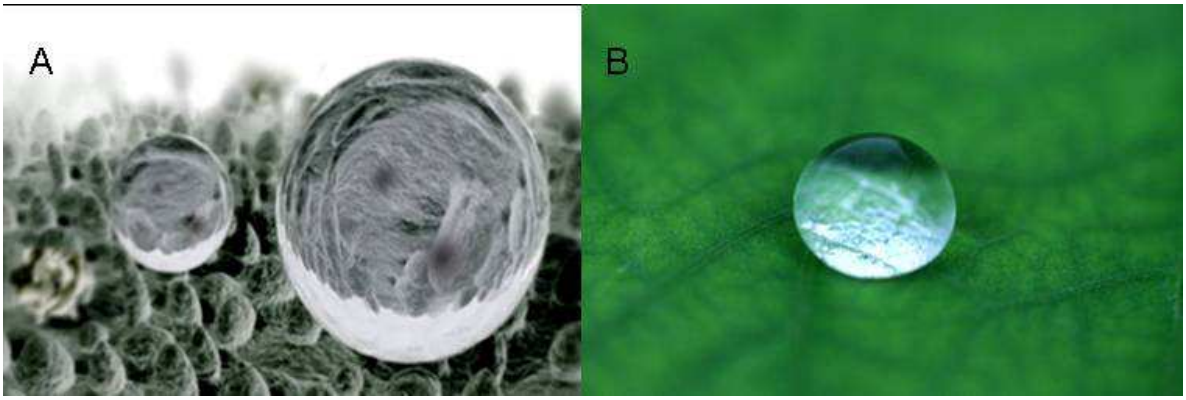


**Figure 1.3: Nanostructures in Nature. (A) Nano-crystals of hydrophobic wax on a Lotus leaf and drops of water; (B) the "Lotus effect" where water floats on a Lotus leaf (Google images, last accessed in September 2011).**

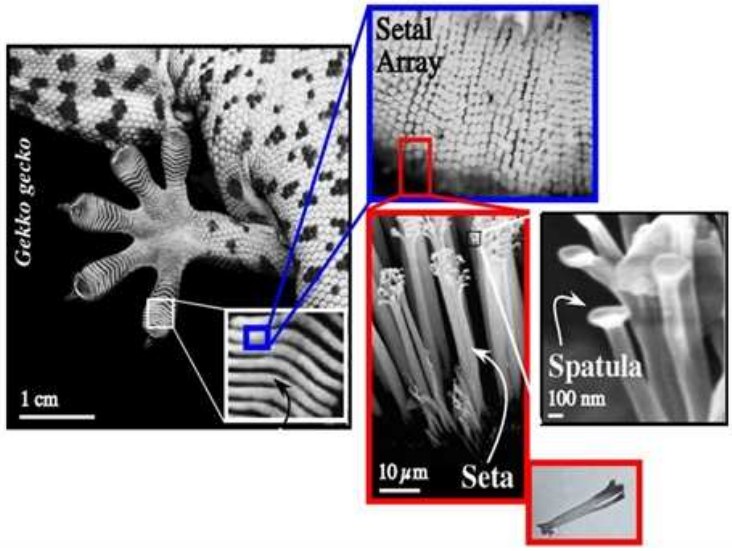


**Figure 1.4: Nanofilaments on the feet of Gecko lizards (http://www.cchem.berkeley.edu/rmgrp/about.html, last accessed in September 2011).**

In contrast, particles specifically produced to exploit the special properties gained at the nanoscale (e.g., high reactivity, optical properties) are examples of engineered NMs. Many products available on the market, for example sunscreens, actually claim to contain a component engineered by nanotechnology (http://www.nanotechproject.org/inventories/consumer/, last accessed in February 2011). Moreover, some particles can be considered to be both engineered materials and incidental components of pollution (e.g., fullerenes and carbon nanotubes).

## 1.3 The potential risk of NMs for human health

Since nanotechnology products have many areas of application, the potential benefits and financial profits are immense. For example, the National Science Foundation has estimated that 2 million people will be employed in the field of nanotechnology by 2015 (http://www.cdc.gov/niosh/nas/RDRP/appendices/chapter7/a7-2.pdf, last accessed in September 2011), and 800 consumer products that claim to contain NMs are already on the market (Singh et al., 2009).

Many different organizations are involved in nanotechnology research, including companies (pharmaceutical, high technology and cosmetic), universities and research

centres. Consequently, estimating the number of people potentially exposed to NMs is very difficult (Aitken et al., 2004). Nevertheless, the potential risks of NMs on human health and the environment must be considered. Potential occupational and public NM exposure occurs via different exposure routes, including inhalation, oral ingestion and dermal absorption and by injection (Bergamaschi et al., 2006).

The toxicity of NMs may be determined or influenced by their physicochemical characteristics, such as size, surface charge, presence or absence of coatings and ability to release ions (Elder et al., 2009). Indeed, evidence suggests that all these characteristics can contribute to the mechanism by which NMs may interfere in or disrupt biological activities (Aillon et al., 2009). Even if NMs originate from the same element, all have unique and diverse physicochemical properties associated with their small size (Oberdorster et al., 2005) that can result in different toxicological profiles (Bergamaschi et al., 2006).

Since the dimensions of NMs are in the same range as many cellular components (Buzea et al., 2007) and NMs can interact with biological molecules, such as proteins (Lynch et al., 2008), it is thought that they may be able to avoid natural defences in humans and other species and damage cells. To endanger humans and other organisms, however, NMs must come into contact with and enter the body, and subsequently participate in cellular reactions to induce damage (Buzea et al., 2007; Singh et al., 2009). Notably, however, the different potential access points of the body for NMs do have efficient defence mechanisms (http://ec.europa.eu/health/scientific_committees/opinions_layman/nanomaterials/en/l-3/4.htm, last accessed in February 2012), such as the production of mucus and presence of cilia in the tracheal epithelium and lung macrophages of the inhalation route (The Royal Society and The Royal Academy of Engineering, 2004; Kreyling et al., 2006).

Scientific and political committees have arranged global conferences and workshops in order to share current knowledge on the toxicology of NMs and to agree common guidelines for the study of NMs (OECD, 2008). The EC's suggestions for a safe and responsible strategy to reinforce the European Union's leading position in the Research and Development of nanotechnology have been reported in a communication that combines the "Towards a European Strategy for Nanotechnology" and "European Action

Plan for Nanosciences and Nanotechnologies" reports (http://cordis.europa.eu/nanotechnology/actionplan.htm, last accessed in February 2011). This communication specifically advocates an increase in nanotoxicology research using proper methods, as well as *in vitro* systems that can reduce, refine and replace animal testing (Hartung et al., 2004) to elucidate the mechanism of action of NMs.

Based on these recommendations, the Joint Research Centre of the European Commission (DG-JRC) has developed a research plan for NM toxicology based on an integrated approach that combines cell-based *in vitro* assays with specific radiochemical and physicochemical techniques (Ponti, 2008). This experimental approach was used in this Ph.D. thesis to study specific NMs, selected according to their importance in industrial applications, and to determine their physicochemical characterization and toxicological profiles using *in vitro* systems that model human exposure (i.e., lung, liver, kidney, skin, gut and blood).

### 1.4 NMs: production and physicochemical characterization

Specifically synthesized NMs are classified as engineered NMs (Buzea et al., 2007). Metals, semiconductors, glass, ceramics and polymers theoretically can all be synthesized in the nanoscale dimension. Depending on the manufacturing process used, examples of engineered NMs that can be synthesized range from the more simple inorganic (metal oxides, semiconductors, alloys) or organic (polymers, dendrimers, composites) particles, to the crystalline or amorphous particles that are produced as powders or dispersed in a matrix, over colloids, suspensions and emulsions, nanolayers and films, and the more complex class of fullerenes and their derivatives (Rao et al., 2007).

Rao et al. have described different synthesis techniques that have been developed to produce engineered NMs with specific characteristics (e.g., size, surface charge, coatings) (Rao et al., 2004). More recent attention has focused on the development of environmentally friendly synthesis protocols; some examples for those of Ag NPs have been reported (Begum et al., 2009; Roy et al., 2010).

The physicochemical characterization of NMs is necessary to understand and control the synthesis and applications of NMs (Warheit, 2008). Moreover, correct physicochemical characterization of NMs is crucial in identifying variables that can affect the

biocompatibility of these materials (Powers et al., 2006; Maynard et al., 2007; Stern & McNeil, 2008). Current NM research is focused on understanding the mechanism of toxicity of NMs, their interaction with biomolecules or cells and the contribution of particle size with respect to particle composition in NM toxicity (Aillon et al., 2009). For example, the different forms of asbestos demonstrate the importance of the physicochemical properties of NMs as determinants of their respective toxicological potentials (Ponti et al., 2011). The surface area and effects of quantum chemistry are one of many characteristics that specifically affect the way in which biological systems function and interact with the physical world (Sweet & Strohm, 2006).

In nanotoxicology, it is important to characterize NMs thoroughly from the time of synthesis onwards (Fubini et al., 2010). Indeed, NM preparations can be contaminated and thus lead to toxic effects that can overlap with the effects of the NMs *per se*. Not only can the shape of NMs influence their biocompatibility (Huang et al., 2011), but the interactions of NMs with a biological environment (e.g., culture media and biological fluids) are also important to study. The dissolution of NMs can cause free ions production that can subsequently induce toxicity (Mazzotti et al., 2002; Fubini et al., 2010).

Compared to chemical toxicants, the quantitative and qualitative characterization of NMs for toxicological analysis is very complex (Powers et al., 2006). For example, it is important to ascertain exactly the actual dose or concentration of NMs tested, particularly as accurate pipetting of NM suspensions is difficult due to the solid status of NMs (Ponti et al., 2010). If such considerations are disregarded, the potential toxicity of a specific NM may be correlated with the wrong concentration of the NM.

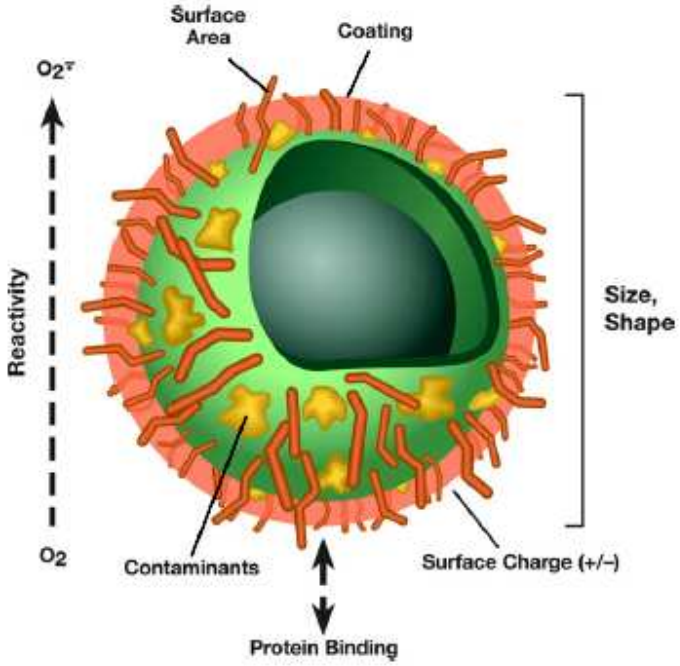


**Figure 1.5: Schematic representation of physicochemical properties of NMs. The main physicochemical properties of NMs that may influence their biocompatibility (including their size, shape, surface area, surface charge, coating, presence of contaminants and reactivity) and that should be considered when assessing their hazard risks (Stern & McNeil, 2008).**

Different techniques, therefore, should be used to obtain information on size distribution, surface charge, morphology and chemical composition of NMs, all of which are important characteristics to be considered when studying the toxicology of NMs (**Figure 1.5**) (Bouwmeester et al., 2011) because the properties that make these NM materials invaluable in industrial and biomedical applications can also cause safety concerns (Jiang et al., 2009; Clark et al., 2011).

The physicochemical characterization of NMs can be achieved using several techniques based primarily on material science. For example, the Scanning Electron Microscopy (SEM), Transmission Electron Microscopy (TEM), Atomic Force Microscopy (AFM), X-ray Photoelectron Spectroscopy (XPS), and powder X-Ray Diffractometry (XRD) techniques can be used to investigate the morphology, size, shape and structure of NMs. These techniques, together with that of Dynamic Light Scattering (DLS), which measures hydrodynamic size distribution and the Z-potential, are the gold standards for the

evaluation of particle size distribution and shape in toxicity screening studies (Powers et al., 2006; Drobne, 2007).

### 1.5 NMs: biological effects

Between 2003 and 2008, the publication of scientific papers related to NMs and their potential toxicity increased by over 1100% (Card et al., 2010). Until recently, however, it has not been possible to identify a single physicochemical characteristic that could explain the toxicological effect of NMs and their interaction with biological systems (Bouwmeester et al., 2011).

Clearly, the toxicological assessment of one type and source of NM is insufficient when evaluating the toxicity induced by a similar NM that may differ only, for example, in its production process (Drobne et al., 2007; Bouwmeester et al., 2011). For example, the coatings or other surface modifications on engineered NMs that are usually used to produce mono-dispersed suspensions may influence their toxicological effect whilst also enhancing their special properties (Drobne et al., 2007; Clift et al., 2008).

Since NMs can differ in many characteristics, every one of which can be responsible for a unique biological effect, it is difficult to generalize NM-induced toxicity (Aillon et al., 2009). Consequently, the characterization, testing and classification of different types of NMs are necessary. The aim in nanotoxicology, however, is not to test every variation of every newly-synthesized NM, but rather to identify the factors that are useful in understanding and predicting NM toxicity (Drobne et al., 2007). Several NP-toxicity screening strategies have been proposed by different research groups and discussed in a number of comprehensive reviews (Donaldson et al., 2004; Oberdorster et al., 2005).

The current consensus is because the actual small physical size of an engineered nanostructure is similar to that of many biological molecules (e.g., antibodies, proteins) and structures (e.g., viruses), nanostructures can readily enter tissues, cells, organelles and functional biomolecular structures (i.e., DNA, ribosomes, etc.) (Elechiguerra et al., 2005). It is thought that nanostructures entering vital biological systems could cause damage there and thus harm human health (Buzea et al., 2007). Both *in vitro* and *in vivo* studies have confirmed the ability of NMs to produce free radicals (Aillon et al., 2009; Stone et al., 2009) and currently, the toxicity of NMs appears to be due to the generation

of reactive oxygen species (ROS) after exposure of cells to particulate matter (Hackenberg et al., 2011; Uchino et al., 2002; Park et al., 2009).

The importance of coatings and surface functionalization for the entry of the nanostructures into biological systems has been highlighted previously. For example, citrate-stabilized gold nanostructures have been shown to enter mammalian cells in endosome-like structures (Chithrani et al., 2006), and engineering the surface chemistry of nanostructures may enhance access to the nucleus or mitochondria (Chen et al., 2004; Nativo et al., 2008). Whilst the intracellular or *in vivo* biodistribution of NMs would be obtained and directed by engineered nanostructures (Chen et al., 2004; Deng et al., 2007; Derfus et al., 2004; Khan et al., 2005), both the final metabolic fate and strategies to avoid secondary, unintentional effects remain unknown (Fischer et al., 2007).

The delivery of NPs by liposomes or the modification of NP surfaces with short peptides (CPPs) to facilitate their cellular uptake are methods by which the well-established endosomal route of cellular uptake of NPs can be bypassed. Nuclear targeting using surface modification with a cocktail of CPPs and a peptide that acts as a nuclear localization signal has been demonstrated (Nativo et al., 2008). Surface functionalization with specific molecules has also been demonstrated as a method by which NMs enter the brain, which is normally protected by the blood-brain barrier (Liu et al., 2008).

The relationship between physicochemical characteristics of NMs, such as size, shape, and surface chemistry, and their intracellular and *in vivo* biodistribution remain largely unknown. However, predictive classification procedures that have already been developed to evaluate this relationship for several drugs and carriers may also be useful for nanostructures (Fischer et al., 2007). Nevertheless, once NMs have entered the body, their behaviour cannot be predicted by their properties alone.

The conventional protocols used for testing chemicals are considered to be a good starting point for the characterization and toxicological evaluation of NMs, but must be refined and specifically adjusted for NMs (Drobne et al., 2007). In order to prevent unwanted effects due to intentional or unintentional exposure to NMs, standard guidelines for toxicity testing strategies of NMs have been developed and validated by regulatory agencies, professional societies, the academic community, National Government Organizations and industry. In particular, these methods and protocols must

also consider the time and cost effectiveness of these analyses giving toxicological information for the variety of NMs (Drobne et al., 2007).

**Figure 1.6** gives a general overview of the common JRC approach for studying the toxicology of NMs. Nanomaterials are synthesized and physicochemically characterized, both as stock suspensions and after dilution in culture medium using Scanning Electron Microscopy (SEM) and Dynamic Light Scattering (DLS) to assess size distribution, and Inductively Coupled Plasma Mass Spectrometry (ICP-MS) to evaluate metal impurities and ion leakage. Moreover, NMs can be radio-activated; this allows their uptake to be quantified and intracellular fate to be estimated. One final consideration is the biological effect that can be related to the internal, not external, concentration of NMs.

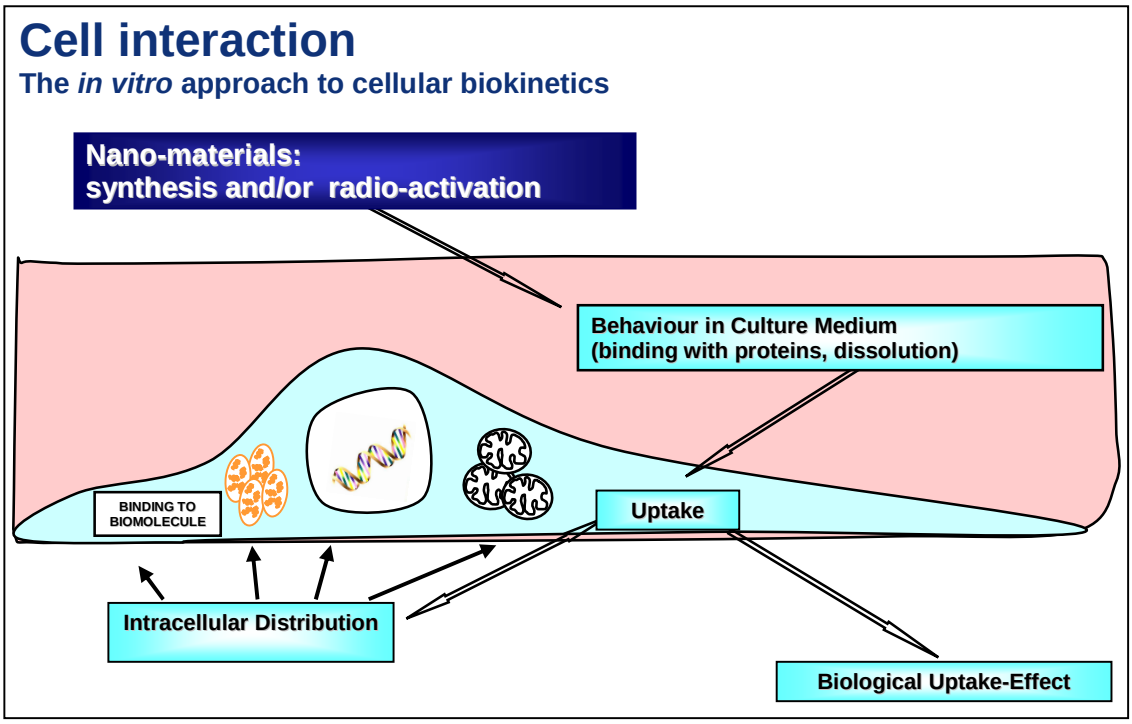


**Figure 1.6: Schematic and general representation of the *in vitro* approach used to assess cellular biokinetics of NMs at the JRC. Nanomaterials are chemically synthesized and radio-activated by neutron, deuteron or proton irradiation. The material is added to culture medium where its behaviour, particularly dissolution, is studied taking advantage of the possibility to measure radioactivity. The interaction of NMs with cells (adsorption/uptake) is then evaluated. Dissolution and uptake of non-radioactive NMs can be measured by ICP-MS. The intracellular distribution is often studied using the TEM technique. Conventional TEM images, however, cannot always distinguish NPs from some small cellular structures (e.g., glycogen granules) so that specific additional techniques must be used (Mühlfeld et al., 2007). The advantage of this approach is that the biological effect can be correlated with the real dose of NM that interacts with the cells (European Commission, JRC-Ispra, NanoBiosciences Unit).**

### 1.6 *In vitro* cell cultures and the characteristics of transformed cells

This study assessed the *in vitro* toxicity induced by specific NPs using six mammalian cell lines (**Table 1.1**). These cell lines were chosen as models of the possible impact that the selected NPs might have on different target organs in the body.

**Table 1.1: The mammalian cell lines used to assess the cytotoxicity of $CoFe_2O_4$ NPs in this study. Mouse Balb3T3 fibroblasts were also used as a cell model to study the concurrent cytotoxicity and cell transformation capacity, as well as genotoxicity induced by specific $CoFe_2O_4$ and Ag NPs.**

| Mammalian cell lines used | | | |
|---|---|---|---|
| **Immortalized cells** | | **Tumorigenic cells** | |
| Bab3T3 | Mouse immortalized fibroblasts | A549 | Human Lung Carcinoma cells |
| HaCat | Human immortalized keratinocyte cells | CaCo2 | Human Caucasian Colon adenocarcinoma cells |
| MDCK | Madin Darby Canine Kidney cells | HepG2 | Human hepatoma cells |

Importantly, the cell lines used in this study could be similar, but not necessarily identical, to the primary cells or cells *in vivo*. Initially, cells taken from a vertebrate organism and cultured *in vitro* multiply, but they then enter a stationary stage where they stop growing (Watanabe et al., 1967). The cell culture then undergoes a crisis stage during which many cells die; some cells may, however, survive and start to grow indefinitely. The ability to overcome the crisis and the time at which it occurs can differ for different cells from organisms of different species. For example, human cells undergo the crisis stage at the fortieth generation and rarely survive this stage, whilst mouse cells enter the crisis stage at the twelfth generation and usually survive.

Cell cultures used to perform *in vitro* experiments can be divided into two main groups (Walum et al., 1990):

- **Primary cell cultures:** these cells represent the direct progeny of cells originating from the donor organ; their phenotype is similar to that of the same cells *in vivo*,

but their lifetime in culture is very short because they reach the crisis stage quickly and then die

- **Cell line cultures:** after an *in vitro* partial transformation, these cells can grow indefinitely with no alteration in phenotype. They are still, for example, anchor-dependent, contact-inhibited and serum growth factor-dependant for growth, and retain the normal cytoskeleton organization that allows the cells to adhere to the substrate with a flat and elongated morphology. Cell lines can also be obtained by selecting cells that can survive to the crisis stage. Their lifetime in culture exceeds that of primary cultures; therefore, the transformed cells are also defined as "stabilized" or "immortalized" and form a cell line with an aneuploid chromosomal set. The immortalized cell lines are not normally tumorigenic.

Tumorigenic cells are completely transformed in neoplastic cells and their morphology differs from normal cells. Tumorigenic cells, via a multi-stage process, can grow without undergoing the processes that usually regulate the cell cycle. The characteristics of the tumorigenic cells are summarized as follows (Walum et al., 1990):

- *Immortalization*: apoptosis is postponed
- *Independence from growth factors*: cells do not need growth factors in the culture medium because they drive their own synthesis
- *Independence from the anchor* (for cells that usually grow whilst attached to a substrate): cells can grow without attaching to a substrate
- *Lose of contact inhibition*: cells grow continuously even when the culture reaches confluence and can grow as a multi-layer
- *Metastatization*: cells can colonize normal tissues, moving from the original tissue to any other part of the body.

Cancer can occur in animals inoculated with tumorigenic cells (Walum et al., 1990). The transformation frequency can be increased by exposure to different carcinogenic agents that can be classified as "initiators" and "promoters" and include several chemical compounds and UV radiation (Asada et al., 2005; Sakai, 2007). In order to produce a

cancer, the carcinogenic agents must affect two main types of genes: the proto-oncogenes (responsible for cell cycle regulation and called oncogenes in the transformed cell) and the anti-oncogenes (so-called tumour suppressor genes because their normal function contrasts with unchecked growth) (Lewin, 1997).

The advantages of using a stabilized cell line are as follows (Ekwall et al., 1990):

- *A homogeneous population of target cells* that can be obtained from a single mother cell due to a high cloning efficiency and unlimited cell growth
- *The availability of a large stock of cells with defined characteristics*
- *Ease of checking* the correlation between the assay endpoint and the neoplastic transformation because stabilized cells require only a few stages to become tumorigenic
- *A higher plating efficiency,* thereby saving resources and simplifying the sub-clone isolation and evaluation of the induced transformation per survived cell
- *Simpler medium for the cell culture* as these cells are adapted to the culturing conditions, resulting in higher reproducibility between laboratories
- *A reproducible dose-effect relationship,* which is not available for diploid cells
- *Sensitivity to promoter agents,* which can be exploited to enhance the sensitivity of cells at the transformation stage

The disadvantages of using stabilized cells include (Ekwall et al., 1990):

- *Abnormality of target cells;* target cells differ from the primary cells because they adapt to the culture conditions
- *Limited ability to metabolize chemical compounds* because (i) most of the chemicals become actively carcinogenic only after being metabolized in the body, and (ii) the stabilized cell lines are clonal in origin and so have limited ability to metabolize chemicals, which reflects the ability of these cells in their original tissue of source

- *Unsure origin and loss of differentiated functions;* cells tend to lose the characteristic functions of their specific cell type after many generations in culture because of reversible and irreversible alterations to genetic patterns. The problems associated with the use of stabilized cell lines are demonstrated both by clonal variation and that which occurs after several passages in culture. With respect to clonal variation, a cell line kept in culture in one laboratory often differs from the very same cell line cultured in another laboratory. In addition, an increase in spontaneous transformation usually occurs at the later passages and can be avoided, therefore, by using cells produced only at earlier passages.

### 1.7 *In vitro* methods to test of NMs: from cytotoxicity to genotoxicity

In this Ph.D. research project, the effects of NPs were tested using *in vitro* methods suggested by the EC, White Paper, Strategy for a Future Chemicals Policy (http://cordis.europa.eu/nanotechnology/actionplan.htm). This report outlines a strategy for toxicological testing using *in vitro* methods as alternatives to animal testing for the Registration, Evaluation and Authorization of Chemicals (REACH) legislation. The estimated number of vertebrate animals (mammals, birds and fish) required for the toxicological assessment of chemicals is approximately 2.6 million in the range of time required by the REACH system (11 years). This corresponds to 2-3% of the total number of vertebrates used every year for experimental and scientific purposes, including pharmacological tests (Perdersen et al., 2003). This number is likely to increase in the future due to the growth in nanotechnology production and subsequent nanotoxicology research. The total cost of these experiments has been evaluated to be approximately 1.5 billion Euros, 90% of which is related to studying the effects on human health.

The development and application of accurate testing strategies may, therefore, contribute to a reduction in the experimental costs and number of animals used (Perdersen et al., 2003). Clearly, the standardization of efficient screening tests based on *in vitro* screening assays is required (Ponti et al., 2006). Moreover, there is increasing interest in the development of alternative *in vitro* methods because the potential toxic effects of engineered NMs, their mechanisms of action and interactions with cells must be understood (Stern & McNeil, 2008). A potential toxic effect may not be explained solely

by toxicity assays because some NMs may induce inflammation and genotoxicity, but not cytotoxicity. This highlights the importance of studying the cell transformation capacity and genotoxicity as well as toxicokinetics using *in vitro* assays (OECD, 2008). Despite the obvious advantages of *in vitro* systems, however, these do have many limitations and one test alone may not suffice for risk assessment purposes (Stone et al., 2009). Currently, *in vitro* nanotoxicology research cannot replace the *in vivo* investigations that are required to verify *in vitro* data, and particularly to test for acute and chronic exposure (Clift et al., 2011).

The most promising *in vitro* tests use human cell lines and can mimic *in vivo* conditions. Other cell lines, such as the immortalized mouse fibroblasts Balb3T3 (A31-1-1 clone) may be of interest when assessing the cell transformation capacity of chemicals or NMs. These cells are actually used in the Cell Transformation Assay (CTA), which is a very promising *in vitro* test for studying the cell transformation capacity of chemicals and NMs. The CTA was the object of a pre-validation study, the goal of which was to optimize and standardize the choice of cell line, methods of culture and exposure protocols, as well as plate reading and data analysis (Ponti, 2004). The observation that results obtained by screening metal compounds using the CTA correlated with cell transformation capacity data in humans (International Agency for Research on Cancer, IARC) and animals confirmed the validity of the assay as a promising *in vitro* method for the evaluation of transformation capacity.

In this study, cytotoxicity was evaluated using the Colony Forming Efficiency (CFE) and Neutral Red uptake assays, and the transformation capacity was assessed using the CTA followed by the Cytokinesis-Block Micronucleus assay (CBMN). The CBMN is a specific assay for genotoxicity that can discriminate between genotoxic and non-genotoxic compounds; it was used here to evaluate genotoxicity because this information cannot be obtained with the CTA.

### *1.7.1 In vitro assays for studying cytotoxicity or viability*

Cytotoxicity is a general term commonly used to indicate the ability of chemicals or NMs to affect cellular structures and/or functions, leading to cell death (Singh et al., 2009). Cytotoxicity assays are often considered to be viability assays, even if they do not always

measure directly the number of living/dead cells, but a cellular function (e.g., mitochondrial activity or release of lactate dehydrogenase) (Stone et al., 2009). Several assays are now available commercially to screen *in vitro* cytotoxicity; however, these should be properly validated with pathogenic and non-pathogenic particulates before they are used to assess NMs (Hillegass et al., 2010).

Among the short-term *in vitro* methods described in the literature and already being used to screen NM-induced cytotoxicity, however, are the so-called "colorimetric assays". These include the Trypan Blue exclusion, Neutral Red uptake and microculture with tetrazolium (MTT, MTS, XTT) assays and use specific dyes to highlight the endpoint. The Trypan Blue assay allows unstained and viable cells to be distinguished from coloured dead cells because the diazo dye, Trypan Blue, can enter cells whose plasma membrane has been damaged. The Neutral Red and tetrazolium assays do not provide direct information on the total number of viable cells, but the viability of the cell population is considered to be directly proportional to the absorbance measured at the end of the experiment. Specifically, Neutral Red dye can be taken up by viable cells and retained by their lysozomes, whilst soluble, yellow tetrazolium dyes are usually metabolized by viable cells with active mitochondrial activity into an insoluble purple formazan product.

Interference in the absorbance measurements of these assays can occur, however, due to the optical properties of some NMs and interactions between the NM/dye or NM/dye-product. This can either invalidate these types of assays or make them inapplicable to all NMs unless some tricks and control experiments are included to minimize over/under-estimation of cell viability (Stone et al., 2009). Indeed, Casey et al. have demonstrated interactions between single-walled carbon nanotubes (swCNTs) and different dyes, commonly used in cytotoxicity studies (i.e., Comassie Blue, Alamar Blue, Neutral Red, MTT and WST-1) using spectroscopic analysis (Casey et al., 2007). Monteiro-Riviere et al. obtained highly variable results due to interactions between the tested materials and dye/dye products when using dye-based assays to screen the toxicity of different carbon NMs (Monteiro-Riviere et al., 2009). It must be stressed, therefore, that whenever possible, more than one method and cell type should be used to accurately study and characterize the properties and effects of each material.

Amongst the cytotoxicity assays, the Colony Forming Efficiency (CFE) "clonogenic assay" measures the cytotoxic effect as a decrease in the number of colonies formed after treatment compared to a control, should also be mentioned (Hillegass et al., 2010). This assay is suitable for testing NMs because it does not use dyes and is usually more sensitive than biochemical methods as it measures cell death in general rather than a specific biological effect (Ponti et al., 2010).

### *1.7.2 In vitro assays for studying the cell transformation capacity*

Carcinogenesis is a multi-step process. It is a series of genetic alterations in a target cell that involves the activation of oncogenes, inactivation of tumour suppressor genes and/or altered activation of cell cycle genes, which cause steady alterations in cell growth control and thus produce cells that can form malignant tumours (Schins, 2002; Lewin, 1997). While carcinogenesis is usually associated with neoplastic fibroblasts, oncogenesis generally refers to any cell type that undergoes neoplastic transformation. A tumorigenic cell has a fully neoplastic transformed phenotype (Walum et al., 1990), and every substance that promotes or initiates cancer is defined as a carcinogen (Singh et al., 2009).

In particular, the morphological transformation in cell cultures implies changes in the behaviour and control of growth characterized (depending on the cellular system) by one or more of the following aspects (Yuspa et al., 1988):

- Alteration of the cellular morphology
- Unorganized growth of the colonies
- Anchorage-independent growth.

Experiments with animals, clinical human material and *in vitro* biomolecular and cellular methods are required to elucidate carcinogenic mechanisms. Several *in vitro* models have been proposed to determine the cell transformation capacity of a material (Combes et al., 1999):

- ❖ The Syrian Hamster Embryo (SHE) cells' morphological transformation assay. The goal of this assay is the formation of transformed colonies by SHE cells, the primary culture. The SHE cells are diploid, have a short lifetime in culture and rarely become tumorigenic unless exposed to a carcinogen (Di

Paolo, 1980). First introduced by Berwald and Sachs in 1963 to test chemicals, this assay produces results within weeks. The results obtained after testing 28 chemicals have shown 78% concordance with rodent bioassays (Engelhardt et al., 2004)

- The Balb3T3 (clone A31-1-1) and C3H/10T½ Cell Transformation Assay (CTA). This assay uses established cell lines of aneuploidy mouse fibroblasts; the endpoint is the loss of contact-inhibition of cell growth. Foci type III are scored as transformed colonies because the normal cells are usually highly sensitive to post-confluence inhibition. This assay can be performed using a standard protocol (72 hours of treatment, refreshing the medium twice weekly and maintaining the culture for a total of 4–6 weeks) or by following a two-stage protocol (treatment with sub-doses of a carcinogenic compound acting as a tumour initiator, e.g., MCA, is followed by a second treatment with a carcinogen that is not genotoxic as a tumour promoter, e.g., TPA). The two-stage protocol is similar to the *in vivo* two-stage carcinogenesis tests and detects the activity of tumour promoters; the latter are usually not genotoxic carcinogens and they do not produce foci in Balb3T3 culture *per se* (Sakai, 2007). The Bhas 42 cell transformation assay is a variation of the two-stage protocol described above, where Bhas 42 cells were established by Sasaki et al. (Sasaki et al., 1988) and obtained after v-Ha-ras-transfection of Balb3T3 cells (Asada et al., 2005)
- The HaCaT cell transformation assay. This human cell line is obtained after the spontaneous immortalization of normal human keratinocytes, most likely caused by p53 gene mutations and the subsequent loss of function of senescence genes. The HaCaT cells are a convenient cell model for studying tumour progression using several carcinogenic agents (Fusening & Boukamp, 1998).

Other assays that detect cell transformation have been documented, such as the soft-agar test with BHK21 (baby hamster kidneys) and JB6 (pre-neoplastic mouse epidermal) cells, where the endpoint is the loss of anchorage dependence for growth (Sakai, 2007).

One of the most promising *in vitro* tests assessing the cell transformation capacity of different organic and inorganic compounds, however, involves the use of the Balb3T3 clone A31-1-1 assay. These mouse fibroblasts are derived from mouse embryo cells that were expanded in culture over 40 years ago (Aaroson & Todaro, 1968) and then selected to obtain the A31-1-1 clone still used in the CTA (Kakunaga, 1973). These cells are contact-inhibited and show a plating efficiency of 50-60%. They can form a monolayer with fibroblast-like morphology and have a division period of approximately 16 hours, depending on the cellular density.

Nevertheless, although Balb3T3 cells show some of the typical characteristics of transformed cells (e.g., immortalization, high cloning efficiency, altered morphology compared to the primary culture, loss of anchor-dependent growth if treated with carcinogenic agents and tumour formation if used to inoculate nude mice after treatment), their frequency of spontaneous transformation is low (about $10^{-5}$ foci per survived cells) (Aaroson & Todaro, 1968; Di Paolo et al., 1972).

The CTA using Balb3T3 cells allows the simultaneous evaluation of cytotoxicity and morphological transformation. It takes 7-10 days and 5 weeks to determine the cytotoxicity and cell transformation capacity, respectively (Ponti et al., 2007). Cytotoxicity is evaluated by the number of colonies formed (CFE), whilst the transformation capacity is evaluated by the formation of type III foci. The range of concentrations of substances to be tested with the CTA has been defined previously by cytotoxicity experiments (usually corresponding to 80%, 50% and 20% of CFE). In the Balb3T3 assay, three different types of foci can be observed after exposure to chemicals and NMs:

- Type I foci: colonies composed of cells with a low level of vertical growth and overlapping
- Type II foci: colonies in which cells grow overlapped and form multi-layers and spindle cells at the boundaries
- Type III foci: basophilic colonies with a high level of overlapping, spindle cells without any specific orientation at the boundaries that appear to run over onto a surrounding monolayer of normal cells.

Only type III foci are scored in this assay since it has been demonstrated that these alone can induce tumour formation in nude mice with 85% frequency (Saffiotti et al., 1984; IARC/INCI/EPA, 1985). One of the larger databases on Balb3T3 cells was developed by Matthews et al. (Matthews et al., 1993) and evaluated 168 chemicals, including 84 carcinogens and 77 non-carcinogens. The Balb3T3 assay was shown to be useful in assessing both carcinogenic and non-carcinogenic chemicals. Notably, surveys of published *in vitro* activities of 131 chemicals, classified as group I carcinogens by the IARC, have shown that morphological transformation assays (in rodents and human cells) had a high level of predictability (IARC, 1987). This is of interest and encouraging for the future development of these assays for regulatory purposes.

### *1.7.3 In vitro assays for studying genotoxicity*

The ability of a test agent, either a chemical or a NM, to damage DNA is defined as genotoxicity (Singh et al., 2009). Genotoxicity testing is an important part of the risk assessment of chemicals for regulatory purposes (DHO, 2000) and identifies chemicals that may damage DNA and be carcinogenic (assuming that mutagenesis plays a key role in the carcinogenic process).

At least two *in vitro* tests are part of the first level of a standard, regulatory genotoxicity test procedure organized into a tier-testing scheme: a bacterial mutagenicity test (OECD TG 471, Ames' test using *Salmonella* or *E. coli*) and a cytogenetic test (OECD TG 473, usually an analysis of the metaphase using either human lymphocytes or rodent cell lines) (Zeiger, 2001). The CTA performed with Balb3T3 allows carcinogens to be detected, but does not distinguish between genotoxic and non-genotoxic compounds. Therefore, a testing strategy that requires CTA experiments to be performed alongside other *in vitro* genotoxicity tests, such as the Cytokinesis-Block Micronucleus assay (CBMN), has been suggested (Hartung et al., 2003).

A number of *in vitro* genotoxicity tests that assess the effects of NMs on the genome have been reported (Singh et al., 2009). The most frequently used was the Comet assay (19 studies, 14 of which had a positive outcome) followed by the CBMN assay (14 studies, 12 of which had a positive outcome), whilst the Ames' test was used less frequently (and almost always showed a negative outcome that may be due to the

bacterial cell wall acting as a barrier against NMs) (Landsiedel et al., 2008). The *in vitro* CBMN test, however, is not yet generally accepted by regulatory authorities as an alternative system in a test battery because it lacks formal validation. It was the object, therefore, of a retrospective validation study carried out by the Validation Management Team (VMT) of the European Centre for the Validation of Alternative Methods (ECVAM). The VMT evaluated existing data to assess the validity of this test when considering seven validity modules:

1. Test definition
2. Intra-laboratory reproducibility
3. Transferability
4. Inter-laboratory reproducibility
5. Predictive capacity
6. Applicability domain
7. Minimum performance standards.

The VMT concluded that the *in vitro* micronucleus test could be considered as a valid alternative to the *in vitro* chromosome aberration test for genotoxicity testing (Corvi et al., 2008). Moreover, following a comprehensive inter-laboratory assessment (Carter, 1967), the OECD approved the *in vitro* Micronucleus Test Guideline 487 (OECD TG 487; Parry et al., 2010), which gave specific recommendations for tests using mammalian cells.

The CBMN assay protocol was improved in 2007 by Fenech (Fenech, 2007); this leads to the development of the Cytokinesis-Block Cytome assay. This procedure allows DNA misrepair, chromosome breakage, chromosome loss, non-disjunction, cytostasis, cytotoxicity, necrosis and apoptosis to be measured. In particular, this refined protocol focuses on the different types of DNA damage that can be detected as (**Figure 1.7**):

- Micronuclei (MN): these are formed either by acentric chromosomes fragments or by entire chromosomes (chromosomal loss) and show the same morphology and nuclear staining, but are smaller and scored only in bi-nucleated cells (BN), which correspond to cells that have divided only once (**Figure 1.8**)

- ❖ Nucleoplasmic bridges (NPBs): these are biomarkers of dicentric chromosomes resulting from telomere end fusions or DNA misrepair, and appear as narrow or wide stalks between the two main nuclei
- ❖ Nuclear buds (NBUDs): these are biomarkers for the elimination of amplified DNA formed during S-phase, and are similar in appearance to micronuclei, but are linked to one of the two main nuclei with a narrow or wide stalk.

The cytostatic effects are measured as the Nuclear Division Index (NDI), which is the ratio of mono-, bi- and poly-nucleated cells, whilst cytotoxicity is represented by the ratio between the necrotic and/or apoptotic cells. More information on the mechanism by which MN, NPBs and NBUDs are formed can be obtained using centromere and/or telomere probes, and specific scoring criteria have been suggested (Fenech, 2007). The NDI assay has been employed successfully for both the monitoring of *in vivo* genotoxin exposure (Migliore et al., 2002) and *in vitro* genotoxicity testing. It has also been used in several research fields, such as nutrigenomics and pharmacogenomics (Fenech, 2010), as well as to predict the sensitivity of normal and tumour tissues to radiation and cancer risks (Saran et al., 2008).

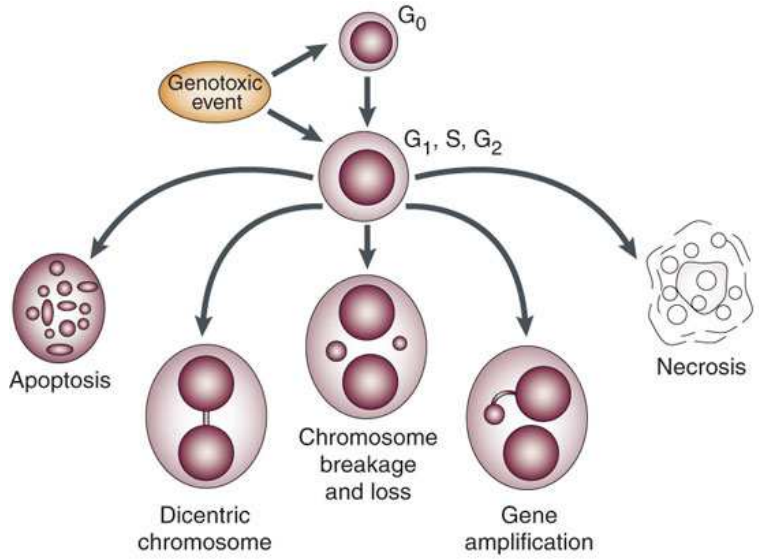


**Figure 1.7: The possible fates of cultured, cytokinesis-blocked cells following exposure to cytotoxic/genotoxic agents. Using CBMN assay, biomarkers, such as the frequency of chromosome breakage (MN), chromosome loss (MN), and chromosome rearrangement, for example, dicentric chromosomes (NPB), gene amplification (NBUDs), necrosis and apoptosis can be measured. In addition, cytostatic effects can be estimated from the ratio of mono-, bi- and multinucleated cells (Fenech, 2007).**

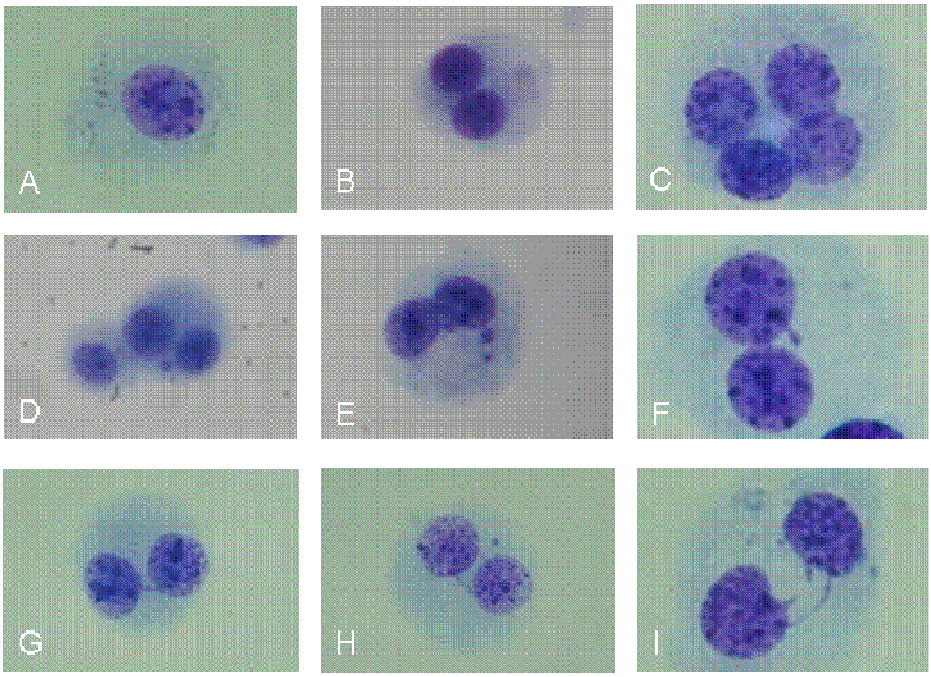


**Figures 1.8A, B, C, D, E, F, G, H and I: Optical microscope images (40X) from positive control slides prepared in the CBMN assay using Balb3T3 mouse fibroblasts. In particular, an example of a mononucleated cell (A), a binucleated cell (B), a polynucleated cell (C), a binucleated cell with one or more micronuclei (D and E respectively), a binucleated cell with nuclear bud (F), a binucleated cell with nucleoplasmic bridge (G), a binucleated cell with double nucleoplasmic bridge and a micronucleus (H) and a binucleated cell with nucleoplasmic bridge and nuclear buds (I) (EC, JRC-Ispra, IHCP, NBS).**
**To calculate the NDI, mononucleated, binucleated (with or without micronuclei) and polynucleated cells are scored. In this study, the genotoxic potential of $CoFe_2O_4$ and Ag NPs, demonstrated by the induction of micronuclei formation, was evaluated on Balb3T3 mouse fibroblasts.**

In addition to genotoxicity investigations, numerous studies related to oxidative stress and inflammation have been reported. These studies are widespread in nanotoxicology research because of the effort invested in understanding the mechanisms by which NMs may induce genetic damages.

Two main hypotheses may explain the possible mechanisms by which NMs can induce DNA damage (Singh et al., 2009):

- Once NMs have entered cells by passive diffusion, receptor-mediated endocytosis and/or clathrin- or caveolae-mediated endocytosis, they can pass through the nuclear membrane (if small enough), be transported through nuclear pores, or be

enclosed in the nucleus during mitosis, and thus physically interact with the DNA to cause genetic damage (primary genotoxicity, **Figure 1.9**)

- NMs can interact with other cellular biomolecules, such as the proteins involved in cell division. They can also cause oxidative stress via reactive oxygen species (ROS) and/or free radical production, inflammation (mediated by inflammatory cells—macrophages and neutrophils—that secrete soluble factors, including cytokines and tumour necrosis factors, which can cause secondary genotoxicity, **Figure 1.9**), and aberrant signalling responses.

Electrophilic molecules (e.g., $H_2O_2$) or free radicals (e.g., OH·) containing an oxygen atom are usually defined as ROS and are produced by metabolic reactions or physicochemical insults. The different ROS species show different reactivity and thus have different potential toxicity profiles. Specific assays can detect the ROS produced by NMs due to their surface properties and thus reactions in biological media in the absence of cells, and to measure intra-/extra-cellular ROS species generated by cells *per se* following treatment with particulates. Assays that can detect changes in the ratio between the reduced form of the natural antioxidant glutathione (GSH) and its oxidized form (GSSG) are also available and used to study oxidative stress (Stone et al., 2009). Oxidative stress studies are important not only to increase understanding of transformation and genotoxicity, but also because they can explain toxicity results; severe oxidative stress *per se* can cause necrosis whilst moderate oxidative stress can cause apoptosis (Curtin et al., 2002).

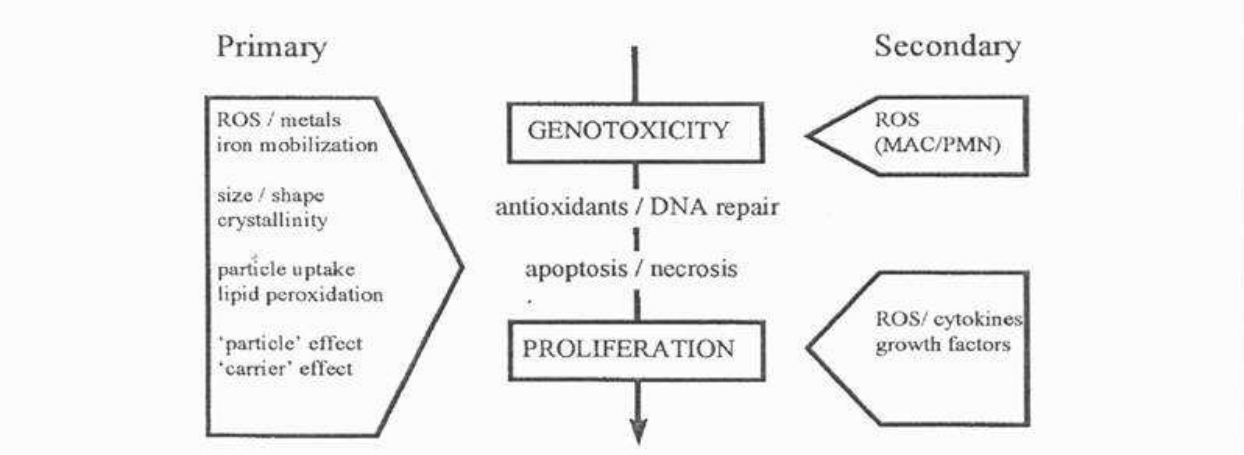


**Figure 1.9: Mechanisms of primary and secondary genotoxicity induced by particles and fibres; ROS may play a major role in primary genotoxicity, whilst the excessive and persistent formation of ROS from inflammatory cells may be responsible for secondary genotoxicity (Schins, 2002).**

## 1.8 Metal NPs investigated in this study

This Ph.D. research study focused on assessing the potential *in vitro* effects induced by different sizes of $CoFe_2O_4$ and Ag NPs. This section describes the current knowledge on the biological effects of $CoFe_2O_4$ and Ag NPs.

### *1.8.1 Cobalt ferrite NPs ($CoFe_2O_4$ NPs): biological background*

Metal oxide NPs are of huge interest because of their unusual and often mass-dependant optical, electronic and magnetic properties. An important group of NPs are the magnetic NPs. Iron oxide NPs with a specific surface chemistry appear to be suitable for several *in vivo* applications (e.g., Magnetic Resonance Imaging contrast enhancement, tissue repair, immunoassay, drug delivery, detoxification of biological fluids and cell separation) that require specific magnetic and physicochemical properties (size ≤100 nm) (Laurent et al., 2008).

For example, the first magnetic NPs to be developed as contrast agents for Magnetic Resonance Imaging (MRI), a useful diagnostic technique because it is non-invasive, were the iron oxide ($Fe_3O_4$) NPs. Magnetic NPs used for MRI can be injected intravenously or directly into a specific site in the body. Particles larger than 100 nm tend to stay into the vascular system, whilst smaller particles can diffuse into neighbouring tissues (Berry, 2005). These NPs are usually coated with dextran or polyethylene glycol derivatives, which allow a longer circulation half-life than uncoated particles and avoid aggregation

(Cormode et al., 2009; Sahoo et al., 2003). The super-paramagnetic iron oxides (SPION) already approved for clinical use include particles larger and even smaller than 50 nm (Kunzmann et al., 2010). Magnetic NPs are also important for drug delivery. The application of an external magnetic field allows magnetic NPs to be transported to the specific target site and drugs released only at the target site, thereby avoiding the undesired effects that occur in radio- and chemo-therapy (Berry, 2005).

Another potential use of magnetic NPs is the hyperthermic treatment of tumour cells, where the tumorigenic area is heated up to 42°C to selectively kill neoplastic cells without damaging healthy neighbouring tissues (Kita et al., 2010). In this procedure, microwave, ultrasound or infrared application to the magnetic NPs leads to oscillation of their magnetic momentum resulting in a temperature increase. The permanent irreversible inhibition or loss of cellular functions is caused by damage to the tumour cellular proteins, including the unfolding and aggregation processes (Kumar et al., 2011).

The $CoFe_2O_4$ NPs have been shown to have higher chemical stability than iron oxide NPs, even at high temperatures. The magnetic momentum of $CoFe_2O_4$ NPs of similar size to the iron oxide NPs relaxes more slowly so that smaller amounts of NPs can be used; therefore, smaller devices can be made to promote cellular uptake (Brigger et al., 2002).

The $CoFe_2O_4$ NPs can be employed in the same ways of the iron oxide NPs described above. The physicochemical stability of $CoFe_2O_4$ NPs also makes them useful for audio and video recording. The $CoFe_2O_4$ NPs can be synthesized in different ways, including the sol-gel method, micro-emulsion with oil in water micelles or reverse micelles, aqueous precipitation and calcination, combustion, and forced hydrolysis in a polyol medium (Baldi et al., 2007; Tartaj et al., 2005), and the NP size is achieved by controlling the growth and nucleation rate (Maaz et al., 2006). These NPs are usually dispersed in different solvents, such as sodium dodecyl sulphate or oleic acid, to avoid their oxidation by atmospheric oxygen and reduce agglomeration.

One of the most interesting applications of $CoFe_2O_4$ NPs is in non-invasive heating in hyperthermic cancer treatment; indeed, most scientific research on $CoFe_2O_4$ NPs has focused on the use of magnetic fluids for cancer therapy. Cancer cells appear to take up magnetic NPs by endocytosis, a process which is greater in highly-proliferating cells.

Direct intra-cancer injection of biocompatible $CoFe_2O_4$ NPs used as magnetic drug carriers in canine breast cancers has shown that endocytosis of $CoFe_2O_4$ NPs occurs just one hour after administration; this non-specific endocytosis is proportional to the NP concentration in the extracellular matrix (Vaishnava et al., 2006).

The cytotoxicity of various ferrite NPs was studied previously by *in vitro* methods as MTT (3-(4,5-Dimethylthiazol-2-yl)-2,5-diphenyltetrazolium bromide assay) on established L929 fibroblasts of the connective tissue of a 100-day-old male mouse. Some of the ferrite NPs tested were found to be cytotoxic, but not $CoFe_2O_4$ and $Co_{0.9}Ni_{0.1}Fe_2O_4$ NPs (Kim et al., 2005). More recently, the *in vitro* and *in vivo* toxicity of $CoFe_2O_4$ NPs was evaluated using the L929 cell line together with the MTT assay and intravenous (IV) injections in male ICR (Imprinting Control Region) mice. *In vitro* cytotoxicity was observed at high doses (IC50 at 2 x $10^3$ μg/mL), while no adverse effects were found *in vivo* on mice, either as changes in growth or behaviour when comparing the test and control groups. Interestingly, $CoFe_2O_4$ NPs were found to be present in almost all organs, including the heart, kidney, liver, spleen and stomach (Kim et al., 2007). The genotoxic potential of three different sizes of $CoFe_2O_4$ NPs (5.6 nm, 10 μm and 120 μm) was also assessed on human peripheral lymphocytes by Colognato et al. using the micronucleus test. They found that the smaller NPs were associated with significant toxicity and mutagenicity, whilst only significant mutagenicity was detected with the 10 μm NPs; no effects were induced by the largest NPs tested (Colognato et al., 2007).

### *1.8.2 Silver NPs (Ag NPs): biological background*

Soluble silver salts have long been used for bacterial disinfection. Metallic silver and its insoluble compounds do not represent a serious health risk because they are not easily taken up by the body. “Argyria”, the irreversible and characteristic grey pigmentation of the skin due to deposits of silver complexes in tissues, is the most common detrimental effect on health. It can be attributed to prolonged exposure to silver compounds and considered to be a mechanism for detoxification of silver by its sequestration as non-toxic, silver-protein complexes or silver sulphide (Casarett and Doull, 2008). Nevertheless, since microbial resistance to metal ions and antibiotics is ever increasing, different types of metallic NPs (copper, zinc, titanium, magnesium, gold and silver

nanoparticles) are being investigated as alternatives, and Ag NPs seem to be valid growth inhibitors of various micro-organisms (Rai et al., 2009; Kim et al., 2007).

Besides their antibacterial properties and associated use in disinfecting medical devices, Ag NPs have many applications, including use in home water treatments and targeted drug delivery. They are also used in electronics, clothing, the food industry, paints, sunscreens and cosmetics. Moreover, their unique plasmon-resonance properties make them invaluable for bio-sensing and imaging applications (Ahamed et al., 2010).

The most common method by which Ag NPs are synthesized is the chemical reduction of a silver salt with a reducing agent. Since there is evidence that the antimicrobial activity may be influenced by particle size, efforts have been made to find synthesis methods that both control particle size and avoid environmental toxicity or biological hazards (Panáček et al., 2006). Moreover, recent attention has focused more on synthetic methods that produce Ag NPs of diverse shape and morphology and which are based on natural biomolecules, such as the aflavins from black tea leaf extract and polyphenolic compounds from Indian propolis (Begum et al., 2009; Roy et al., 2010).

Another, almost unexplored field relates to the study of the interactions between metal NPs and viruses. Elechiguerra et al. demonstrated that PVP-coated Ag NPs with an average size of 6.53 nm can interact in a size dependent way with the HIV-1 virus, binding preferentially to the gp120 glycoprotein knobs (Elechiguerra et al., 2005).

In addition, a colloidal aqueous suspension of spherical Ag NPs of 7-20 nm in size was studied for *in vitro* toxicity and oxidative stress on A431 human skin carcinoma and HT-1080 human fibrosarcoma cells in order to develop a topical antimicrobial agent for the treatment of burn wound infections; a reduction in the GSH level and increased levels of ROS and lipid peroxidation were found (Arora et al., 2008).

The same research team then tested these Ag NPs in a further study, again using primary mouse fibroblasts as a model of dermal exposure for the wound healing process and primary liver cells as a model for accumulation (Arora et al., 2009). The IC50 values determined by the XTT assay were 61 μg/mL and 449 μg/mL for fibroblasts and liver cells, respectively, indicating that fibroblasts were more sensitive to the Ag NPs tested and suggesting that primary cells have a higher tolerance to these NPs than the

concentrations found in the gel formulation (~ 20 μg/mL) of topical antimicrobial preparations (Arora et al., 2009).

Foldbjerg et al. investigated in parallel the effects of $Ag^+$ and of PVP-coated Ag NPs of 30-50 nm in size on A549 cells, a human alveolar cell line. They found that $Ag^+$ decreased mitochondrial activity to a greater extent than Ag NPs, but Ag NPs induced higher ROS production than $Ag^+$, suggesting that Ag NP-induced ROS production is not due to the potential release of $Ag^+$ alone. The administration of an antioxidant GSH precursor (NAC) was found to protect the cells against cytotoxicity in both silver treatments, probably due to the antioxidant ROS-scavenging action of NAC and possible $Ag^+$ binding effects (Foldbjerg et al., 2011).

Asharani et al. also observed an increase in ROS production due to treatment with Ag NPs; they tested starch-coated Ag NPs of 6-20 nm in size on normal human lung fibroblasts (IMR-90) and human glioblastoma cells (U251). Interestingly, they also observed a dose-dependent reduction in the ATP but increase in DNA damage (Asharani et al., 2009).

In accordance with these studies, 30 nm Ag nanospheres were found to be cytotoxic and genotoxic on the OLHNI2 medaka fish cell line, extensively used as a model for human health (Wise et al., 2010). Cytotoxicity was assessed by a colony forming assay.

In addition, Larese and colleagues demonstrated that PVP-coated Ag NPs of 25 nm were able to pass through intact and damaged human skin *in vitro* (Filon Larese et al., 2009).

Lu et al. reported the effects of surface coating on the toxicity and genotoxicity of Ag NPs by the MTT and Comet assays, respectively, in HaCaT keratinocytes. Whilst colloidal citrate-coated Ag NPs were neither cyto- nor geno-toxic, they were both cyto- and geno-toxic if dried and converted into powder form. The authors suggested PVP-coated Ag NPs were safe for use in daily life because they did not show toxicity (Lu et al., 2010).

Data can still be found in the literature on the *in vivo* and *in vitro* toxicity of Ag NPs on mammalian cells. It is difficult, however, to compare all the scientific data as they vary depending on the characteristics of the NPs (e.g., surface chemistry, coatings, size, doses administered, exposure time, etc.), the cell types and tests employed (Ahamed et al., 2010; Johnston et al., 2010).

# Chapter 2: Materials and Methods

## 2.1 Cell lines, cell culture and media

### *2.1.1 A549* (source: ATCC)

The A549 Human Lung Carcinoma cells were chosen as a model of lung toxicity. They were cultivated with HAM F-12 containing GlutaMAX-I (Cat N. 31765, GIBCO Invitrogen) medium completed with 50 mL of Newborn Calf Serum (10% v/v) (New Zealand origin, Cat N. 26010-074, GIBCO Invitrogen), 5 mL of penicillin/streptomycin (1% v/v) ($10^4$ Units/mL, Cat N.15140, GIBCO Invitrogen) and 2.5 mL of Hepes buffer (0.5% v/v) (Cat N. 15630, GIBCO Invitrogen). The cells were maintained as described below (see **Sections 2.2** and **2.3**).

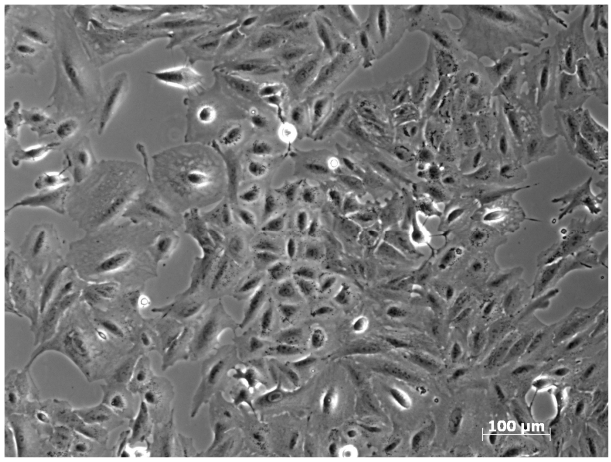


**Figure 2.1: A549 cells in culture (100X magnification at the optical microscope) (NBS, IHCP, JRC).**

### *2.1.2 Balb3T3* (source: Hatano Research Institute, Japan)

These immortalized mouse fibroblasts were cultured in MEM (Minimum Essential Medium with Earle's salts and L-glutamine, Cat N. 31095, GIBCO Invitrogen) with low glucose (1000 mg/L), L-glutamine (292 mg/L) and sodium bicarbonate (2200 mg/L) completed with 50 mL (10% v/v) of Foetal Bovine Serum (Australian origin, Cat N. 10099-141, Lot N. 6792117Y, GIBCO Invitrogen) and 5 mL of penicillin/streptomycin (1% v/v) ($10^4$ Units/mL, Cat N.15140, GIBCO Invitrogen). The cells were maintained as described below (see **Sections 2.2** and **2.3**).

The Foetal Bovine Serum Lott was tested using the Colony Forming Efficiency (CFE) assay and the Cell Transformation Assay (CTA) before use in the Balb3T3 cell culture and both CFE and CTA experiments with NPs. The Lott of serum was selected both to maintain the normal contact-inhibited monolayer of untreated cells and support the type III foci formation by 3-methylcolantrene, as recommended by the IARC (IARC, 1985).

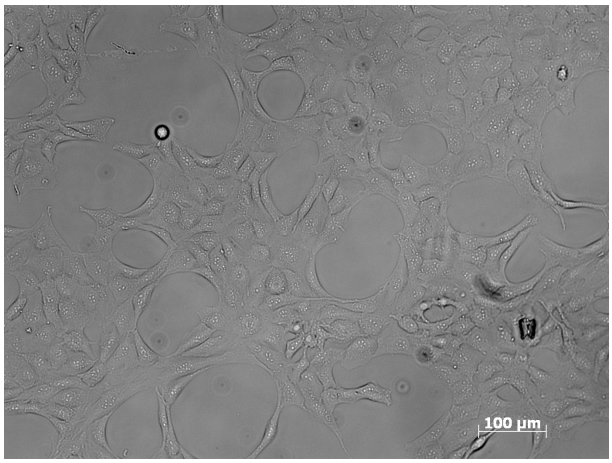


**Figure 2.2: Balb3T3 cells in culture (100X magnification at the optical microscope) (NanoBioSciences Unit, IHCP, JRC).**

### *2.1.3 CaCo2* (source: Istituto Superiore di Sanita', Rome)

Human Caucasian Colon adenocarcinoma cells were selected as a model of the intestine. They were maintained in culture using DMEM (Dulbecco's Modified Eagle Medium, Cat N. 41965, GIBCO Invitrogen) high glucose (4500 mg/L) without sodium and magnesium and completed with 50 mL of Foetal Bovine Serum (10% v/v) (US origin, Cat N. 16000-044, GIBCO Invitrogen), 12 mL of L-glutamine (4 mM) (Cat N. 25030, GIBCO Invitrogen), 5 mL of penicillin/streptomycin (1% v/v) ($10^4$ Units/mL, Cat N.15140, GIBCO Invitrogen) and 5 mL of non-essential amino acids (1% v/v) (Cat N. 11140, GIBCO Invitrogen). The cells were maintained as described below (see **Sections 2.2** and **2.3**).

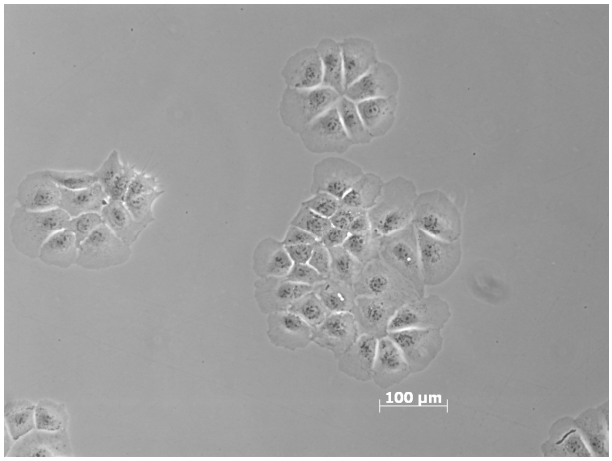


**Figure 2.3: CaCo2 cells in culture (100X magnification at the optical microscope) (NanoBioSciences Unit, IHCP, JRC).**

### *2.1.4 HaCaT* (source: Prof. Norbert E. Fusening, Deutsches Krebsforghungszentrum)

This spontaneously immortalized human keratinocyte cell line has been used in many studies as a model of epidermal cells and keratinocyte functions. The HaCaT cells were cultured in DMEM (Dulbecco's Modified Eagle Medium, Cat N. 41965, GIBCO Invitrogen) high glucose (4500 mg/L) without sodium and magnesium completed with 50 mL of Foetal Clone II Serum (10% v/v) (Cat N. SH30066.03, HyClone), 12 mL of L-glutamine (4 mM) (Cat N. 25030, GIBCO Invitrogen) and 5 mL of penicillin/streptomycin (1% v/v) ($10^4$ Units/mL, Cat N.15140, GIBCO Invitrogen). The cells were maintained as described below (see **Sections 2.2** and **2.3**).

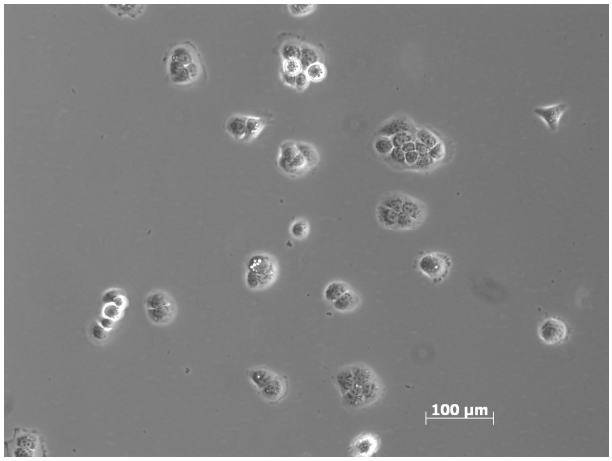


**Figure 2.4: HaCaT cells in culture (100X magnification at the optical microscope) (NanoBioSciences Unit, IHCP, JRC).**

### *2.1.5 HepG2* (source: Interlab Cell Line Collection)

The HepG2 human hepatoma cell line has been used as an *in vitro* model of liver hepatocytes. These cells were cultured in DMEM (Dulbecco's Modified Eagle Medium, Cat N. 41965, GIBCO Invitrogen) high glucose (4500 mg/L) without sodium and magnesium completed with 50 mL of Foetal Clone II Serum (10% v/v) (Cat N. SH30066.03, HyClone), 5 mL of penicillin/streptomycin (1% v/v) ($10^4$ Units/mL, Cat N.15140, GIBCO Invitrogen) and 5 mL of non-essential amino acids (1% v/v) (Cat N. 11140, GIBCO Invitrogen). The cells were maintained as described below (see **Sections 2.2** and **2.3**).

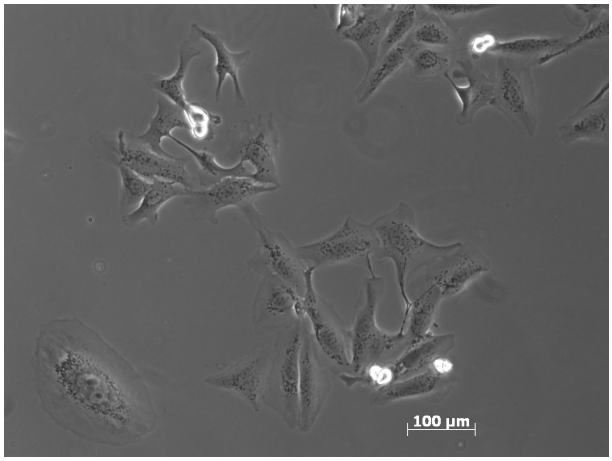


**Figure 2.5: HepG2 cells in culture (100X magnification at the optical microscope) (NBS, IHCP, JRC).**

### *2.1.6 MDCK* (source: European Collection of Cell Culture)

The MDCK Madin Darby Canine Kidney cells are used to model the impact of NPs on the kidney. These cells were cultured in DMEM (Dulbecco's Modified Eagle Medium, Cat N. 41965, GIBCO Invitrogen) high glucose (4500 mg/L) without sodium and magnesium completed with 50 mL (10% v/v) of Foetal Bovine Serum (Australian origin, Cat N. 10099-141, GIBCO Invitrogen), 6 mL of L-glutamine (2 mM) (Cat N. 25030, GIBCO Invitrogen) and 5 mL of penicillin/streptomycin (1% v/v) ($10^4$ Units/mL, Cat N.15140, GIBCO Invitrogen). The cells were maintained as described below (see **Sections 2.2** and **2.3**).

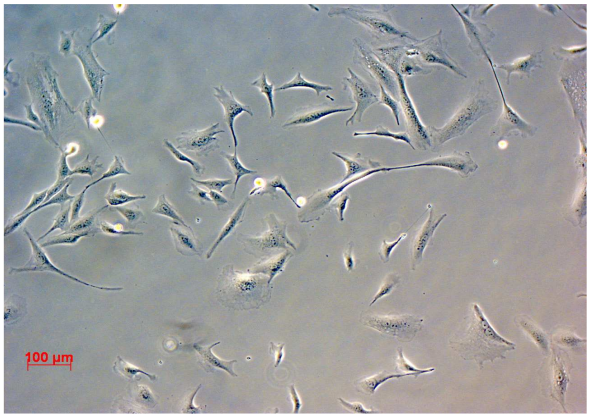


**Figure 2.6: MDCK cells in culture (100X magnification at the optical microscope) (NBS, IHCP, JRC).**

## 2.2 Cell line maintenance

All cell lines were maintained in culture under standard conditions (37°C, 5% $CO_2$, 90% humidity) in an incubator (HERAEUS, Hera cell 150, ThermoElectron Corporation, Germany) and sterile conditions were preserved by performing every step under a laminar flow biological hood (BIOAIR S@femate 1.2, EuroClone Division, Italy). The cells were sub-cultured twice a week. To aid the detachment of cells from the bottom of a 75 $cm^2$ culture flask (Cat N. 430641, Corning plastic) using Trypsin-EDTA (Cat N. 25300, GIBCO Invitrogen), the culture medium was removed and cells were washed twice with 10 mL of PBS (Phosphate Buffer Saline, 1X, without calcium, magnesium and sodium bicarbonate, Cat N. 20012, GIBCO Invitrogen) to remove the $Ca^{2+}$ and $Mg^{2+}$ ions involved in integrin-based binding. Cells were detached by adding 1 mL of Trypsin-

EDTA to the culture flask and incubating this for a period of either 1 minute (A549, Balb3T3 cells) or 5 minutes (CaCo2, HaCaT, HepG2 and MDCK cells). The Trypsin-EDTA activity was stopped by harvesting the detached cells in 9 mL of fresh complete medium. An aliquot of 10 µL of the cell suspension was added to 90 µL of Trypan Blue dye (0.4% solution, CAS N. 72-57-1, Cat N.15250061 GIBCO Invitrogen) for cell counting in a Bürker chamber (0.0025 $cm^2$). The number of cells/mL was calculated using the following formula **(2.1)**:

$$\mathbf{N = \{[(a + b)/2]/ 9 \times 10^4 \times DF\}} \qquad \mathbf{(2.1)}$$

where:

**N** = Number of cells/mL

**a** = Number of cells counted in 9 squares of the first chamber

**b** = Number of cells counted in 9 squares of the second chamber

$\mathbf{10^4}$ = Conversion factor of the chamber volume

**DF** = Dilution factor of the cell suspension (usually equal to 10 or 2)

The required volume of cells was then taken directly from the cell suspension and cultured with 10 mL of complete culture medium.

### 2.3 Cell freezing and thawing procedures

***Freezing***. Cells were detached from the culture flask and re-suspended as described previously (see **Section 2.2**). After calculating the number of cells per mL, the number of cells in the total volume of the suspension was determined. In order to prepare each criovial (NUNC, Nalgene, Milan, Italy) with $10^6$ cells, 0.5 mL of cell suspension was added to 0.5 mL of freezing solution, composed of 80% v/v of complete medium, 10% v/v of serum and 10% v/v of filtered dimethyl sulphoxide (DMSO, CAS N. 67-68-5, Cat N. D5879-100mL, Sigma Aldrich). Every criovial was labelled to indicate the cell type, their number, passage and the date. The criovials were then frozen at –80°C and stored in liquid nitrogen until use.

***Thawing***. Criovials containing the cells to be used were drawn from the liquid nitrogen and heated to 37°C. The defrosted cells were then re-suspended in complete culture

medium in a 15 mL tube to a final volume of 10 mL. After 24 hours, the medium was replaced with 10 mL of fresh medium. When the cells reached 80% confluence in the culture flask, they were sub-cultured (as described in **Section 2.2**) three times before use in the cytotoxicity assays.

### 2.4 The basis for the *in vitro* toxicity assays

Incubation times of 24 and 72 hours were chosen for evaluating the cytotoxicity of $CoFe_2O_4$ and Ag NPs using the Colony Forming Efficiency (CFE) assay. These treatment times were chosen as they were involved in the following study of the NP-induced genotoxicity and cell transformation capacity assessed by Cytokinesis-Block Micronucleus assay (CBMN) and Cell Transformation Assay (CTA,) respectively.

Before starting the experiments on the $CoFe_2O_4$ NPs, however, the maximum dose of the NP dispersant, dialyzed diethylene glycol (DEG), was determined. The cytotoxicity induced by DEG was evaluated in all six cell lines using both NR and CFE, specifically for 0.05, 0.1, 0.5, 1, 1.5, and 2% v/v DEG concentrations and a 72-hour exposure time. Thus, it was possible to select the concentration range of NPs to be tested whilst avoiding false positives due to effects of DEG. In particular, the effects of P601 and P703 NPs were tested at concentrations ranging from 10 to 120 µM for cytotoxicity. More specifically, cytotoxicity was evaluated after 72-hour treatment of five cell lines (A549, CaCo2, HaCaT, HepG2, MDCK) with 10, 20, 40, 60, 80, 100 and 120 µM concentrations of NPs using NR, and 10, 20, 30, 40, 50, 60, 80, 100 and 120 µM concentrations of NPs using CFE. In parallel with these tests, cytotoxicity was also evaluated in mouse Balb3T3 fibroblasts using (i) NR after 72-hour treatment with 10, 20, 40, 60, 80, 100 and 120 µM concentrations of NPs, and (ii) CFE after both 72-hour treatment with 1, 5, 10, 20, 30, 40, 50, 60, 80, 100 and 120 µM concentrations of NPs, and 24-hour treatment with 1, 10, 60 and 120 µM concentrations of NPs. In addition, P601 and P703 NPs were tested from 1–60 µM for both cell transformation capacity (specifically on Balb3T3 after 72 hours of treatment at concentrations of 1, 5, 20 and 60 µM and assessed using CTA) and for genotoxicity (specifically on Balb3T3 after 24 hours of exposure at concentrations of 1, 10 and 60 µM and assessed using CBMN).

Controls of the dispersant were also considered for all Ag NPs studied. In the experiment done to assess the *in vitro* toxicity of Ag NPs using Balb3T3 fibroblasts, the chosen concentration range for cytotoxicity was 0.01–10 µM (specifically, the concentrations tested using CFE were 0.1, 0.5, 1, 5 and 10 µM for 24 hours of treatment and 0.01, 0.1, 0.5, 1, 2.5, 5 and 10 µM for 72 hours of treatment). The transformation capacity was tested on Balb3T3 cells at concentrations ranging from 0.5–5 µM (specifically, the concentrations tested using CTA were 0.5, 2.5 and 5 µM for 72 hours of treatment), whilst genotoxicity was tested at concentrations ranging from 1–10 µM (specifically, concentrations tested using CBMN and Balb3T3 were 1, 5 and 10 µM for 24 hours of treatment). The dose range of Ag NPs to be screened was chosen based on data available in literature for Ag NPs and $AgNO_3$. In particular, both *in vivo* and *in vitro* studies have described the effects induced by excessively high Ag NP doses, which are far likely to be encountered by humans in consumer and occupational environments (Johnston et al., 2010). A previous *in vitro* investigation of $AgNO_3$ cytotoxicity using CFE to evaluate concentrations of 1–100 µM of $AgNO_3$ incubated with Balb3T3 cells for 72 hours found a dose-effect curve with IC50 values corresponding to 11.2 µM and complete cell death at higher doses (Mazzotti et al., 2002).

The molarity of NPs test concentrations were calculated considering the molar NPs stock suspensions concentration, as stated by the supplier, according to the following formulas for the dilutions (**2.2 and 2.3**)

**Ci/Cf = DF** **(2.2)**

where:

**Ci** = Initial concentration (corresponding to stock or intermediate concentrations of NPs)

**Cf** = Desired or final concentration (corresponding to concentrations of NPs to be tested)

**DF** = Dilution factor

**Vf/DF = volume of NPs to be added to obtain the Cf** **(2.3)**

where:

**Vf** = Final volume (corresponding to 100 µL, 3 mL, 6 mL and 4 mL in the NR, CFE, CTA and CBMN experiments, respectively)

Moreover, for the highly concentrated NP stock suspensions (both $CoFe_2O_4$ P601 and P703, and Ag NM-300), intermediate NP suspensions in culture medium were prepared before preparation of the NP test suspensions. This approach was also used in the preparation of NP dilutions to be analysed in the physicochemical characterization experiments.

In addition, a working stock of the different cell lines to be used in the experiments was created from a master stock. Cells were maintained in culture for a maximum of 10–15 passages, after which they were disposed of and new cells were defrosted from the working stock for the next experiments. Defrosted cells were sub-cultured three times before starting toxicity experiments. This approach allowed different runs of the same experiment for each cell line to be compared. The Balb3T3 fibroblasts were sub-cultured only once before use in the CTA.

## 2.5 *In vitro* toxicity assays

### *2.5.1 Neutral Red uptake*

The Neutral Red (NR) assay is an *in vitro* colorimetric viability test, which exploits the ability of living cells to accumulate Neutral Red dye within their lysosomes. The NR is usually carried out with adherent cells. The NR dye can pass through the cell membrane and once inside the cell, can be accumulated in lysosomes (lysosomal pH < cytoplasmic pH) where it binds to the anionic sites of the lysosomal matrix (Griffon et al., 1995). Any modification of cellular or lysosomal membranes can cause irreversible lysosomal changes. The NR uptake and binding decrease when a xenobiotic induces such alterations in a cell. The amount of NR taken up by viable cells is measured by spectrometry at 540 nm; the absorbance values measured are directly proportional to the number of viable cells.

In order to perform the assay as accurately as possible, the optimized number of cells (**Table 2.1**) were seeded in 100 µL/well of fresh medium in a 96 well/plate (Cat n.353072, Falcon plastic).

Twenty four hours after seeding, the cells were treated with $CoFe_2O_4$ NPs test suspensions ranging from 10–120 μM (specifically 10, 20, 40, 60, 80, 100 and 120 μM; 4 replicates for each concentration). For each cell line, a control for the DEG effect (0.1% v/v of dialyzed DEG, corresponding to the percentage of DEG present in the maximum dose of $CoFe_2O_4$ tested) and a positive control ($Na_2CrO_4$ $10^{-3}$M, CAS N. 10034-82-9, Cat N. 013453, AlfaAesar, Johnson Matthey GmbH) were done in parallel. After an exposure time of 72 hours, the treatment was removed and every well washed twice with 100 μL/well of PBS without calcium or magnesium. A Neutral Red (CAS N. 553-24-2, Cat N. N4638-1G, Sigma Aldrich) 1:40 solution was freshly prepared in the respective complete culture medium (1 mL of Neutral Red in PBS, 2 mg/mL of PBS), 39 mL of complete culture medium) and 100 μL/well were added and incubated for 2 hours under standard conditions. The NR solution was then removed and every well washed twice with 100 μL of PBS to remove excess Neutral Red from the cells. Finally, 100 μL/well of bleaching solution (50% v/v ethanol, CAS N. 64-17-2, Cat N. 02860, Fluka), 49% v/v ultrapure water, 1% v/v acetic acid (acetic acid, glacial 99.8%, CAS N. 64-19-7, Sigma-Aldrich)) was added. After 20 minutes, the absorbance was measured by an Omega Spectrophotometer at a wavelength of 544 nm (λ = 544 nm). The results were expressed as percentage of dialyzed DEG control viability.

**Table 2.1: Number of cells seeded per well in the Neutral Red assay for an incubation period of 72 hours.**

| Cell line | Number of cells/well |
|---|---|
| A549 | 2500 |
| Balb3T3 | 5000 |
| MDCK | 2500 |
| CaCo2 | 5000 |
| HaCaT | 5000 |
| HepG2 | 5000 |

### *2.5.2 Colony Forming Efficiency*

The Colony Forming Efficiency (CFE) is a sensitive clonogenic assay that can be performed in different adherent cell lines, provided that the cells can form colonies because cytotoxicity is detected as inhibition of colony growth. The CFE was employed previously for the successful evaluation of the toxic effects induced both by chemicals and NMs (Ponti et al., 2009; Ponti et al., 2010).

On the first day, 200 cells (300 cells for A549) were seeded in 3 mL of fresh complete medium in each Petri dish (60 mm x 15 mm, Cat n. 353004, Falcon plastic) (3 replicates/concentration). After 24 hours of incubation, (37°C, 5% $CO_2$, 90% humidity), the treatment suspensions were added as aliquots to the cells (day 1). Concentrations of $CoFe_2O_4$ ranged from 10–120 µM (more specifically, 10, 20, 30, 40, 50, 60, 80, 100 and 120 µM concentrations of NPs were tested with 72 hours treatment of five cell lines (A549, CaCo2, HaCaT, HepG2, MDCK); in parallel, 1, 5, 10, 20, 30, 40, 50, 60, 80, 100 and 120 µM concentrations of NPs with 72-hour treatment, and 1, 10, 60 and 120 µM concentrations of NPs with 24 hour treatment were both tested using Balb3T3 fibroblasts). For each cell line, a control for the DEG effect (0.1% v/v of dialyzed DEG, corresponding to the percentage of DEG present in 120 µM of $CoFe_2O_4$ tested as a maximum dose) and a positive control ($Na_2CrO_4$ $10^{-3}$M, CAS N. 10034-82-9, Cat N. 013453, AlfaAesar, Johnson Matthey GmbH) were done in parallel. Cells were exposed to the treatment for 24 or 72 hours, after which the treatment was removed and replaced with complete culture medium. After 72 hours, cells were fixed and stained (days 8 or 9). A fixing solution of 10% v/v of formaldehyde (formaldehyde 37% v/v, CAS N. 50-00-0, Cat N. 252549, Sigma-Aldrich) in PBS was used, whilst a staining solution of 10% v/v of Giemsa (GIEMSA stain modified, Cat N. GS500-500mL, Sigma-Aldrich) in ultrapure water was prepared and filtered (NALGENE, Nalge Nunc International, U.S.A.). Dishes were air-dried before colony counting. The data obtained were used to define the dose-effect curve.

At the stereo microscopic level, the colonies from the cell lines used appeared to differ in morphology and dimensions (**Figures 2.7A -2.7F**).

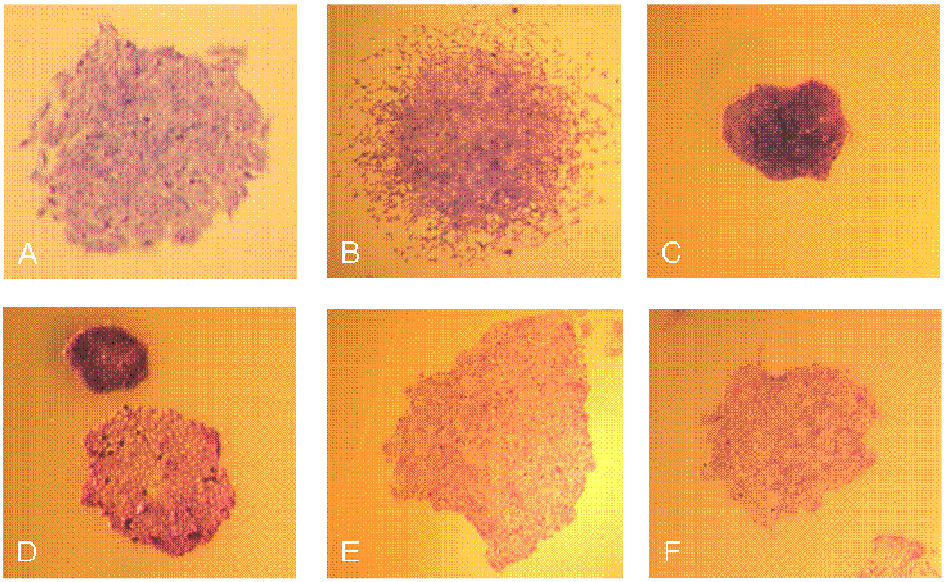


**Figures 2.7A, B, C, D, E and F: Images of colonies from negative controls at the end of a CFE assay: (A) A549 colonies (45X magnification), (B) Balb3T3 colonies (15X magnification), (C) CaCo2 colonies (45X magnification), (D) HaCaT colonies (45X magnification), (E) HepG2 colonies (15X magnification) and (F) MDCK colonies (15X magnification) (EC, JRC-Ispra, IHCP, NBS).**

Cytotoxicity induced by treatment with $CoFe_2O_4$ NPs for 24 hours (at 1, 10, 60 and 120 µM) was additionally investigated on Balb3T3 cells using CFE, an essential step in determining the dose-range for a further genotoxicity study with the Cytokinesis-Block Micronucleus assay (CBMN).

The CFE was also used as an *in vitro* assay to detect the cytotoxicity induced in Balb3T3 mouse fibroblasts by Ag NPs at concentrations of 0.01–10 µM (specifically 0.01, 0.1, 0.5, 1, 2.5, 5 and 10 µM) and 0.1–10 µM (specifically 0.1, 0.5, 1, 5 and 10 µM) for treatment times of 72 and 24 hours, respectively. The CFE protocol employed was the same as described previously (see **Section 2.5.2**) and appropriate controls for the Ag NPs dispersant were done.

The CFE results were expressed as CFE% of the solvent control (mean of three independent experiments) ± SEM (standard error of the mean = standard deviation/√number of replicates) following formula (**2.4**)

**CFE% (of solvent control) = (A/ B) x 100** **(2.4)**

where:

**A** = Number of colonies counted per dish

**B** = The average of colonies counted in three replicates of the solvent control

Cytotoxicity data produced by NR and CFE were both statistically analyzed using one-way ANOVA using GraphPadPrism4 statistical software (GraphPad Inc., CA, USA) to highlight results significantly different ($p<0.05$) from the respective solvent control. For more information, please see **Section 2.6**.

### *2.5.3 Cell Transformation Assay*

The Cell Transformation Assay (CTA) is a two-step assay because the procedure requires a cytotoxicity assay (CFE) to be performed in parallel. This simple assay allows the transformation capacity of different chemicals and NMs to be assessed without using time-consuming and expensive procedures. Here, the CTA was performed using Balb3T3 mouse fibroblasts.

On Day 0, 2 x $10^4$ cells were seeded in 6 mL of complete fresh medium (MEM completed as described in **Section 2.1.2**) in each Petri dish (100 mm x 20 mm, Cat n. 353003, Falcon plastic) (5 replicates/concentration). After 24 hours, the chosen concentrations of treatment (corresponding to 1, 5, 20, 60 µM for $CoFe_2O_4$ NPs, and 0.5, 2.5 and 5 µM for Ag NPs) were achieved by adding aliquots of NP preparations. Cells were either untreated or treated with a well-known carcinogenic compound (3-methylcholanthrene, MCA, CAS N. 56-49-5, Cat N.213942-100mg, Sigma-Aldrich stock solution prepared in DMSO at the concentration of 0.8 mg/mL) (4 µg/mL final concentration) as negative and positive controls, respectively. In addition, a control for the dispersant effect was done (dialyzed DEG for $CoFe_2O_4$ NPs and the appropriate dispersants for Ag NPs) for each NP preparation.

After 72 hours of exposure (Day 4), the treatment was removed and replaced with fresh complete medium, DMEM/F12 (Dulbecco's modified Eagle's medium/F12, Cat. N. 31330-038, GIBCO Invitrogen) with high glucose (3151 mg/L), L-glutamine (365 mg/L) and sodium bicarbonate (1200 mg/L) levels, and supplemented with 2% v/v Foetal Bovine Serum-Australian Origin (Cat. N. 10099-141; Lot N. 6792117Y, GIBCO Invitrogen), 2 µg/mL Insulin (Cat. N. I5500, Sigma-Aldrich) and 1% v/v antibiotics ($10^4$

Units/mL penicillin and $10^4$ µg/mL streptomycin, Cat. N. 15140-122; Lot N. 708414, GIBCO Invitrogen).

The medium was then changed twice a week. During the last week of the CTA (days 24–31), the culture medium was left unchanged so that after 5 weeks (Day 31), cells were fixed with 10% v/v of formaldehyde in PBS. Cells were then stained with a 10% v/v Giemsa solution in ultrapure water for 1 hour. The dishes were air-dried and studied at the stereo microscopic level to detect and quantify only type III foci, as described by the International Agency for Cancer Research Working-Group (IARC/NCI/EPA Working-Group, 1985).

Transformation results were expressed as Transformation frequency (Tf) (average of three independent experiments) ± SEM using the following formula (**2.5**):

$$\mathbf{T_f = A/B} \qquad \mathbf{(2.5)}$$

where:

**A** = Total number of type III foci per treatment

**B** = Number of surviving cells

The number of surviving cells for each treatment and control was calculated using the following formula (**2.6**):

$$\mathbf{Surviving\ number\ of\ cells = [(2x10^4)\ x\ 5x\ CFE\%]/100\ x\ (Plating\ Efficiency/100)} \qquad \mathbf{(2.6)}$$

where:

**$2x10^4$ =** Number of cells seeded per dish

**5** = Number of replicates per treatment

**CFE**% = see formula (**2.4)**

**Plating Efficiency** = (Number of colonies formed in the control/Number of cells seeded in one CFE dish) x 100.

Data were analysed and statistical significance was calculated using Fishers' exact test (http://www.langsrud.com/fisher.htm) to highlight results significantly different ($p<0.05$) to the respective solvent controls. For more information, please see **Section 2.6**.

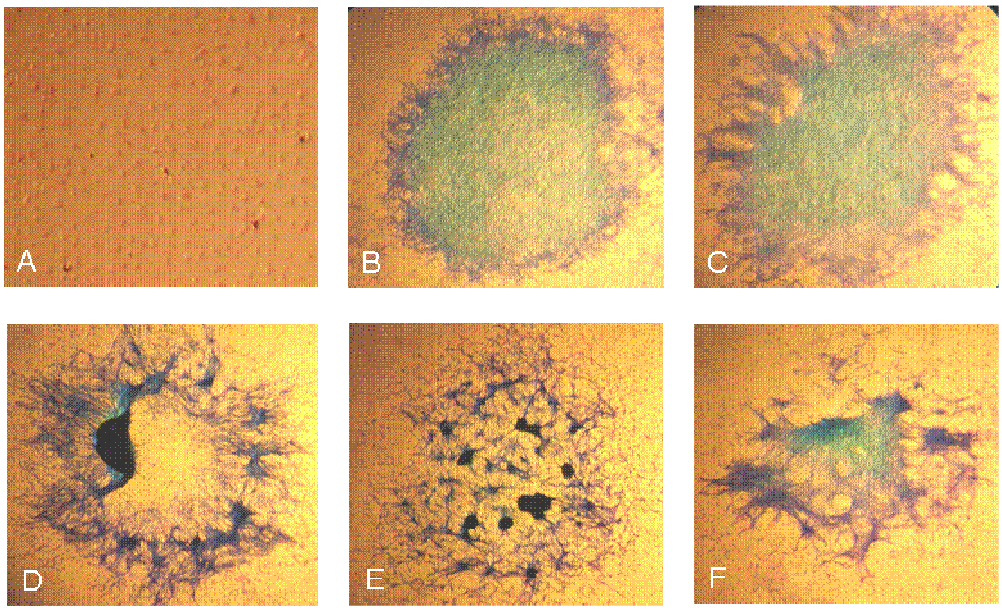


**Figures 2.8A, B, C, D, E and F: Normal and morphologically transformed Balb3T3 mouse fibroblasts as seen at the stereo microscopic level after the CTA: (A) negative control cells (45X of magnification) and some examples of type III foci from positive control dishes (B, C, D, E and F) (15X magnification). In the negative control dishes, cells grow in a monolayer as they retain their morphology and contact-inhibition. When cells are transformed into tumorigenic cells, they lose contact-inhibition and begin to grow spindle shaped with no ordered orientation and as a multilayer (EC, JRC-Ispra, IHCP, NBS). Only type III foci are scored because these alone can induce tumour formation in nude mice with an 85% frequency (Saffiotti et al., 1984; IARC/INCI/EPA, 1985).**

### *2.5.4 Cytokinesis-Block Micronucleus assay*

The Cytokinesis-Block Micronucleus assay (CBMN) is a reliable standard and reproducible assay for testing genotoxicity in both human and mammalian cells. When counting micronuclei, only once-divided, binucleated cells are considered. These are obtained by blocking cytokinesis with cytochalasin B, which specifically inhibits the assembly of the microfilament ring required for completion of cytokinesis. Micronuclei are scored only in binucleated cells in order to avoid the effects caused by suboptimal or altered cell division kinetics (Fenech, 2007).

On Day 0, 3 x $10^5$ Balb3T3 mouse fibroblasts were seeded in 4 mL of complete medium in each well (1 replicate/concentration) of a 6 well/plate (Cat n. 3506, Corning plastic).

Twenty four hours after seeding (Day 1), cells were treated with NP suspensions and incubated for 24 hours (concentrations of 1, 10, 60 µM and 1, 5, 10 µM were used for $CoFe_2O_4$ and Ag NPs, respectively). As a positive control, 0.5 µM of mitomycin C (MMC, CAS N. 50-07-7, Cat N. L01DC03, Kyowa Italiana Farmaceutici) was used and dispersant controls were done for all NPs investigated. On Day 2, the treatment was removed and each well was washed twice with Phosphate Buffer Saline (PBS). In order to block cell division, 4.5 µg/mL of cytochalasin B (cytochalasin B from *Dreschslera dematioidea*, CAS N. 14930-96-2, Cat N. C6762-5MG, Sigma-Aldrich) were then added to 4 mL of fresh complete culture medium per each well. After 24 hours of incubation (Day 3), cells were detached and harvested in PBS. The cell suspensions were centrifuged (250 G) and the cell pellets were treated first with a prefixing solution (3:5) followed by a fixing (6:1) solution prepared with different methanol (CAS N. 67-56-1, Lot N. 34885, Sigma-Aldrich): acetic acid (acetic acid, glacial 99.8%, CAS N. 64-19-7, Sigma-Aldrich) ratios. The solutions obtained were dropped onto glass slides and dried overnight at room temperature. The slides (two replicates for each sample) were stained with a 2% v/v of Giemsa solution in ultrapure water and air-dried.

Binucleated cells with micronuclei were scored under an optical microscope, and the NDI (Nuclear Division Index) was calculated using the following formula (**2.7**):

$$\mathbf{NDI = [(MNx1)+(BNx2)+(PNx3)]/500} \qquad \mathbf{(2.7)}$$

where:

**MN** = Mononucleated cells

**BN** = Binucleated cells with or without micronuclei

**PN** = Polynucleated cells.

Statistical analysis was conducted using the Fisher exact test (http://www.langsrud.com/fisher.htm) to identify statistically significant differences ($p<0.05$) between solvent control and NP-treated samples. For more information, please see **Section 2.6.**

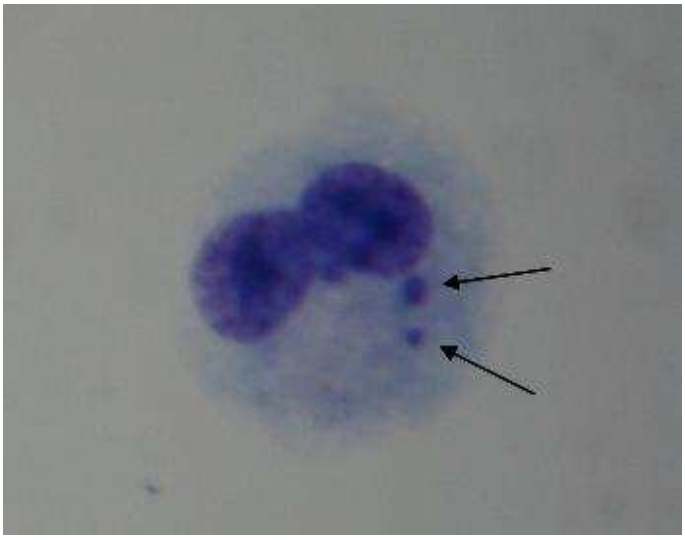

**Figure 2.9: A typical binucleated, micronucleated Balb3T3 cell after 24-hour exposure to mytomicin C (0.5 µM) as a positive control. The black arrows highlight micronuclei in the cytosol (400X of magnification, EC, JRC-Ispra, NBS). In this study, the genotoxic potential of $CoFe_2O_4$ and Ag NPs in Balb3T3 mouse fibroblasts was indicated by the induction of micronuclei formation.**

## 2.6 Statistical data analysis

A description of the statistics used in the analysis of toxicity data obtained by NR, CFE, CTA and CBMN now follows. Computer programmes were used for all the statistical analyses performed.

### 2.6.1 Statistical methods

***Student t-test.*** The Student t-test is a parametric test commonly used to compare the means of two groups (e.g., untreated/control group vs. treated group) when data follow a Gaussian (or normal) distribution. This distribution is symmetrical and the data spread around the true value is caused by random effects (e.g., imprecise pipetting, use of different media/reagents, etc.). If the data to be analysed are not Gaussian-distributed, they can be normalized before the statistical analysis by mathematical transformation that limits data to a defined interval of values (e.g., 0-100). For example, data related to the "control/untreated" group can be defined as 100, while those related to a "treated" group can be expressed as percentage of the control. Therefore, raw data are not necessary for this statistical method and statistical calculations can be made using the mean, standard error of the mean (SEM) and sample size for each group.

There are two types of t-test: the "unpaired t-test", used when the two data groups to be compared are independently collected, and the "paired t-test", which is used to analyse two groups of data with matched samples (e.g., before and after treatment/measurement) (Motulsky, 1995). Here, the unpaired t-test was used to compare the CFE% (of the solvent control) values obtained by treating Balb3T3 cells with $CoFe_2O_4$ NPs for 24 and 72 hours, and the CFE% (of the negative control) values from a previous study where the same cell line was treated with soluble $CoCl_2$ for the same exposure time (Ponti et al., 2009). More specifically, this statistical analysis was done to calculate the probability that the difference in the CFE% values observed between the two groups (NP-treated and ion-treated cells, respectively) were due to chance.

Before the statistical analysis, the mean CFE values (of at least three runs in total) related to $CoFe_2O_4$ NPs were normalized and expressed as a percentage of the CFE solvent control mean to obtain CFE% values. Only after mathematical transformation these data were statistically compared using the unpaired t-test for CFE% values (of at least three runs in total) corresponding to concentrations of $CoCl_2$ similar to those of Co ions released by the $CoFe_2O_4$ NPs. Results with $p<0.05$ were considered to be statistically significant with respect to the $CoCl_2$ treatment and meant that the probability of a difference between NPs and ion treatment due to chance was less than 5%.

***One-way ANOVA.*** It has been suggested that when more than two groups of data are collected, they should be compared using one-way ANOVA instead of separate t-tests for each pair of groups. In fact, the one-way ANOVA analysis also allows the comparison of more than two groups with the same mean, thereby avoiding the 5% chance that each comparison result is significant, as would be found after separate t-test comparisons.

The one-way ANOVA is a parametric test, which means that data to be analysed (as for the t-test) follow a Gaussian distribution. As described above for the Student t-test, data that are not Gaussian distributed can be normalized to approximate a Gaussian distribution before statistical analysis. If the collected data are matched (e.g., they represent measures before, during and after treatment), the repeated-measures ANOVA should be used so that the difference between the ordinary and repeated-measures ANOVA resembles that of the unpaired and paired t-test.

The Bonferroni post-test is one of the multiple comparison posts-tests available after ANOVA to compare all pairs of groups (Motulsky, 1995). The one-way ANOVA with the Bonferroni post-test was chosen to calculate the statistically significant differences between treatment and solvent control values (normalized absorbance in NR and CFE% in CFE experiments, respectively) and to compare cytotoxicity results obtained from different cell lines (NR and CFE with $CoFe_2O_4$ NPs). All data were normalized prior to statistical analysis. Results with $p<0.05$ were considered to be statistically different from those of the solvent control, meaning that the probability of a difference between NP-treatment and solvent control being due to chance is less than 5%. This statistical method was used previously by Ponti et al. (Ponti et al., 2010) with the same experimental procedures and objectives as described here.

***Fisher's exact test.*** The Fisher's exact test is a non-parametric test and can, therefore, be used when data do not follow a Gaussian distribution. It is used to compare two unpaired groups when analysing moderate-sized data (<100) (Motulsky, 1995). This statistical analysis was used to determine if the morphological cell transformation and the micronuclei observed after NP-treatment in the CTA and the CBMN assays, respectively, were significantly different to those observed in the solvent control.

In particular, morphological transformation (CTA) data were statistically analysed to compare both the number of surviving cells (calculated using **formula 2.6**) and the respective total number of type III foci formed in the solvent control to the corresponding values of the NP treatment. The statistical significance of genotoxicity results (CBMN) was calculated by comparing the total number of binucleated cells with micronuclei found per 1000 binucleated cells scored in the solvent control to those found in the NP treatments. Results with $p<0.05$ were considered to be significantly different from those of the solvent control, indicating that the probability of a difference between NP treatment and solvent control due to chance is less than 5%. This statistical method was used previously by Ponti et al. (Ponti et al., 2010) with the same experimental procedures and objectives as described here.

### 2.6.2 Experimental procedures

Here, each assay (NR, CFE, CTA and CBMN) was performed at least three times (three independent experiments) and replicas for each concentration (or experimental point) were done in every experiment (e.g., 4 wells/concentration for NR, 3 Petri dishes/concentration for the CFE, 5 Petri dishes/concentration for the CTA, 2 slides/concentration for the CBMN).

Data obtained from the NR and CFE experiments were normalized prior to statistical analysis. In particular, the mean absorbance of the blank was subtracted from the absorbance of the solvent control and treatments values (raw data-blank average) in the NR. The absorbance was then expressed as a percentage of the solvent control average; these absorbance values were then analysed using one-way ANOVA. In the CFE experiments, colonies scored in each dish were expressed as a percentage of the average of colonies in the solvent control (CFE% of solvent control) and these values were used for the ANOVA calculations.

Data from the CTA and CBMN experiments were not normalised here. The surviving number of cells (calculated using **formula 2.6**) together with the total number of type III foci scored in each concentration, and the number of binucleated, micronucleated cells together with the total number of binucleated cells scored per slide, respectively, as determined using CTA and CBMN, were the input data for the Fisher's analysis. The statistical significance with respect to the proper solvent control was considered to be $p<0.05$ and indicated in graphs by star symbols (e.g., $*p<0.05$).

**Table 2.2: A summary of statistical methods and experimental procedures used to analyse toxicity data.**

| Assay | Experiments | Replicas | Normalization | Statistics | Data input | Data output |
|---|---|---|---|---|---|---|
| NR | 3 | 4 | yes | ANOVA | Normalized absorbance | $p<0.05$ |
| CFE | 3 | 3 | yes | ANOVA, t-test | CFE% | $p<0.05$ |
| CTA | 3 | 5 | no | Fisher's | Surviving cells, total type III foci | $p<0.05$ |
| CBMN | 3 | 2 | no | Fisher's | Binucleated micronucleated cells, total binucleated cells scored | $p<0.05$ |

# Appendix A: Materials and Methods for the physicochemical characterization of NPs

## A. 1 Nanoparticles tested

### *A.1.1 Cobalt ferrites nanoparticles ($CoFe_2O_4$ NPs)*

The following uncoated/functionalized $CoFe_2O_4$ NPs were used in this study:

**P601**: supplied by Colorobbia (Colorobbia S.p.A., Vinci, Italy) and made available as a 120 mM suspension of $CoFe_2O_4$ in 100% diethylene glycol (DEG); particle sizes provided by the supplier on the material data sheet and determined using Dynamic Light Scatter (DLS) were 28.81 nm for particles in DEG and 13.56 nm for particles in ultrapure water;

**P703**: supplied by Colorobbia (Colorobbia S.p.A., Vinci, Italy) and made available as a 118 mM suspension of $CoFe_2O_4$ in 100% DEG; particle sizes provided by the supplier on the material data sheet and determined using DLS were 83.22 nm for particles in DEG and 63.62 nm for particles in ultrapure water.

Dialyzed DEG was also provided by the NP supplier to be used as a control for the NP dispersant in the biological experiments. Testing the dialyzed DEG prior to the NPs allowed the concentration range of NPs to be selected for the study, thereby avoiding false positives due to potential effects of DEG.

Since there is still no consensus on how to express nanomaterial (NM) concentrations, a selection of the possible methods for P601 and P703 NPs are shown in **Table B.3**, found in "Appendix B: Results for the physicochemical characterization of NPs", **Section B.1.3**.

### *A.1.2 Silver nanoparticles (Ag NPs)*

The following uncoated/functionalized Ag NPs were used in this study:

**NM-300**: supplied by OECD and made available as an aqueous dispersion containing stabilizing agents, 4% each of polyoxyethylene glycerol trioleate and polyxyethylene (20) sorbitan mono-laurate (Tween 20), 10.16% w/w of silver ($10^5$ ppm of silver, corresponding to 930 mM). The particle size provided by the supplier on the material data sheet and determined using Transmission Electron Microscope (TEM) was <20 nm;

**Ag 44 nm**: synthesized in the JRC chemistry laboratory by Thierry Darmanin, Ph.D., and made available as an aqueous dispersion containing 0.25% w/v D-lactose as a stabilizing agent and 1 mM of silver. The particle size provided on the material data sheet and determined using DLS was 44 nm;

**Ag 84 nm**: synthesized in the JRC chemistry laboratory by Thierry Darmanin, Ph.D., and made available as an aqueous dispersion containing 0.18% w/v D-(+)-maltose as a stabilizing agent and 1 mM of silver. The particle size provided on the material data sheet and determined using DLS was 84 nm;

**Ag 100 nm**: synthesized in the JRC chemistry laboratory by Thierry Darmanin, Ph.D., and made available as an aqueous dispersion containing 0.15% w/v L-(+)-arabinose as a stabilizing agent and 1 mM of silver. The particle size provided on the material data sheet and determined using DLS was 100 nm.

The NP dispersants used for each Ag NP were also provided to be used as controls for dispersant toxicity in the biological experiments, thereby avoiding false positive results due to dispersant effects.

**Table B.12**, found in "Appendix B: Results for the physicochemical characterization of NPs", **Section B.2.4**, shows the different ways in which Ag NP concentrations are tested.

The terms "NP dispersant" and "NP solvent" used in this study refer to both types of NPs studied ($CoFe_2O_4$ and Ag), and are synonyms for the liquid phase free of NPs in a NP stock suspension.

**Section 2.4** "Premise to the *in vitro* toxicity assays" of "Chapter 2: Materials and Methods" describes how the molarity of the NP dilutions to be tested for the physicochemical characterization of NPs was calculated.

## A.2 Characterization of the NPs

### *A.2.1 Zeta Potential assessment using Dynamic Light Scattering*

When a particle is dispersed in an aqueous solution, charge can distribute on its surface. The charged particle can then generate an ion distribution in the surrounding region, leading to an increase of oppositely charged ions next to its surface. The film of liquid around the particle is composed by two regions: the inner, so-called "Stern layer" where

ions are strongly bound, and an external, so-called "diffuse layer", where interactions are weaker. The combination of these regions results in a double electrical layer around each particle. A theoretical boundary, in which ions and particles form stable entities, can be identified on the diffuse layer; when the particle moves, ions found in this area move together with the particle, whilst ions outside this region do not. This boundary is called "slipping plane". The potential corresponding to this boundary is known as the Zeta potential (Z-potential).

Measurements of the Z-potential provide information about chemical and physical characteristics of particles in suspension. A high Z-potential value (more positive than +30 mV or more negative than -30 mV) is usually associated with moderate or high dispersion stability since electrostatic repulsions between the particles are strong. In contrast, a low Z-potential value (between -30 and +30 mV) indicates aggregate/agglomerate formation, causing colloidal instability (http://www.malvern.com/LabEng/technology/zeta_potential/zeta_potential_LDE.htm, last accessed in September 2011).

In general, the Z-potential is useful in determining the surface charge of NPs suspended in ultrapure water. The surface charge should change when NPs are in culture medium (with or without serum).

Here, samples were prepared by diluting aliquots of $CoFe_2O_4$ P601 and P703 NP stock suspensions up to 2 mL to achieve a concentration of 100 µM in ultrapure water and basal media (HAM, MEM and DMEM; for more information on media, please see **Section 2.1,** "Cell lines, cell culture and media") without serum. Similar samples of Ag NPs in ultrapure water were prepared and measured.

All samples were vortexed and then immediately tested using DLS (Nano-ZS, Malvern Instruments).

Samples were prepared by Francesca Broggi and data were generated by Guido Giudetti, Ph.D.

### *A.2.2 Size distribution assessed using Dynamic Light Scattering*

Particles in suspension move by Brownian motion, which is the result of the particles' thermal energy and also occurs when particles collide with solvent molecules that are also moving. Particles or molecules can scatter light when illuminated by a laser. The fluctuations of the light intensity vary depending on particle size. In particular, after collision with solvent molecules, smaller particles can move faster than larger particles. Analysis of the fluctuations of the light intensity allows the rate of particles and thus their size to be determined using the Stokes-Einstein relationship (http://www.malvern.com/LabEng/technology/dynamic_light_scattering/dynamic_light_scattering.htm, last accessed in September 2011).

Dynamic Light Scattering can be used to measure the particle hydrodynamic diameter, which corresponds to that of a sphere with the same translational diffusion coefficient. The size, core and surface structure of a particle together with the type of solvent used all influence the translational diffusion coefficient. Therefore, the particle size measured with DLS can be larger than that determined by electron microscopy. In fact, in the latter procedure, particles are removed from the solution and analysed as dried samples. The DLS technique was used to determine the size distribution profile of suspensions of the NPs investigated here in different solvent/media. Together with the DLS technique, therefore, the aggregation/agglomeration state of the NP preparations could be checked.

Firstly, DLS measurements were made for HAM, MEM, DMEM, dialyzed DEG and the six complete culture media, in order to verify the absence of NPs and to exclude any background. Samples of P601 and P703 NPs prepared in basal and completed Balb3T3 media, which were considered as baseline references of the behaviour of NPs as a function of time under standard cell culture conditions (37°C, 5% $CO_2$, 90% humidity), were measured after 0, 24 and 72 hours of incubation. These media were chosen as reference points, since Balb3T3 cells are used in the subsequent Cell Transformation Assay (CTA) and the Cytokinesis-Block Micronucleus assay (CBMN).

The P601 and P703 NP stock suspensions were then diluted to obtain a final concentration of 2% v/v in dialyzed DEG and of 100 µM in ultrapure water, basal media without serum (HAM, DMEM) and complete media (for A549, CaCo2, HaCaT, HepG2 and MDCK cells culture; please see **Section 2.1** "Cell lines, cell culture and media).

These samples were analysed after 72 hours of incubation under standard culture conditions and vortexed before analysis using DLS.

The results were analysed with respect to the correlogram, the polydispersity index (PdI) and the comparison of particle size measured by intensity, and the respective particle size measured by volume. Conventionally and in accordance to the International Organization for Standardization directive ISO 22412:2008(E) for Particle size analysis-Dynamic Light Scattering (DLS), data with PdI $\geq$0.1 are considered to be unreliable because the samples are too polydispersed.

Dynamic Light Scattering measurements were also made for Ag NP preparations in ultrapure water, Phosphate Buffer Saline solution (PBS), MEM basal medium and Balb3T3 complete culture medium. All Ag NP samples were analysed at time 0 hours and even after 24 and 72 hours of incubation under standard culture conditions (37°C, 5% $CO_2$, 90% humidity) in the Balb3T3 culture medium.

All the samples were tested using a DLS instrument (Nano-ZS, Malvern Instruments). The refractive index and absorption coefficient were set at 1.71 and 0.90 for $CoFe_2O_4$ NP samples, respectively, and at 0.560 and 4.27 for Ag NP samples, respectively (as suggested by the user manual from Malvern Instruments).

Samples were prepared by Francesca Broggi and data were generated by Guido Giudetti, Ph.D.

### *A.2.3 Size distribution by Nanoparticle Tracking Analysis*

The Nanoparticle Tracking Analysis (NTA) is a useful technique that allows the hydrodynamic size of NPs to be measured in a liquid environment. The basic principle is that the NPs in a liquid medium are subject to Brownian motion; when a laser illuminates the NPs, the intensity of the particle-scattered light can be used to analyse the path followed by the particles and subsequently to determine the hydrodynamic size of the NPs. The advantage of NTA compared to DLS is its ability to track and size single NPs or single aggregates/agglomerates: moreover, signals arising from smaller NPs are not hidden by those of larger NPs (http://www.nanosight.com, last accessed in September 2011).

The Ag NP samples in ultrapure water were vortexed and immediately analysed with the instrument set at standard acquisition parameters (Nanoparticle Analysis System, LM20-20X-FT, Nanosight Salisbury, UK).

Samples were prepared by Francesca Broggi and data were generated by Guido Giudetti, Ph.D.

### *A.2.4 Quantification of cobalt and silver in stock suspensions and determination of the release of ions by Inductively Coupled Plasma Mass Spectrometry*

Inductively Coupled Plasma Mass Spectrometry (ICP-MS) is a sensitive technique that allows the presence of inorganic substances in a sample to be determined with a sensitivity in the range of parts per billion (ppb = parts per billion, which correspond to μg/L).

Here, the ICP-MS technique was used to identify and quantify possible metal impurities in the stock suspensions of NPs and to quantify cobalt (Co) and silver (Ag) in their respective stock suspensions. This technique was also useful when measuring the presence of $Co^{2+}$ or $Ag^{+}$ ions released by NPs in culture medium after different incubation times relevant to the toxicity experiments, and detected these ions as Co or Ag following separation from NPs by centrifugal filtration.

The $CoFe_2O_4$ P601 and P703 NP preparations of 20, 40, 60, 120 μM (2 mL samples for each concentration) in MEM and Balb3T3 culture medium were incubated for 0 and 72 hours under standard cell culture conditions (37°C, 5% $CO_2$, 90% humidity) in an incubator (HERAEUS, Hera cell 150, ThermoElectron Corporation, Germany). Similar samples of P601 and P703 NPs at concentrations of 1, 10 and 60 μM were also incubated for 0 and 24 hours. After incubation, two fractions were prepared for each sample: an unfiltered aliquot (1 mL) and a filtered aliquot (1 mL). The unfiltered samples were used to quantify the total amount of NPs diluted from the stock suspension, as an indicator of the pipetting accuracy. The filtered samples were obtained by centrifugation (3000 rpm corresponding to 1810 G for 20 min) in 4 mL membrane tubes ($10^4$ K, Amicon® Ultra-4, Millipore) and the filtered liquids were analysed. Prior to the ICP-MS analysis (PerkinElmer, ELAN DRC II SCIEX™ - Ontario, Canada), an aliquot of each $CoFe_2O_4$

NP sample was mineralized with concentrated nitric acid (nitric acid ultrapure RS, 408051, Carlo Erba) and then suitably diluted with ultrapure water to achieve a final acidity of 5% and a maximum Co concentration <100 ppb.

An example of a nominal 60 µM Co sample preparation (not-filtered):

Aliquot from the sample = 50 µL

Nitric acid added = 500 µL

Final volume = 10 mL

Obtained dilution = 200.

Results expressed as Co ppb were converted into Co µM concentration.

Toxicity data were elucidated by determining the release of ions. Here, ion release was calculated as the difference between the amount of Co detected in filtered fractions at 24 or 72 hours and the amount of Co detected at time 0.

A similar approach was employed in the Ag NP study in order to quantify Ag in the NP stock suspensions and detect all impurities present. The $Ag^+$ ion leakage was investigated by analysing 10 µM Ag NP preparations in MEM basal medium and Balb3T3 complete culture medium after different incubation times (0, 24 and 72 hours) under standard culture condition (37°C, 5% $CO_2$, 90% humidity). For all Ag NPs samples, 1 mL was mineralized with concentrated nitric acid and digestion was achieved using a microwave oven (CEM Explorer) at a temperature of 200°C and pressure of 140 PSI (Pounds per Square Inch, 1 PSI = 0.069 bar) maintained for 5 minutes. The Ag NP samples were then analysed using ICP-MS (Agilent Technologies, 7700 series, Canada, for Ag NPs analyses).

Samples were prepared by Francesca Broggi and data were generated by Fabio Franchini, Ph.D.

### *A.2.5 Sedimentation assessed using UV-Vis Spectroscopy*

The UV-Vis spectroscopy is a simple technique that was used to obtain information on the sedimentation of NP preparations in culture medium during a test period of 72 hours. In fact, considering the **Lambert-Beer law (A.1):**

$$\mathbf{A=\varepsilon_{\lambda}Cl} \qquad \textbf{(A.1)}$$

where:

A = Absorbance

$\boldsymbol{\varepsilon_{\lambda}}$ **=** Molar absorption coefficient

**C =** Molar concentration

**l = S**ample depth,

the absorbance measured at a certain height of the sample or liquid column is considered to be directly proportional to the concentration of the sample in that region. Therefore, any changes in the concentration at a certain height of a sample over a chosen time can be detected.

The sedimentation/precipitation of the NPs was determined by preparing samples of both $CoFe_2O_4$ P601 and P703 NPs by diluting aliquots of the stock suspensions in Balb3T3 complete culture medium w/o Phenol Red (thus avoiding interference in the wavelength range of 400-700 nm) to a final concentration of 60 µM. The UV-Vis spectra were recorded every 30 minutes over 72 hours (144 total cycles) using spectrophotometery (Nicolet Evolution 300, Thermo Electron Corporation) at constant room temperature. The sample size of both P601 and P703 NPs for all UV-Vis measurements was always 1 mL.

Samples were prepared by Francesca Broggi and data were generated by Hubert Rauscher, Ph.D.

### *A.2.6 NP imaging using Scanning Electron Microscopy*

The Scanning Electron Microscopy (SEM) allows heterogeneous organic or inorganic objects with dimensions in the range of a nanometer to micrometer to be observed and characterized. Typical SEM images are three-dimensional and are obtained by irradiating the sample with a finely focused, high energy electron beam. The electrons of the beam interact with the sample atoms, scanning it and thus producing signals that arise primarily from secondary electrons other than x-rays and photons of various energies. These signals are converted into images containing information on the surface topography or the

composition of the sample (Goldstein et al., 2003). The sample is usually prepared completely dry, since the specimen chamber is at high vacuum.

The Ag NP samples of 100 μM prepared in ultrapure water were investigated using this imaging technique. The $SiO_2$ wafers were previously cleaned via 30 minutes of ultrasonication in ethanol followed by 30 minutes of sterilization under a UV lamp. A solution of 1% v/v 3-aminopropyltriethoxysilane (APTS, CAS N. 919-30-2, Sigma Aldrich) in ethanol was freshly prepared and used to incubate $SiO_2$ substrates for 30 minutes. The substrates were then rinsed twice in ethanol (10 minutes per wash). The Ag NP samples were spotted on these surfaces and after 5-10 minutes, any drops still remaining were blown away with nitrogen at room temperature.

The preparations were studied in the Scanning Electron Microscope (FEI NOVA nanolab 600I) using relatively low voltages (5 KV) to avoid excessive scattering and enabling the in-lens detector to be used.

Samples were prepared by Guido Giudetti, Ph.D. and images were generated by Cesar Pascual Garcia, Ph.D.

# Chapter 3: Results

## 3.1 *In vitro* toxicity of $CoFe_2O_4$ NPs

### *3.1.1 Toxicity of the dispersant DEG*

The stock suspensions of the $CoFe_2O_4$ NPs selected for study were supplied in diethylene glycol (DEG). In order to select an appropriate concentrations range of test NPs and to avoid false positive results due to the dispersant, the potential effect of DEG was assessed using dialyzed DEG provided by the supplier of the $CoFe_2O_4$ NPs.

The cytotoxicity induced by 72-hour treatment with dialyzed DEG was investigated using the NR and CFE assays at concentrations of 0.05, 0.1, 0.5, 1, 1.5, and 2% v/v; the results obtained are shown in **Figures 3.1** and **3.2,** respectively.

In the NR experiments (**Figure 3.1**), no toxic effects of 0.05% v/v of dialyzed DEG on any of the cell lines employed were observed. In fact, at this concentration of dialyzed DEG, the viability was almost 100% when compared to the negative control for the six cell lines. At 0.1% v/v of dialyzed DEG, the toxic effect induced by the dispersant on HepG2 and MDCK increased; viability was approximately 90% and 80%, respectively, when compared to the negative control, whilst the toxic effects on the other cell types were unchanged. At 0.5% v/v of dialyzed DEG, CaCo2 and MDCK showed a viability of 40% and 25%, respectively, when compared to the negative control, and these values were not acceptable for subsequent NP tests. The maximum dose of dispersant that was chosen to be administered to the six cell lines with the NP treatment in the NR experiments was 0.1% v/v of dialyzed DEG (highlighted by the red ring in **Figure 3.1**) instead of 0.05% v/v. This allowed NP toxicity to be tested at concentrations of up to120 μM instead of 60 μM using the NR assay.

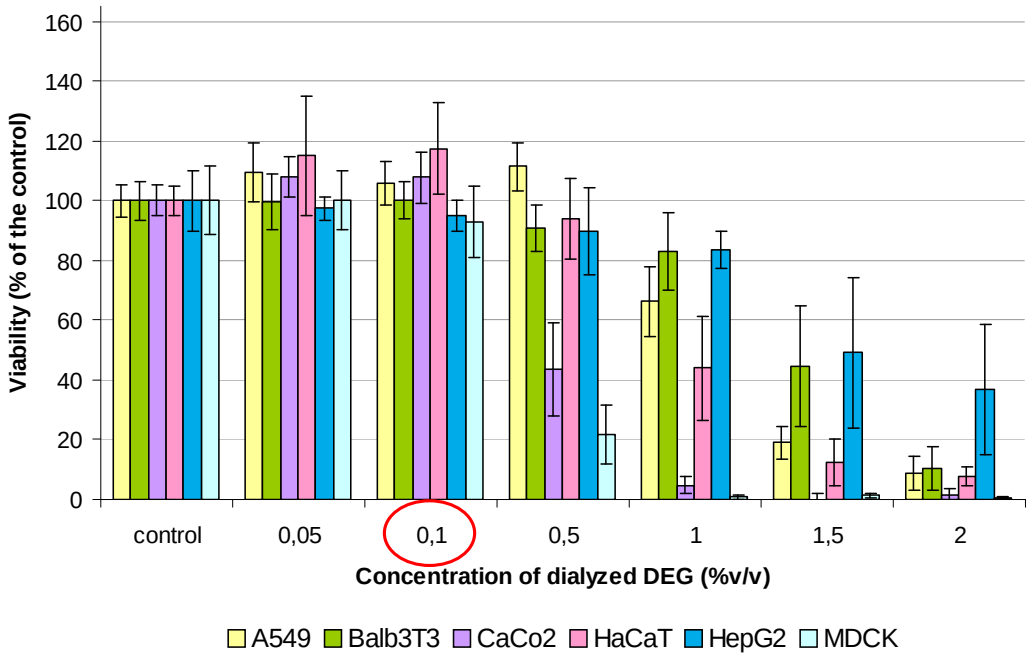


**Figure 3.1: Six cell lines exposed to dialyzed diethylene glycol (DEG) for 72 hours. Cytotoxicity was evaluated using Neutral Red uptake. Results are expressed as Cell Viability (% of control) and are a mean of three independent experiments, ± standard error of the mean (SEM). The red ring highlights the concentration of dialyzed DEG that was chosen as control for the solvent (Control DEG 0.1% v/v) in the experiments with cobalt ferrites.**

In the CFE assay (**Figure 3.2**), at 0.05% v/v of dialyzed DEG, all the cell lines tested showed viability of 90–100% when compared to the negative control. Similar viability values were observed when 0.1% v/v of dialyzed DEG was tested, with the exception of MDCK cells where viability decreased to 80%. Based on the comparisons of toxicity data obtained for dialyzed DEG using NR and CFE, the maximum dose of dialyzed DEG selected for administration to cells during treatment with NPs in both assays was 0.1% v/v. This allowed the cells treated with NPs to reach the same maximum concentration (120 µM) in both assays. In particular, the cytotoxicity of the P601 and P703 $CoFe_2O_4$ NPs was evaluated at concentrations of 10–120 µM. In fact, the highest $CoFe_2O_4$ concentration (120 µM) tested used 0.1% v/v of DEG. The toxic effect due to the dispersant was then considered in the statistical data analysis for $CoFe_2O_4$ NPs (one-way ANOVA was used to compare NP treatments with the dialyzed DEG 0.1% v/v control with significance of $p<0.05$).

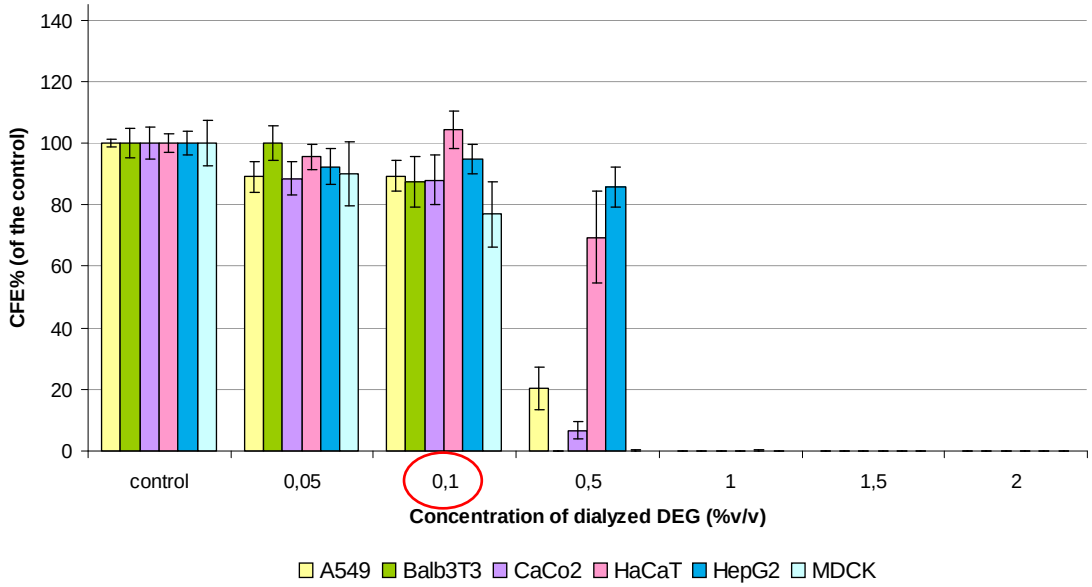


**Figure 3.2: Six cell lines exposed to dialyzed diethylene glycol (DEG) for 72 hours. Cytotoxicity was evaluated by Colony Forming Efficiency (CFE). Results are expressed as CFE (% of control) and are the mean of three independent experiments, ± standard error of the mean (SEM). The red ring highlights the concentration of dialyzed DEG that was chosen as control for the solvent (control DEG 0.1 % v/v) in the experiments with cobalt ferrites.**

### *3.1.2 Cytotoxicity induced by P601*

The results obtained after treating cells for 72 hours with $CoFe_2O_4$ NPs P601 at concentrations of 10, 20, 40, 60, 80, 100 and 120 µM and 10, 20, 30, 40, 50, 60, 80, 100 and 120 µM in the NR and CFE experiments, respectively, are shown in **Figure 3.3** for NR and **Figure 3.4** for CFE. None of the cell lines used to evaluate the cytotoxic effect of $CoFe_2O_4$ P601 using NR decreased to a viability of 50% of the solvent control at the concentrations tested (**Figure 3.3**).

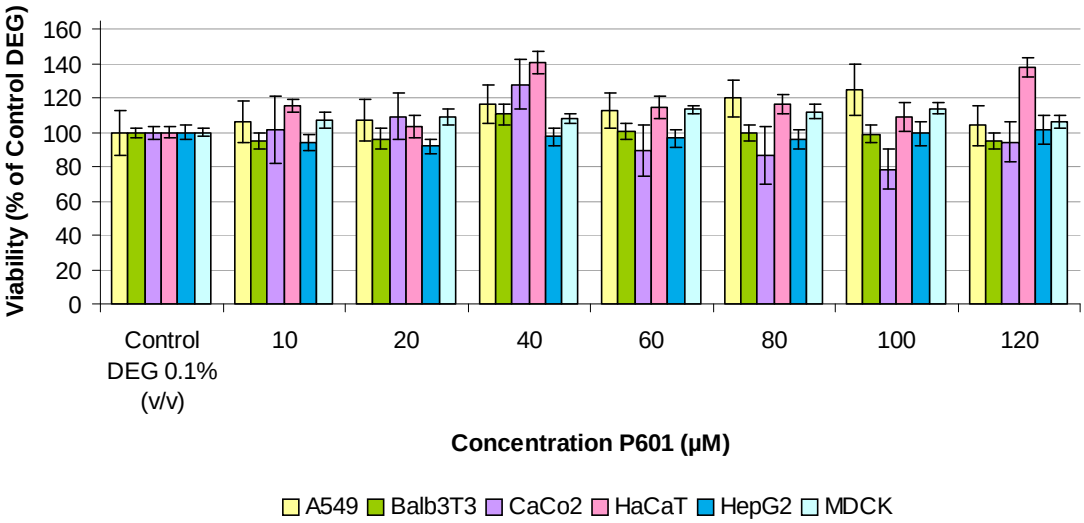


**Figure 3.3: Six cell lines exposed to $CoFe_2O_4$ NPs P601 for 72 hours. Cytotoxicity was evaluated using the Neutral Red assay. Results are expressed as Cell Viability (% of the dialyzed DEG 0.1% v/v) and are the mean of three independent experiments, ± standard error of the mean (SEM).**

In the NR experiments, it was not possible to define an IC50 value for the cell lines studied. Statistical analysis of the NR data using one-way ANOVA did not highlight any significant differences compared to the dialyzed DEG control.

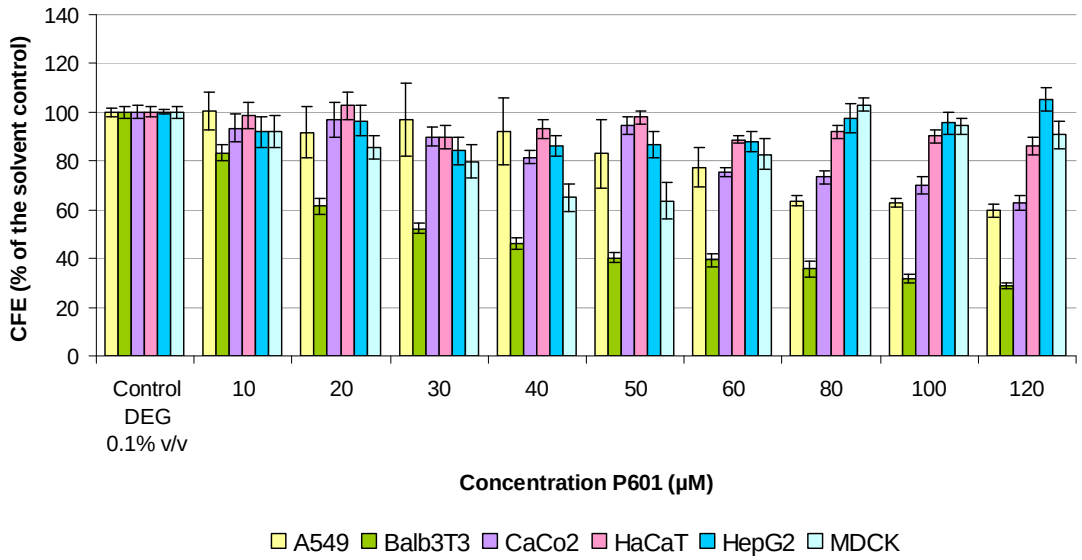


**Figure 3.4: Six cell lines exposed to $CoFe_2O_4$ NPs P601 for 72 hours. Cytotoxicity was evaluated using CFE. Results are expressed as Colony Forming Efficiency (CFE% of the solvent control, i.e., CFE% of dialyzed DEG 0.1% v/v) and are the mean of three independent experiments, ± standard error of the mean (SEM).**

In the CFE experiments (**Figure 3.4A** and **3.4B**), a significant toxic effect (* $p<0.05$ and ** $p<0.01$) of P601 NPs was observed in three cell lines: A549 (80, 100, 120 µM), Balb3T3 (20, 30, 40, 50, 60, 80, 100, 120 µM) and CaCo2 (60, 100, 120 µM), but only for Balb3T3 was it possible to determine an IC50 value (35 µM; determined graphically, see **Figure 3.8A**). The MDCK cells showed a significant response to P601 NPs with respect to the DEG control at two concentrations (40 and 50 µM), while no significant effects were found in HaCaT and HepG2 cells.

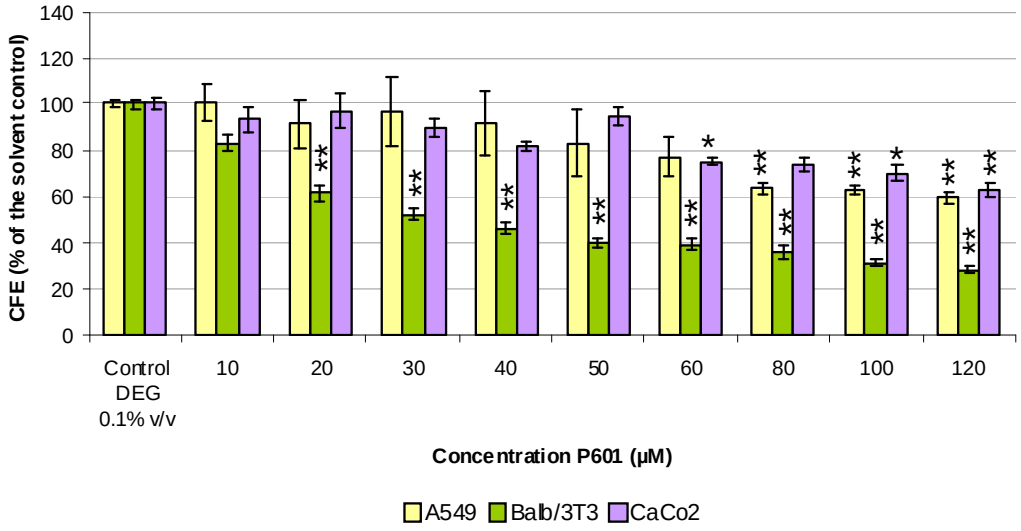


**Figure 3.4A: Three cell lines exposed to $CoFe_2O_4$ NPs P601 for 72 hours. The statistical significance was evaluated by one-way ANOVA (*p<0.05 and **p<0.01) with respect to dialyzed DEG 0.1% v/v control. Significant differences were found in A549, Balb3T3 and CaCo2 cells when compared to dialyzed DEG 0.1% v/v control. Results are the mean of three independent experiments, ± standard error of the mean (SEM).**

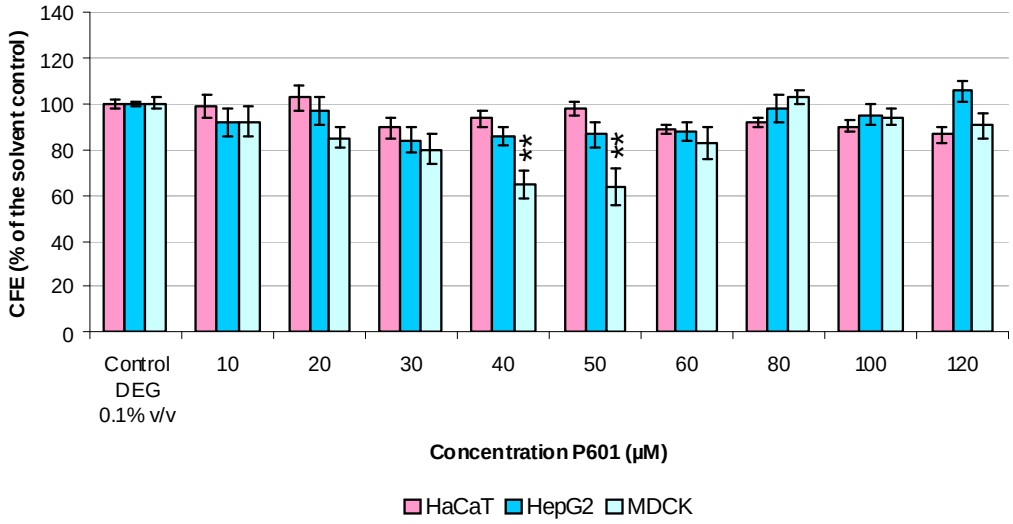


**Figure 3.4B: Three cell lines exposed to $CoFe_2O_4$ NPs P601 for 72 hours. The statistical significance was evaluated by one-way ANOVA (*p<0.05 and **p<0.01) with respect to dialyzed DEG 0.1% v/v control. Significant differences were found in MDCK cells compared to dialyzed DEG 0.1% v/v control. Results are the mean of three independent experiments, ± standard error of the mean (SEM).**

### *3.1.3 Cytotoxicity induced by P703*

Parallel NR and CFE experiments were also performed to assess the cytotoxicity of $CoFe_2O_4$ NPs P703 (at concentrations of 10, 20, 40, 60, 80, 100, 120 µM and 10, 20, 30, 40, 50, 60, 80, 100, 120 µM for the NR and CFE experiments, respectively) (**Figures 3.5** and **3.6** for NR and CFE, respectively). The following graphs show P703 NP concentrations as expected test concentrations to allow an easy comparison of the toxicity data of both P601 and P703 NPs. In the NR experiments with $CoFe_2O_4$ P703, it was not possible to identify IC50 values since all cell lines showed a viability of at least 70% at the concentration ranges tested.

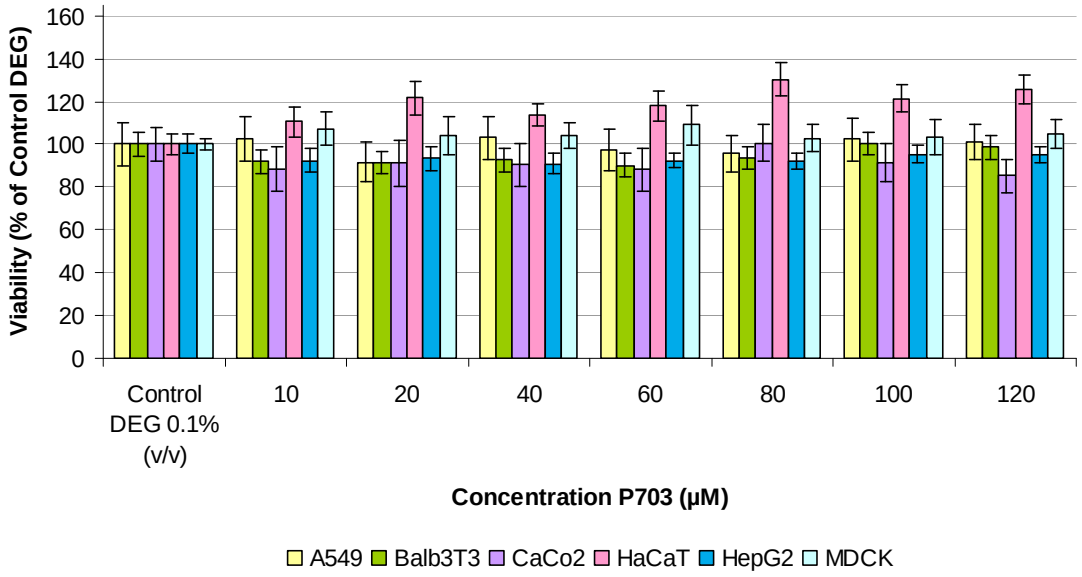


**Figure 3.5: Six cell lines exposed to $CoFe_2O_4$ NPs P703 for 72 hours. Cytotoxicity was evaluated using NR. Results are expressed as Cell Viability (% of dialyzed DEG 0.1% v/v control) and are the mean of three independent experiments, ± standard error of the mean (SEM). For ease of comparing the cytotoxicity results of P601 NPs to those of the P703 NPs, the concentrations of P703 NPs reported in the cytotoxicity graphs were the expected ones.**

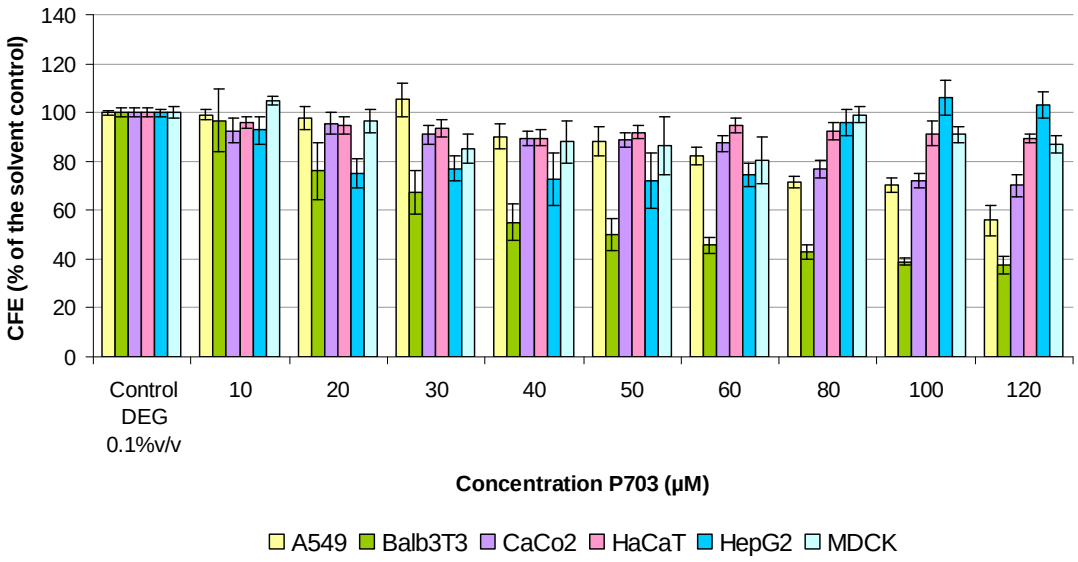


**Figure 3.6: Six cell lines exposed to $CoFe_2O_4$ NPs P703 for 72 hours. Cytotoxicity was evaluated using CFE. Results are expressed as Colony Forming Efficiency (% of the dialyzed DEG 0.1% v/v control) and are the mean of three independent experiments, ± standard error of the mean (SEM).**

In CFE experiments, P703 induced significant toxicity (*p<0.05 and **p<0.01) in A549 (120 µM), Balb3T3 (30, 40, 50, 60, 80, 100, 120 µM) and HepG2 (60 µM) cells (**Figures 3.6A** and **3.6B** for NR and CFE, respectively). The IC50 value could only be derived using the graph for Balb3T3 fibroblasts and corresponded to 50 µM (as expected concentration on the graph in **Figure 3.8B**, but corresponding to real 41.53 µM as reported in **Table B.3**).

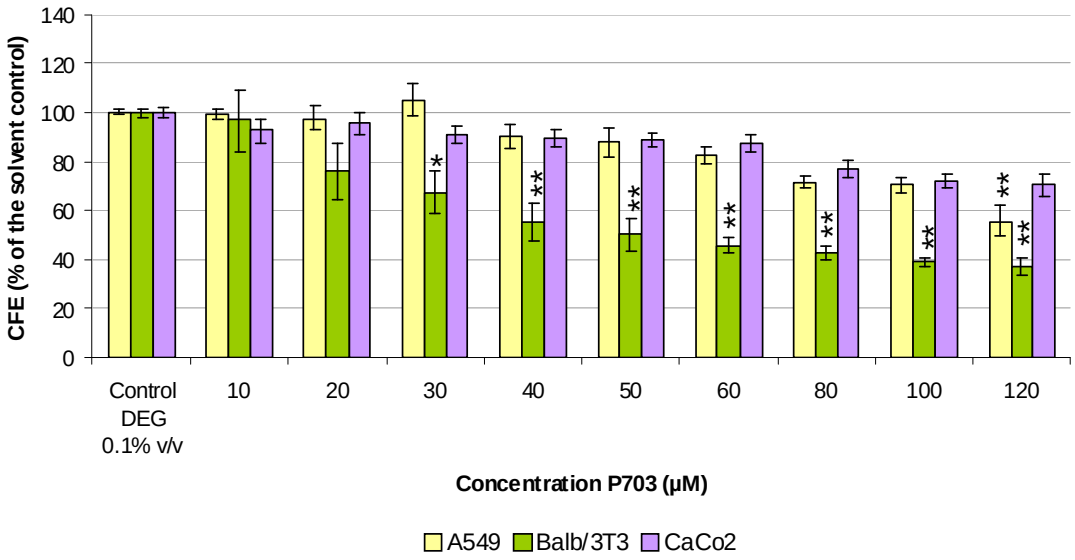


**Figure 3.6A: Three cell lines exposed to $CoFe_2O_4$ NPs P703 for 72 hours. The statistical significance was evaluated by one-way ANOVA (*p<0.05 and **p<0.01) with respect to dialyzed DEG 0.1% v/v control. Significant differences compared to dialyzed DEG 0.1% v/v control were found in A549 and Balb3T3 cells. Results are the mean of three independent experiments, ± standard error of the mean (SEM).**

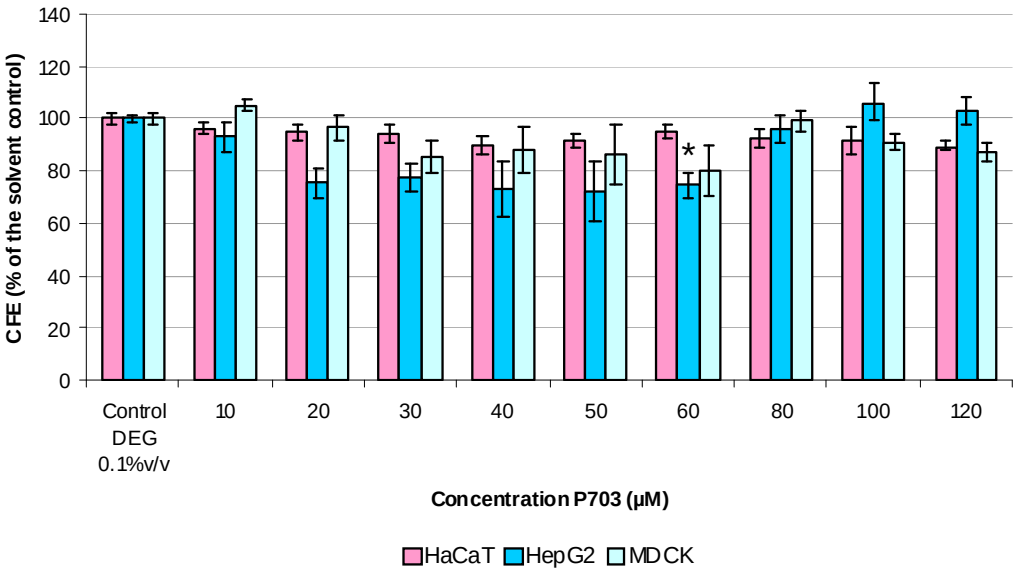


**Figure 3.6B: Three cell lines exposed to $CoFe_2O_4$ NPs P703 for 72 hours. The statistical significance was evaluated by one-way ANOVA (*p<0.05 and **p<0.01) with respect to dialyzed DEG 0.1% v/v control. Significant differences were found in HepG2 cells (p<0.05) compared to the dialyzed DEG 0.1% v/v control. Results are the mean of three independent experiments, ± standard error of the mean (SEM).**

Amongst all the cell lines tested by CFE, the Balb3T3 cells were found to be the most sensitive to $CoFe_2O_4$ NPs. The CFE data were compared to data previously reported on $CoCl_2$-treated Balb3T3 cells (Ponti et al., 2009) in order to determine if the observed cytotoxicity could be attributed only to P601 and P703 NPs or whether the $Co^{2+}$ ion release also contributed. This comparison was possible due to the data produced by ICP-MS analysis of P601 and P703 NPs samples diluted in Balb3T3 complete culture medium (**Table B.6** and **B.7**), taking into account the amount of Co detected in filtered fractions after 72 hours of incubation, and using these values as reference concentrations to determine the corresponding CFE% values reported by Ponti et al. (Ponti et al. 2009).

This approach was also used when interpreting the cytotoxicity data produced by CFE after 24 hours of treatment with the NPs (see **Section 3.1.4** and **Figure 3.9A** and **B**). The comparisons between cytotoxicity results obtained after 72 hours of exposure to P601 and P703 NPs and $Co^{2+}$ (for information on $Co^{2+}$ toxicity, please refer to Ponti et al., 2009) on Balb3T3 cells using CFE assays are shown in **Figures 3.7A** and **3.7B**. Viability is expressed as CFE% of the solvent control for both P601 and P703 NPs and as CFE% of the negative control for $Co^{2+}$. To simplify the data presentation, the concentrations related to the NPs, as expected in the total fractions, are shown in **Figures 3.7A** and **3.7B**, whilst data for the corresponding $Co^{2+}$ concentrations, detected by ICP-MS in filtered fractions, are presented in **Tables B.6** and **B.7**.

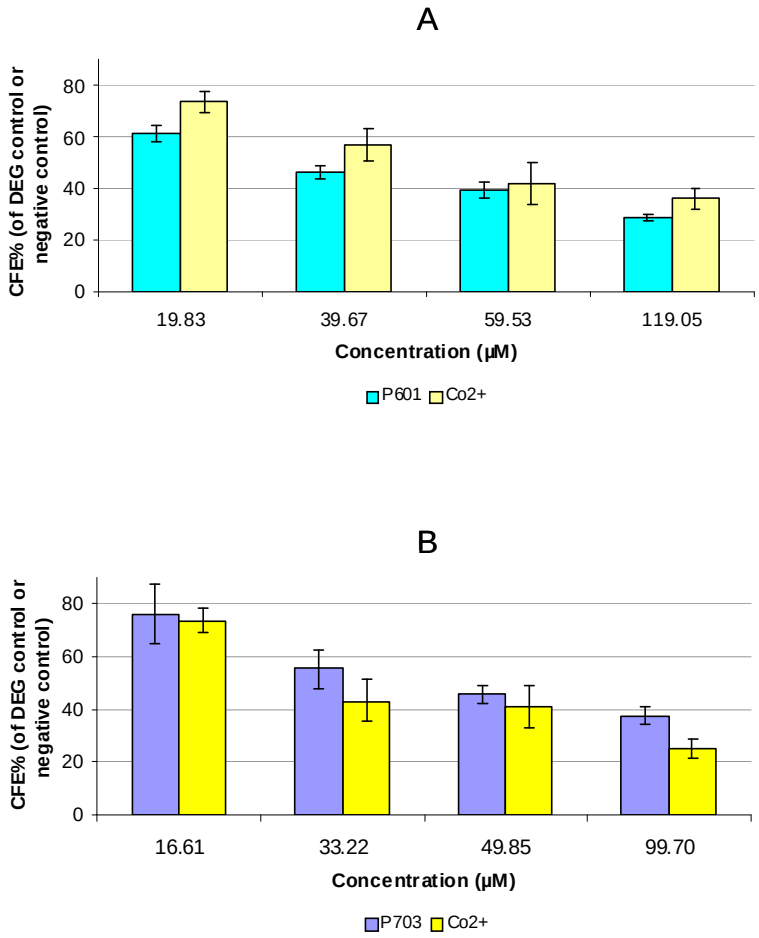


**Figures 3.7A and 3.7B. The comparison of cytotoxicity in Balb3T3 cells induced by P601 (A, light blue histograms) and P703 (B, dark blue histograms), NPs and $Co^{2+}$ (A and B, yellow histograms) after 72 hours of exposure, evaluated using the CFE assay. Results are the mean of three independent experiments, ± standard error of the mean (SEM = standard deviation/√number of experiments or replicates). The CFE values for $Co^{2+}$ treatments of 72 hours were extrapolated from a previous study (Ponti et al., 2009). Concentrations indicated in the graphs are related to the expected µM concentrations of NPs in total fraction samples, considering 119 and 98 mM as concentration of the stock suspensions of P601 and P703; see Tables B.6 and B.7 for the respective $Co^{2+}$ concentrations detected in Balb3T3 complete culture medium after 72 hours of incubation for both P601 and P703 NPs.**
**The P601 NPs showed the highest cytotoxicity with respect to $Co^{2+}$ at all doses considered; in contrast, P703 NPs showed less cytotoxicity than $Co^{2+}$. Data were statistically analyzed using t-test (http://www.graphpad.com/quickcalcs/ttest1.cfm). There was no significant difference when P601 or P703 data were compared to those of $Co^{2+}$.**

Since the P601 NPs have shown CFE values lower than those of $Co^{2+}$, this suggests that P601 NPs may have a higher toxic effect on Balb3T3 cells than that of ion release alone. In contrast, P703 NPs have shown higher CFE values than those of $Co^{2+}$, suggesting that P703 NPs are less toxic than $Co^{2+}$. In this context, it should be noted that for the test $CoFe_2O_4$ NPs, generally both the NPs and ions ultimately released in the stock

suspensions (the amounts of which could not be measured) were tested at the same time. Therefore, the effects that were attributed to the NPs were actually due to NPs and ions present in the stock suspension. Statistical analysis was performed using the t-test (http://www.graphpad.com/quickcalcs/ttest1.cfm). There was no statistically significant difference in toxicity of either P601 or P703 compared to that $Co^{2+}$.

### *3.1.4 Cell transformation capacity and genotoxicity induced by P601 and P703*

The transformation capacity of both $CoFe_2O_4$ NPs was studied using concurrent CFE and CTA tests on the Balb3T3 model after 72 hours of exposure at concentrations of 1, 5, 20, 60 µM. In order to define this concentration range as accurately as possible, the cytotoxicity induced by both $CoFe_2O_4$ NPs was investigated in earlier CFE experiments considering only to Balb3T3 fibroblasts, by contrast to the other cell lines, additional concentrations (including 1 and 5 µM) so that 1, 5, 10, 20, 30, 40, 50, 60, 80, 100 and 120 µM were the concentrations tested by CFE to Balb3T3 with 72 hours of exposure (see **Figure 3.8A and B)**. Therefore 1, 5, 20 and 60 µM were chosen as the concentrations to be tested for assessing the transformation capacity and corresponded to viability values higher, similar and lower than those indicated by IC50 values (CFE% of 50).

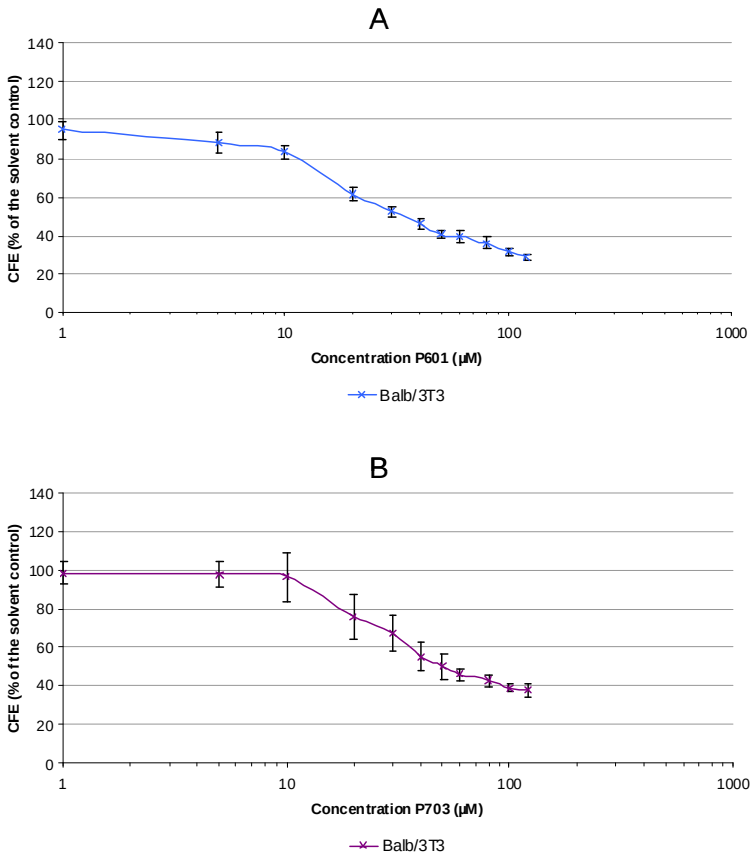


**Figure 3.8A and 3.8B: CFE results after exposing Balb3T3 cells to P601 (A) and P703 (B) NPs for 72 hours. In order to define the concentrations at which the transformation capacity of these NPs could be assessed as accurately as possible, the cytotoxicity on Balb3T3 fibroblasts (in contrast to the other cell lines) was investigated testing additional concentrations including 1 and 5 µM. Statistically significant differences are not shown here (please see Figures 3.4A and 3.6A).**

Results from concurrent CFE and CTA assays are shown in **Figures 3.9A** and **3.9B**. Cytotoxicity data were statistically analyzed using one-way ANOVA. Significant differences with respect to the control DEG were found in the CFE for both P601 and P703 at 20 and 60 µM (**Figure 3.9A**) and confirmed the cytotoxic potential of these NPs. No statistically significant differences between NP treatments and DEG control were found in the CTA results using Fisher's exact test, suggesting that both P601 and P703 NPs had not transformation capacity across the selected concentration range (**Figure 3.9B**).

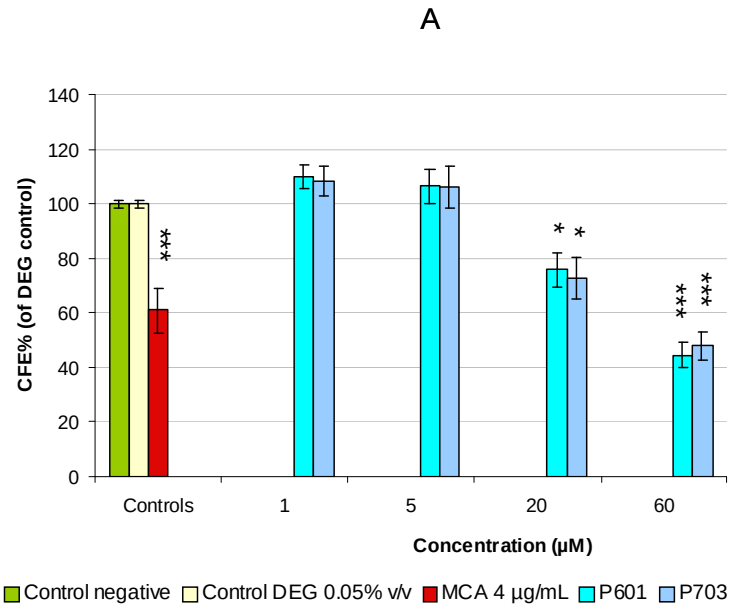


**Figure 3.9A: The cytotoxicity induced by P601 and P703 NPs after 72 hours of exposure, evaluated by concurrent CFE and CTA assays. Results are the mean of three independent experiments, ± standard error of the mean (SEM = standard deviation/√number of experiments or replicates). Statistical significance was evaluated using one-way ANOVA (*p<0.05, ***p<0.001).**

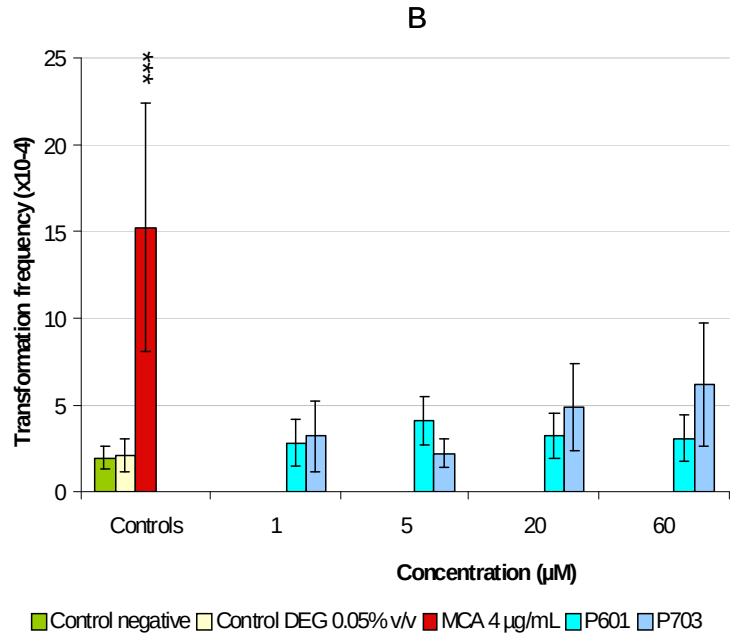


**Figure 3.9B: The cell transformation capacity induced by P601 and P703 NPs in Balb3T3 cells after 72 hours of exposure, evaluated using CTA. Results are a mean of three independent experiments, ± standard error of the mean (SEM = standard deviation/√number of experiments or replicates). Statistical significance was evaluated by Fisher's exact test for CTA data (***p<0.001).**

Cytotoxicity studies using CFE were done for both P601 and P703 NPs at concentrations of 1, 10, 60 and 120 µM and 24 hours of exposure (**Figure 3.10**) in order to determine the concentrations to be tested in subsequent CBMN experiments.

The potential genotoxicity of $CoFe_2O_4$ NPs on Balb3T3 was then investigated using the CBMN assay at concentrations of 1, 10, 60 µM for both $CoFe_2O_4$ NPs.

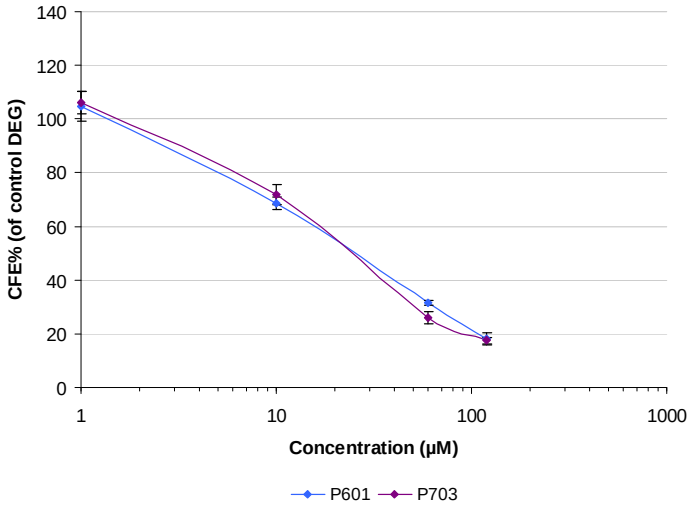


**Figure 3.10: The cytotoxicity induced by P601 and P703 NPs in Balb3T3 cells after 24 hours of exposure, evaluated by CFE. Results are the mean of three independent experiments, ± standard error of the mean (SEM = standard deviation/√number of experiments or replicates). Results of the statistical analysis are not shown here (please see Figure 3.11A).**

Concentrations of 1, 10 and 60 µM of both $CoFe_2O_4$ NPs were selected for testing in the CBMN experiments because they corresponded with viabilities that were higher, similar and lower than the IC50. Both the P601 and P703 NPs were significantly cytotoxic compared to the solvent control after 24 hours of incubation (**Figure 3.11A**), but did not show a significant induction of micronuclei across the concentration range studied (**Figure 3.11B**).

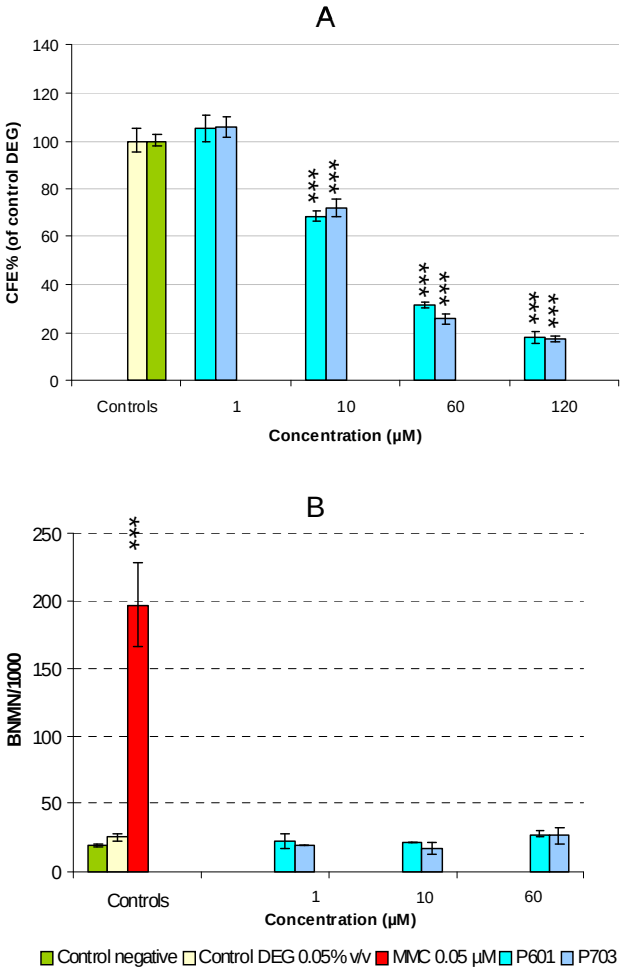


**Figure 3.11A and 3.11B: The cytotoxicity (A) and genotoxicity (B) induced by P601 and P703 NPs after 24 hours of exposure on Balb3T3 cells evaluated by CFE and CBMN assays. Results are the mean of three independent experiments, ± standard error of the mean (SEM = standard deviation/√number of experiments or replicates). The statistical significance of CFE and CBMN data was evaluated using one-way ANOVA and Fisher's exact test, respectively (***p<0.001).**

As described previously for cytotoxicity after 72 hours of exposure, the CFE results obtained by treating Balb3T3 cells for 24 hours with P601 and P703 NPs were compared to those of Ponti et al. (Ponti et al., 2009) (**Figure 3.12A** and **3.12B**). Both P601 NPs and P703 NPs showed the greatest cytotoxicity with respect to $Co^{2+}$ at two of the doses studied (9.92 and 59.63 µM and 8.31 and 49.85 µM, respectively). Statistical analysis of these data using the t-test showed that the difference between the CFE% value for P601 and the corresponding value for $Co^{2+}$ at 59.63 µM was statistically significant (**p<0.01), and also the difference between CFE% of P703 and $Co^{2+}$ was statistically significant (*p<0.05).

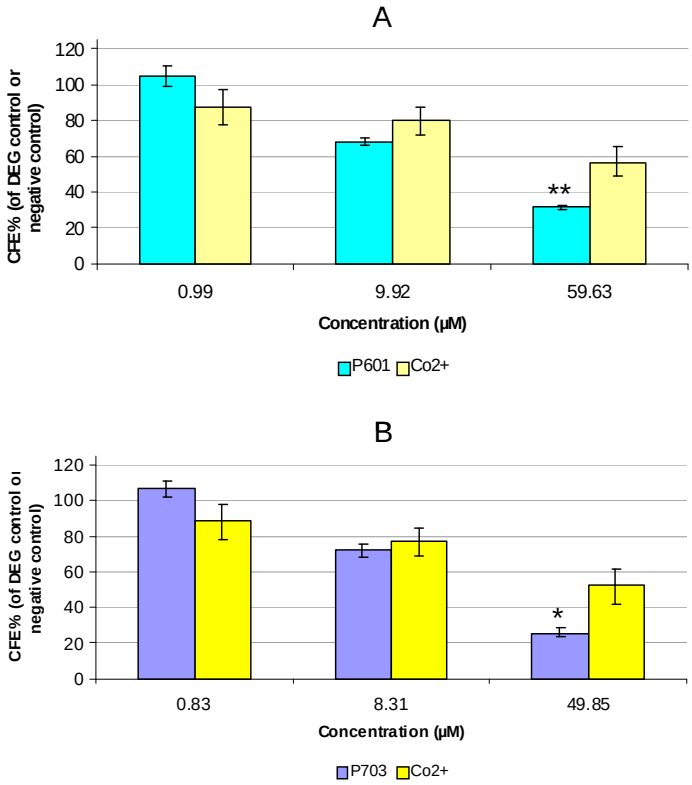


**Figure 3.12A and 3.12B: The comparison between cytotoxicity induced by P601 (A, light blue histograms), P703 (B, dark blue histograms) NPs and $Co^{2+}$ (A and B, yellow histograms) in Balb3T3 cells after 24 hours of exposure, evaluated using the CFE assay. Results are the mean of three independent experiments, ± standard error of the mean (SEM = standard deviation/√number of experiments or replicates). The CFE values for $Co^{2+}$ treatments of 24 hours were extrapolated from a previous study (Ponti et al., 2009). The concentrations shown relate to the expected µM concentrations of NPs in total fraction samples, considering 119 and 98 mM as the concentration of the stock suspensions of P601 and P703, respectively; please see Tables B.6 & B.7 for the respective $Co^{2+}$ concentrations detected in Balb3T3 complete culture medium after 24 hours of incubation for both P601 and P703 NPs.**
**Statistical analysis was done using the t-test (http://www.graphpad.com/quickcalcs/ttest1.cfm) and significant differences were found when comparing P601 or P703 data to those of $Co^{2+}$ (*p<0.05; **p<0.01).**

## 3.2 *In vitro* toxicity of Ag NPs

### *3.2.1 Cytotoxicity of Ag NPs*

Cytotoxicity induced by 0.01, 0.1, 0.5, 1, 2.5, 5 and 10 µM of Ag NPs on Balb3T3 fibroblasts was assessed after 72 hours of exposure using CFE. The dose-effect curves from these experiments are shown in **Figures 3.13**, **3.14**, **3.15** and **3.16** for NM-300, Ag 44 nm, Ag 84 nm and Ag 100 nm, respectively. Statistical analysis of the data by one-way ANOVA showed a significant cytotoxic effect in respect to the dispersant control for

NM-300 (at concentrations of 0.5, 1, 2.5, 5 and 10 µM), Ag 44 nm (1, 2.5, 5 and 10 µM), Ag 84 nm (2.5, 5 and 10 µM) and Ag 100 nm (2.5, 5 and 10 µM).

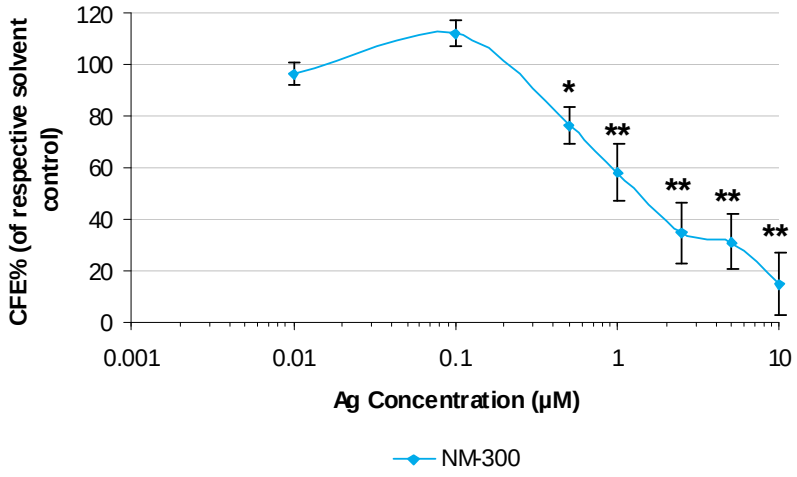


**Figure 3.13: The cytotoxicity of NM-300 NPs on Balb3T3 cells after 72 hours of exposure, assessed using CFE; the NP concentration is expressed as µM. Results are the mean of three independent experiments, ± standard error of the mean (SEM = standard deviation/√number of experiments or replicates). Statistical significance was evaluated using one-way ANOVA (*p<0.05; **p<0.01).**

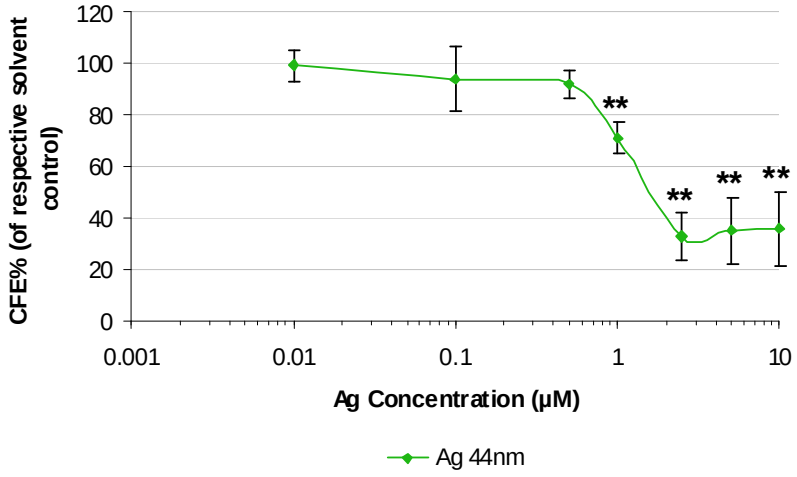


**Figure 3.14: The cytotoxicity of Ag 44 NPs on Balb3T3 cells after 72 hours of exposure, assessed using CFE; the NP concentration is expressed as µM. Results are the mean of three independent experiments, ± standard error of the mean (SEM = standard deviation/√number of experiments or replicates). Statistical significance was evaluated using one-way ANOVA (**p<0.01).**

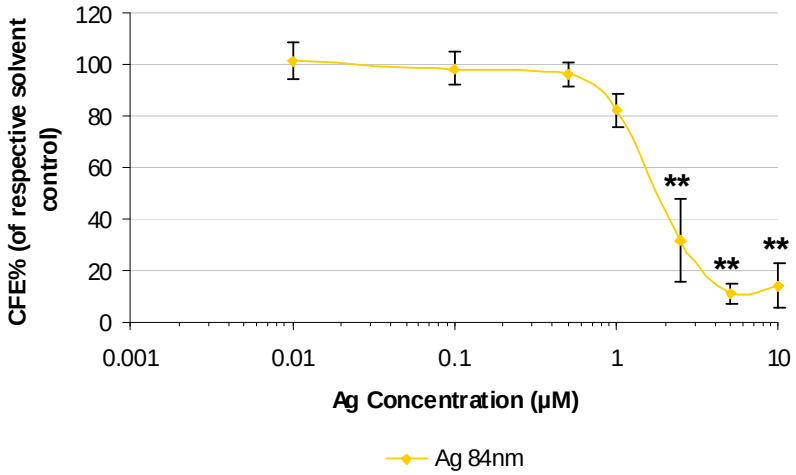


**Figure 3.15: The cytotoxicity of Ag 84 NPs on Balb3T3 cells after 72 hours of exposure, assessed using CFE; the NP concentration is expressed as µM. Results are the mean of three independent experiments, ± standard error of the mean (SEM = standard deviation/√number of experiments or replicates). Statistical significance was evaluated using one-way ANOVA (**p<0.01).**

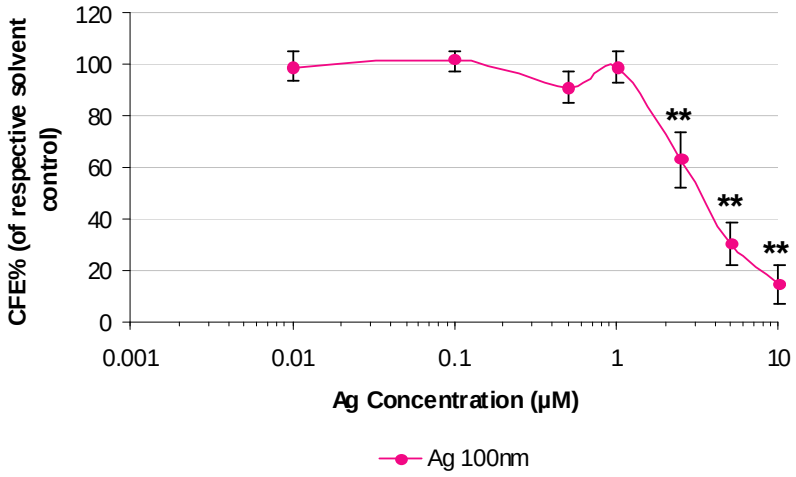


**Figure 3.16: The cytotoxicity of Ag 100 NPs on Balb3T3 cells after 72 hours of exposure, assessed using CFE; the NP concentration is expressed as µM. Results are the mean of three independent experiments, ± standard error of the mean (SEM = standard deviation/√number of experiments or replicates). Statistical significance was evaluated using one-way ANOVA (**p<0.01).**

It was thought to be of interest to present the above cytotoxicity data both as µM and the number of NPs per mL (**Figure 3.17A** and **3.17B**). When the CFE results were shown as a function of Ag NP concentration expressed as µM, the dose-effect curves covered the same concentration range, and the smaller Ag NPs (e.g., NM-300 and Ag 44 nm) appeared to be more toxic than the larger ones since the IC50 values (~1.5 µM for NM-

300, ~1.7 µM for Ag 44 nm, ~1.9 µM for Ag 84 nm and ~3.2 µM for Ag 100 nm) increase with NP size (**Figure 3.17A**). In contrast, when the concentration of Ag NP was expressed as the number of particles (see **formula B.1** and **Section B.2.4**), the dose-effect curves shifted and did not cover exactly the same Ag concentration range for all the NPs. This also resulted in a change in IC50 values since smaller NPs appeared to be less toxic than the larger ones (**Figure 3.17B**).

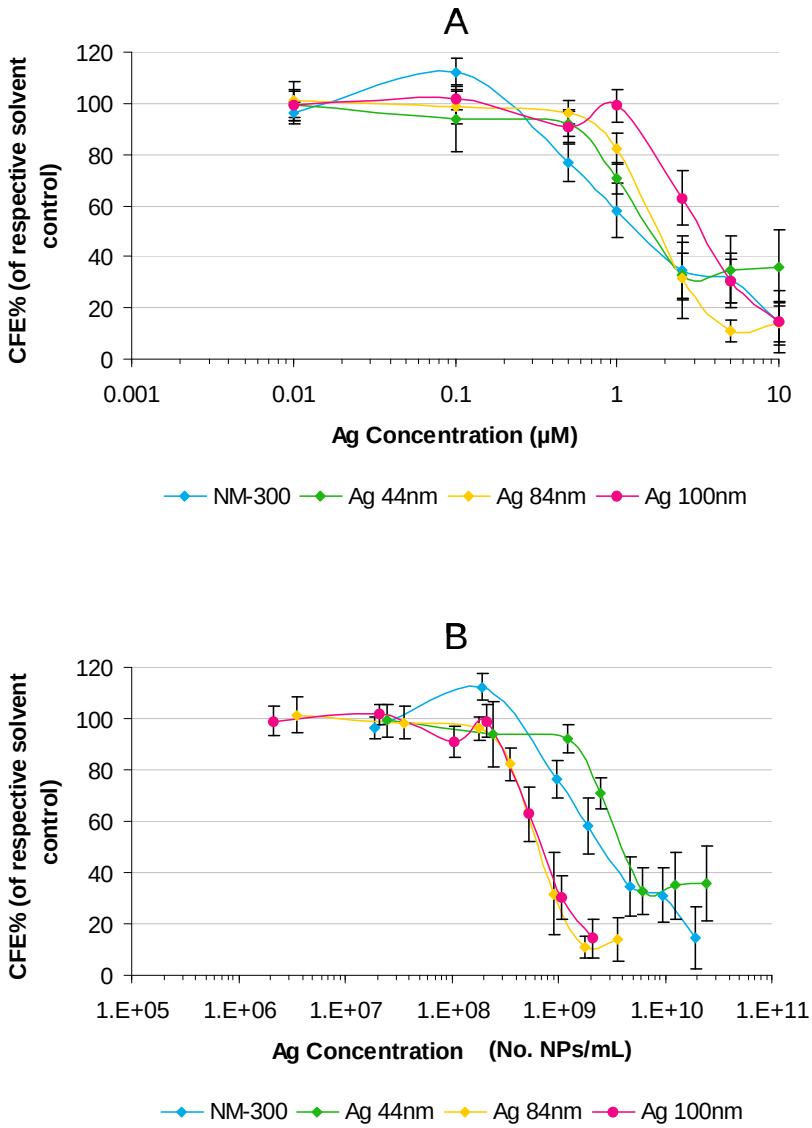


**Figures 3.17A and 3.17B: The cytotoxicity of Ag NPs on Balb3T3 cells after 72 hours of incubation, assessed using CFE and expressed as a function of the NP concentration in either µM (A) or the number of NPs/mL (No. NPs/mL) (B). Results are the mean of three independent experiments, ± standard error of the mean (SEM = standard deviation/√number of experiments or replicates).**

### *3.2.2 Cell transformation capacity and genotoxicity of Ag NPs*

The transformation capacity and genotoxic potential of all the Ag NPs studied here was investigated using Balb3T3 mouse fibroblasts. The cell transformation capacity was assessed using CTA after exposing cells to Ag NPs for 72 hours at concentrations ranging from 0.5 to 5 µM (specifically 0.5, 2.5 and 5 µM) and previously selected by CFE, as concentrations with CFE% values higher, near and lower than the IC50. Results from concurrent CFE and CTA procedures are shown in **Figure 3.18A** and **3.18B**. Both NM-300 and Ag 44 nm induced a statistically significant toxic effect on Balb3T3 cells in respect to the appropriate NP dispersant control at concentrations of 2.5 and 5 µM, whilst Ag 84 nm and Ag 100 nm did so at 5 µM. Since no type III foci were observed, the transformation frequency (x $10^{-4}$) was zero for Ag 100 nm at 2.5 and 5 µM, and zero for Ag 44 nm at 5 µM. Statistical analysis with Fisher's exact test showed no significant cell transformation capacity with respect to the appropriate solvent control.

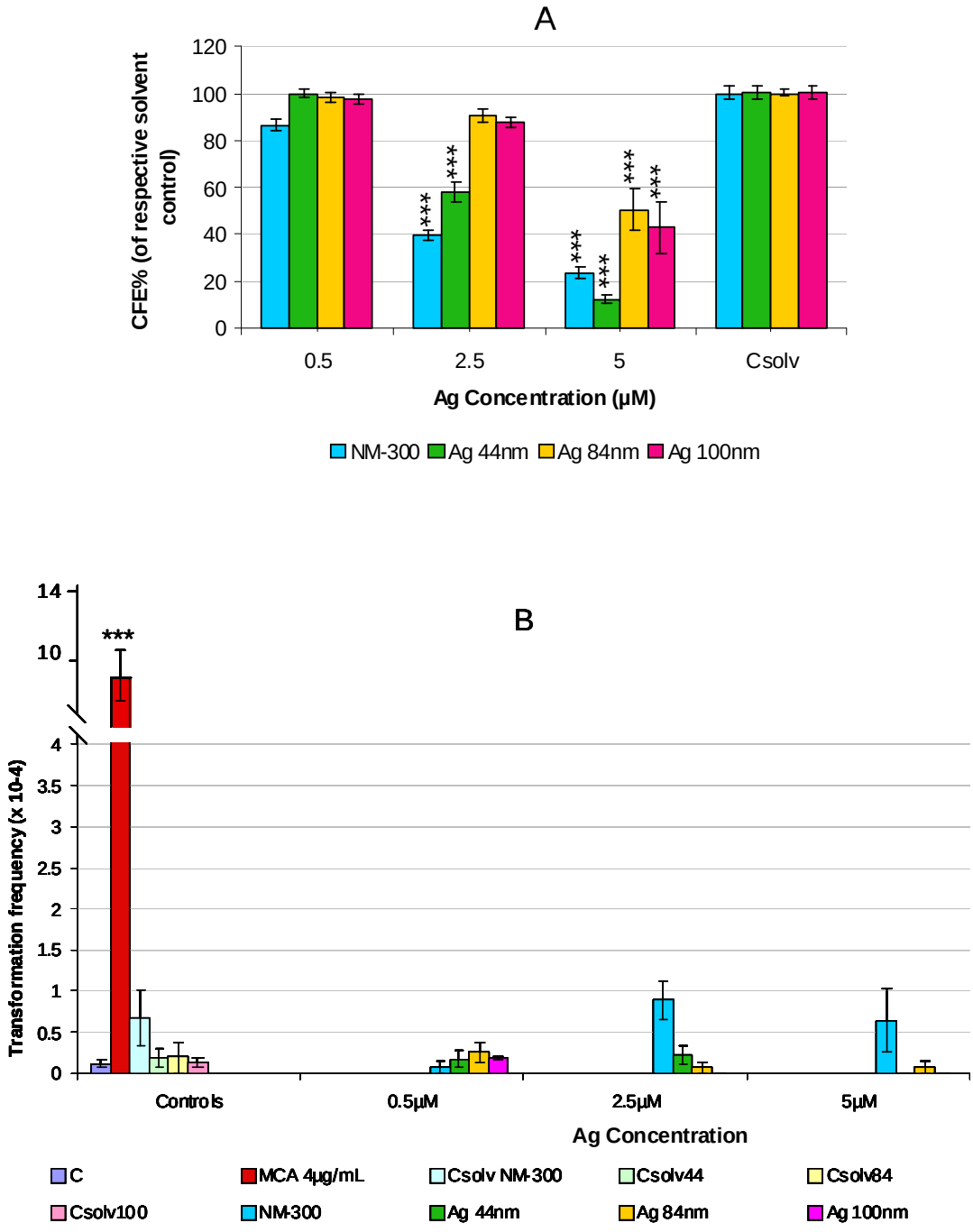


**Figures 3.18A and 3.18B: The cytotoxicity and cell transformation induced by Ag NPs in Balb3T3 cells after 72 hours of exposure as evaluated with concurrent CFE and CTA assays. Due to the absence of type III foci, the transformation frequency (x $10^{-4}$) was zero for Ag 100 nm at 2.5 and 5 µM, and zero for Ag 44 nm at 5 µM. The results are the mean of three independent experiments, ± standard error of the mean (SEM = standard deviation/√number of experiments or replicates). Statistical significance was evaluated using one-way ANOVA and Fisher's exact test for CFE and CTA results, respectively (***p<0.001).**

The genotoxic potential of all Ag NPs on Balb3T3 fibroblasts, indicated by the induction of micronuclei in binucleated cells, was evaluated using the CBMN assay. The concentrations of Ag NPs investigated in the CBMN assay (1, 5 and 10 µM) were selected after CFE experiments in which Balb3T3 were treated for 24 hours at Ag NP concentrations of 0.1, 0.5, 1, 5 and 10 µM (**Figure 3.19**).

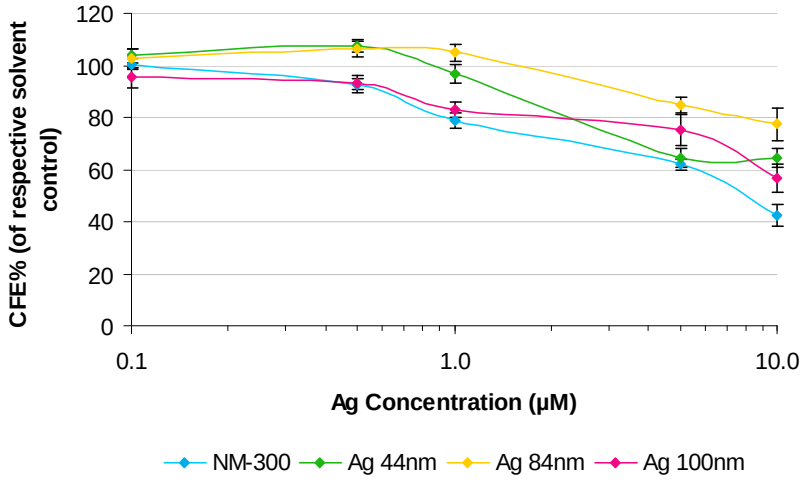


**Figure 3.19: The cytotoxicity of Ag NPs on Balb3T3 cells after 24 hours of exposure, assessed using CFE. Results of the statistical analyses are shown in Figure 3.20A. Results are the mean of three independent experiments, ± standard error of the mean (SEM = standard deviation/√number of experiments or replicates).**

Statistical analysis of CFE data using one-way ANOVA showed significant toxicity compared to the appropriate solvent controls at Ag NP concentrations of 1, 5 and 10 µM for NM-300, 5 and 10 µM for Ag 44 nm and Ag 100 nm, and 10 µM for Ag 84 nm (**Figure 3.20A**). In contrast, statistical analysis of CBMN data using Fisher's exact test showed no significant differences, suggesting that the Ag NPs have no genotoxic potential over the concentration range investigated (**Figure 3.20B**).

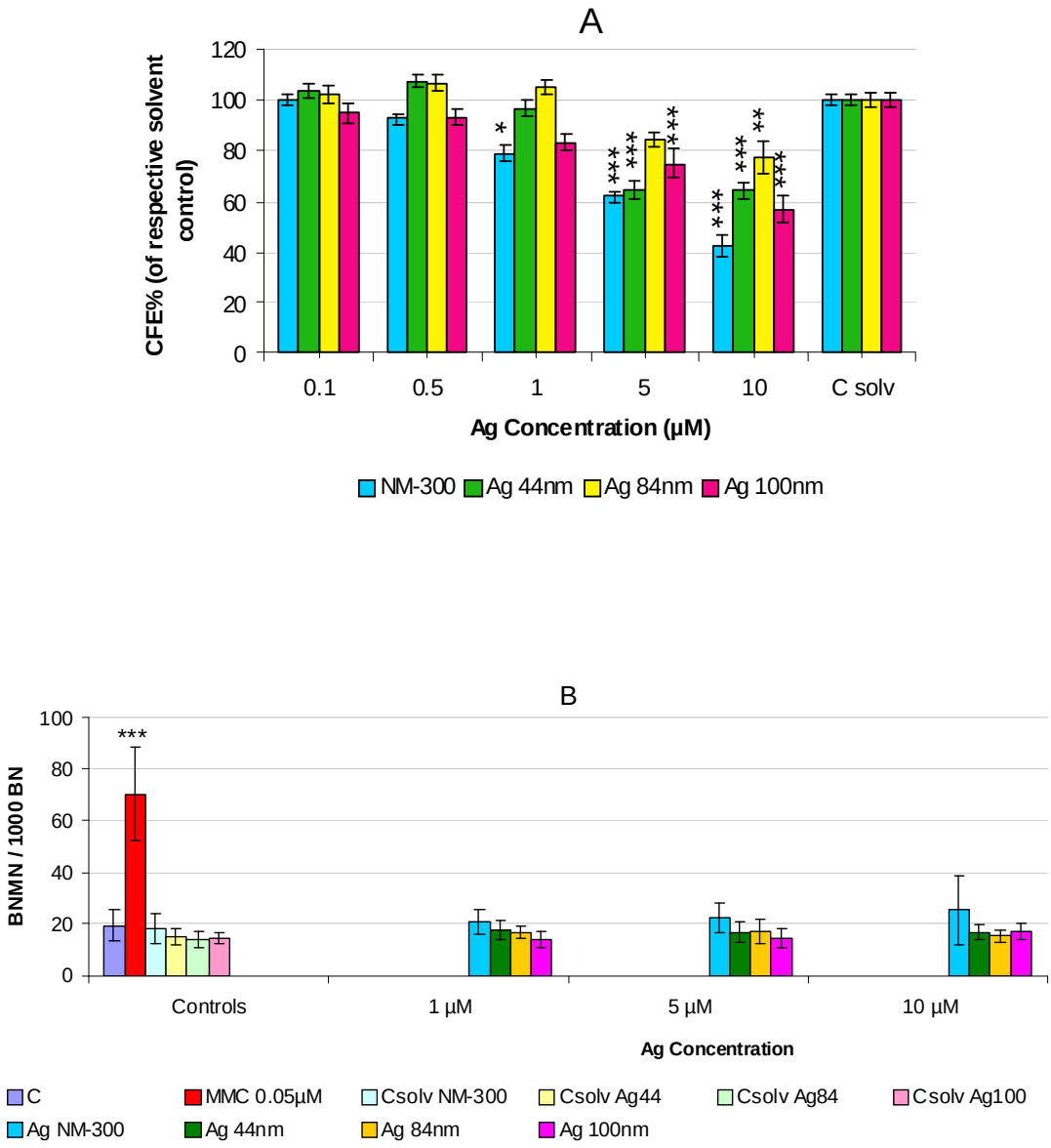


**Figures 3.20A and 3.20B: The cytotoxicity of Ag NPs in Balb3T3 cells after 24 hours of exposure, assessed using CFE (A), and genotoxicity of Ag NPs in Balb3T3 cells after 24 hours of exposure (B), assessed using the CBMN assay. Results are the mean of three independent experiments, ± standard error of the mean (SEM = standard deviation/√number of experiments or replicates). Statistical significance was evaluated by one-way ANOVA (*p<0.05; ***p<0.001) and Fisher's exact test for CFE and CBMN assay data, respectively.**

# Appendix B: Results for the physicochemical characterization of NPs

## B.1 The characterization of $CoFe_2O_4$ NPs

### *B.1.1 Zeta potential*

The Z-potential results for $CoFe_2O_4$ P601 and P703 NPs preparations in ultrapure water and in the three basal media (HAM, MEM and DMEM without serum and other additives) at time 0 are shown in **Table B.1.** The Z-potential in ultrapure water was 40 ± 0.31 mV and 35 ± 0.55 mV for 100 µM of both P601 and P703 NPs, respectively, which suggested that these particles were stable in ultrapure water. The Z-potential values for both P601 and P703 NPs dilutions in the three basal media all ranged from +30 mV to -30 mV. This suggested that $CoFe_2O_4$ NPs were unstable and tended to aggregate and/or agglomerate when suspended in culture media, probably due to the salts, glucose or glutamine commonly found in cell culture media.

**Table B.1: The Z-potential measurements of $CoFe_2O_4$ P601 and P703 NPs dilutions (100 µM) in ultrapure water and in the three cell culture media used for the toxicological studies. Values are expressed in mV ± standard deviation (SD).**

| Sample name | Zpot (mV) ± SD |
|---|---|
| **P601 prepared in:** | |
| ultrapure water | 40 ± 0.31 |
| HAM | -12 ± 0.95 |
| MEM | -6.10 ± 0.11 |
| DMEM | -7.63 ± 0.94 |
| **P703 prepared in:** | |
| ultrapure water | 35 ± 0.55 |
| HAM | -12.9 ± 0.75 |
| MEM | -6.24 ± 0.23 |
| DMEM | -7.05 ± 0.12 |

### *B.1.2 Size distribution*

The DLS results obtained from the three cell culture media, the dialyzed DEG (NPs dispersant), and the ultrapure water are summarized in **Figures B.1A-B, B.2A-B and B.3.**

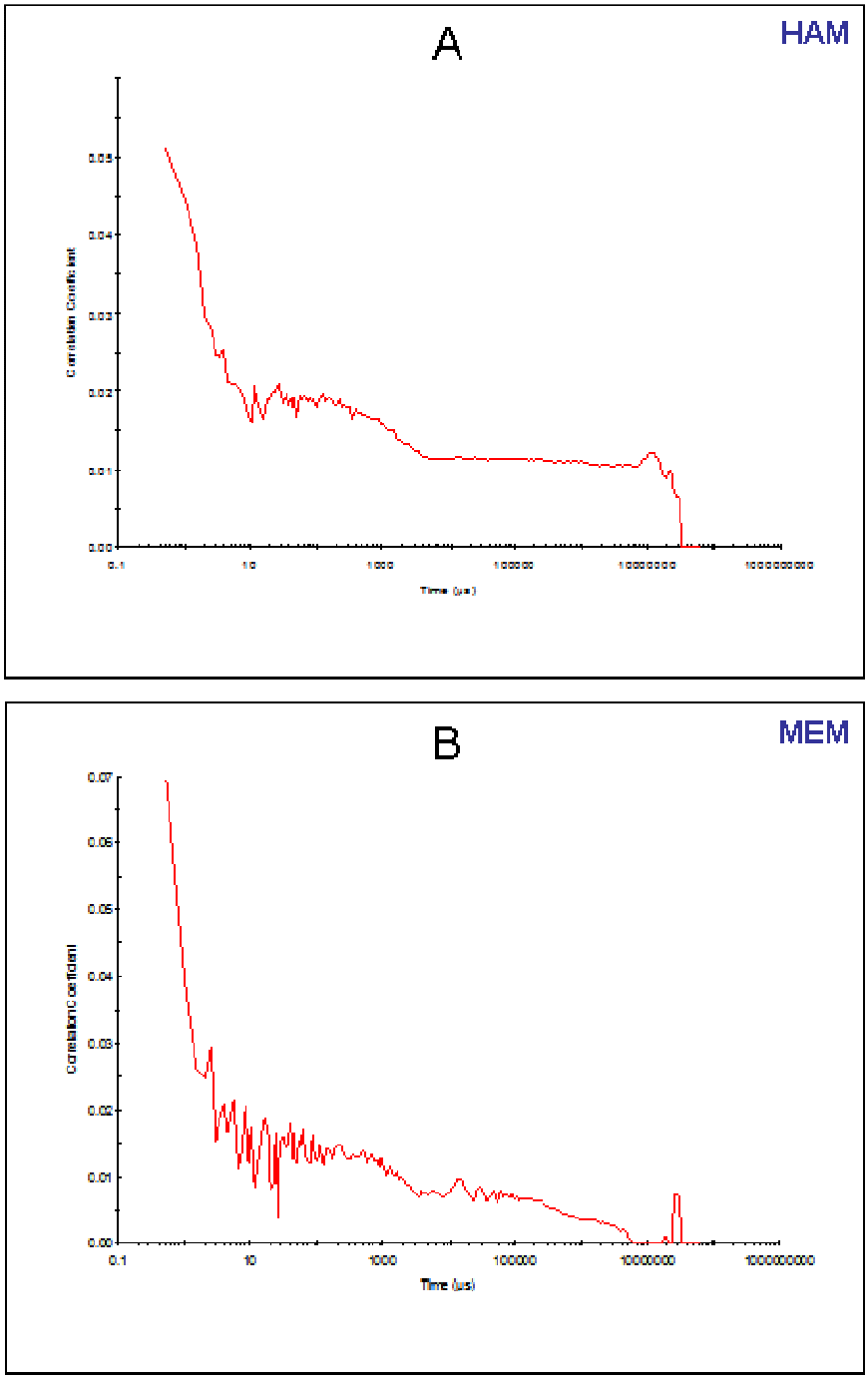


**Figure B.1A and B.1B: DLS correlograms of basal media HAM and MEM, used to dilute $CoFe_2O_4$ P601 and P703 NPs for DLS sample analysis. The correlation coefficient is expressed as a function of time (µs). The Y intercepts at time 0 were lower than 0.1 and no correlogram had a sigmoid shape. These observations indicated that no nano-sized objects were detected in these samples using DLS and thus suggested they were particle-free.**

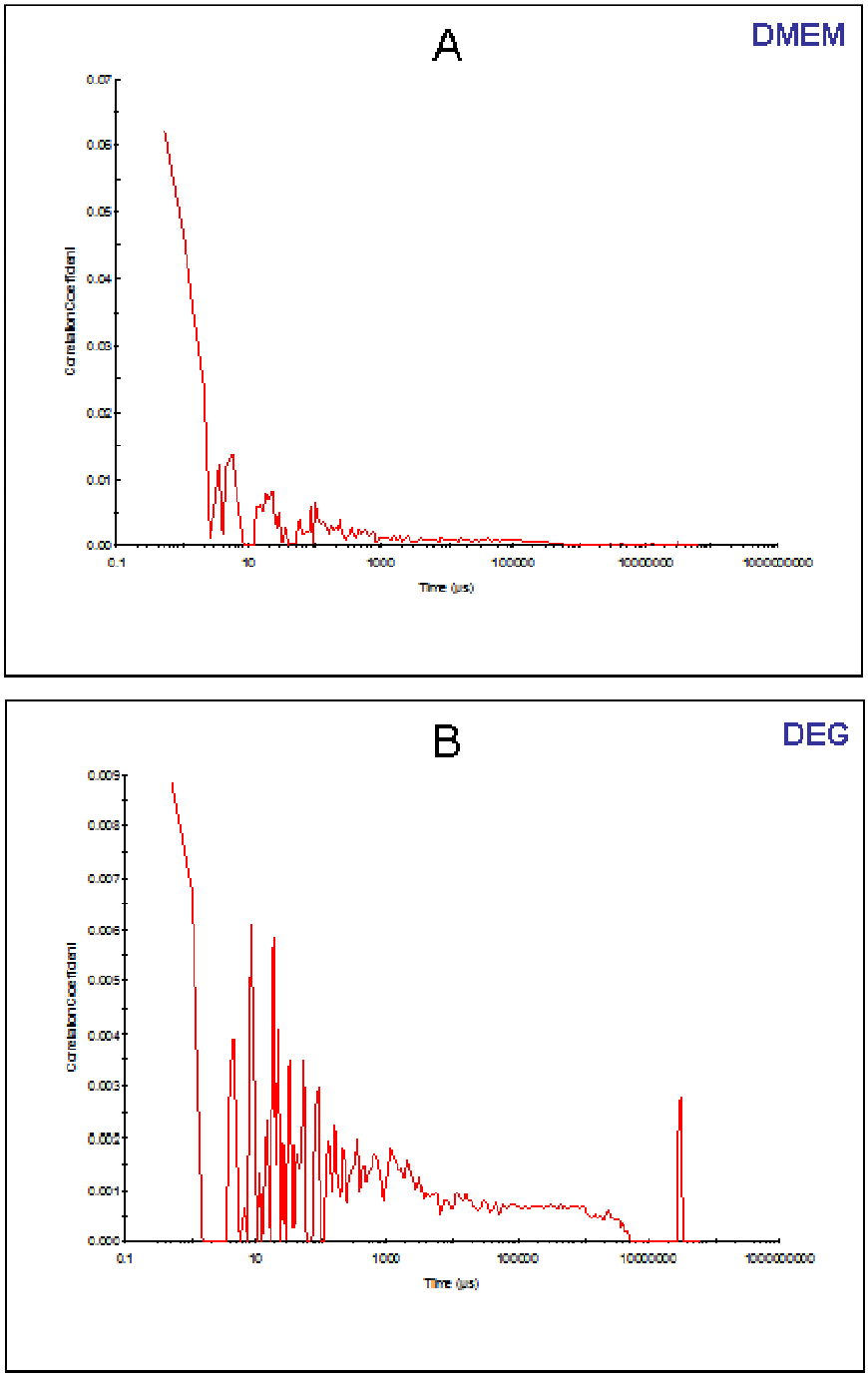


**Figure B.2A and B.2B: DLS correlograms of basal media DMEM and NPs dispersant DEG, used to dilute $CoFe_2O_4$ P601 and P703 NPs for DLS sample analysis. The correlation coefficient is expressed as a function of time (µs). The Y intercepts at time 0 were lower than 0.1 and no correlogram had a sigmoid shape. These observations indicated that no nano-sized objects were detected in these samples using DLS and thus suggested they were particle-free.**

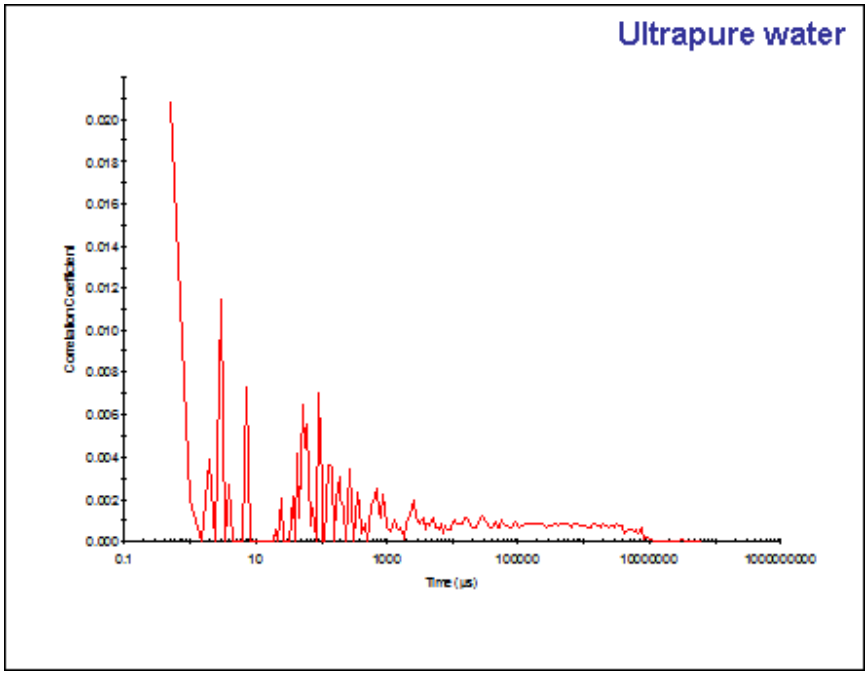


**Figure B.3: DLS correlograms of ultrapure water, used to dilute $CoFe_2O_4$ P601 and P703 NPs for DLS sample analysis. The correlation coefficient is expressed in function of time (µs). The Y intercept at time 0 was lower than 0.1 and the correlogram did not show a sigmoid shape. These observations indicated that no nano-sized objects were detected in these samples using DLS and thus suggested they were particle-free.**

The Y intercepts for all basal media (HAM, MEM, DMEM), ultrapure water and DEG were always below 0.1 and no correlogram had a sigmoid shape. These findings both indicated that the DLS technique did not detect any nano-sized objects in the samples, suggesting that they were actually particle-free.

The DLS measurements of the completed culture media used for the six cell lines showed a sigmoid-shaped correlogram with Y intercept values between 0.8 and 1.0 at time 0 (**Figures B.4A-B, B.5A-B** and **B.6A-B**). This suggested that nano-sized objects were present in these media, possibly due to additives used to complete them for the cell culturing (e.g., serum proteins, glutamine, etc.).

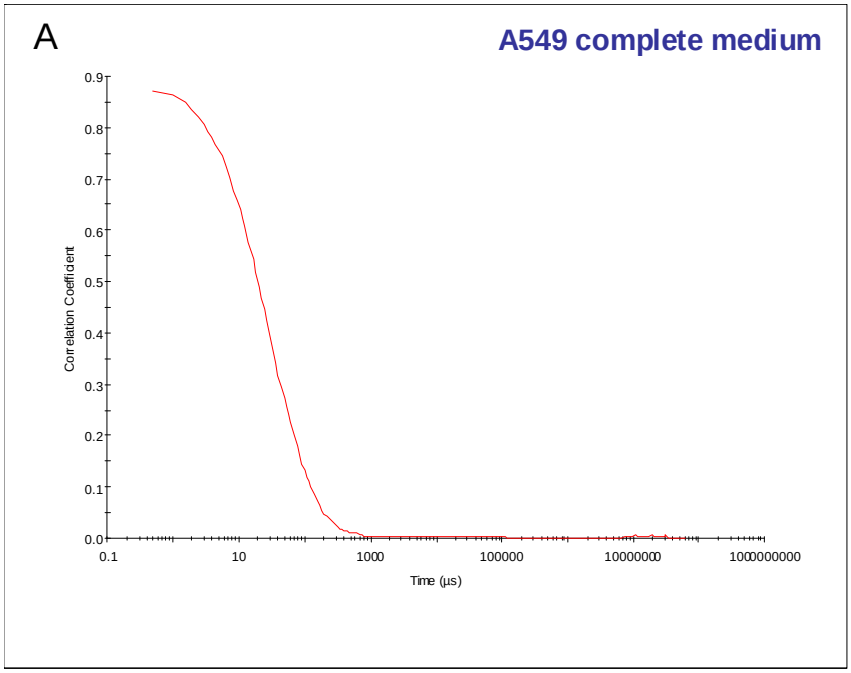


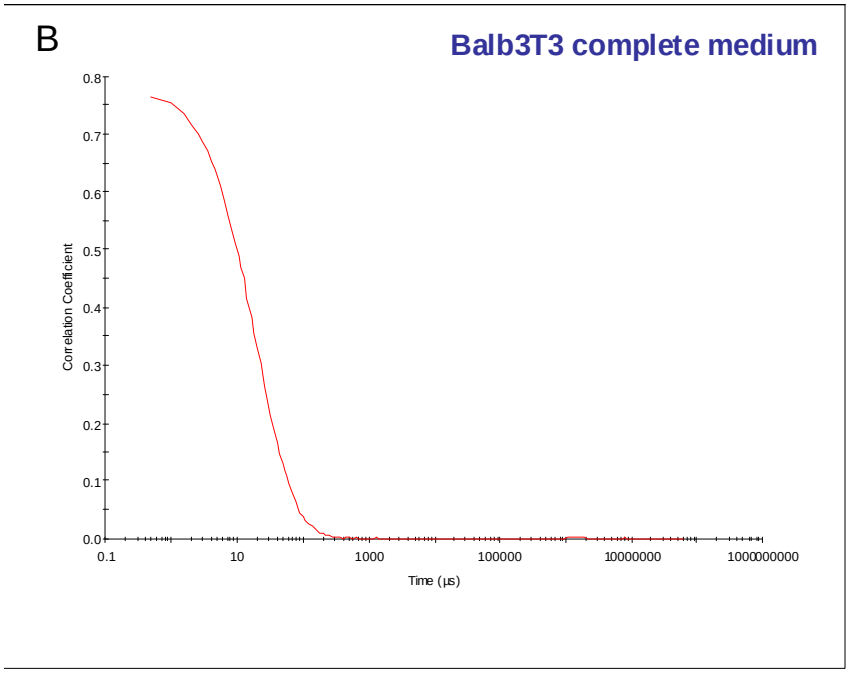


**Figures B.4A and B.4B: DLS correlograms of A549 and Balb3T3 complete culture media. The curves showed a sigmoid shape and Y intercepts at time 0 had values close to 1. Correlograms of this type are usually associated with samples that contain nano-sized objects.**

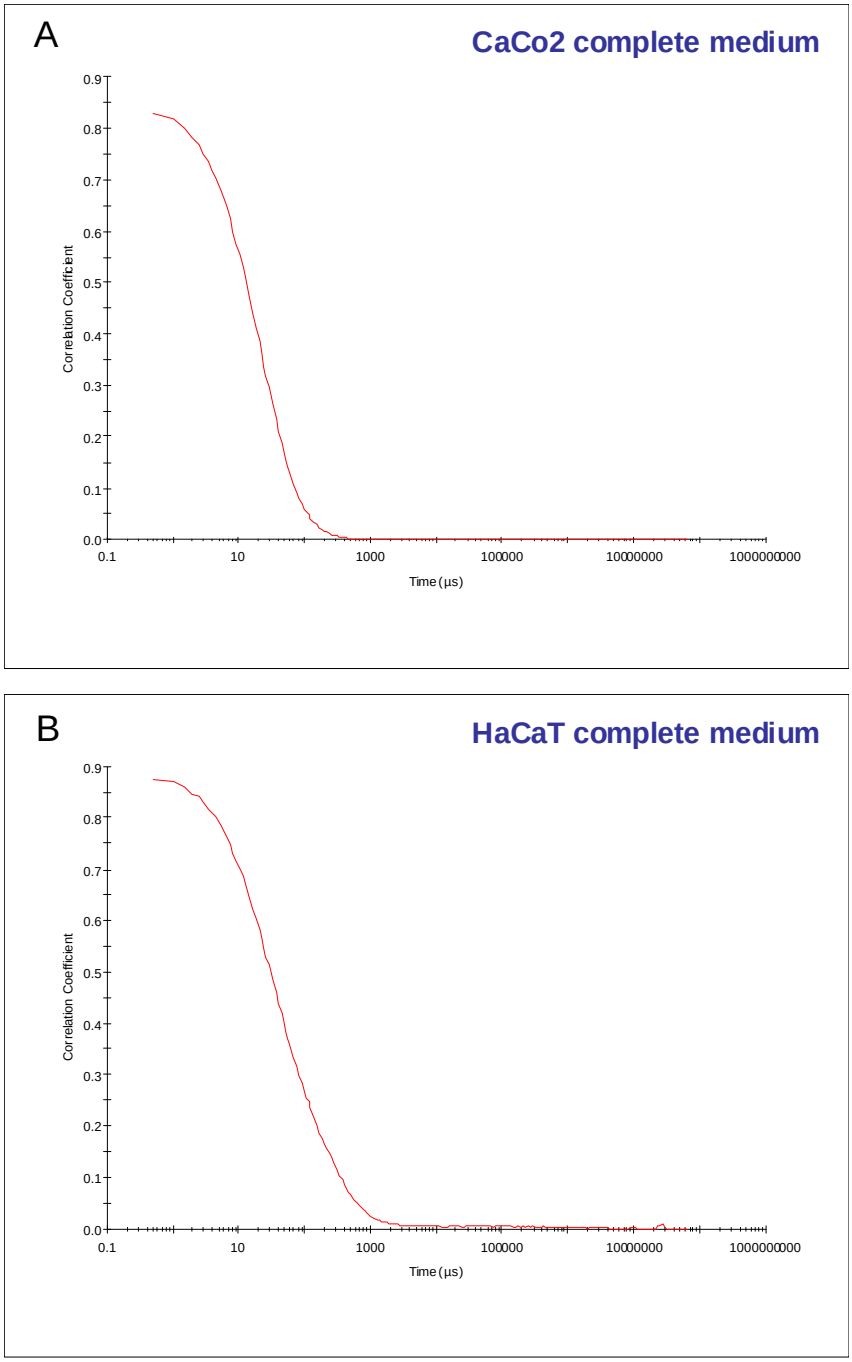


**Figures B.5A and B.5B: DLS correlograms of CaCo2 and HaCaT complete culture media. The curves showed a sigmoid shape and Y intercepts at time 0 had values close to 1. Correlograms of this type are usually associated with samples that contain nano-sized objects.**

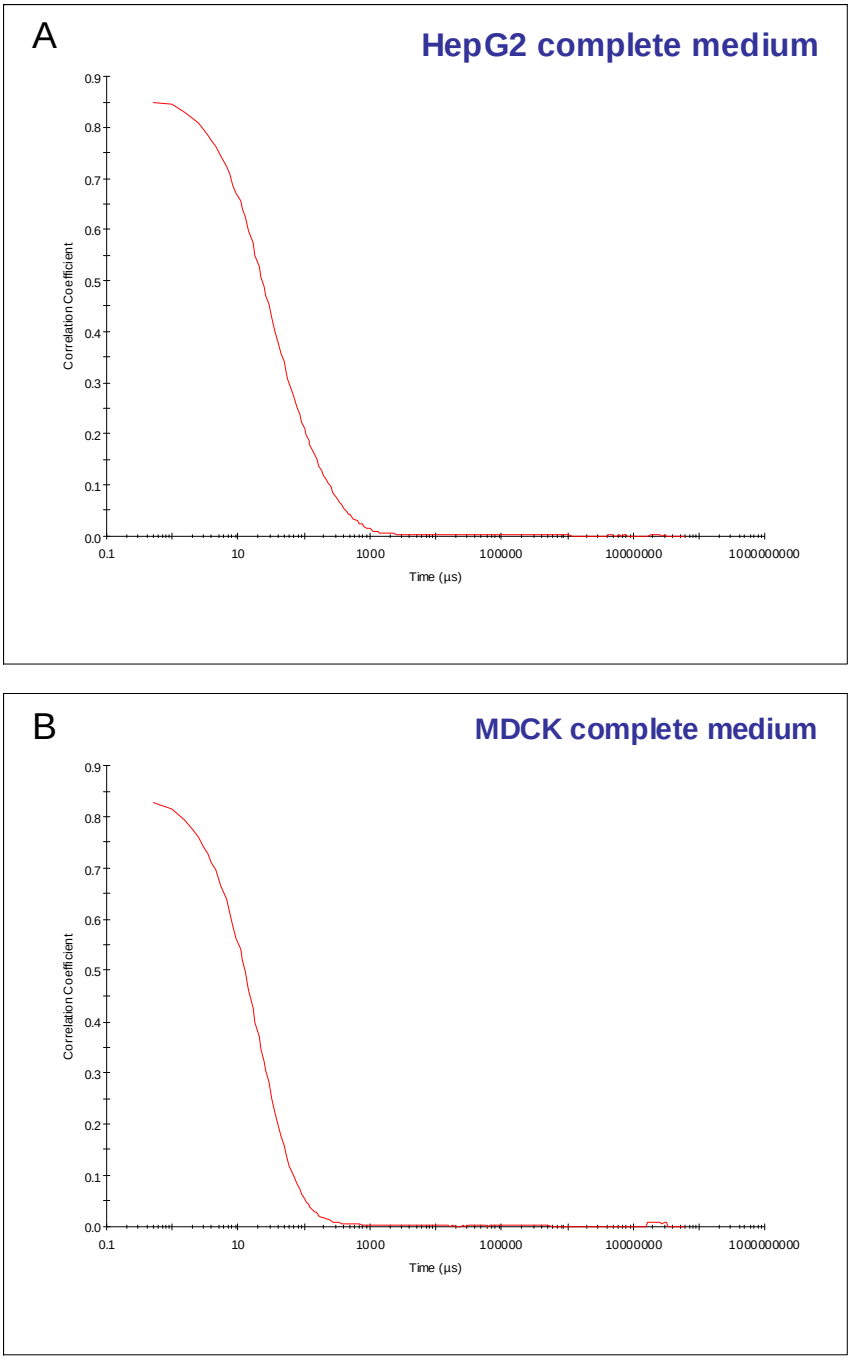


**Figures B.6A and B.6B: DLS correlograms of HepG2 and MDCK complete culture media. The curves showed a sigmoid shape and Y intercepts at time 0 had values close to 1. Correlograms of this type are usually associated with samples that contain nano-sized objects.**

The presence of nano-sized objects in these media resulted in subsequent analysis of their corresponding size distribution graphs. **Figures B.7** to **B.12** show the size distribution by both intensity and volume for each complete culture medium. The peaks in intensity were likely to be associated with the presence of cell culture medium components. In fact, a peak of approximately 8 nm was observed for all the complete media in the size distribution by volume graphs. This peak in volume might have been due to the bovine serum albumin, which is one of the most abundant proteins in sera used for cell culture (Foster, 1977).

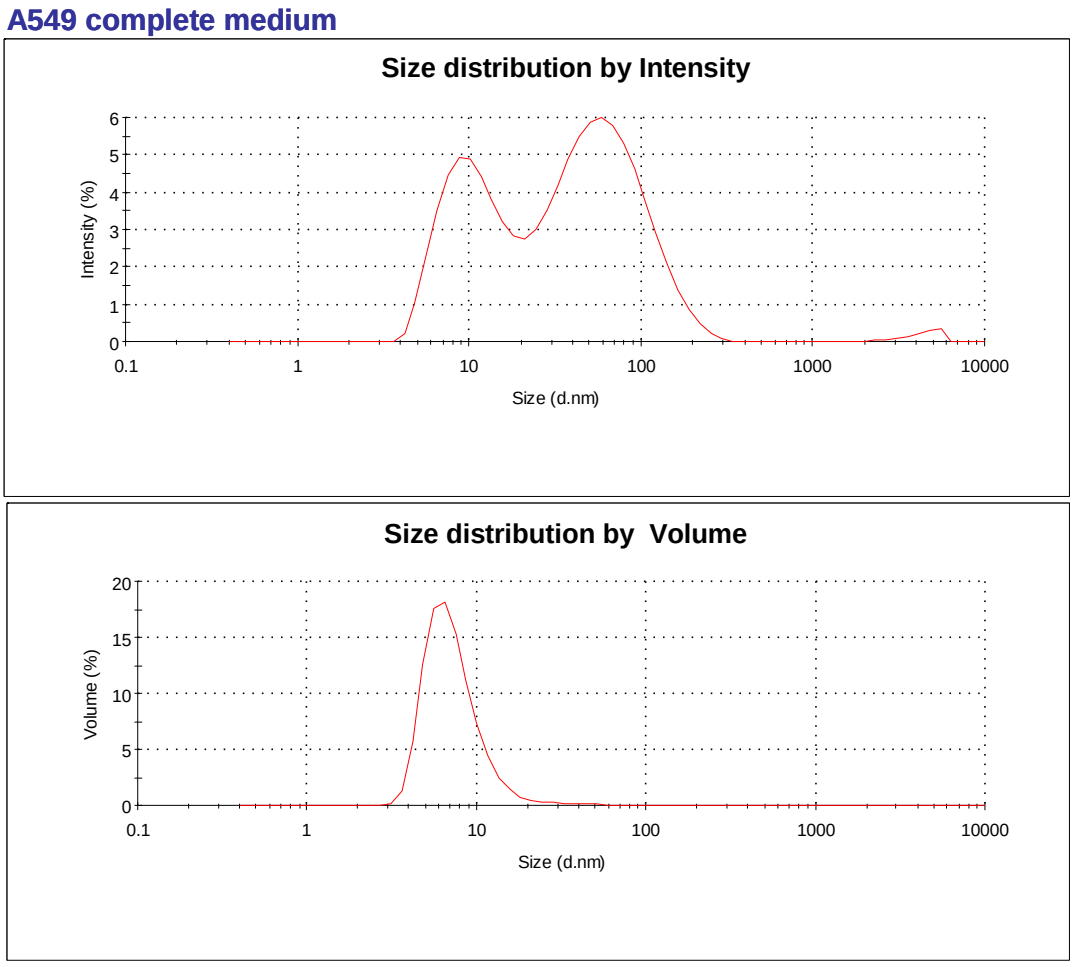


**Figure B.7: DLS size distribution average of six measurements by intensity (upper graph) and volume (lower graph) of complete culture medium employed for A549 cells. In both graphs, the percentage values (% Intensity and % Volume) are shown as a function of the nanometer size.**

**Balb3T3 complete medium**

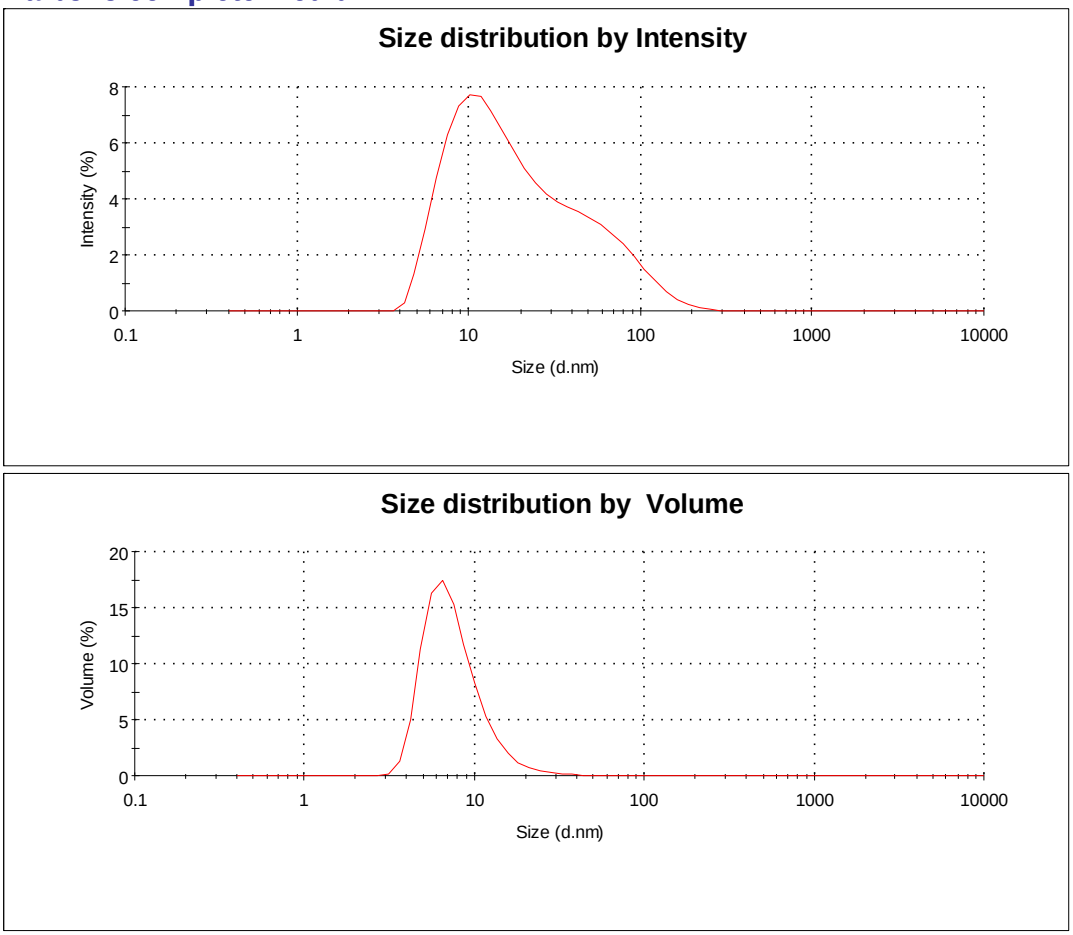


**Figure B.8: DLS size distribution average of six measurements by intensity (upper graph) and volume (lower graph) of complete culture medium employed for Balb3T3 cells. In both graphs, the percentage values (% Intensity and % Volume) are shown as a function of the nanometer size.**

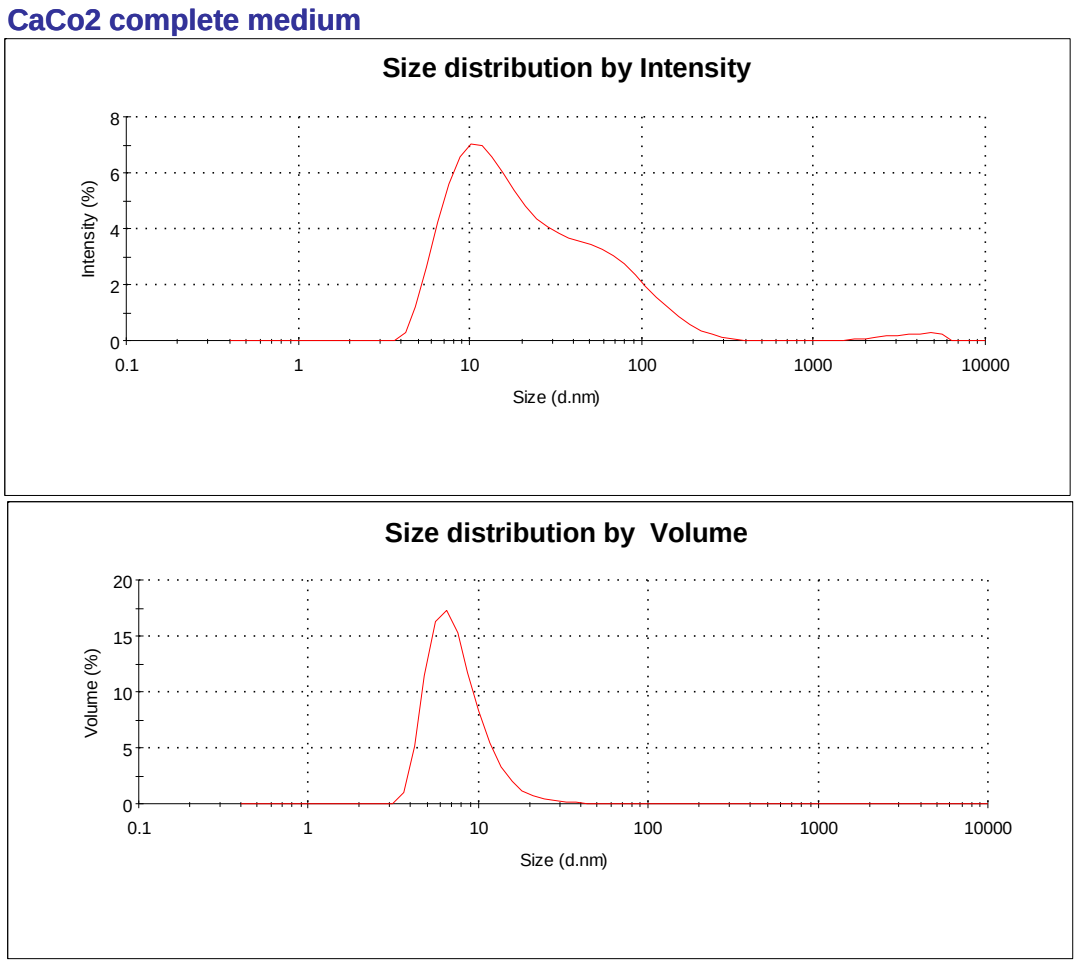


**Figure B.9: DLS size distribution average of six measurements by intensity (upper graph) and volume (lower graph) of complete culture medium employed for CaCo2 cells. In both graphs, the percentage values (% Intensity and % Volume) are shown as a function of the nanometer size.**

**HaCat complete medium**

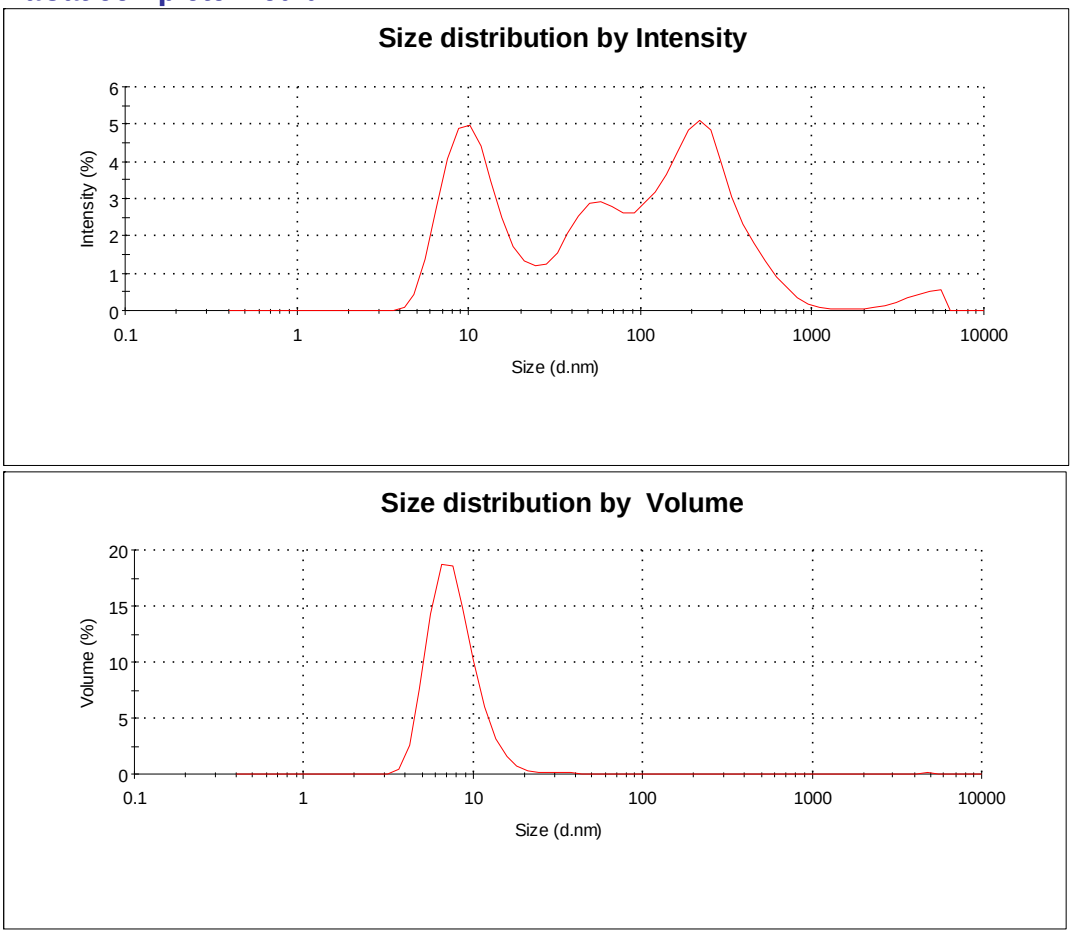


**Figure B.10: DLS size distribution average of six measurements by intensity (upper graph) and volume (lower graph) of complete culture medium employed for HaCaT cells. In both graphs, the percentage values (% Intensity and % Volume) are shown as a function of the nanometer size.**

**HepG2 complete medium**

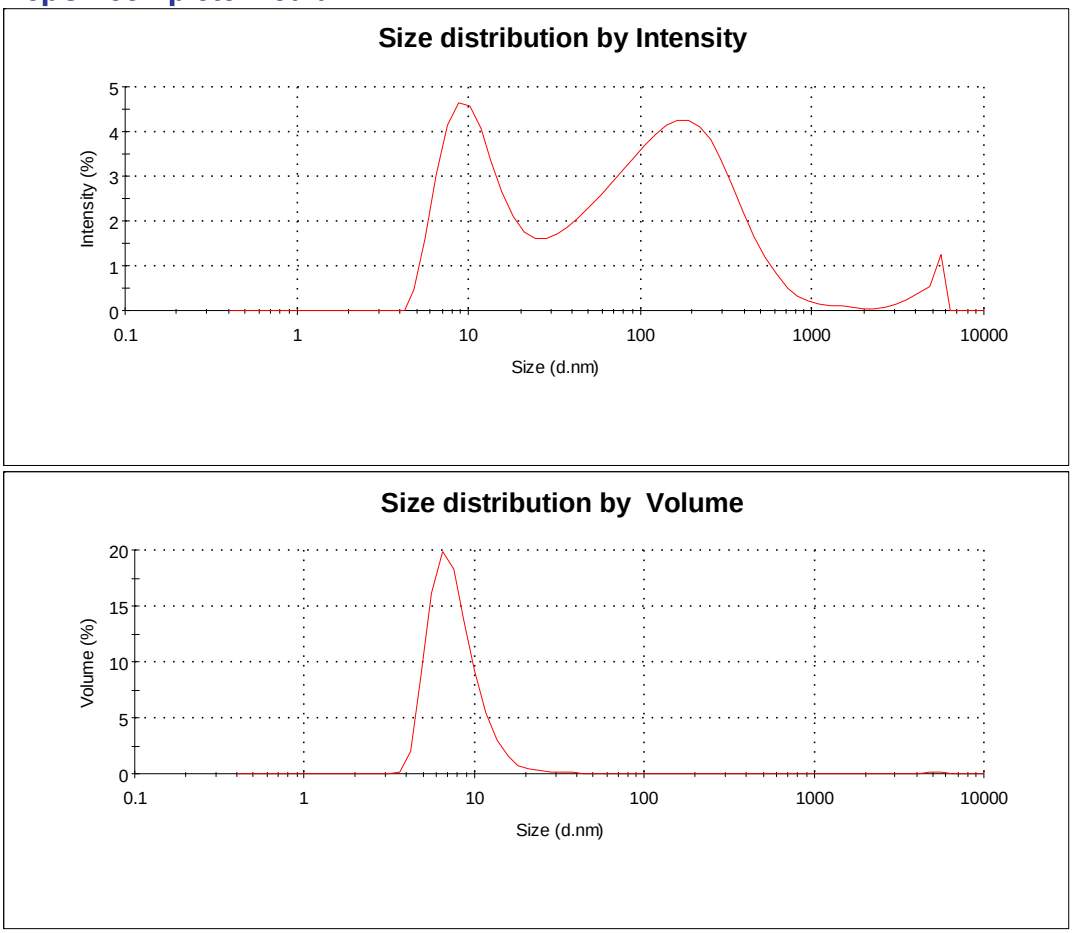


**Figure B.11: DLS size distribution average of six measurements by intensity (upper graph) and volume (lower graph) of complete culture medium employed for HepG2 cells. In both graphs, the percentage values (% Intensity and % Volume) are shown as a function of the nanometer size.**

**MDCK complete medium**

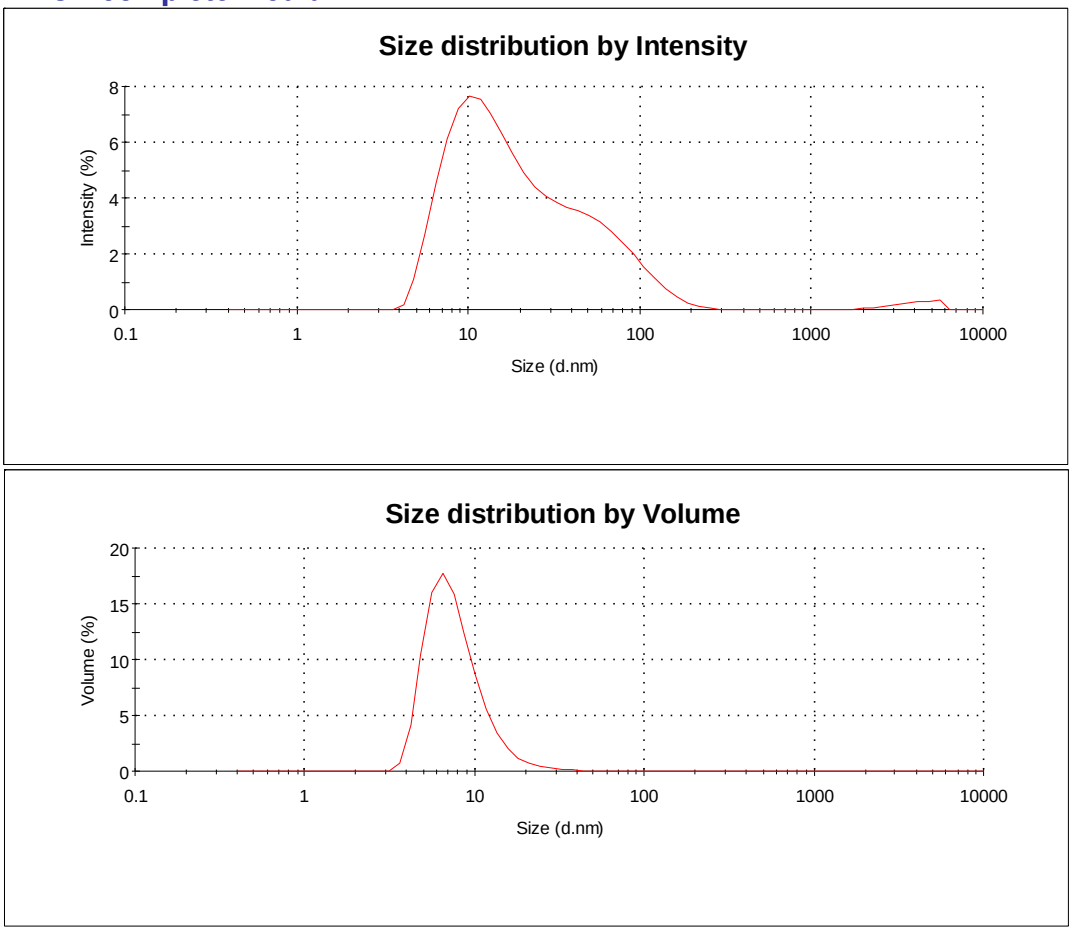


**Figure B.12: DLS size distribution average of six measurements by intensity (upper graph) and volume (lower graph) of complete culture medium employed for MDCK cells. In both graphs, the percentage values (% Intensity and % Volume) are shown as a function of the nanometer size.**

Different P601 and P703 NPs preparations were incubated for 72 hours at 37°C, 5% $CO_2$ and 90% humidity to reproduce the actual experimental conditions. **Table B.2** shows the data obtained from these NP preparations after DLS analysis; the mean NP diameters (Mean NP Ø) are reported in nanometers (nm).

**Table B.2: DLS measurements of $CoFe_2O_4$ P601 and P703 NP dilutions in dialyzed DEG (2% v/v), ultrapure water, basal media and complete culture media (100 µM) used in the toxicological studies. Only data on the main intensity peaks are shown. The standard deviation (SD) was used to assess variability in the measurements.**

| Sample Name | Polydispersity Index | ± SD | Mean NP Ø (nm) by intensity | ± SD |
|---|---|---|---|---|
| **P601 in:** | | | | |
| DEG | 0.160 | 0.020 | 35.6 | 1.08 |
| ultrapure water | 0.230 | 0.060 | 16.47 | 0.65 |
| HAM | 0.316 | 0.040 | 1593 | 151.26 |
| MEM | 0.361 | 0.030 | 1921 | 813.99 |
| DMEM | 0.293 | 0.040 | 2132 | 566.80 |
| A549 complete | 0.926 | 0.182 | 757.1 | 248.60 |
| Balb3T3 complete | 0.468 | 0.010 | 567.1 | 67.57 |
| CaCo2 complete | 0.580 | 0.040 | 784.0 | 118.20 |
| HaCat complete | 0.591 | 0.090 | 812.7 | 287.90 |
| HepG2 complete | 0.488 | 0.030 | 789.7 | 230.70 |
| MDCKcomplete | 0.542 | 0.040 | 623.2 | 96.89 |
| **P703 in:** | | | | |
| DEG | 0.180 | 0.050 | 59.5 | 10.64 |
| ultrapure water | 0.180 | 0.000 | 65.4 | 0.48 |
| HAM | 0.240 | 0.020 | 1642.0 | 465.95 |
| MEM | 0.390 | 0.100 | 1687.0 | 260.55 |
| DMEM | 0.400 | 0.080 | 1869.3 | 555.05 |
| A549 complete | 0.560 | 0.020 | 656.9 | 141.66 |
| Balb3T3 complete | 0.500 | 0.020 | 417.4 | 43.02 |
| CaCo2 complete | 0.330 | 0.040 | 381.7 | 23.22 |
| HaCat complete | 0.630 | 0.130 | 758.5 | 210.15 |
| HepG2 complete | 0.510 | 0.040 | 544.9 | 47.36 |
| MDCK complete | 0.470 | 0.040 | 423.5 | 55.69 |

When NP samples were prepared in DEG or ultrapure water, the size of the NPs did not change from that stated on the synthesis data sheet (28.81 nm for P601 and 83.22 nm for P703 in DEG, and 13.56 nm for P601 and 63.62 nm for P703 in ultrapure water) and the

polidispersity index (PdI) was at the maximum 0.2. The PdI value that was used as a reference for monodispersity in this study was 0.1, in accordance with the International Organization for Standardization directive ISO 22412:2008(E) for Particle size analysis-Dynamic Light Scattering (DLS). When NPs were diluted in basal media or in complete culture media and incubated for 72 hours, the size increased by several hundred nanometers. In particular, the largest NP diameters were found for NP dilutions in basal media (a maximum value of 2132 nm for P601 and 1869 nm for P703, both in DMEM), while the mean NP diameters found in complete culture media ranged from 300–800 nm. The PdI was greater than 0.3 in all these preparations. The comparison between mean NP diameter related to preparations in basal media with those in complete culture media suggested that serum proteins could stabilize the size of NPs. **Figures B.13A** and **B.13B** show the mean NP diameter (nm) for all preparations as histograms; standard deviations are given.

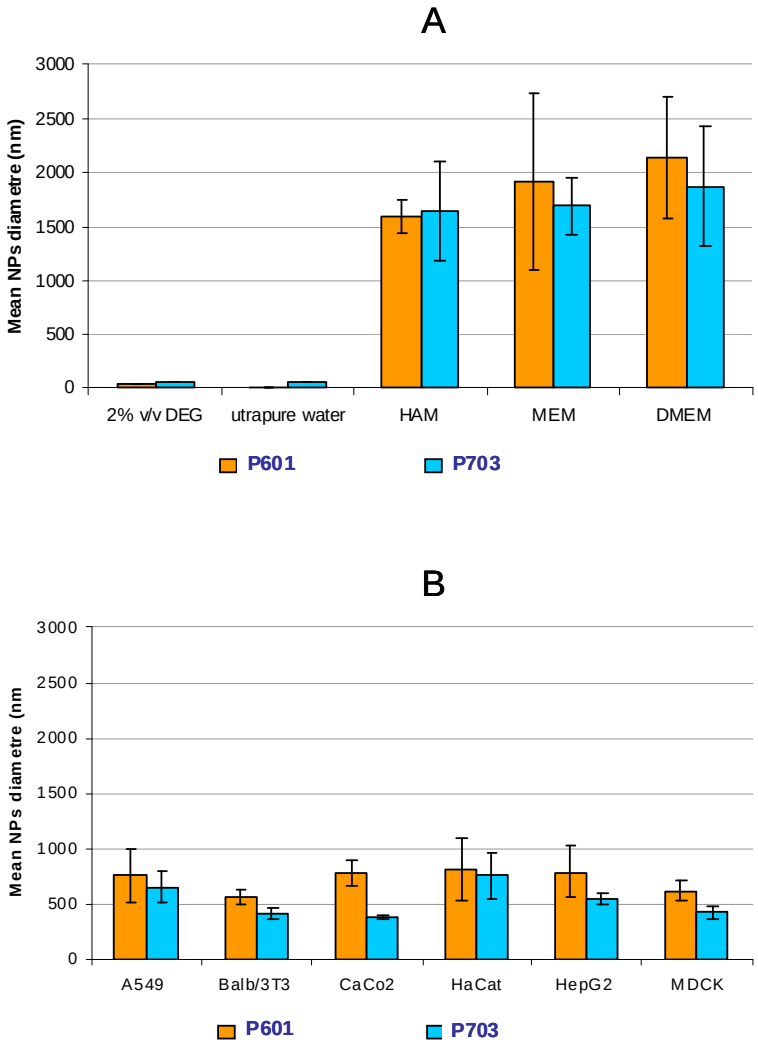


**Figures B.13A and B.13B: DLS measurements of P601 and P703 NPs dilutions in dialyzed DEG (2% v/v), ultrapure water, basal media and complete culture media (100 µM expected test concentration) after 72 hours of incubation in standard culture conditions (37°C, 5% $CO_2$, 90% humidity). The standard deviation (SD) is shown. Both $CoFe_2O_4$ NPs increase in size in the basal media environment (>1.5 µm); neither of the P601 and P703 preparations in dialyzed DEG and in ultrapure water increased in size. The PdI values for 2% v/v of P601 in dialyzed DEG and ultrapure water were 0.16 ± 0.02 and 0.23 ± 0.06, respectively. The PdI values for all other P601 preparations were ≥0.3. The PdI values for P703 preparations showed behaviour similar to that of P601 and corresponded to 0.180 ± 0.05 in both dialyzed DEG and ultrapure water.**

The P601 and P703 preparations were also characterized after 0 and 24 hours of incubation in MEM and Balb3T3 complete culture medium. The results are shown in **Figures B.14A** and **B.14B** and were compared to those after 72 hours of incubation. The P601 NPs prepared in MEM basal medium increased in size during the incubation period,

while P601 samples prepared in Balb3T3 complete medium had constant dimensions of approximately 500 nm **(Figure B.14A**).

The size of P703 NPs prepared in MEM basal medium increased to reach a maximum at 24 hours (2045 nm), but decreased after 72 hours (1687 nm) (**Figure B.14B**). As with P601 NPs, the size of the P703 NPs in Balb3T3 complete medium at all the time points studied were lower than that of NPs in MEM (approximately 500 nm) and remained constant. This suggested that the size of NPs could be stabilized by serum proteins.

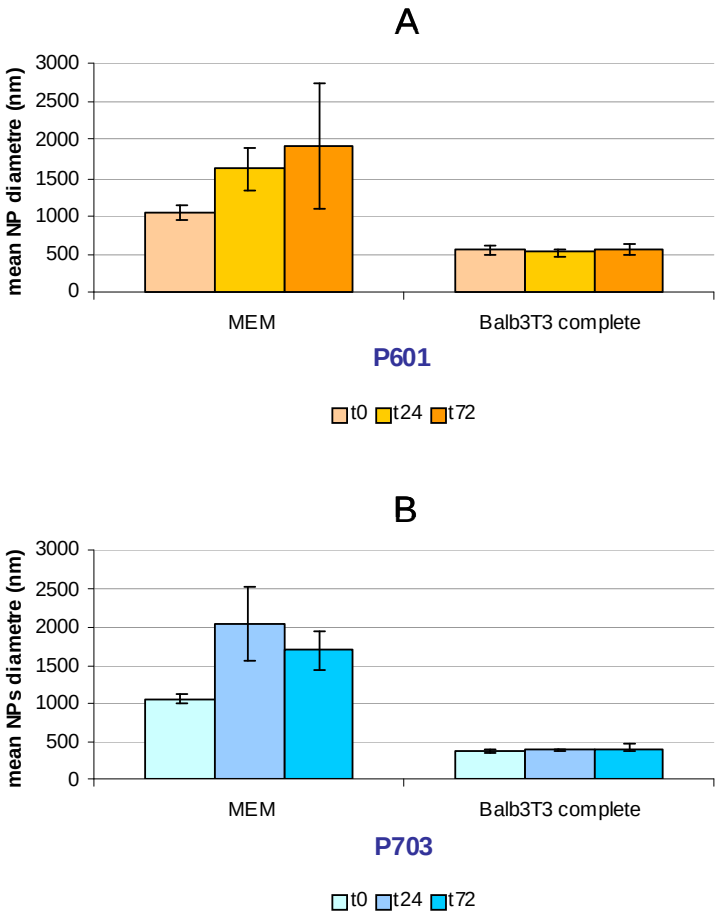


**Figures B.14A and B.14B: DLS measurements of $CoFe_2O_4$ P601 and P703 NP (100 µM) dilutions in basal medium MEM and Balb3T3 complete culture medium after 0, 24 and 72 hours of incubation, under standard culture conditions (37°C, 5% $CO_2$, 90% humidity). The standard deviation (SD) is shown. Both P601 and P703 NPs tended to form aggregates/agglomerates that were larger in medium without serum than those in the completed medium at all incubation time points studied. The PdI values for P601 were consistently >0.3; the PdI ranged between 0.361 ± 0.03 and 0.399 ± 0.04, and 0.468 ± 0.01 and 0.587 ± 0.04 for samples in MEM and Balb3T3 complete medium, respectively. In contrast, the PdI values for P703 ranged between 0.289 ± 0.03 and 0.390 ± 0.10, and 0.378 ± 0.05 and 0.500 ± 0.02 for MEM and Balb3T3 complete medium, respectively.**

### *B.1.3 Determination of impurities and quantification of Co in stock suspensions and $Co^{2+}$ ion release from $CoFe_2O_4$ NPs in culture medium*

Levels of cobalt in both the P601 and P703 NP stock suspensions were quantified using ICP-MS. The expected concentration (120 mM) of cobalt in the P601 NP stock suspension was similar to the real concentration (119 mM). In contrast, the cobalt concentration detected in the P703 NP stock suspension was lower than expected (98 mM vs. 118 mM). Therefore, P703 concentrations used in the biological studies that were supposedly in the range of 10–120 μM were actually lower.

The comparison of expected and real concentrations for P703 NPs is shown in **Table B.3**. Real concentrations were calculated using 119 and 98 mM as stock suspension concentrations for P601 and P703 NPs, respectively, as determined by ICP-MS analysis of stock suspensions in this study. Expected concentrations were calculated using 120 and 118 mM as stock suspension concentrations for P601 and P703 NPs, respectively, as stated by the manufacturer on the data sheets. Notably, the concentrations in **Table B.3** are expressed as micro Molarity (μM), micrograms of cobalt per milliliter (μg Co/mL), micrograms of $CoFe_2O_4$ per milliliter (μg $CoFe_2O_4$/mL) and the number of NPs per milliliter (No. NPs/mL).

The number of NPs per mL was calculated under the assumption that all NPs in a sample were spherical and homogeneous in size (i.e., no agglomerates or aggregates present) and using the following **formula (B.1)**:

$$\textbf{No. NPs/mL} = \mathbf{a}/\mathbf{m} \qquad \textbf{(B.1)}$$

where:

**a** = Concentration of NPs as grams per litre (g/L)

**m** = 1 NP mass as volume of a single spherical NP multiplied by the $CoFe_2O_4$ density (1.06 g/cm$^3$, as stated by the supplier for both P601 and P703 NPs),

and using 16.5 nm and 65.4 nm as the hydrodynamic diameters of P601 and P703, respectively, as determined using DLS analysis in ultrapure water in this study.

Finally, in the context of tested concentrations and related number of NPs employed, it should be noted that cells were treated with $CoFe_2O_4$ NPs diluted in complete culture

medium in the biological experiments. The volumes used were 100 µL, 3 mL, 6 mL and 4 mL per well/Petri dish in the NR, CFE, CTA and CBMN assays, respectively (please see **sections 2.5.1**, **2.5.2**, **2.5.3** and **2.5.4** for information on the protocols used for the biological assays).

**Table B.3: Conversion into different units of measure for P601 and P703 $CoFe_2O_4$ NP concentrations tested in the experiments described. Expected concentrations were calculated using 120 and 118 mM as stock suspension concentrations for P601 and P703 NPs, respectively, as stated by the manufacturer. Real concentrations were calculated using 119 and 98 mM as stock suspension concentrations for P601 and P703 NPs, respectively, as determined by ICP-MS analysis of the stock suspensions. The number of NPs per mL was calculated using formula B.1 and 16.5 nm and 65.4 nm as diameters of P601 and P703, respectively, as determined by DLS analysis in ultrapure water.**

| | µM | | µg Co /mL | | µg CoFe2O4 /mL | | No.NPs/mL | |
|---|---|---|---|---|---|---|---|---|
| | *expected* | *real* | *expected* | *real* | *expected* | *real* | *expected* | *real* |
| **P601** | | | | | | | | |
| | 10 | 9.92 | 0.59 | 0.59 | 2.35 | 2.33 | 9.41E+11 | 9.34E+11 |
| | 20 | 19.83 | 1.18 | 1.17 | 4.69 | 4.65 | 1.88E+12 | 1.87E+12 |
| | 30 | 29.75 | 1.77 | 1.76 | 7.04 | 6.98 | 2.82E+12 | 2.80E+12 |
| | 40 | 39.67 | 2.36 | 2.34 | 9.38 | 9.30 | 3.77E+12 | 3.73E+12 |
| | 50 | 49.59 | 2.95 | 2.93 | 11.73 | 11.63 | 4.71E+12 | 4.67E+12 |
| | 60 | 59.53 | 3.54 | 3.51 | 14.07 | 13.96 | 5.65E+12 | 5.60E+12 |
| | 80 | 79.34 | 4.72 | 4.68 | 18.77 | 18.61 | 7.53E+12 | 7.47E+12 |
| | 100 | 99.17 | 5.90 | 5.85 | 23.46 | 23.26 | 9.41E+12 | 9.34E+12 |
| | 120 | 119.05 | 7.08 | 7.02 | 28.15 | 27.93 | 1.13E+13 | 1.12E+13 |
| **P703** | | | | | | | | |
| | 10 | 8.31 | 0.59 | 0.49 | 2.35 | 1.95 | 1.51E+10 | 1.26E+10 |
| | 20 | 16.61 | 1.18 | 0.98 | 4.69 | 3.90 | 3.02E+10 | 2.51E+10 |
| | 30 | 24.92 | 1.77 | 1.47 | 7.04 | 5.84 | 4.53E+10 | 3.77E+10 |
| | 40 | 33.22 | 2.36 | 1.96 | 9.38 | 7.79 | 6.05E+10 | 5.02E+10 |
| | 50 | 41.53 | 2.95 | 2.45 | 11.73 | 9.74 | 7.56E+10 | 6.28E+10 |
| | 60 | 49.85 | 3.54 | 2.94 | 14.07 | 11.69 | 9.07E+10 | 7.54E+10 |
| | 80 | 66.44 | 4.72 | 3.92 | 18.77 | 15.58 | 1.21E+11 | 1.00E+11 |
| | 100 | 83.05 | 5.90 | 4.90 | 23.46 | 19.48 | 1.51E+11 | 1.26E+11 |
| | 120 | 99.70 | 7.08 | 5.88 | 28.15 | 23.39 | 1.81E+11 | 1.51E+11 |

The P601 and P703 NPs dilutions in complete (Balb3T3) and serum free (MEM) culture media of 1, 10 and 60 µM (for 0 and 24 hours of incubation) and of 20, 40, 60, 120 µM (for 0 and 72 hours of incubation) were prepared for analysis by ICP-MS to determine $Co^{2+}$ ion leakage. In order to determine the release of $Co^{2+}$ ions, the amount of Co was measured by ICP-MS in total and filtered fractions for each dilution after 0, 24 and 72 hours. Data collected were then analysed to determine the $Co^{2+}$ ions released. The $Co^{2+}$ ion release was considered to be the difference between Co detected in filtered fractions

at 24 or 72 hours and the amount of Co detected in filtered fractions at time 0 hours (**Tables B.4-B.7**). The ion leakage was also expressed as percentage of the average of cobalt detected in total fractions. The expected values of Co in the total fractions were obtained using 119 and 98 mM as the concentration of P601 and P703, respectively. Hereafter, only results related to the MEM and Balb3T3 culture medium are presented because cytotoxicity was detected using CFE only in this instance. These data were later used to determine if cytotoxicity was induced by NPs or by $Co^{2+}$ ions *per se*.

The release in MEM appeared to be dose-dependent for both P601 and P703 NPs (**Tables B.4** and **B.5).**

**Table B.4: Cobalt concentrations (µM) detected by ICP-MS in P601 $CoFe_2O_4$ samples prepared in MEM basal medium in total and filtered fractions, both at time 0 and after 24 and 72 hours of incubation under standard culture conditions (37°C, 5% $CO_2$, 90% humidity). Expected concentrations in total fractions were calculated using 119 mM as concentration of the stock suspension for P601. The release of cobalt ($Co^{2+}$) was calculated as the difference between the cobalt detected at 24 or 72 hours and at time 0 in filtered fractions. The percentage release was calculated using the corresponding average of the total fractions.**

| | Concentration of Co (µM) in MEM | | | | | | | |
|---|---|---|---|---|---|---|---|---|
| | expected in total fractions | detected in total fractions | | average | detected in filtered fractions | | release | % |
| | | t0 | t24 | | t0 | t24 | | |
| P601 | | | | | | | | |
| | 0.99 | 1.11 | 1.11 | 1.11 | 0.23 | 0.33 | 0.10 | 9.01 |
| | 9.92 | 10.88 | 10.32 | 10.60 | 1.45 | - | | |
| | 59.53 | 69.29 | 51.98 | 60.64 | 7.68 | 14.80 | 7.12 | 11.74 |
| | | t0 | t72 | | t0 | t72 | | |
| | 19.83 | 19.98 | 18.77 | 19.38 | 3.80 | 5.44 | 1.64 | 8.46 |
| | 39.67 | 41.80 | 39.67 | 40.74 | 7.80 | 10.48 | 2.68 | 6.58 |
| | 59.53 | 60.38 | 61.37 | 60.88 | 11.54 | 16.46 | 4.92 | 8.08 |
| | 119.05 | 117.99 | 115.02 | 116.51 | 21.83 | 30.42 | 8.59 | 7.37 |

**Table B.5: Cobalt concentrations (µM) detected by ICP-MS in P703 $CoFe_2O_4$ samples prepared in MEM basal medium in total and filtered fractions, both at time 0 and after 24 and 72 hours of incubation under standard culture conditions (37°C, 5% $CO_2$, 90% humidity). Expected concentrations in total fractions were calculated using 98 mM as concentration of the stock suspension for P703. The release of cobalt ($Co^{2+}$) was calculated as the difference between the cobalt detected at 24 or 72 hours and at time 0 in filtered fractions. The percentage release was calculated using the corresponding average of the total fractions.**

| Concentration of Co (µM) in MEM | | | | | | | | |
|---|---|---|---|---|---|---|---|---|
| | expected in total fractions | detected in total fractions | | average | detected in filtered fractions | | release | % |
| | | t0 | t24 | | t0 | t24 | | |
| P703 | | | | | | | | |
| | 0.83 | 0.96 | 0.81 | 0.89 | 0.15 | 0.31 | 0.16 | 18.08 |
| | 8.31 | 9.65 | 8.08 | 8.87 | 2.70 | 4.44 | 1.74 | 19.63 |
| | 49.85 | 68.51 | 41 | 54.76 | 9.64 | 12.06 | 2.42 | 4.42 |
| | | t0 | t72 | | t0 | t72 | | |
| | 16.61 | 12.14 | 11.02 | 11.58 | 4.90 | 7.08 | 2.18 | 18.83 |
| | 33.22 | 26.73 | 26.17 | 26.45 | 9.70 | 14.15 | 4.45 | 16.82 |
| | 49.85 | 58.20 | 62.52 | 60.36 | 14.30 | 21.75 | 7.45 | 12.34 |
| | 99.70 | 74.10 | 82.39 | 78.25 | 27.60 | 51.93 | 24.33 | 31.09 |

When comparing results related to P601 and P703 NPs dilutions in Balb3T3 culture medium (**Tables B.6** and **B.7**), the release of $Co^{2+}$ ions again appeared to be dose-dependent for both NPs.

**Table B.6: Cobalt concentrations (µM) detected by ICP-MS in P601 $CoFe_2O_4$ samples prepared in Balb3T3 complete culture medium in total and filtered fractions, both at time 0 and after 24 and 72 hours of incubation under standard culture conditions (37°C, 5% $CO_2$, 90% humidity). Expected concentrations in total fractions were calculated using 119 mM as concentration of the stock suspension for P601. The release of cobalt ($Co^{2+}$) was calculated as the difference between the cobalt detected at 24 or 72 hours and at time 0 in the filtered fractions. The percentage release was calculated using the corresponding average of the total fractions.**

| Concentration of Co (µM) in Balb3T3 culture medium | | | | | | | | |
|---|---|---|---|---|---|---|---|---|
| | expected in total fractions | detected in total fractions | | average | detected in filtered fractions | | release | % |
| | | t0 | t24 | | t0 | t24 | | |
| P601 | | | | | | | | |
| | 0.99 | 1.12 | 0.76 | 0.94 | 0.21 | 0.24 | 0.03 | 3.19 |
| | 9.92 | 10.45 | 9.06 | 9.76 | 2.00 | 3.12 | 1.12 | 11.48 |
| | 59.53 | 61.74 | 50.24 | 55.99 | 11.74 | 13.21 | 1.47 | 2.63 |
| | | t0 | t72 | | t0 | t72 | | |
| | 19.83 | 19.95 | 20.34 | 20.15 | 2.70 | 5.10 | 2.40 | 11.91 |
| | 39.67 | 41.37 | 40.52 | 40.95 | 4.80 | 8.62 | 3.82 | 9.33 |
| | 59.53 | 59.61 | 59.47 | 59.54 | 7.30 | 11.94 | 4.64 | 7.79 |
| | 119.05 | 120.71 | 98.41 | 109.56 | 13.60 | 21.91 | 8.31 | 7.58 |

**Table B.7: Cobalt concentrations (µM) detected by ICP-MS in P703 $CoFe_2O_4$ samples prepared in Balb3T3 complete culture medium in total and filtered fractions, both at time 0 and after 24 and 72 hours of incubation under standard culture conditions (37°C, 5% $CO_2$, 90% humidity). Expected concentrations in total fractions were calculated using 98 mM as concentration of the stock suspension for P703. The release of cobalt ($Co^{2+}$) was calculated as the difference between the cobalt detected at 24 or 72 hours and at time 0 in filtered fractions. The percentage release was calculated using the corresponding average of the total fractions.**

| | Concentration of Co (µM) in Balb3T3 culture medium | | | | | | | |
|---|---|---|---|---|---|---|---|---|
| | expected | detected | | | detected | | | |
| | in total fractions | in total fractions | | average | in filtered fractions | | release | % |
| | | t0 | t24 | | t0 | t24 | | |
| P703 | | | | | | | | |
| | 0.83 | 0.86 | 0.72 | 0.79 | 0.22 | 0.24 | 0.02 | 2.53 |
| | 8.31 | 8.67 | 8.48 | 8.58 | 1.87 | 3.78 | 1.91 | 22.27 |
| | 49.85 | 61.95 | 38.39 | 50.17 | 11.39 | 18.74 | 7.35 | 14.65 |
| | | t0 | t72 | | t0 | t72 | | |
| | 16.61 | 16.96 | 14.95 | 15.96 | 2.90 | 5.00 | 2.10 | 13.16 |
| | 33.22 | 33.01 | 30.14 | 31.58 | 5.80 | 10.07 | 4.27 | 13.52 |
| | 49.85 | 50.69 | 47.37 | 49.03 | 8.60 | 12.68 | 4.08 | 8.32 |
| | 99.70 | 92.79 | 81.72 | 87.26 | 16.80 | 27.78 | 10.98 | 12.58 |

The $Co^{2+}$ released by P601 NPs in Balb3T3 complete medium was, on average, less than that released in MEM after 24 hours of incubation. In contrast, the $Co^{2+}$ released by P601 after 72 hours was slightly higher in Balb3T3 complete medium than in MEM (**Tables B.6 and B.4**). A similar comparison of $Co^{2+}$ released in Balb3T3 and MEM media was also done for P703 NPs; the $Co^{2+}$ released by P703 NPs was, on average, greater in Balb3T3 complete medium after 24 hours and in MEM after 72 hours of incubation (**Tables B.7 and B.5**).

Both P601 and P703 NPs stock suspensions were analysed using ICP-MS to identify and quantify potential metal impurities. **Table B.8** shows the metal impurities found in P601 and P703 NPs as a percentage of the $CoFe_2O_4$ stock suspension, as well as their µM concentration in the $CoFe_2O_4$ stock suspension. The concentration of each metal contaminant related to the maximum concentration of $CoFe_2O_4$ tested (120 µM and 99.7 µM for P601 and P703, respectively) is shown. At these levels, any of the impurities found have the potential to induce toxic effects on Balb3T3 cells, which appear to be the most sensitive of the cell lines used to test the $CoFe_2O_4$ NPs (Ponti, unpublished data).

**Table B.8: Metal impurities detected by ICP-MS analysis in P601 and P703 $CoFe_2O_4$ stock suspensions. The metal amounts detected are reported as a percentage of the stock suspension (119 mM and 98 mM stock concentrations for P601 and P703, respectively), the corresponding concentration as micromolarity and the maximum concentration present in the maximum dose of $CoFe_2O_4$ tested. At these levels, any of the impurities can potentially induce toxic effects after 72 hours of treatment on Balb3T3 cells, which appear to be the most sensitive culture of the cell lines used to test the $CoFe_2O_4$ NPs (Ponti, unpublished data).**

| P601 | | | |
|---|---|---|---|
| **metal** | **% Stock $CoFe_2O_4$** | **Concentration in stock (µM)** | **Max. concentration in test (µM)** |
| Aluminium (Al) | 1.8 | 0.0125 | $1.25x10^{-5}$ |
| Boron (B) | 2.4 | 0.0409 | $4.09x10^{-5}$ |
| Magnesium (Mg) | 1.1 | 0.0082 | $8.2x10^{-6}$ |
| Nickel (Ni) | 3 | 0.0095 | $9.5x10^{-6}$ |
| **P703** | | | |
| **metal** | **% Stock $CoFe_2O_4$** | **Concentration in stock (µM)** | **Max. concentration in test (µM)** |
| Aluminium (Al) | 3 | 0.0122 | $1.24x10^{-5}$ |
| Magnesium (Mg) | 1 | 0.0047 | $4.76x10^{-6}$ |

### *B.1.4 Sedimentation*

**Figure B.15A** shows some of the 144 cycles completed during the sedimentation experiment with $CoFe_2O_4$ NPs P601 using the spectrophotometer. The absorbance was measured close to the upper end of the liquid column in the cuvette every 30 minutes over 72 hours, and decreased cycle by cycle. A similar solution was measured under the same conditions close to the lower end of the liquid column.

**Figure B.15B** shows the absorption measured at 500 nm wavelength at the upper end of the column as a function of time, whilst **Figure B.16A** shows the temporal behaviour of the absorption at the lower end of the column. The figures show that the absorption towards the upper end of the column decreased (depletion regime), but increased at the lower end (accumulation regime), indicating that sedimentation/precipitation for P601 NPs occurred. Similar measurements were made for $CoFe_2O_4$ NPs P703, but in this case only close to the bottom of the cuvette **(**see **Figure B.16B)**. The increased absorption also

indicated accumulation of NPs at the bottom of the cuvette and suggested that sedimentation had occurred.

It was concluded from these observations that the timescale for experiments involving the exposure of cell cultures at the bottom of a dish/well has to be considered carefully. In fact, if experiments are to be based on a timescale of minutes, sedimentation effects probably can be ignored, but should be taken into consideration in experiments using a treatment period of days.

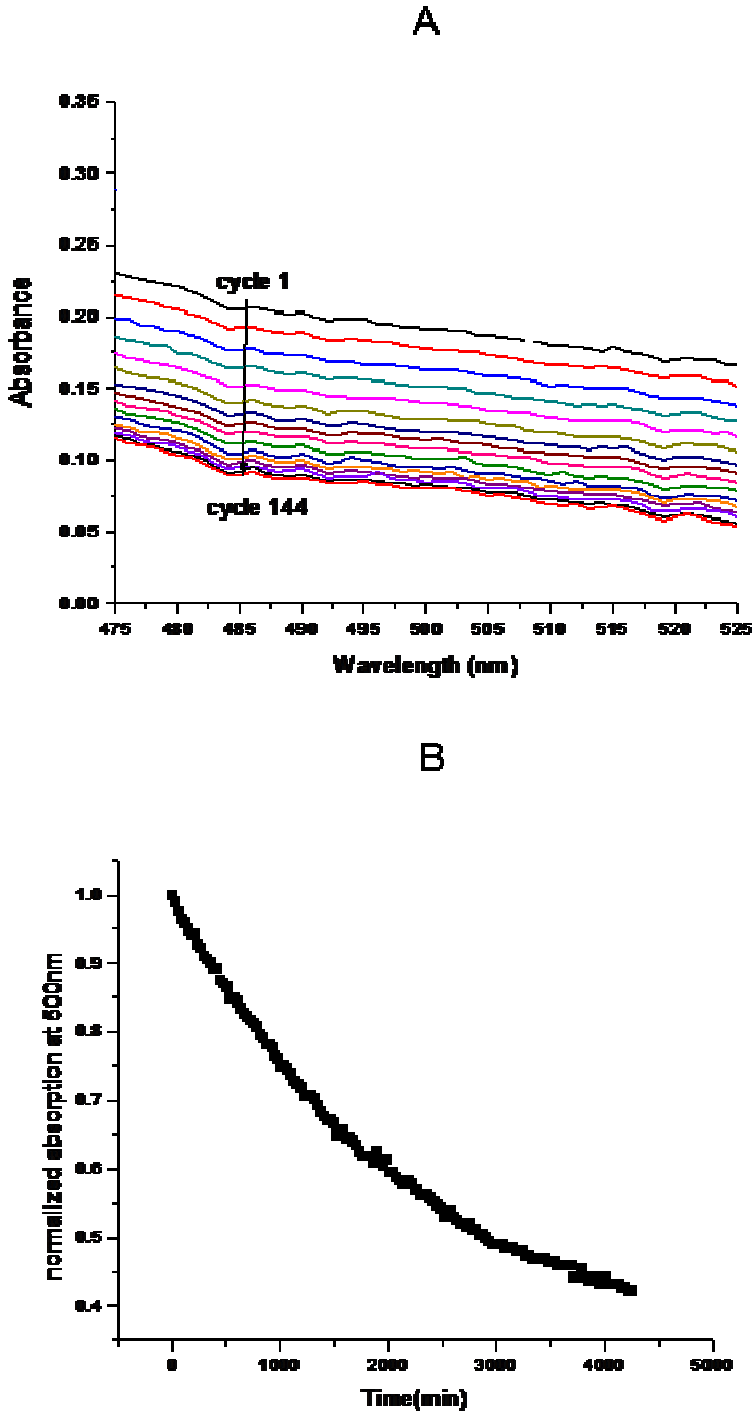


**Figures B.15A and B.15B: Some of the 144 cycles of the UV-Vis measurements in a $CoFe_2O_4$ P601 sample (60 µM) in complete culture medium without Phenol Red at fixed height (upper cuvette region) made every 30 minutes over 72 hours (A), and normalized absorption of the same sample at 500 nm (upper cuvette region) (B).**

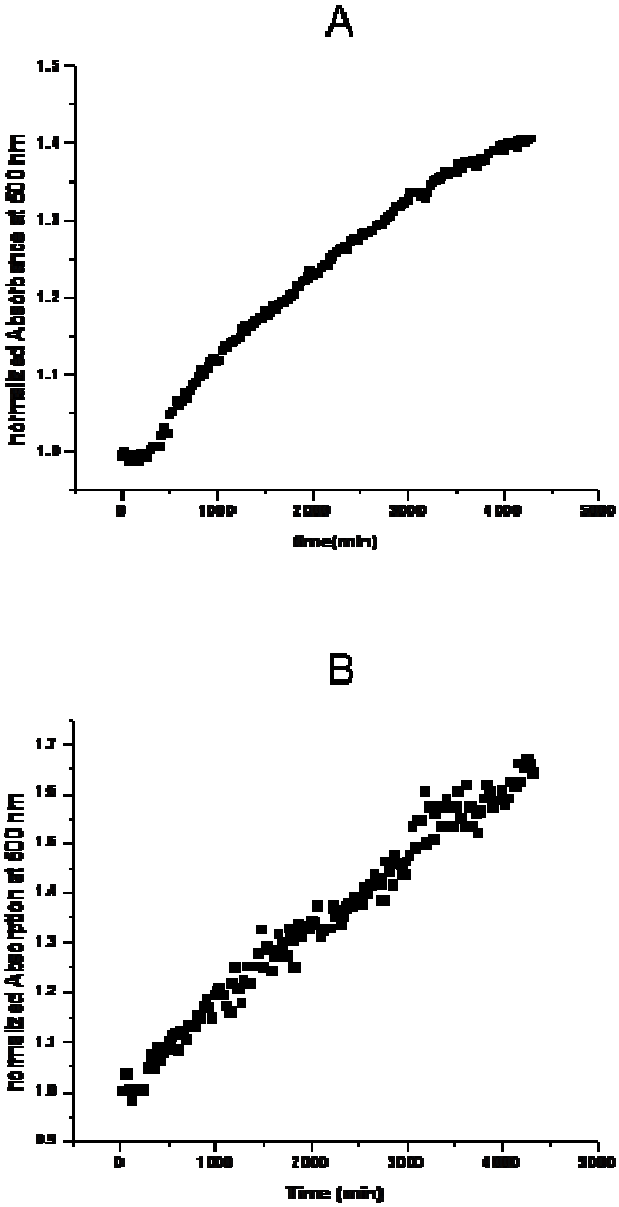


**Figures B.16A and B.16B: Normalized absorption of a sample of $CoFe_2O_4$ P601 (A) and P703 (B) at a concentration of 60 µM in complete culture medium at fixed height (bottom cuvette region) in complete culture medium without Phenol Red at 500 nm.**

## B.2 Characterization of Ag NPs

### *B.2.1 Zeta potential*

The Zeta potential values (Z-potential), expressed as mV ± SD, measured for dilutions of 100 µM of NM-300, Ag 44 nm, Ag 84 nm, and Ag 100 nm in ultrapure water are shown in **Table B.9**. All the Ag NPs studied exhibited a negative surface charge and NM-300 was the only Ag NP unstable in an aqueous environment because its Z-potential was in the range of +30 mV to -30 mV.

**Table B.9: Z-potential measurements of all Ag NPs evaluated in this study. The Ag NPs dilutions in ultrapure water were investigated to determine their surface charge. Values are expressed as mV ± standard deviation (SD). All Ag NPs had a negative surface charge, but only Ag 44 nm, Ag 84 nm and Ag 100 nm showed values lower than -30 mV, which indicated that they were stable in an aqueous environment.**

| Sample name | Zpot (mV) ± sd |
|---|---|
| **NM-300 prepared in:** | |
| ultrapure water | -11 ± 2.77 |
| **Ag 44 nm prepared in:** | |
| ultrapure water | -54.5 ± 12.2 |
| **Ag 84 nm prepared in:** | |
| ultrapure water | -49.4 ± 0.42 |
| **Ag 100 nm prepared in:** | |
| ultrapure water | -45.3 ± 1.20 |

### *B.2.2 Size distribution*

**Table B.10** shows the results of DLS measurements of dilutions of each Ag NP studied in different media. The mean diameter of each NP measured by DLS at time 0 in ultrapure water confirmed the nominal sizes stated for Ag 44 nm, Ag 84 nm and Ag 100 nm and determined after their synthesis. It should be noted that the diameter of a NM-300 dilution in ultrapure water measured using DLS was 46 nm compared to the stated diameter of 20 nm obtained by TEM micrographs of the stock suspension. The difference in these two values may be explained by the fact that the TEM technique measures the NP core disregarding any surfactant effect, while DLS measures the hydrodynamic diameter. The hydrodynamic diameter may, therefore, includes molecules of the surfactant surrounding the particle.

**Table B.10: The mean NP diameter (Mean NPs Ø) (nm) of all Ag NPs investigated in this study. The DLS measurements were done for Ag NP dilutions in ultrapure water, Phosphate Buffer Saline (PBS), MEM basal medium and Balb3T3 complete culture medium (100 µM for all Ag NPs investigated) at time 0 and after 24 and 72 hours of incubation under standard culture conditions (37°C, 90% humidity, 5% $CO_2$). The standard deviation (SD) was used to assess variability in the measurements.**

| Sample Name | Polydispersity Index | ± SD | Mean NPs Ø (nm) by intensity | ± SD |
|---|---|---|---|---|
| **Ag NM-300** | | | | |
| **time 0 hours** | | | | |
| ultrapure water | 0.502 | 0.002 | 46.0 | 1.31 |
| PBS | 0.232 | 0.151 | 62.1 | 5.17 |
| MEM | 0.395 | 0.199 | 174.5 | 61.33 |
| Balb3T3 complete | 0.279 | 0.008 | 41.9 | 10.64 |
| **time 24 hours** | | | | |
| Balb3T3 complete | 0.560 | 0.101 | 147.3 | 7.07 |
| **time 72 hours** | | | | |
| Balb3T3 complete | 0.476 | 0.068 | 117.8 | 16.58 |
| **Ag 44 nm** | | | | |
| **time 0 hours** | | | | |
| ultrapure water | 0.174 | 0.009 | 44.9 | 0.29 |
| PBS | 0.230 | 0.003 | 363.6 | 24.82 |
| MEM | 0.259 | 0.019 | 389.9 | 57.16 |
| Balb3T3 complete | 0.279 | 0.008 | 83.4 | 2.33 |
| **time 24 hours** | | | | |
| Balb3T3 complete | 0.286 | 0.011 | 99.6 | 1.05 |
| **time 72 hours** | | | | |
| Balb3T3 complete | 0.316 | 0.005 | 98.4 | 1.47 |
| **Ag 84 nm** | | | | |
| **time 0 hours** | | | | |
| ultrapure water | 0.146 | 0.006 | 83.7 | 0.84 |
| PBS | 0.271 | 0.026 | 173.7 | 28.01 |
| MEM | 0.278 | 0.012 | 283.0 | 29.99 |
| Balb3T3 complete | 0.157 | 0.005 | 112.5 | 0.95 |
| **time 24 hours** | | | | |
| Balb3T3 complete | 0.220 | 0.013 | 124.6 | 3.41 |
| **time 72 hours** | | | | |
| Balb3T3 complete | 0.274 | 0.005 | 120.6 | 0.90 |
| **Ag 100 nm** | | | | |
| **time 0 hours** | | | | |
| ultrapure water | 0.159 | 0.010 | 101.6 | 0.95 |
| PBS | 0.271 | 0.019 | 151.9 | 13.31 |
| MEM | 0.285 | 0.009 | 313.7 | 25.68 |
| Balb3T3 complete | 0.153 | 0.005 | 121.1 | 1.24 |
| **time 24 hours** | | | | |
| Balb3T3 complete | 0.179 | 0.008 | 146.4 | 1.14 |
| **time 72 hours** | | | | |
| Balb3T3 complete | 0.247 | 0.011 | 147.5 | 5.05 |

Five of the samples shown in **Table B.10** had a polydispersity index (PdI) >0.3, four of which were dilutions of NM-300 in ultrapure water and in MEM measured at time 0, and in Balb3T3 complete culture medium measured after 24 and 72 hours of incubation. The fifth sample (with a PdI >0.3) was Ag 44 nm diluted in Balb3T3 complete culture medium and was analysed after 72 hours of incubation. These PdI values indicated that samples were not monodispersed. As with $CoFe_2O_4$ NPs, all of the Ag NPs studied appeared to be stabilized by serum proteins in complete culture medium and achieved relatively constant dimensions during the incubation time, with exception of NM-300, which increased in size between 0 and 24 hours (**Figures B.17A-B.17D**).

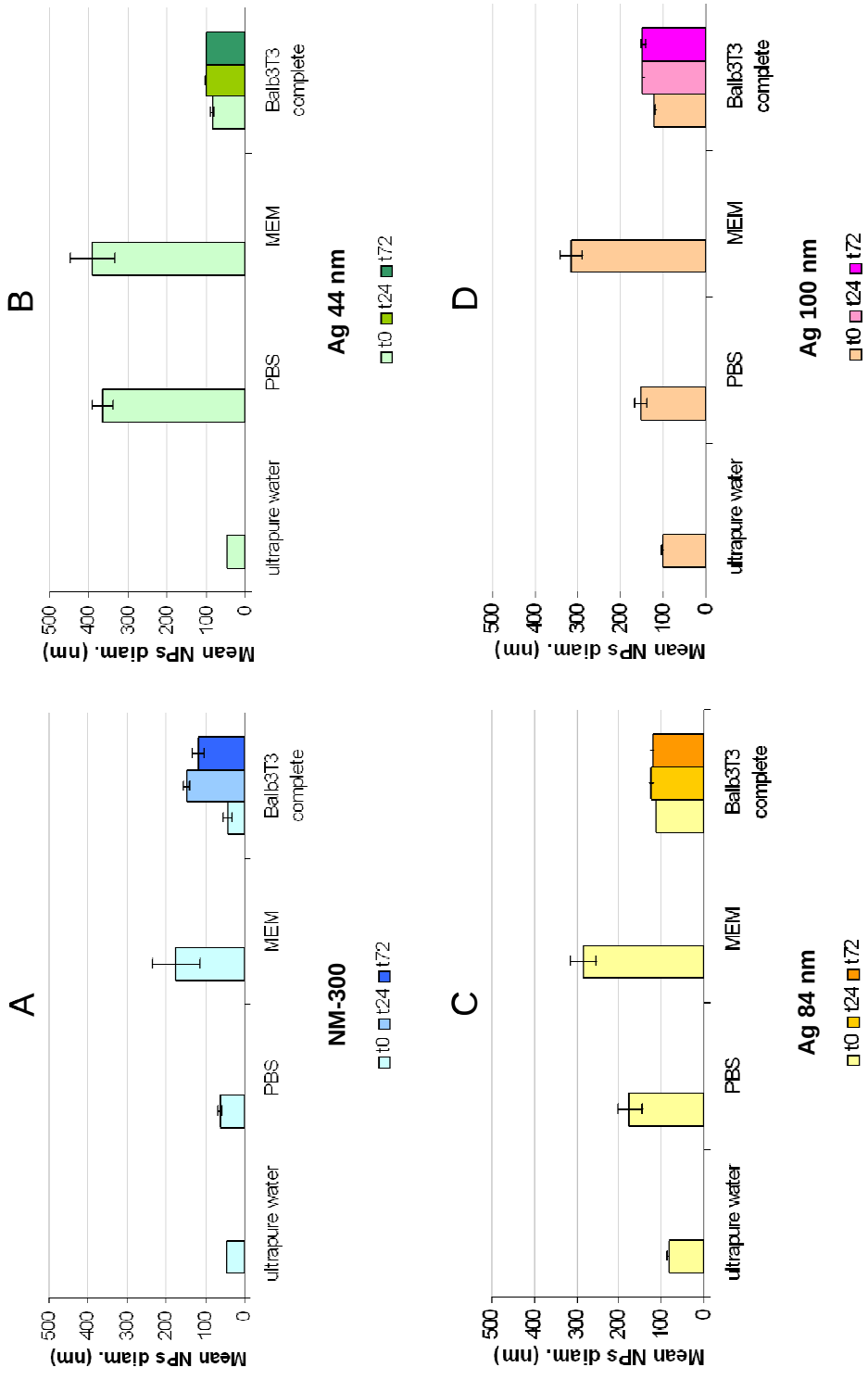


**Figures B.17A, B.17B, B.17C and B.17D: Mean NP diameter (nm) of all Ag NPs investigated in this study. DLS measurements were done for Ag NP dilution in ultrapure water, Phosphate Buffer Saline (PBS), MEM basal medium and Balb3T3 complete culture medium (100 µM for all Ag NPs investigated) at time 0 and after 24 and 72 hours of incubation (for preparations in Balb3T3 complete culture medium) under standard culture conditions (37°C, 90% humidity, 5% $CO_2$). The standard deviation (SD) was used to assess variability in the measurements.**

In addition, samples of Ag NPs (100 µM) were prepared in ultrapure water and immediately analysed using Nanoparticle Tracking Analysis to determine their size distribution. The mean NP diameter (nm) of NM-300 was 56 nm, while those of Ag 44 nm, Ag 84 nm and Ag 100 nm were 36 nm, 65 nm and 89 nm, respectively (**Table B.11).**

**Table B.11: Mean NP diameter (Mean NPs Ø) (nm) of 100 µM Ag NP samples prepared in ultrapure water and determined by Nanoparticle Tracking Analysis. Standard deviation (SD) is shown.**

| Sample Name | Mean NPs Ø (nm) by intensity ± SD |
|---|---|
| **Ag NM-300 prepared in:** | |
| ultrapure water | 56 ± 26 |
| **Ag 44 nm prepared in:** | |
| ultrapure water | 36 ± 14 |
| **Ag 84 nm prepared in:** | |
| ultrapure water | 65 ± 18 |
| **Ag 100 nm prepared in:** | |
| ultrapure water | 89 ± 45 |

### *B.2.3 Determination of impurities and quantification of Ag in stock suspensions and $Ag^+$ ion release from Ag NPs in culture medium*

Levels of metal impurities in the stock suspensions, as measured using ICP-MS, were lower than the instrument detection limit. For Ag quantification in stock suspensions, the nominal concentration was confirmed for all Ag NP stock suspensions. **Table B.12** shows the concentrations used in the biological experiments expressed as micromolarity (µM), micrograms of Ag per mL (µg Ag/mL) or number of Ag NPs per mL (No. NPs/mL). The number of NPs per mL (No. NPs/mL) was calculated using **formula B.1** and the hydrodynamic diameters measured in ultrapure water by DLS (46 nm, 44 nm, 84 nm and 100 nm for NM-300, Ag 44 nm, Ag 84 nm and Ag 100 nm, respectively). The densities of Ag 44 nm, Ag 84 nm and Ag 100 nm were determined by weighing (AM50 balance, Mettler Toledo) three samples of 500 µL of stock suspension for each Ag NP; the average densities were 0.9885, 0.9779 and 0.9773 g/cm$^3$ for Ag 44 nm, Ag 84 nm and Ag 100 nm, respectively. The density considered for NM-300 was 1.113 g/cm$^3$, as stated on the material data sheet.

**Table B.12: The different units of measure by which Ag NP concentration can be expressed. The number of NPs per mL (No. NPs/mL) was calculated using formula B.1, the hydrodynamic diameters measured in ultrapure water by DLS (46 nm, 44 nm, 84 nm and 100 nm for NM-300, Ag 44 nm, Ag 84 nm and Ag 100 nm, respectively) and the densities determined by weighing three samples of 500 µL of stock suspension for each Ag NP (1.113, 0.9885, 0.9779 and 0.9773 g/cm$^3$ for NM-300, Ag 44 nm, Ag 84 nm and Ag 100 nm, respectively).**

**NM-300**

| µM | µg Ag/mL | No.NPs/mL |
|---|---|---|
| 0.01 | 0.00108 | 1.90E+07 |
| 0.1 | 0.01079 | 1.90E+08 |
| 0.5 | 0.05393 | 9.51E+08 |
| 1 | 0.10787 | 1.90E+09 |
| 2.5 | 0.26967 | 4.76E+09 |
| 5 | 0.53934 | 9.51E+09 |
| 10 | 1.07868 | 1.90E+10 |

**Ag 44 nm**

| µM | µg Ag/mL | No.NPs/mL |
|---|---|---|
| 0.01 | 0.00108 | 2.45E+07 |
| 0.1 | 0.01079 | 2.45E+08 |
| 0.5 | 0.05393 | 1.22E+09 |
| 1 | 0.10787 | 2.45E+09 |
| 2.5 | 0.26967 | 6.12E+09 |
| 5 | 0.53934 | 1.22E+10 |
| 10 | 1.07868 | 2.45E+10 |

**Ag 84 nm**

| µM | µg Ag/mL | No.NPs/mL |
|---|---|---|
| 0.01 | 0.00108 | 3.56E+06 |
| 0.1 | 0.01079 | 3.56E+07 |
| 0.5 | 0.05393 | 1.78E+08 |
| 1 | 0.10787 | 3.56E+08 |
| 2.5 | 0.26967 | 8.89E+08 |
| 5 | 0.53934 | 1.78E+09 |
| 10 | 1.07868 | 3.56E+09 |

**Ag 100 nm**

| µM | µg Ag/mL | No.NPs/mL |
|---|---|---|
| 0.01 | 0.00108 | 2.11E+06 |
| 0.1 | 0.01079 | 2.11E+07 |
| 0.5 | 0.05393 | 1.05E+08 |
| 1 | 0.10787 | 2.11E+08 |
| 2.5 | 0.26967 | 5.27E+08 |
| 5 | 0.53934 | 1.05E+09 |
| 10 | 1.07868 | 2.11E+09 |

Ag NP samples of 10 µM concentration (obtained by diluting stock suspensions in MEM and Balb3T3) medium were analysed using ICP-MS after 0, 24 and 72 hours of incubation under standard culture conditions (37°C, 5% of $CO_2$, 90% of humidity). No Ag was detected in filtered fractions at any time point studied (results not reported but discussed in "Chapter 4: Discussion").

### *B.2.4 Imaging*

The Ag NP characterization profile previously determined using DLS and NTA was completed using a Scanning Electron Microscope; the images obtained from dried samples are shown in **Figures B.18A-D**. Qualitative analysis of the images confirmed the

stability of Ag NPs in ultrapure water because no aggregates of relevance were found (monodispersed NPs).

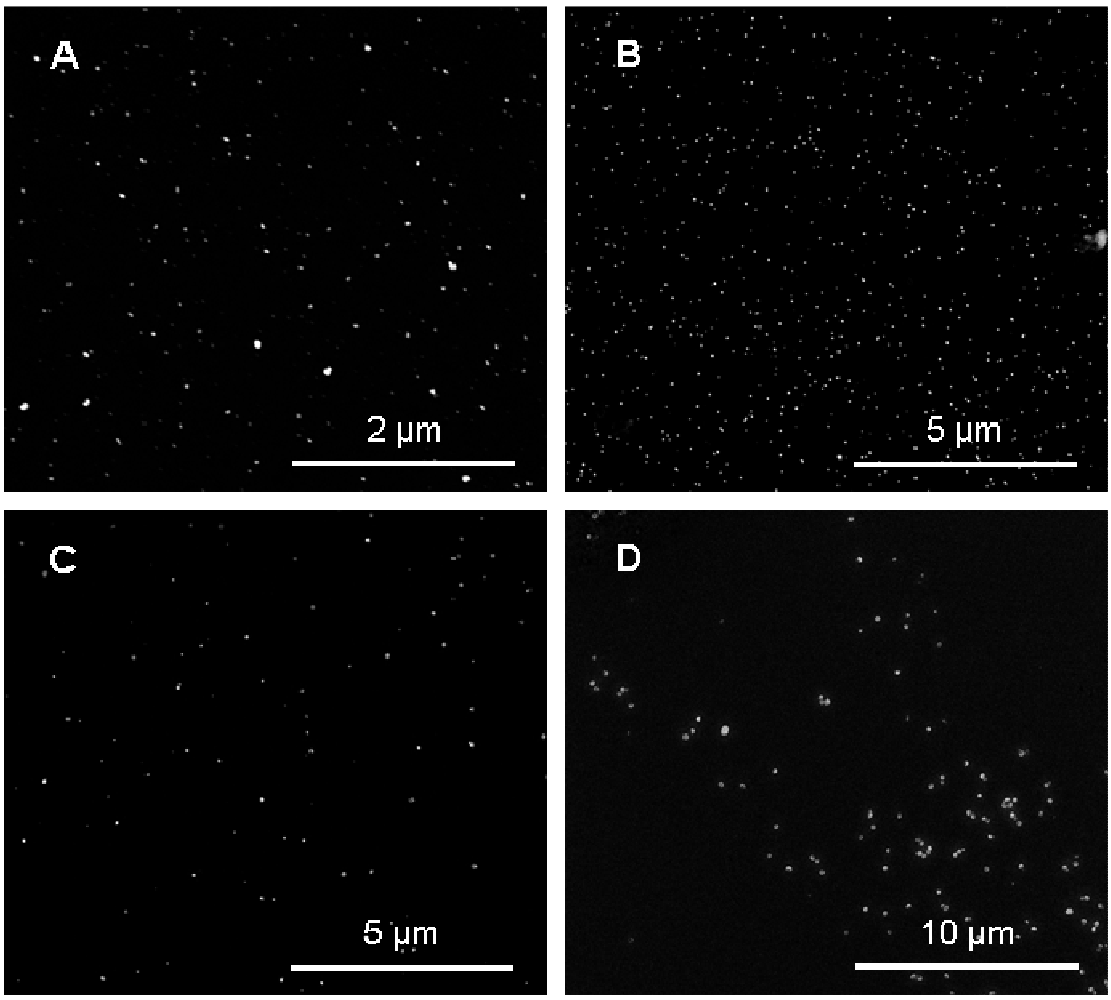


**Figures B.18A, B.18B, B.18C and B.18D: Scanning Electron Microscope images of 100 µM samples of Ag NM-300 (A), Ag 44 nm (B), Ag 84 nm (C) and Ag 100 nm (D) prepared in ultrapure water. No aggregates/agglomerates of relevance were found in these preparations.**

# Chapter 4: Discussion

The main objective of this Ph.D. research project was to study and elucidate the *in vitro* toxicological effects induced by NPs of industrial and biomedical interest, such as the nanoparticles of cobalt ferrites ($CoFe_2O_4$ NPs) and silver (Ag NPs). In particular, $CoFe_2O_4$ NPs were selected for study as part of the European Commission-funded STREP project "Cellular Interaction and Toxicology with Engineered Nanoparticles" (CellNanoTox) (FP6-2004-NMP-TI-4- 032731), while Ag NPs were chosen as part of "The Reactivity and Toxicity of Engineered Nanoparticles: Risks to the Environment and Human Health" project (NanoReTox), (NMP-2007-1.3-2).

This experimental work was carried out at the NanoBioSciences Unit (NBS) in the Institute for Health and Consumer Protection (IHCP) of the Joint Research Centre (JRC) of the European Commission (EC) located in Ispra (Varese, Italy). The NBS focuses on nanotechnology research, both producing nanomaterials (NMs) (nanoparticles and nanosurfaces) and evaluating their potential *in vitro* toxicity using cell models as alternatives to animal models (Russell et al., 1959). The use of *in vitro* methods is supported by the "3 Rs" principle (**R**eduction of the number of animals used for experimental and scientific purposes; **R**efinement of the animal's suffering during experimentation; **R**eplacement of animals in the toxicological tests requested by law) (Russell et al., 1959), which inspired the EC Directive (86/609/EEC) regulating the use of animals for experimental purposes (Anon, 1986).

Therefore, the toxicological profiles of $CoFe_2O_4$ NPs and Ag NPs were studied using *in vitro* mammalian cell cultures proposed either as possible examples of different targets of exposure to NMs (A549, CaCo2, HaCaT, HepG2 and MDCK cells) or chosen for their suitability for specific bioassays (Balb3T3 cells).

Some superparamagnetic NPs are already on the market and are used as contrast agents in magnetic resonance imaging (MRI), such as Lumirem®, Endorem® and Sinerem®. These NPs are classified into two groups according to their size, including particles larger than 50 nm (superparamagnetic iron oxides, SPIOs) or smaller than 50 nm (ultrasmall superparamagnetic iron oxides, USPIOs) (Brigger et al., 2002).

Potential NP candidates that can improve cancer therapy through targeted drug delivery, hyperthermia treatment and MRI of solid tumours are being sought and the magnetic $CoFe_2O_4$ NPs are of interest for these biomedical purposes. Nevertheless, these NPs must be both characterized and their potential biocompatibility assessed before they can be exploited safely as regards human health.

For a thorough characterization, therefore, it has been suggested that each NM is studied for more than one property and by more than one technique (Stone et al., 2009; Bouwmeester et al., 2011). In addition, a reliable toxicity assessment is recommended using more than one *in vitro* toxicity assay so as to avoid artefacts and/or false positive/negative results due to the method used and its limitations (Ponti et al., 2010). Here, a series of tests was performed to define the physicochemical characteristics of $CoFe_2O_4$ NPs and to elucidate their behaviour in culture medium.

Both $CoFe_2O_4$ NPs (P601 and P703) were positively charged and stable when dispersed in ultrapure water, but became unstable in a saline environment, such as the culture media with or without serum (Balb3T3 and MEM media, respectively). The $CoFe_2O_4$ NPs tended to aggregate/agglomerate immediately in MEM, the serum free medium considered as a reference, and became larger (reaching micrometre dimensions, 2 µm) as incubation time increased.

In addition, both P601 and P703 NPs prepared in the complete culture medium containing 10% v/v of serum and used for Balb3T3 cells were shown to aggregate/agglomerate immediately; they reached a maximal size of 500 nm, which remained constant over 72 hours. In general this different behaviour of NPs in the culture medium, depending on serum content, was observed after 72 hours of exposure for both P601 and P703 NPs. Similar behaviour was also observed in the media used for culturing the other mammalian cell lines tested. These results support the hypothesis that serum proteins interact immediately with the NP surface and start to form the evolving protein

corona (Lynch et al., 2008), thereby stabilizing the NPs and preventing their aggregates/agglomerates from reaching 1 µm in size.

The ICP-MS analysis of stock suspensions confirmed the theoretical concentration for P601 NPs, while the stock suspension concentration detected for P703 NPs was 17% lower than the expected concentration. Therefore, lower than expected concentrations were obtained during the preparation of P703 NPs samples for both the characterization and toxicity experiments.

Some metal NPs are reported to release ions in biological media; therefore, distinguishing between the effects induced by NPs *per se* and those of the released ions is a critical issue for NP toxicology studies. The dissolution of metal or metal oxide NPs in biological media is of great interest to study so as to understand the observed toxicity effects better. The determination of Co ions release ($Co^{2+}$) in complete Balb3T3 culture medium using ICP-MS showed that leakage from P601 and P703 NPs occurred at all the incubation times considered (24 and 72 hours); the $Co^{2+}$ ions release from the NP was dose-dependent for both P601 and P703. It was not possible, however, to measure the amount of $Co^{2+}$ ions in the stock suspensions provided by the supplier, since neither filtration using Millipore membranes nor ultracentrifugation was effective in separating the NPs from the solvent phase. In fact, even after these attempts the NPs remained in suspension. Iron (Fe) ion release from $CoFe_2O_4$ NPs was previously found to be between 0–2% and not to be dose- or time-dependent (Mariani et al., 2011).

Both $CoFe_2O_4$ NPs have shown to undergo sedimentation over 72 hours (Rauscher et al., 2010). This observation appears to correspond with the instability and polydispersity of the NP preparations in complete culture medium as assessed by DLS. It is reasonable to suggest that the larger aggregates/agglomerates underwent sedimentation and reached the cells more quickly than the smaller aggregates/agglomerates, which precipitated later in the 72-hour incubation period.

When studying the toxicity of $CoFe_2O_4$ NPs, the NP size, cell type and *in vitro* methods used are factors that are considered to potentially influence the outcomes of NP tests. In particular, two different sizes of $CoFe_2O_4$ NPs were investigated for *in vitro* cytotoxicity using six mammalian cell lines. The TEM images and measurements of both $CoFe_2O_4$ NPs were presented in the first CellNanoTox project activity report and corresponded to

6-7 nm for P601 and 50 nm for P703, respectively, whilst the A549, Balb3T3, CaCo2, HaCaT, HepG2 and MDCK cell lines were selected as potential examples of target organs for 72 hours exposure to NPs. Two different *in vitro* assays were performed in parallel and compared, namely the colorimetric Neutral Red uptake (NR) test and the clonogenic Colony Forming Efficiency (CFE) assay. After the evaluation of the maximum dispersant (dialyzed DEG) concentration tolerated by the cells (0.1% v/v by NR and CFE), the dose range of $CoFe_2O_4$ NPs was set between 10–120 µM (corresponding to a dose range of 0.59–7.08 µg of Co/mL or 2.35–28.15 µg of $CoFe_2O_4$/mL), with the higher value representing the NP concentration with a maximum DEG content of 0.1% v/v.

Under the experimental conditions in this study, a dose-effect relationship was not detected by NR for either size of $CoFe_2O_4$ NP in all cell lines showing a high level of viability which never decreased to 50%. The statistical analysis of the NR results using one-way ANOVA highlighted no significantly different ($p<0.05$) viability compared to the DEG control for each cell line and $CoFe_2O_4$ NPs tested. In contrast, a dose-dependent effect was observed using CFE in the A549, Balb3T3 and CaCo2 cell lines for both sizes of $CoFe_2O_4$ NPs. The IC50 values were graphically derived for Balb3T3 fibroblasts (35 µM or 2.06 µg Co/mL for P601, and 50 µM or 2.95 µgCo/mL expected concentration, corresponding to a real concentration of 41.5 µM or 2.45 µg Co/mL for P703). In contrast, IC50 values were not graphically derived for the other cell lines because at the highest concentration tested, their CFE% values were still greater than 50.

These observations reflect previous studies (Ceriotti et al., 2007; Ponti et al., 2010) showing that the CFE assay is more sensitive than the NR assay. The difference between the two methods may be due to the fact that the viability in the NR assay is measured immediately after treatment cessation, whilst cells are kept in culture for at least a week in the CFE assay. Since some NMs have been reported to interact with reagents used in most common colorimetric assays (Casey et al., 2007) and since CFE is usually one of the most sensitive *in vitro* assays to assess cytotoxicity, the CFE should be used to test the effect of NMs on adherent cell lines (Ponti et al., 2010).

Of all the cell lines used, only the Balb3T3 cells allowed the IC50 value to be determined; this may be due to the different biotransformation ability of xenobiotics by

fibroblast cells compared to other cell types, such as HepG2 (Coecke et al., 2006). In addition, normal cell lines have shown to be more sensitive to NMs than carcinoma cell lines in a clonogenic assay (Herzog et al., 2007). It has also been reported that 10 mg/mL of $CoFe_2O_4$ NPs (size not specified) tested *in vivo* for 7 weeks using ICR (Imprinting Control Region) mice did not show significant adverse effects on either the growth or the behaviour of the treated animal compared to the negative control group (Kim et al., 2007).

Here, the cytotoxicity in Balb3T3 cells after 24 hours of treatment using CFE was also evaluated. The IC50 values graphically determined for both $CoFe_2O_4$ NPs were in the range of 25–30 µM (i.e., in the range of 1.47–1.77 µg Co/mL and 5.86–7.04 µg $CoFe_2O_4$/mL, respectively). The ICP-MS measurements of cobalt ion release in complete Balb3T3 culture medium allowed the CFE results for the NPs to be compared with those reported previously when treating the same cell line with soluble cobalt chloride ($CoCl_2$) (Ponti et al., 2009). After 24 hours of treatment, both P601 and P703 NPs were more toxic than the $Co^{2+}$ ions released from the NPs. After treatment for 72 hours, the P601 NP was again more toxic than the $Co^{2+}$ ions released, unlike P703, which was less toxic than the ions released. It is not possible, however, to exclude the possibility that the toxicity observed in NP treatments was induced by a combination of NPs and $Co^{2+}$ ions. Ponti et al. reported similar conclusions for cobalt NP-induced cytotoxicity compared to that of $CoCl_2$ treatments (Ponti et al., 2009).

The uptake and intracellular distribution of $CoFe_2O_4$ NPs have been demonstrated by Synchrotron Radiation X-Ray Fluorescence (SR-XRF) in Balb3T3 cells as a function of the NP concentration (Marmorato et al., 2011). Based on the results of this study, it is reasonable to suggest that the ions released from NPs once they have entered the cell contribute to cytotoxicity according to the Trojan-horse theory proposed for metal NPs by Park et al. (Park et al., 2010a). Currently, little information is available on the *in vitro* and *in vivo* biocompatibility of $CoFe_2O_4$ NPs. The information that does exist relates to other sizes or doses of $CoFe_2O_4$ NPs and other *in vitro* methods or cell lines (see **Section 1.8.1** for examples), so it is difficult to directly compare published results with those found here.

Notably, however, Kim and co-workers have tested different ferrite particles (Fe-, Li-, Ni/Zn/Cu-, Ba-, Sr-, Co-, Co/Ni-ferrites) using MTT and agar diffusion assays in L929 fibroblasts and found that the $CoFe_2O_4$ particles (170 nm in size) were not cytotoxic in either assay (Kim et al., 2005). Moreover, the biocompatibility of magnetic NPs, such as $Fe_3O_4$ (20-30 nm), $ZnFe_2O_4$ (15-30 nm) and $NiFe_2O_4$ (20-30 nm), was investigated using the colony forming assay and Trypan Blue exclusion method in HeLa cells. These NPs were not found to be cytotoxic at the lowest tested concentrations (10 µg/mL), although $NiFe_2O_4$ was cytotoxic at the highest tested concentration (100 µg/mL) (Tomitaka et al., 2009).

Here, the cytotoxicity studies on Balb3T3 fibroblasts assessed at 24 and 72 hours using CFE were the first step of the *in vitro* investigations on $CoFe_2O_4$ NPs. The dose-effect curves obtained after CFE analysis allowed the chosen concentrations to be tested by the Cell Transformation Assay (CTA; concentrations of 1, 5, 20, 60 µM corresponding to 0.059, 0.295, 1.18 and 3.54 or 0.235, 1.175, 4.69 and 14.07 µg Co/mL and $CoFe_2O_4$/mL, respectively) and the Cytokinesis-Block-Micronucleus assay (CBMN; concentrations of 1, 10, 60 µM corresponding to 0.059, 0.59 and 3.54 µg or 0.235, 2.35 and 14.07 µg Co/mL and $CoFe_2O_4$/mL, respectively).

The Balb3T3 mouse fibroblasts, and specifically the A-31-1-1 clone, were used as a well-established *in vitro* model in this study. These cells are suitable for not only the CFE, but also the CTA and CBMN assays. The advantage of using Balb3T3 fibroblasts, therefore, was using single cell type to generate a toxicological profile for the $CoFe_2O_4$ NPs that included potential cytotoxicity, cell transformation capacity and genotoxicity. The results showed that both $CoFe_2O_4$ NPs did not significantly induce type III foci formation or micronuclei under the experimental conditions of this study.

Since there is no information available on the transformation capacity and genotoxic potential for $CoFe_2O_4$ NPs, data found here were compared to those of cobalt NPs and $CoCl_2$. Cobalt and its compounds have been classified as possible human carcinogens (Group 2B) by the IARC (Agents classified by the IARC Monographs, Volumes 1-102; http://monographs.iarc.fr/ENG/Classification/index.php, last accessed in February 2011).

Morphological transformation assessed with CTA and genotoxicity assessed with both the CBMN and Comet assays have been observed in Co NP-treated Balb3T3 cells; whilst

treating the same cell line with $CoCl_2$ did not induce morphological effects, significant genotoxicity was found using the Comet assay (Ponti et al., 2009). In contrast, Colognato et al. found that Co NPs had a smaller genotoxic effect on human peripheral lymphocytes than $CoCl_2$, indicated by the presence of micronuclei and a reduced cell proliferation index (Colognato et al., 2008). Clearly more investigations on the potential effects of $CoFe_2O_4$ NPs on DNA are required to determine if these particles are genotoxic or not.

As yet, the transformation capacity of NPs has not been investigated often. Although there are a few reports on using the CTA to assess the transformation capacity of NPs (Ponti et al., 2009; Ponti et al., 2011), there are none on using CTA to test the $CoFe_2O_4$ NPs. This study, therefore, is the first to report the use of CTA in assessing the cell transformation capacity of $CoFe_2O_4$ NPs.

Other methods, such as the Soft Agar Colony Forming assay where the biomarker for neoplastic cell transformation is the loss of the anchorage-dependence for growth, can, however, be used to study the genotoxic potential of NPs on adherent cells. Previously, this type of test has been demonstrated as valid for the screening of antitumor drugs (Shoemaker et al., 1985), and it has also been used to assess the ability of NPs to act as drug delivery systems against cancer cell lines, detected as the inhibition of cell proliferation and thus non-formation of colonies (Bisht et al., 2007). Indeed, the transformation capacity of NPs could potentially be evaluated using the soft agar assay; the endpoint would be the detection of colonies formed in soft agar gel by transformed cells that have lost the anchor-dependence for growth after NP treatment. Anchorage-independent transformation, for example, has been demonstrated in JB6 mouse epithelial cells after treatment with <20 nm alumina NPs ($Al_2O_3$ NPs) (Dey et al., 2008). The advantage of this method is the possibility of using Balb3T3 cells so that the transformation capacity of NPs can be determined both with this method and the CTA.

In contrast, the genotoxic potential of NPs evaluated using the CBMN assay is well documented. The CBMN assay has been shown to give positive outcomes for a wide range of nanomaterials, such as Co NPs (100-500 nm), Co-Cr alloy NPs (30 nm), $TiO_2$ NPs (25; 10-20; ≤20 nm), $SiO_2$ NPs (6.6, 8.2, 196 nm), polyaspartic acid-coated magnetite NPs (8.5 nm), water soluble $C_{60}$ (7.1 nm) and mwCNTs (11.3 nm diameter, 700 nm length) (Singh et al., 2009), using different cell types.

The Comet assay is an alternative *in vitro* assay for testing the genotoxicity of NPs; the genetic damage is identified as single and double DNA strand breaks (Rojas et al., 1999). A recent review on the use of the Comet assay in nanotoxicology investigations reported positive outcomes in A549 cells after 4 hours of treatment with 2-80 μg/mL of iron oxide NPs (e.g., $Fe_2O_3$ and $Fe_3O_4$ 20-40 that are 30-60 nm in size, respectively) (Karlsson, 2010). Numerous positive outcomes have been obtained using the Comet assay to test different NPs; this is unsurprising due to the high reactivity of NPs (Karlsson, 2010). Nevertheless, it cannot be excluded that the positive outcomes detected using the Comet assay for several NPs were due to NP-assay interactions, as observed for NPs, such as $TiO_2$ and CuO (Karlsson, 2010). In addition, particles of iron oxide, which have shown to induce little DNA damage using the Comet assay, were seen in the comet head (Karlsson, 2010). Therefore, a thorough investigation of the genotoxic potential of $CoFe_2O_4$ NPs using additional methods with protocols specifically adjusted for NP testing is clearly required.

Oxidative stress studies must be considered when evaluating the genotoxicity of NPs because most NPs have been shown to induce oxidative stress, which itself appears to be involved in DNA damage that is associated with cancer formation (Karlsson, 2010). In this context, a modified version of the Comet assay using specific enzymes, such as formamidopyrimidine glycosylase (FPG) and endonuclease III, allows the detection of oxidative stress and repair. These enzymes recognize and nick the DNA in correspondence of oxidized purines and pyrimidines, thereby increasing the number of DNA fragments; information on oxidative stress is obtained by comparing the cells treated/untreated with these enzymes (Karlsson, 2010).

Other assays that measure NP-induced production of reactive oxygen species (ROS) in the absence or presence of cells have been reported (Stone et al., 2009). In the absence of cells, however, NP ROS production is considered to be associated with the physicochemical characteristics of NPs, whilst ROS production in the presence of cells (both extracellular and intracellular) is considered to be a marker of oxidative stress (Stone et al., 2009). One assay which can detect intracellular ROS is the DCFH (2, 7-dichlorofluorescein) assay; this exploits the conversion of a precursor into a fluorescent dye. Meanwhile, the cytochrome C assay allows the quantification of extracellular ROS,

such as superoxide anions produced by cells. Additional markers of oxidative stress in NP studies include changes in the ratio between the reduced (GSH) and oxidized (GSSG) forms of glutathione (GSH:GSSG), lipid peroxidation and mRNA expression of oxidative stress-dependent genes (Stone et al., 2009). Future studies following on from this work will include investigation of oxidative stress induced by the NPs tested here.

The results found in this study differ depending on the assay and cell lines chosen when screening the toxicity of $CoFe_2O_4$ NPs. As regards the potential influence of $CoFe_2O_4$ NP size on the biocompatibility studies, there were no relevant differences in the toxicity induced by P601 and P703 $CoFe_2O_4$ NPs using the NR uptake, CFE, CTA and CBMN assays. The similar effects induced by the P601 and P703 NPs can be explained by the fact that both sizes were shown to behave similarly in terms of formation of aggregates/agglomerates, ion leakage and sedimentation when in media, such that cells would reasonably "see" and interact with P601 and P703 NPs in an analogous manner.

Additional toxicity experiments comparing NPs that differ by more than 50 nm in size (e.g., 16 nm vs. 160 nm particles) would be necessary to clarify the role of the NPs size in toxicity. For example, Colognato et al. studied three different sizes of $CoFe_2O_4$ NPs (5.6 nm, 10 µm and 120 µm) using the CBMN assay in order to assess the genotoxic potential of these NPs in human peripheral lymphocytes (Colognato et al., 2007). They showed that the smallest NPs induced significant toxicity and mutagenicity, while the 10 µm NPs induced significant mutagenicity only and no effects were induced by the largest NPs (Colognato et al., 2007).

In order to hypothesize a mechanism of toxicity and explain the differences observed with CFE analysis of the six cell lines studied here, it might be of interest to assess the toxic potential of $CoFe_2O_4$ NPs with different surface properties (i.e., surface charge, presence of different coatings) that can influence the NP protein corona. Experiments that allow characterization of the protein corona of $CoFe_2O_4$ NPs would be useful in understanding the interaction of NPs with cells and subsequently their toxicology since the protein corona may be involved in the absorption of the NPs (Fischer et al., 2007).

*In vitro* studies, such as those described in this work, are a good foundation for the safety assessment of $CoFe_2O_4$ NPs, but still have limitations and are insufficient when compared to complex *in vivo* conditions. Even if *in vitro* systems are in general relatively

inexpensive, time effective and easy to perform and interpret, they cannot reproduce, for example, either the NP changes or interactions among different cell types that occur *in vivo* (Stone et al., 2009). Fischer et al. highlighted the need for *in vivo* investigations to be carried out in the first step of NP toxicity research so as to identify the cells/organs that can take up the NPs, and thus the need to design more focused *in vitro* experiments (Fischer et al., 2007).

Nevertheless, based on this work, it is clear that more studies are required to enable *in vitro* and *in vivo* results to be correlated. For example, a comparison of the concentrations of $CoFe_2O_4$ NPs used in our *in vitro* experimental conditions with the results of *in vivo* studies testing similar NPs is difficult and no direct correlation can be found. The superparamagnetic NP formulations already in use for MRI contain iron oxide NPs and their concentrations are usually expressed as µg of iron (Fe) or mL of NP suspension per kilogram (Kg) of weight. For example, Resovist®, a carboxydestran-coated iron oxide NP, is one of the superparamagnetic NPs used for MR imaging of liver lesions (Reimer et al., 2003). The hydrodynamic diameter of this NP ranges from 45–60 nm and the recommended dose for intravenous (IV) injection on the material data sheet is 0.9 mL (corresponding to 0.45 mmol of Fe) in patients weighing less than 60 kg, and 1.4 mL (corresponding to 0.7 mmol of Fe) in patients weighing 60 kg or more (http://radiologie-uni-frankfurt.de/sites/radiologie-uni-frankfurt.de/content/e43/e2321/e2331/resofinal_eng.pdf, last accessed in September 2011).

To enable the concentration of $CoFe_2O_4$ NPs used in this study to be compared with the Resovist® iron oxide NP doses, the Fe concentrations in toxicity experiments of this study could be calculated using the amount of Fe declared on the material data sheet (e.g., 259.25 mM for P601 NPs) and the dilutions used during the toxicity tests with cells. Using this approach, the amount of Fe in P601 NP treatments was 2.2 µM–259 µM (corresponding to 0.12–14.50 µg Fe/mL). Since the usual dose of Resovist® to be injected IV into a patient weighing 60 kg or more corresponds to 0.7 mmol of Fe, an amount that should be distributed in a blood volume of approximately 4 litres (i.e., the blood volume of a person weighing 70 kg), the Resovist® blood concentration is 175 µM. This value can now be compared to the Fe amounts calculated as described above and supposedly

administered to the cells when testing P601 NPs *in vitro*. Specifically, the P601 $CoFe_2O_4$ NP test concentration of 80 µM in this study corresponds to 173 µM of Fe, and reflects the recommended dose of Resovist® used in the IV injection. In order to compare the concentrations injected *in vivo* with those tested *in vitro* in this work, however, the amount of Fe that reaches a single cell should be measured.

In addition, the dose of NP that actually reaches a target organ *in vivo* is influenced by the physicochemical characteristics of NPs and their changes when NPs enter the body (Elder et al., 2009). Even if NPs are specifically engineered to directly reach a target cell/organ, their metabolic fate is unknown, and thus the effects induced by altered/metabolized NPs are unpredictable (Fischer et al., 2007). *In vivo* studies reported by Kim et al. showed that in ICR (Imprinting Control Region) mice treated with an IV injection of 10 mg/mL of specific $CoFe_2O_4$ NPs for 7 weeks, the $CoFe_2O_4$ NPs were able to reach and be distributed in different organs, such as the heart, liver, kidney, stomach and spleen (Kim et al., 2007). The elimination of NPs may also depend on their physicochemical properties and affect the NP dose at a target site. For example, 20-25% of two dextran-coated superparamagnetic oxide NPs of 80 nm and 30 nm in size and injected into rats is eliminated via urine and faeces within 19 days and 7 weeks, respectively (Kunzmann et al., 2010).

In this study, four aqueous suspensions of Ag NPs, with different sizes and stabilizing agents, were characterized and assessed for their potential cytotoxicity (CFE), cell transformation capacity (CTA) and genotoxicity (CBMN) in Balb3T3 fibroblasts. Indeed, Balb3T3 fibroblasts are used to study NP toxicity because they are connective tissue cells and thus found throughout the body; therefore, they represent a potential target tissue and represent a model for evaluating the transformation capacity of chemicals. Fibroblasts in particular appear to be a good target cell model since Ag NPs of 25 nm can enter the body via damaged skin (Filon Larese et al., 2009) and many of the available consumer products containing Ag NPs involve skin application or contact.

Recent attention has focused on Ag NPs because of the need for new antimicrobial substances to which microorganisms have not yet developed resistance (Rai et al., 2009). Because the Ag NPs are suitable for applications requiring antimicrobial or antiviral

effects, they have been used in many consumer products. Indeed, Ag NPs are the most common NPs used in nanotechnology-based products, as reported in the Woodrow Wilson inventory (http://www.nanotechproject.org/inventories/silver/, last accessed in February 2011). Concerns about the potential effects of Ag NPs and their derivatives on human and environmental health, however, have stimulated the need to identify and evaluate the toxicity induced by these NPs.

The physicochemical characterization studies performed here showed that all Ag NPs considered in this study had a negatively-charged surface and were monodispersed in ultrapure water. The DLS measurements showed that the Ag NPs increased in size under conditions of both complete (Balb3T3) and serum free (MEM) culture media. In particular, all Ag NPs were found to be larger in MEM compared to Balb3T3 complete medium, again supporting the theory of an immediate size-stabilizing role of serum proteins (Lynch et al., 2008).

A number of studies on the effects of Ag NPs on bacterial and eukaryotic cells have been reported (Panáček et al., 2006; Kim et al., 2007; Rai et al., 2009; Ahamed et al., 2010; Johnston et al., 2010). The available toxicity data are often related to different cellular models, methods employed or different Ag NP characteristics (e.g., surface charge, presence/absence of coatings, size, etc.). A distinction between the toxicity induced by either Ag NPs or released $Ag^+$ ions, however, is not always clear. As mentioned above, some metal NPs, such as $CoFe_2O_4$, can release ions in the biological environment, so studies on particle solubility are important in understanding the toxicology of NPs.

The toxicity induced by Ag NPs is related frequently to their potential of being oxidized, which subsequently produces $Ag^+$ ions and ROS, such as $H_2O_2$ (Auffan et al. 2009; Rai et al., 2009). The ICP-MS is a powerful technique that can detect and measure traces of several elements in a sample: therefore, it was used here to assess $Ag^+$ ion release induced by the NPs in media with/without serum. No Ag was detected in filtered fraction samples at any of the incubation times investigated (0, 24 and 72 hours); these results reflect those of Gaiser et al. (Ag NPs less than 1% soluble) (Gaiser et al., 2009).

Nevertheless, Ag NPs can react with hydrochloric acid (HCl) to produce the insoluble salt, silver chloride (AgCl) (El-Ansary et al., 2009). For this reason, and in order to critically assess the $Ag^+$ release data of this study, the MEM medium formulation should

be taken into account. In fact, the MEM medium itself contains three different soluble chloride salts, namely calcium (1.8 mM), potassium (5.33 mM) and sodium chloride (117.24 mM), which can be regarded as sources of $Cl^-$ ions that can react with and bind to $Ag^+$ ions released by the NPs. Since the amount of $Cl^-$ ions in the culture medium is very high, the possibility of finding $Ag^+$ ions in filtered fractions is low. Even if it assumed that the maximum dose of Ag NP administered to the cells (10 µM) is completely dissolved, this amount of $Ag^+$ would be completely precipitated by the $Cl^-$ ions. In fact, for each chloride ion in the culture medium, the ionic product calculated for the reaction with Ag is higher than the silver chloride solubility product (corresponding to $1.7 \times 10^{-10}$ at 25°C), confirming the formation of AgCl precipitates (Gillespie et al., 1990). Due to its insoluble nature, any AgCl produced would be stopped by the filter membrane used in this study protocol for sample preparation, making it unavailable for detection using ICP-MS. These observations suggest that the toxicity observed in Balb3T3 cells is associated with Ag NPs *per se*. Nevertheless, even if insoluble silver salts are not easily taken up by the body (Casarett & Doull, 2008), it would be interesting to perform experiments that clarify whether or not the AgCl could induce or participate in *in vitro* toxicity to cells.

The release of $Ag^+$ ions from Ag NPs can also be influenced by varying the chemical and physical parameters, such as pH and temperature (Liu et al., 2010). In this study, samples for the measurements of the ion release were incubated under standard cell culture conditions (37°C, 5% $CO_2$, 90% humidity) and in the absence of cells. The cells were excluded from these experiments to avoid the loss of Ag due to the cellular uptake reported previously in both bacteria and eukaryotic cells (Panáček et al., 2006; Arora et al., 2009). Therefore, the pH changes were only those associated with the incubation conditions and pH changes in the medium caused by cellular metabolic activities were disregarded. Further investigations using protocols that have been optimized to detect and quantify AgCl would be valuable in refining the release experiments and clarifying the behaviour of Ag NPs in culture media.

The Ag NPs in this study were associated with significant cytotoxicity at both incubation times considered (24 and 72 hours) compared to the respective dispersant controls; in contrast, no cytotoxicity associated with the dispersants was observed in the concentration range studied for NP testing. Based on the ICP-MS analysis of stock

suspensions, the effect of metal impurities that may have influenced the toxicity outcomes was disregarded. The cytotoxic effect of Ag NPs, however, could reasonably be explained by the Trojan-horse mechanism, which involves intracellular ion release by NPs as suggested previously for other NPs that easily release ions (Park et al., 2010a).

As described previously (see Chapter 2: Materials and Methods), the concentrations of Ag NPs assessed in this study were selected based on data available in the literature. As for the $CoFe_2O_4$ NPs investigated, the concentrations of Ag NPs used here were reported both as µM and as µg/mL to allow the data to be compared to those of other research groups. It is very difficult, however, to compare the concentration of Ag NPs used in this study with that used in consumer products, particularly as the amounts of Ag NPs, their size, aggregation/agglomeration states and ion release capacity in these products are often not available (Wijnhoven et al., 2009).

After treatment of Balb3T3 cells with Ag NPs for 72 hours, the graphically determined IC50 values were approximately 1.5 µM (0.162 µg/mL) for NM-300, 1.7 µM (0.184 µg/mL) for Ag 44 nm, 1.9 µM (0.205 µg/mL) for Ag 84nm, and 3.2 µM (0.346 µg/mL) for Ag 100 nm. Following 24 hours of treatment, only NM-300 showed an identifiable IC50 value that corresponded to 8 µM (0.864 µg/mL) in the concentration range studied. These results suggest that the smaller Ag NPs (e.g., NM-300 and Ag 44 nm) have a greater cytotoxic effect than the larger Ag NPs (e.g., Ag 100 nm). This may be due to their greater surface area and thus a greater potential to interact with cells or molecules. In addition, differences of NP surface chemistry, possibly due to different synthesis processes and dispersants (Johnston et al., 2010), may also explain the different toxicity results of NM-300 compared to Ag 100 nm.

There is evidence showing Ag NP-induced cytotoxicity in fibroblasts, such as the human lung fibroblasts (IMR-90). Specifically, starch-coated Ag NPs 6-20 nm in size were tested on human lung fibroblasts (IMR-90) using several assays to assess cell viability, metabolic activity and oxidative stress. As a possible mechanism by which Ag NPs induce toxicity, was suggested the mitochondrial respiratory chain impairment, causing the production of ROS and inhibition of ATP synthesis (Asharani et al., 2009). Ahamed et al. have also reported mitochondrial-dependent toxicity on fibroblast cells (Ahamed et al., 2010). Moreover, Ag NPs 40 and 80 nm in size were found to damage the

mitochondrial membrane permeability of rat liver mitochondria, thus disrupting their function (Teodoro et al., 2011). The generation of ROS due to mitochondrial dysfunction, however, should not be considered as a toxic effect specific to Ag NPs because this effect has also been reported for other particles, for example, titanium dioxide ($TiO_2$) (Freyre-Fonseca et al., 2011).

The cytotoxicity results of this study can be compared to data related to *in vitro* testing of Ag NPs on bacteria in order to understand if the test Ag NPs could be used safely as antimicrobial agents. Kim et al. have shown that the minimal inhibitory concentration required for the antimicrobial effect of 13.5 nm sized-Ag NPs on *S. aureus* after 24 hours of incubation was approximately 33 nM (Kim et al., 2007). This suggests that the Ag NPs investigated in this study could be used for their antimicrobial properties without cytotoxic effects on mammalian cells. Moreover, the antimicrobial effects of different sizes of Ag NPs (44, 50, 25 and 35 nm) after 24 hours of treatment on *S. aureus* have been shown to be size-dependent; however, the NP doses were not converted into the number of NPs per millilitre so the size-dependence toxicity conclusions must be confirmed (Panáček et al., 2006).

One possible way to express the NP concentration proposed in this study is to consider the corresponding number of NPs per millilitre (No. NPs/mL). It was shown (Chapter 3: Results, **Section 3.2.1**, **Figures 3.17A and B**) that this approach would lead to different conclusions than those reported above because the number of NPs/mL is generally greater for smaller NPs than for larger ones for a fixed concentration, causing a shift in the dose-effect curves. This observation highlights the need for a standard method of conveniently expressing the amount of NPs used in experiments, thereby allowing data of different research groups to be compared (Stone et al., 2009).

The toxicity of different sizes of Ag NPs (22, 42, 71 and 323 nm in diameter) following oral administration of 1 mg/kg to ICR mice over 14 days has also been investigated (Park et al., 2010b). Although there were no differences in the body or organ weight between the treated and the control groups, the smaller—but not the larger—Ag NPs were found to be distributed in several tissues (brain, lung, liver, kidney and testis) (Park et al., 2010b). The same team has also shown that repeated doses of 42 nm bare Ag NPs induced significant inflammation (involving increased levels of cytokines produced), B-

cell distribution and tissue infiltration of inflammatory cells (Park et al., 2010b). Another research group investigated the distribution and accumulation of three different sizes of Ag NPs (20, 80 and 110 nm) administered by IV injection to rats once daily for 5 days, and found that the smallest Ag NPs (20 nm) were distributed in the liver, kidneys and spleen, while larger Ag NPs (80 and 110 nm) were distributed in the spleen, liver and lung (Lankveld et al., 2010). The size-dependent distribution suggested that toxicity may be also size-dependent and the liver, lung, kidneys and spleen may be potential targets for Ag NPs (Lankveld et al., 2010).

As regards the carcinogenic potential of Ag, the United States Environmental Protection Agency has reported Ag as belonging to group D, thus "not classified as to human carcinogenicity" (US EPA, http://www.epa.gov/IRIS/subst/0099.htm, last accessed in September 2011). Since Ag NPs can induce oxidative stress and inflammation, conditions that may be associated with genetic damage, it is important to assess the transformation capacity and genotoxic potential of Ag NPs. In this work, therefore, the cell transformation capacity and genotoxicity of Ag NPs in Balb3T3 cells were evaluated using the CTA and CBMN assays, respectively. The data indicated that all the Ag NPs studied did not significantly induce type III foci or micronuclei formation compared to their dispersant controls under the applied experimental conditions.

As yet, no studies on the transformation capacity of Ag NPs assessed using the CTA appear to have been reported. This study, therefore, is the first to report on the use of the CTA in evaluating Ag NPs. Nevertheless, as explained for the $CoFe_2O_4$ NPs, further experiments, including other both *in vitro* and *in vivo* methods, are required for a comprehensive evaluation of the potential of Ag NPs to damage DNA. Although neither *in vitro* nor *in vivo* experiments alone provide a definitive evaluation of NP toxicity, exploiting the advantages of both these approaches and combining *in vitro–in vivo* testing would produce more meaningful assessments of NP toxicity.

Both *in vitro* and *in vivo* evaluations that focus on long-term treatments with NPs should also be done to clarify if chronic exposure with NPs can induce morphological cell transformation and carcinogenesis, respectively (Ng et al., 2010). The importance of such studies is confirmed by the fact that chronic exposure by subcutaneous administration of Ag NPs (1.75–2.5 mg/week) was found to cause malignant tumour formation at the

injection site in 31% of the rats which survived for more than 16 months; no tumours were found in rats treated with intramuscular injection of AgNPs (Wijnhoven et al., 2009).

Studies on Ag NP-induced DNA damage reported in the literature mostly concern the expression of DNA repair protein, micronuclei formation and DNA double strand breakage (Singh et al., 2009; Ahamed et al., 2010). For example, Ag NPs of similar size (25 nm), but different surface chemistry induce DNA damage in mouse embryonic stem cells and fibroblasts (Ahamed et al., 2008). In particular, the polysaccharide-coated Ag NPs induced greater DNA damage than uncoated particles, as demonstrated by measurements of the double strand breaks' repair protein Rad51 (Ahamed et al., 2008). This type of test allows NP-induced genotoxicity to be evaluated by measuring a cellular response (changes in protein expression); therefore, it would be a useful test to complement the CBMN or Comet assays that measure DNA alteration (micronuclei or DNA fragmentation) in genotoxicity studies.

In addition, Ag NPs <50 nm and at concentrations of 0.1, 1 and 10 μg/mL were shown to induce significant genotoxic effects on primary human mesenchymal stem cells (primary cells very proliferating) using Comet and chromosome aberration tests (Hackenberg et al., 2011). The chromosome aberration assay can be performed either *in vitro* or *in vivo* and detects alterations of both the number and structure of the chromosomes in metaphase-arrested cells. The metaphase stage occurs immediately prior to the separation of replicated chromosomes into newly-forming nuclei and cells can be arrested at this stage using a specific chemical (Singh et al., 2009). The advantage of this assay is that it provides information on the damaged chromosome that cannot be obtained using, for example, the CBMN or Comet assays. In contrast, no significant genotoxicity, indicated by micronuclei induction in erythrocytes of the bone marrow, was shown in *in vivo* studies involving the oral administration of 30, 300 and 1000 mg/kg Ag NPs of 60 nm in size for 28 days in Sprague-Dawley rats (Ng et al., 2010).

Based on the reported genotoxic potential of Ag NPs, further investigations that use other methods to complement the CTA and CBMN assays are clearly needed to better elucidate the specific effects of Ag NPs on DNA. Oxidative stress studies, such as those mentioned above, should also be considered. Attention should particularly focus on distinguishing

between the effects induced by NPs *per se* and ion-induced effects. Indeed, oxidative stress and interference with intracellular zinc homeostasis were found in human skin fibroblasts after treatment with $AgNO_3$, suggesting that oxidative stress observed in Ag NP-treated cells may be due to the $Ag^+$ ions released by the NPs (Cortese-Krott et al., 2009). Additional experiments are required to clarify the mechanism by which Ag NPs exert their toxicity on cells.

The *in vitro* studies and results of this research project highlight the advantages of using *in vitro* methods to elucidate the mechanism by which NPs exert their effects. The advantage of an *in vitro* approach in nanotoxicology with respect to human health is that different time points, types of NPs, NP doses and study endpoints can be investigated (Clift et al., 2011). *In vitro* methods have attracted increasing attention for NP testing (Stern & McNeil, 2008) and have also been promoted by the European Union for assessment of new cosmetics (Clift et al., 2011). The effects induced by NPs, however, cannot be explained simply by *in vitro* cytotoxicity assessments. In this context, priority research areas highlight the importance of studying carcinogenic potency, genotoxicity and toxicokinetics using *in vitro* tests (OECD, 2008). *In vitro* tests using human cell lines that mimic the *in vivo* situation are the most promising for toxicological studies.

*In vivo* experiments, however, are required to identify target organs and NP kinetics, and include adsorption, distribution, metabolism and excretion studies. Nevertheless, it is still difficult to correlate *in vitro* toxic effects with *in vivo* data both for chemicals and NPs, and to predict the toxicological effects on humans from animal studies because of species' differences. A qualitative *in vitro*/*in vivo* comparison is usually considered to be sufficient because it is difficult to establish a quantitative *in vitro*/*in vivo* relationship (Ekwall, 1992).

Predictive toxicity models for nanotoxicology are also required. In particular, these models should be designed to predict how changes in the physicochemical characteristics of NPs may affect their potential toxicity in humans (Clark et al., 2011). However, much experimental work is required to achieve this objective because many high quality data are needed to develop predictive models, and information on NPs are usually collected using different methods (and thus endpoints) or materials, thereby preventing a thorough evaluation of NMs (Clark et al., 2011).

In this study, the $CoFe_2O_4$ and Ag NPs were found to induce cytotoxic, but not genotoxic effects on cells, and had no effect on cell transformation. This study, therefore, can be considered as the first screening study to suggest the potentially safe use of these NPs. Clearly, other assays using both *in vitro* and *in vivo* models must be considered when studying NPs based on their potential future applications (e.g., studies on the kinetics of NPs that may be used for drug delivery) to increase confidence in the safety of these materials.

# Chapter 5: Conclusions

This work contributes to nanotoxicology research by proposing a strategy for the evaluation of NM genotoxicity using *in vitro* studies.

The study of $CoFe_2O_4$ and Ag NPs confirmed that a multidisciplinary approach is needed to understand NM toxicity. Nanotoxicology represents a complex research field; the main purpose is the identification of a relationship between the special physicochemical characteristics of the NMs and their effects on cells. Chemistry, physics and biology are just a few examples of the merging disciplines that are involved in NM research.

Indeed, effects on cells induced by $CoFe_2O_4$ and Ag NPs cannot be explained without investigating the physicochemical properties of the particles (e.g., size, surface charge, ion release, etc.) and considering the different techniques/methods or cell lines used as parameters that can affect experimental outcomes. Here, it was demonstrated that differently-sized NPs of the same element (Ag) or compound ($CoFe_2O_4$) induce cytotoxicity in Balb3T3 fibroblasts; the smallest NPs appear to be the most cytotoxic. The correlation between NP size and cytotoxicity, however, should be investigated further because it was shown that the way in which NP concentrations are expressed can affect the conclusions. In addition, it was shown that differently-sized NPs immediately tend to form aggregates/agglomerates when in complete culture medium, reaching larger hydrodynamic dimensions that remain constant over the 72-hour incubation time investigated. In order to understand the role of aggregates/agglomerates on cellular toxicity, experiments designed to elucidate the NPs' behaviour in complete culture medium should be done.

Determination of ion release into the culture medium can be used to distinguish between toxicity induced by NPs *per se* and toxicity induced by the released ions. Moreover, it was verified here that the choice of cell type and *in vitro* assay (e.g., NR, CFE) can also influence results. The CFE assay detected the cell-specific toxicity of $CoFe_2O_4$ NPs in Balb3T3 fibroblasts; in contrast, the NR assay was less sensitive than the CFE in detecting the cytotoxic effect under the exposure conditions used.

More techniques should be employed to complete the characterization of the NPs studied here. For example, studies on the surface changes of NPs in culture medium (e.g., oxidation, interaction with proteins, etc.) would generate a comprehensive array of

information that can be used to elucidate the toxicity data and formulate a hypothesis for the mechanism of action of $CoFe_2O_4$ and Ag NPs.

Both the $CoFe_2O_4$ and Ag NPs did not significantly induce cell transformation and micronuclei in Balb3T3 cells, as measured using the CTA and CBMN assays. Nevertheless, although these results were generated using *in vitro* assays, the effectiveness of which had already been proven when testing for NP genotoxicity, they cannot be considered as sufficient to definitively discard the potential of these NPs to damage DNA. Thus, future investigations must include assessments of the ability of NPs to generate ROS on their surface or induce ROS production by cells would help to clarify the genotoxicity of NPs.

The long-term exposure to NPs should also be investigated in future studies to determine whether chronic exposure can induce morphological transformation or carcinogenesis *in vitro* and *in vivo*, respectively. Moreover, additional genotoxicity endpoints should be considered for *in vitro* testing of NPs (e.g., measurements of repair protein expression, Comet and chromosomal aberration assays) and, whenever possible, these endpoints should also be investigated using *in vivo* models. *In vitro* tests cannot reproduce the *in vivo* environment that NPs encounter in the body and the alterations NPs may undergo due to metabolic processes; this reduces the correlation between *in vitro* and *in vivo* data.

In summary, the use of *in vitro* tests is largely advantageous due to the simplicity of the systems and reproducibility of the data. *In vitro* tests, therefore, appear to be an acceptable compromise when studying NMs. Protocols for *in vitro* testing should, however, be optimized for each NM and the results compared to *in vivo* investigations.

## References

Aaroson S.A. & Todaro G. J., 1968, "Development of 3T3-like lines from Balb/c mouse embryo cultures: Transformation susceptibility to SV40", Journal Cellular Physiology, 72, 141-148

Ahamed M. et al., 2008, "DNA damage response to different surface chemistry of silver nanoparticles in mammalian cells", Toxicology and Applied Pharmacology, 233, 404-410

Ahamed M. et al., 2010, "Silver nanoparticle applications and human health", Clinica Chimica Acta, 411, 1841-1848

Ahamed M. et al., 2011, "Oxidative stress mediated apoptosis induced by nickel ferrite nanoparticles in cultured 549 cells", Toxicology, 283, 101-108

Aillon K. et al., 2009, "Effects of nanomaterial physicochemical properties on in vivo toxicity", Advanced Drug Delivery Reviews, 61, 457-466

Aitken R.J. et al., 2004, "Nanoparticles: an occupational hygiene review", Research report 274, prepared by the Institute of Occupational Medicine for the Health and Safety Executive

Aitken R. J. et al., 2006, "Manufacture and use of nanomaterials: current status in the UK and global trends", Occupational Medicine, 56, 300-306

Anon, 1986, Council Directive 86/609/EEC of 24 November 1986, Official Journal of the European Communities, L358, 1-29

Arora S. et al., 2008, "Cellular responses induced by silver nanoparticles: *in vitro* studies", Toxicology Letters, 179, 93-100

Arora S. et al., 2009, “Interactions of silver nanoparticles with primary mouse fibroblasts and liver cells”, Toxicology and Applied Pharmacology, 236, 310-318

Asada S. et al., 2005, “Detection of initiating as well as promoting activity of chemicals by a novel cell transformation assay using v-Ha-ras-transfected Balb/c 3T3 cells (Bhas 42 cells)”, Mutation Research, 588, 7-21

Asada S. et al., 2005, “Detection of initiating as well as promoting activity of chemicals by a novel cell transformation assay using v-Ha-ras-transfected BALB/c 3T3 cells (Bhas 42 cells)”, Mutation Research, 588, 7-21

Asharani P. V. et al., 2009, “Cytotoxicity and Genotoxicity of silver nanoparticles in human cells”, ACS Nano, Vol 3, No.2, 279-290

Auffan M. et al., 2009, “Chemical stability of metallic nanoparticles: a parameter controlling their potential cellular toxicity in vitro”, Environmental pollution, 157, 1127-1133

Baldi G. et al., 2007b, “Synthesis and coating of cobalt ferrite NPs: a first step toward the obtainment of new magnetic nanocarrier”, Langmuir, 23, 4026-4028

Baldi G. et al., 2007a, “Cobalt ferrite nanoparticles: the control of the particle size and surface state and their effects on magnetic properties”, Journal of Magnetism and Magnetic Materials, 311, 10-16

Begum N. A. et al., 2009, “Biogenic synthesis of Au and Ag nanoparticles using aqueous solutions of Black Tea leaf extracts”, Colloids and Surfaces B: Biointerfaces, 71, 113-118

Bergamaschi E. et al., 2006, “Nanomaterials and lung toxicity: interactions with airways cells and relevance for occupational health risk assessment”. International Journal of Immunopathology and Pharmacology 19, 3-10

Berry C. C. 2005, “Possible exploitation of magnetic nanoparticle-cell interaction for biomedical applications”, Journal of Materials Chemistry, 15, 543-547

Bisht S. et al., 2007, “Polymeric nanoparticle-encapsulated curcumin (“nanocurcumin”): a novel strategy for human cancer therapy”, Journal of Nanobiotechnology, 5, 3

Borm P. J. A. et al., 2006, “The potential risks of nanomaterials: a review carried out for ECETOC”, Particle and Fibre Toxicology, 3, 11

Bouwmeester H. et al., 2011, “Minimal analytical characterization of engineered nanomaterials needed for hazard assessment in biological matrices”, Nanotoxicology, 5(1), 1-11

Brigger I. et al., 2002, “Nanoparticles in cancer therapy and diagnosis”, Advanced Drug Delivery Reviews, 54, 631-651

Buzea C. et al., 2007, “Nanomaterials and nanoparticles: sources and toxicity”, Biointerphases 2(4)

Card J. W. et al., 2010, “A method to assess the quality of studies that examine the toxicity of engineered nanomaterials”, International Journal of Toxicology, 29(4), 402-410

Carter S. B., 1967, “Effects of Cytochalasins on mammalian cells”, Nature, 21

Casarett and Doull’s, 2008, “Toxicology - The Basic Science of Poisons”, McGraw-Hill, Seventh edition

Casey A. et al., 2007, “Spectroscopic analysis confirms the interactions between single walled carbon nanotubes and various dyes commonly used to assess cytotoxicity”, Carbon, 45, 1425-1432

Casey A. et al., 2007, "Probing the interaction of single walled carbon nanotubes within cell culture medium as a precursor to toxicity testing", Carbon, 45, 34-40

Ceriotti L. et al., 2007, "Real-time assessment of cytotoxicity by impedance measurement on a 96-well plate", Sensors and Actuators B, 123, 769-778

Chen F. et al., 2004, "Fluorescent CdSe/ZnS nanocrystal-peptide conjugates for long-term, nontoxic imaging and nuclear targeting in living cells", Nano Letters, 4, 1827-1832

Chithrani B. D. et al., 2006, "Determining the size and shape dependence of gold nanoparticle uptake into mammalian cells", Nano Letters, 6, 662-668

Clark K. A. et al., 2011, "Predictive models for nanotoxicology: current challenges and future opportunities", Regulatory Toxicology and Pharmacology, 59, 361-363

Clift M. et al., 2008, "The impact of different nanoparticle surface chemistry and size on uptake and toxicity in a murine macrophage cell line", Toxicology and Applied Pharmacology, 232, 418-427

Clift M. J. D. et al., 2011, "Nanotoxicology: a perspective and discussion of whether or not in vitro testing is a valid alternative", Archives of Toxicology, 85, 723-731

Coecke S. et al., 2006, "Metabolism: a bottleneck in *in vitro* toxicological test development", ATLA, 34, 49-84

Colognato R. et al., 2007, "Analysis of cobalt ferrite nanoparticles induced genotoxicity on human peripheral lymphocytes: comparison of size and organic grafting-dependent effects", Nanotoxicology, 1(4), 301-308

Colognato R. et al., 2008, "Comparative genotoxicity of cobalt nanoparticles and ions on human peripheral leukocytes in vitro", Mutagenesis, 23, 377-382

Combes R. et al., 1999, "Cell transformation assay as predictors of human carcinogenicity. The report and recommendations of ECVAM, Workshop 39", ATLA, 27, 745-767

Cormode D. P. et al., 2009, "Nanotechnology in medical imaging probe design and applications", Arteriosclerosis Thrombosis and Vascular Biology, 29, 992-1000

Cortese-Krott M. M. et al., 2009, "Silver ions induce oxidative stress and intracellular zinc release in human skin fibroblasts", Free Radical Biology & Medicine, 47, 1570-1577

Corvi R. et al., 2008, "ECVAM retrospective validation of *in vitro* micronucleus test (MNT)", Mutagenesis, 3(4), 271-283

Curtin J. F. et al., 2002, "Regulation and measurement of oxidative stress in apoptosis", Journal of Immunological methods, 265 (1-2), 49-72

Deng X. et al., 2007, "Translocation and fate of multi-walled carbon nanotubes *in vivo*", Carbon, 45, 1419-1424

Derfus A. M. et al., 2004, "Probing the cytotoxicity of semiconductor quantum dots", Nano Letters, 4, 11-18

Dey S. et al., 2008, "Interactions between SIRT1 and AP-1 reveal a mechanistic insight into the growth promoting properties of alumina ($Al_2O_3$) nanoparticles in mouse skin epithelial cells", Carcinogenesis, 29(10), 1920-1929

DHO (Department of Health), 2000, "Report on health and social subjects, guidelines for the testing of chemicals for mutagenicity", Committee on Mutagenesis of Chemicals in Food, Consumer Products and the Environment. London, UK, HMSO

Di Paolo J. A. et al., 1972, "Quantitation of chemically induced neoplastic transformation of Balb/3T3 cloned cell lines", Cancer Research, 32, 2686-2695

Di Paolo J. A., 1980, "Quantitative *in vitro* transformation of Syrian golden hamster embryo cells with the use of frozen stored cells", Journal of the National Cancer Institute, 64, 1485-1489

Donaldson K. et al., 2004, "Nanotoxicology", Occupational and Environmental Medicine, 61, 727-728

Drobne D., 2007, "Nanotoxicology for safe sustainable nanotechnology", Archives of Industrial Hygiene and Toxicology, 58, 471-478

Dunphy Guzmán K. A. et al., 2006, "Environmental risks of nanotechnology: National Nanotechnology Initiative Funding, 2000-2004", Environmental Science & Technology, 40, 1401-1407

Ekwall B., 1992, "Validation of *in vitro* tests for general toxicity", AATEX, 1, 127-141

Ekwall B. et al., 1990, "Short-term toxicity tests for non-genotoxic effects", Scope, published by John Wiley and Sons, Chapter 7

El-Ansary A. et al., 2009, "On the toxicity of therapeutically used nanoparticles: an overview", Journal of Toxicology

Elder A. et al., 2009, "Physicochemical factors that affect metal and metal oxide nanoparticle passage across epithelial barriers", WIREs Nanomedicine Nanobiotechnology, 1, 434-450

Elechiguerra J. L. et al., 2005, "Interaction of silver nanoparticles with HIV-I", Journal of Nanobiotechnology, 3(6)

Engelhardt G. et al., 2004, "The testing of chemicals in the Syrian Hamster Embryo (SHE) cell transformation assay for assessment of carcinogenic potential", Toxicology in Vitro, 18, 213-218

Fenech M., 2007, "Cytokinesis-block micronucleus cytome assay", Nature Protocols, 2(2)

Fenech M., 2010, "Nutriomes and nutrient arrays- the key to personalised nutrition for DNA damage prevention and cancer growth control", Genome Integrity, 1(11)

Filon Larese F. et al., 2009, "Human skin penetration of silver nanoparticles through intact and damaged skin", Toxicology, 255, 33-37

Fischer H. C. et al., 2007, "Nanotoxicity: the growing need for in vivo study", Current Opinion in Biotechnology, 18, 565-571

Foldbjerg R. et al., 2011, "Cytotoxicity and genotoxicity of silver nanoparticles in the human lung cancer cell line, A549", Archives of Toxicology, 85(7), 743-50

Foster J. F., 1977, "Some aspects of the structure and conformational properties of serum albumin", in *Albumin, Structure, Function and Uses V.M. Rosenoer, M. Oratz, M.A. Rothschild (Eds.), Pergamon Press, Oxford*, 58-84

Freyre-Fonseca V. et al., 2011, "Titanium dioxide nanoparticles impair lung mitochondrial function", Toxicology Letters, 202, 111-119

Fubini B. et al., 2010, "Physico-chemical features of engineered nanoparticles relevant to their toxicity", Nanotoxicology, 4(4), 347-363

Fusenig N. E. & Boukamp P., 1998, "Multiple stages and genetic alterations in immortalisation, malignant transformation, and tumor progression of human skin keratinocytes", Molecular Carcinogenesis, 23, 144-158

Gaiser B. K. et al., 2009, "Assessing exposure, uptake and toxicity of silver and cerium dioxide nanoparticles from contaminated environments", Environmental Health, 8 (I):S2

Gillespie R. J. et al., 1990, "Chimica", Società Editrice Scientifica, prima edizione italiana

Goldstein J. et al., 2003, "Scanning Electron Microscopy and X-Ray microanalysis", third edition, (accessed by Google books)

Griffon G. et al., 1995, "Comparison of sulforhodamine B, tetrazolium and clonogenic assays for in vitro radiosensitivity testing in human ovarian cell lines", Anti-Cancer Drugs, 6, 115-123

Hackenberg S. et al., 2011, "Silver nanoparticles: evaluation of DNA damage, toxicity and functional impairment in human mesenchymal stem cells", Toxicology Letters, 201, 27-33

Hartung T. et al., 2003, "ECVAM's Response to the changing political environment for alternatives: consequence of the European Union Chemical and Cosmetic Policies", ATLA, 31, 473-481

Hartung T. et al., 2004, "New hepatocytes for toxicology?", Trends in Biotechnology, 22, 613-5

Hartung T. et al., 2004, "A modular approach to the ECVAM principles on test validity", ATLA, 32, 467-472

Herzog E. et al., 2007, "A new approach to the toxicity testing of carbon-based nanomaterials-the clonogenic assay", Toxicology Letters, 174, 49-60

Hillegass J. M. et al., 2010, "Assessing Nanotoxicity in cells *in vitro*", WIREs Nanomedicine and Nanobiotechnology, 2, 219-231

http://copublications.greenfacts.org/en/nanotechnologies/l-3/7-exposure-nanoparticles.htm#2p0, last accessed in February 2012

http://cordis.europa.eu/nanotechnology/actionplan.htm, last accessed in October 2010

http://cordis.europa.eu/projects/index.cfm?fuseaction=app.search&TXT=nanomaterials&FRM=1&STP=10&SIC=SICNNT&PGA=FP7-NMP&CCY=&PCY=&SRC=&LNG=en&REF=, last accessed in February 2012

http://ec.europa.eu/health/scientific_committees/opinions_layman/nanomaterials/en/l-3/4.htm, last accessed in February 2012

http://www.langsrud.com/fisher.htm, last accessed in February 2011

http://www.malvern.com/LabEng/technology/dynamic_light_scattering/dynamic_light_scattering.htm, last accessed in September 2011

http://www.malvern.com/LabEng/technology/zeta_potential/zeta_potential_LDE.htm, last accessed in September 2011

http://www.nanosight.com/, last accessed in September 2011

http://www.nanotechproject.org/inventories/consumer/, last accessed in February 2011

http://www.nanotechproject.org/inventories/silver/, last accessed in February 2011

http://radiologie-uni-frankfurt.de/sites/radiologie-uni-frankfurt.de/content/e43/e2321/e2331/resofinal_eng.pdf, last accessed in September 2011

Huang X. et al., 2011, "The shape effect of Mesoporous Silica Nanoparticles on biodistribution, clearance, and biocompatibility *in vivo*", ACS Nano, 5(7), 5390-5399

IARC/NCI/EPA Working-Group, 1985, "Cellular and molecular mechanisms of cell transformation and standardization of transformation assays of established cell lines for the prediction of carcinogenic chemicals: overview and recommended protocols", Cancer Research, 45, 2395-2399

IARC, 1987, Monographs on the evaluation of Carcinogenic Risks to Humans, Suppl. 6. Genetic and Related Effects: An Updating of selected IARC Monographs from Vol. 1 to 42: 729

IARC Monographs, Volumes 1-102; http://monographs.iarc.fr/ENG/Classification/index.php, last accessed in February 2011

Jiang J. et al., 2009, "Characterization of size, surface charge, and agglomeration state of nanoparticle dispersions for toxicological studies", Journal of Nanoparticle Research, 11, 77-89

Johnston H. et al., 2010, "A review of the in vivo and in vitro toxicity of silver and gold particulates: particle attributes and biological mechanisms responsible for the observed toxicity", Critical Reviews in Toxicology, 40(4), 328-46

Kakunaga T., 1973, "A quantitative system for assay of malignant transformation by chemical carcinogens using a clone derived from Balb/3T3", International Journal of Cancer, 12, 463-473

Karlsson H. L., 2010, “The comet assay in nanotoxicology research”, Analytical and Bioanalytical Chemistry, 398, 651-666

Khan M. K. et al., 2005, “In vivo biodistribution of dendrimers and dendrimer nanocomposites—implications for cancer imaging and therapy”, Technology in Cancer Research and Treatment, 4, 603-613

Kim D. H. et al., 2005, “Cytotoxicity of ferrites particles by MTT and agar diffusion methods for hyperthermic application”, Journal of Magnetism and Magnetic Materials, 293, 287-292

Kim D. H. et al., 2007, “*In vitro* and *in vivo* toxicity of $CoFe_2O_4$ for application to magnetic hyperthermia”, Nano Science and Technology Institute-Nanotech, 2

Kim J. S. et al., 2007, “Antimicrobial effects of silver nanoparticles”, Nanomedicine: Nanotechnology, Biology and Medicine, 3, 95-101

Kita E. et al., 2010, “Ferromagnetic nanoparticles for magnetic hyperthermia and thermoablation therapy”, Journal of Physics D, 43

Keyling W. G. et al., 2006, “Health implications of nanoparticles”, Journal of Nanoparticle Research, 8, 543-562

Kumar C. S. S. R. et al., 2011, “Magnetic nanomaterials for hyperthermia-based therapy and controller drug delivery”, Advanced Drug Delivery Reviews, 63, 789-808

Kunzmann A. et al., 2010, “Toxicology of engineered nanomaterials: focus on biocompatibility, biodistribution and biodegradation”, Biochimica et Biophysica Acta, 1810(3), 361-73

Landsiedel R. et al., 2008, “Genotoxicity investigations on nanomaterials: methods, preparation and characterization of test material, potential artefacts and limitations- Many questions, some answers”, Mutation Research, 681, 241-258

Lankveld D. P. K. et al., 2010, “The kinetics of the tissue distribution of silver nanoparticles of different sizes”, Biomaterials, 31, 8350-8361

Laurent S. et al., 2008, “Magnetic iron oxide nanoparticles: synthesis, stabilization, vectorization, physicochemical characterizations, and biological applications”, Chemical Reviews, 108, 2064-2110

Lewin B., 1997, "Genes VI", International Student Edition, chapter 37, pp. 1131-1171

Liu M. et al., 2008, “Pharmacokinetics and biodistribution of surface modification polymeric nanoparticles”, Archives of Pharmaceutical Research, 31, 547-554

Liu J. et al., 2010, “Ion release kinetics and particle persistence in aqueous nano-silver colloids”, Environmental Science & Technology, 44, 2169-2175

Lu S. et al., 2009, “Efficacy of simple short-term in vitro assays for predicting the potential of metal oxide nanoparticles to cause pulmonary inflammation”, Environmental Health Perspectives, 117, 241-247

Lu W. et al., 2010, “Effect of surface coating on the toxicity of silver nanomaterials on human skin keratinocytes”, Chemical Physics Letters, 487, 92-96

Lynch I. et al., 2008, “Protein-nanoparticle interactions”, Nanotoday, 3, 1-2

Maaz K. et al., 2006, “Synthesis and magnetic properties of cobalt ferrite nanoparticles prepared by wet chemical route”, Journal of Magnetism and Magnetic Materials, 308, 289-295

Mariani V. et al., 2011, "Online monitoring of cell metabolism to assess the toxicity of nanoparticles: the case of cobalt ferrite", Nanotoxicology

Marmorato P. et al., 2011, "Cellular distribution and degradation of Cobalt Ferrite Nanoparticles in Balb/3T3 Mouse Fibroblasts", Toxicology Letters, 207, 128-136

Matthews E. J. et al., 1993, "Transformation of Balb/c-3T3 cells: V. Transformation responses of 168 chemicals compared with mutagenicity in *Salmonella* and carcinogenicity in rodent bioassays", Environmental Health Perspective, 101, 347-482

Maynard A. D. et al., 2007, "Assessing exposure to airborne nanomaterials: Current abilities and future requirements", Nanotoxicology, 1, 26-41

Mazzotti F. et al., 2002, "*In vitro* setting of dose–effect relationships of 32 metal compounds in the Balb/3T3 cell line as a basis for predicting their carcinogenic potential", ATLA, 30, 209-217

McNeil S. E., 2005, "Nanotechnology for the biologist", Journal of Leukocyte Biology, 78

Migliore L. et al., 2002, "Assessment of sperm DNA integrity in workers exposed to styrene", Human Reproduction, 17, 2912-2918

Min'ko N. I. et al., 2008, "Nanotechnology in glass materials", Glass and Ceramics, 65, 5-6, 148-153

Monteiro-Riviere N. A. et al., 2009, "Limitations and relative utility of screening assays to assess engineered nanoparticle toxicity in a human cell line", Toxicology and Applied Pharmacology, Vol 234, Issue 2, 222-235

Motulsky H., 1995, “Intuitive biostatistics”, Oxford University Press

Mühlfeld C. et al., 2007, “Visualization and quantitative analysis of nanoparticles in the respiratory tract by transmission electron microscopy”, Particle and Fibre Toxicology, 4(11)

Nativo P. et al., 2008, “Uptake and intracellular fate of surface-modified gold nanoparticles”, ACS Nano, 2, 1639-44

Ng C.-T. et al., 2010, “Current studies into the genotoxic effects of nanomaterials”, Journal of Nucleic Acids

NIOSH (National Institute for Occupational Safety and Health), “Approaches to safe Nanotechnology: an information exchange with NIOSH”, available at http://www.cdc.gov/niosh/nas/RDRP/appendices/chapter7/a7-2.pdf, accessed on September 2011

Oberdörster G. et al., 2005, “Nanotoxicology: An emerging Discipline Evolving from Studies of Ultrafine Particles”, Environmental Health Perspectives, 113 (7), 823-839

OECD TG 471, available at http://www.oecd.org/dataoecd/18/31/1948418.pdf

OECD TG 473, available at http://www.alttox.org/ttrc/existing-alternatives/genotoxicity.html

OECD TG 487, available at http://www.oecd.org/dataoecd/33/22/37865944.pdf

OECD, 2008, Current Developments/Activities on the Safety of Manufactured Nanomaterials/Nanotechnologies.(http://www.olis.oecd.org/olis/2008doc.nsf/LinkTo/NT00000E8A/$FILE/JT03243507.PDF) ENV/JM/MONO (2008)7

Panáček A. et al., 2006, "Silver colloid nanoparticles: synthesis, characterization and their antibacterial activity", The Journal of Physical Chemistry B, 110,16248-16253

Park E. J. et al., 2009, "Oxidative stress and pro-inflammatory responses induced by silica nanoparticles *in vivo* and *in vitro*", Toxicology Letters, 184, 18-25

Park E. J. et al., 2010a, "Silver nanoparticles induce cytotoxicity by Trojan-horse type mechanism", Toxicology in Vitro, 24, 872-878

Park E. J. et al., 2010b, "Repeated-dose toxicity and inflammatory responses in mice by oral administration of silver nanoparticles", Environmental Toxicology and Pharmacology, 30, 162-168

Parry J. M. et al., 2010, "Special issue on *in vitro* MN trial", Mutation Research, 702, 132-134

Perdersen F. et al., 2003, "Assessment of additional testing needs under REACH-effects of (Q)SARs, risk based testing and voluntary industry initiatives", JRC Report EUR 20863, 33pp, Ispra, Italy: European Commission Joint Research Centre

Ponti J., 2004, "*In vitro* metal toxicology research. A study carried out by Balb/3T3, HaCaT and CaCo-2 cell lines", Traball de Magíster UAB

Ponti J. et al., 2006, "Comparison of Impedance-based Sensors for Cell Adhesion Monitoring and *In Vitro* Methods for Detecting Cytotoxicity Induced by Chemicals", ATLA, 34, 515-525

Ponti J. et al., 2007, "An optimised data analysis for the Balb/c 3T3 transformation assay and its application to metal compounds", International Journal of Immunopathology and Pharmacology, 20, 673-684

Ponti J., 2008, "*In vitro* toxicology activities at the Joint Research Centre (JRC)", Nanotoxicology, 2(I), Abstract of ICONTOX 2008, Lucknow India, February 5-7

Ponti J. et al., 2009, "Genotoxicity and morphological transformation induced by cobalt nanoparticles and cobalt chloride: an in vitro study on Balb/3T3 mouse fibroblasts", Mutagenesis, 24(5), 439-445

Ponti J. et al., 2010, "Colony Forming Efficiency and microscopy analysis of multi-wall carbon nanotubes cell interaction", Toxicology Letters, 197, 29-37

Ponti J. et al., 2011, "*In vitro* carcinogenic potential induced by multiwall carbon nanotubes on Balb/3T3 cell model", paper submitted to Nanotoxicology

Powers K. W. et al., 2006, "Research strategies for safety evaluation of nanomaterials, Part VI, Characterization of nanoscale particles for toxicological evaluation", Toxicological Science, 90, 296-303

Rai M. et al., 2009, "Silver nanoparticles as a new generation of antimicrobials", Biotechnology Advances, 27, 76-83

Rao C. N. R. et al., 2004, "The chemistry of nanomaterials: Synthesis, properties and applications", Wiley-VCH

Rao C. N. R. et al., 2007, "Synthesis of inorganic nanomaterials", Dalton Transactions, 34, 3728-3749

Rauscher H. et al., 2010, "Sedimentation of nanoparticles in in vitro toxicity assays", European cells and Materials, 20(3), 120

Reimer P. et al., 2003, "Ferucarbotran (Resovist): a new clinically approved RES-specific contrast agent for contrast-enhanced MRI of the liver: properties, clinical development and applications", European radiology, 13(6), 1266-1276

Resovist® leaflet, available at http://radiologie-uni-frankfurt.de/sites/radiologie-uni-frankfurt.de/content/e43/e2321/e2331/resofinal_eng.pdf, last accessed in September 2011

Rojas E. et al., 1999, "Single cell gel electrophoresis assay: methodology and applications", Journal of Chromatography B, 722, 225-254

Roy N. et al., 2010, "Biogenic synthesis of Au and Ag nanoparticles by Indian propolis and its constituents", Colloids and Surfaces B: Biointerfaces, 76, 317-325

Russel W. M. S. et al., 1959, "The Principles of Humane Experimental Technique", London, Methuen; 69-154

Saffiotti U. et al., 1984, "Studies on chemically induced neoplastic transformation and mutation in the Balb/3T3 Cl A31-1-1 cell line in relation to the quantitative evaluation of carcinogens", Toxicology and Pathology, 12, 383-390

Sahoo S. K. et al., 2003, "Nanotech approaches to drug delivery and imaging", Drug Discovery Today, 8(24), 1112-20

Sakai A., 2007, "Balb/c 3T3 cell transformation assays for the assessment of chemicals carcinogenicity", AATEX Journal, 14, 367-373

Saran R. et al., 2008, "Risk assessment of oral cancer in patients with pre-cancerous states of the oral cavity using micronucleus test and challenge assay", Oral Oncology, 44, 354-360

Sasaki K. et al., 1988, “Isolation and characterization of ras-transfected BALB/3T3 clone showing morphological transformation by 12-O-tetradecanoyl-phorbol-13-acetate”, Japanese Journal of Cancer Research, 79, 921-930

Schins R. P. F., 2002, “Mechanisms of genotoxicity of particles and fibresa”, Inhalation Toxicology, 14, 57-78

Shoemaker R. H. et al., 1985, “Application of a human tumour Colony-forming assay to new drug screening”, Cancer Research, 45, 2145-2153

Singh M. et al., 2008, “Nanotechnology in medicine and antibacterial effect of silver nanoparticles”, Digest Journal of Nanomaterials and Biostructures, 3 (3), 115-122

Singh N. et al., 2009, “NanoGenotoxicology: the DNA damaging potential of engineered nanomaterials”, Biomaterials, 30, 3891-3914

Stern S. T. & McNeil S. E., 2008, “Nanotechnology Safety Concerns Revisited”, Toxicological Sciences, 101, 4-21

Stone V. et al., 2009, “Development of *in vitro* systems for nanotoxicology: methodological consideration”, Critical Reviews in Toxicology, 39(7), 613-626

Stone V. et al., 2010, “Nanomaterials for environmental studies: classification, reference materials issues, and strategies for physico-chemical characterization”, Science of the total environment, 408, 1745-1754

Sweet L. & Strohm B., 2006, “Nanotechnology - Life-cycle risk management”, Human and Ecological Risk Assessment, 12, 528-551

Tartaj P. et al., 2005, “Advances in magnetic nanoparticles for biotechnology applications”, Journal of Magnetism and Magnetic Materials, 290-291, 28-34

Teodoro J. S. et al., 2011, "Assessment of the toxicity of silver nanoparticles *in vitro*: a mitochondrial perspective", Toxicology in Vitro, 25, 664-670

The Royal Society and The Royal Academy of Engineering, 2004, "Nanoscience and nanotechnologies: opportunities and uncertainties", Nanoscience and Nanotechnologies

Tomitaka A. et al., 2009, "Biocompatibility of various ferrite nanoparticles evacuate by *in vitro* cytotoxicity assays using HeLa cells", Journal of Magnetism and Magnetic Materials, 321, 1482-1484

Uchino T. et al., 2002, "Quantitative determination of OH radical generation and its cytotoxicity induced by $TiO_2$-UVA treatment", Toxicology In Vitro, 16, 629-635

US EPA, http://www.epa.gov/IRIS/subst/0099.htm, last accessed in September 2011

Vaishnava P. P. et al., 2006, "Magnetic properties of cobalt-ferrite nanoparticles embedded in polystyrene resin", Journal of applied Physics 99

Walum E. et al., 1990, "Understanding cell toxicology. Principles and practice", Hellis Horwood

Warheit D. B., 2008, "How meaningful are the results of nanotoxicity studies in the absence of adequate material characterization?" Toxicological Sciences, 101(2), 183-185

Watanabe I. et al., 1967, "Stationary phase of cultured mammalian cells (L5178Y)", Journal of Cell Biology, 35(2), 285-294

Wijnhoven S. W. P. et al., 2009, "Nano-silver: a review of available data and knowledge gaps in human and environmental risk assessment", Nanotoxicology, 3(2), 109-138

Wise Sr. J. P. et al., 2010, “Silver nanospheres are cytotoxic and genotoxic to fish cells”, Aquatic Toxicology, 97, 34-41

Yuspa S. H. et al., 1988, “Chemical carcinogenesis: from animal models to molecular models in one decade”, Advances in cancer Researcher, 50, 25-70

Zeiger E., 2001, “Genetic toxicity test for predicting carcinogenicity, in Genetic Toxicology and Cancer Risk Assessment” (ed. W.N. Choy), pp 29-46. New York, NY, USA: Marcel Dekker